

# **TASK 3.4 – IMPACTS OF COFIRING BIOMASS WITH FOSSIL FUELS**

Final Report

*(for the period April 1, 1999, through March 31, 2001)*

*Prepared for:*

AAD Document Control  
U.S. Department of Energy  
National Energy Technology Laboratory  
PO Box 10940, MS 921-143  
Pittsburgh, PA 15236-0940

Cooperative Agreement No. DE-FC26-98FT40320; UND 4255  
Performance Monitor: Mr. Philip Goldberg

*Prepared by:*

Christopher J. Zygarlicke  
Donald P. McCollor  
Kurt E. Eylands  
Melanie D. Hetland  
Mark A. Musich  
Charlene R. Crocker  
Jonas Dahl  
Stacie Laducer

Energy & Environmental Research Center  
University of North Dakota  
PO Box 9018  
Grand Forks, ND 58202-9018

## **DOE DISCLAIMER**

This report was prepared as an account of work sponsored by an agency of the United States Government. Neither the United States Government, nor any agency thereof, nor any of their employees makes any warranty, express or implied, or assumes any legal liability or responsibility for the accuracy, completeness, or usefulness of any information, apparatus, product, or process disclosed or represents that its use would not infringe privately owned rights. Reference herein to any specific commercial product, process, or service by trade name, trademark, manufacturer, or otherwise does not necessarily constitute or imply its endorsement, recommendation, or favoring by the United States Government or any agency thereof. The views and opinions of authors expressed herein do not necessarily state or reflect those of the United States Government or any agency thereof.

This report is available to the public from the National Technical Information Service, U.S. Department of Commerce, 5285 Port Royal Road, Springfield, VA 22161; phone orders accepted at (703) 487-4650.

## **ACKNOWLEDGMENT**

This report was prepared with the support of the U.S. Department of Energy (DOE) National Energy Technology Laboratory Cooperative Agreement No. DE-FC26-98FT40320. However, any opinions, findings, conclusions, or recommendations expressed herein are those of the authors(s) and do not necessarily reflect the views of DOE.

## **EERC DISCLAIMER**

**LEGAL NOTICE** This research report was prepared by the Energy & Environmental Research Center (EERC), an agency of the University of North Dakota, as an account of work sponsored by DOE. Because of the research nature of the work performed, neither the EERC nor any of its employees makes any warranty, express or implied, or assumes any legal liability or responsibility for the accuracy, completeness, or usefulness of any information, apparatus, product, or process disclosed, or represents that its use would not infringe privately owned rights. Reference herein to any specific commercial product, process, or service by trade name, trademark, manufacturer, or otherwise does not necessarily constitute or imply its endorsement or recommendation by the EERC.

## TABLE OF CONTENTS

LIST OF FIGURES .....	iv
LIST OF TABLES .....	vii
EXECUTIVE SUMMARY .....	ix
INTRODUCTION .....	1
GOAL AND OBJECTIVES .....	3
EXPERIMENTAL .....	4
Biomass Processing .....	4
Combustion Testing .....	5
Fuel, Fly Ash, and Ash Deposit Analyses .....	7
RESULTS .....	8
Background on Processing of Biomass Fuel Types .....	8
The Effects of Plant Cell Chemistry on Cofiring Biomass with Coal .....	9
Introduction .....	9
Intrinsic Properties of Biomass .....	9
Plant Physiology .....	10
Elements of Interest .....	12
Elemental Occurrence in Biomass .....	14
Potassium, Calcium, Phosphorus, Chlorine, and Sodium .....	16
Wheat .....	17
Rice .....	20
Switchgrass .....	22
Hybrid Poplar .....	24
Alfalfa .....	24
Silica .....	24
Extrinsic Properties of Biomass .....	27
Environmental Factors .....	27
Toxicities .....	28
pH .....	29
Summary .....	29
GEOGRAPHIC AND SEASONAL DIFFERENCES IN SWITCHGRASS ELEMENTAL COMPOSITION .....	30
Background .....	30
Analysis Results .....	31

Continued . . .

## TABLES OF CONTENTS (Continued)

Geographical Variations by County and Township .....	34
Seasonal Variations .....	35
Combustion Characteristics .....	38
Discussion .....	39
K <sub>2</sub> O, Na <sub>2</sub> O, and Cl Correlations .....	39
Geographical Variations .....	40
Seasonal Variations .....	40
Conclusions .....	41
<b>BIOMASS CHARACTERISTICS .....</b>	<b>42</b>
Effects of Chemical Composition on Power-Generating Equipment .....	42
Effects of Physical Characteristics on Process Design and Equipment .....	43
Biomass Production, Harvesting, Transport, and Storage Issues .....	43
Biomass Grinding and Feeding Methods and Equipment .....	44
Chipping and Grinding .....	44
Feeding Biomass to a Combustor .....	45
Results of Biomass–Coal Cofiring Studies .....	47
Summary of Literature and Background on Biomass Processing .....	49
Biomass Processing Data Results .....	49
<b>BIOMASS CHARACTERIZATION .....</b>	<b>51</b>
Analytical Technique Development and Fuel Characterization Results .....	52
Combustion Testing and Biomass Cofiring Results .....	61
Slagging Deposit .....	61
<b>MODELING OF FLY ASH AND AEROSOL FORMATION DURING COMBUSTION OF BIOMASS BY MODIFYING A CODE DEVELOPED FOR COAL COMBUSTION ...</b>	<b>89</b>
The TraceTran (ATRAN) Program .....	91
General Algorithms and Data Flow in TraceTran .....	93
Calculations with the TraceTran Code .....	97
Discussion of Results .....	99
Results from Mineral Classification of Biomass Fuels .....	100
Discussion .....	100
Implementation of Aerosol Model Calculations .....	101
The General Dynamic Equation .....	101
Improvements to the TraceTran Code .....	106
Suggestions on Changes to the TraceTran (ATRAN) Code .....	107
<b>CONCLUSIONS .....</b>	<b>107</b>
Survey of Literature on Biomass Processing and Cofiring .....	107

Continued . . .

## TABLE OF CONTENTS (Continued)

The Effects of Plant Cell Chemistry on Cofiring Biomass with Coal .....	108
Geographic and Seasonal Differences in Switchgrass Elemental Composition .....	109
Characterization and Processing of Test Fuels .....	110
Analytical Techniques Improvement .....	110
Ash Formation and Deposition .....	111
Modeling of Biomass Ash Transformations .....	114
FUTURE WORK .....	115
REFERENCES .....	115
BIOMASS LITERATURE SEARCH .....	Appendix A
PLANT CELL CHEMISTRY LITERATURE SEARCH .....	Appendix B
GLOSSARY OF BIOMASS TERMS .....	Appendix C
SWITCHGRASS PROXIMATE, ULTIMATE, AND ASH CHEMISTRY ANALYSES .....	Appendix D
ANALYTICAL CHARACTERIZATIONS FOR VARIOUS TYPES OF BIOMASS .....	Appendix E
FUEL CCSEM ANALYSIS RESULTS .....	Appendix F
CLUSTER ANALYSIS OF BIOMASS FUEL CCSEM DATA .....	Appendix G
FLY ASH CCSEM ANALYSIS RESULTS .....	Appendix H

## LIST OF FIGURES

1	Biomass availability by region . . . . .	2
2	Conversion and environmental process simulator . . . . .	6
3	Simplified scheme of a mesophyll cell (43) . . . . .	11
4	Process of nutrient uptake in soil–plant system (43) . . . . .	13
5	Transverse section of corn root showing the symplastic (A) and apoplastic (B) pathways of ion transport across the root (43) . . . . .	13
6	Distribution of nutrients in different plant parts of wheat (43) . . . . .	21
7	Distributions of N, P, and K in roots, tops, and grains of two upland rice cultivars (43) . . . . .	23
8	K <sub>2</sub> O versus Cl in harvested switchgrass . . . . .	33
9	Water-soluble alkalies versus moisture in harvested switchgrass . . . . .	34
10	Switchgrass dry-basis county averages for October and November 1999 . . . . .	36
11	Seasonal changes of unharvested switchgrass from the Schultz farm . . . . .	37
12	Seasonal changes of unharvested switchgrass from the Sellers farm . . . . .	37
13	Ash and alkali content for unharvested switchgrass . . . . .	38
14	Sellers farm switchgrass ash viscosity by season . . . . .	39
15	Wheat straw and alfalfa stems before and after shredding . . . . .	50
16	Hybrid poplar tree being harvested from an experimental tree farm in northwestern Minnesota . . . . .	51
17	Phytolith structures of wheat straw . . . . .	53
18	SEM BEI image of wheat straw . . . . .	58
19	SEM BEI image of alfalfa stems . . . . .	58

Continued . . .

## LIST OF FIGURES (Continued)

20	SEM BEI image of hybrid poplar . . . . .	59
21	SEM BEI image of Illinois No. 6 coal . . . . .	59
22	SEM BEI image of Absaloka coal . . . . .	60
23	Particle-size distribution of quartz and silica-rich material . . . . .	60
24	Comparison of deposit growth rates and crushing strengths . . . . .	65
25	Illinois No. 6 fouling deposit . . . . .	65
26	Absaloka fouling deposit . . . . .	66
27	Wheat straw fouling deposit . . . . .	66
28	Alfalfa stem fouling deposit . . . . .	67
29	Hybrid poplar fouling deposit . . . . .	67
30	80% Illinois No. 6–20% wheat straw fouling deposit . . . . .	68
31	80% Illinois No. 6–20% alfalfa stem fouling deposit . . . . .	68
32	80% Illinois No. 6–20% hybrid poplar stem fouling deposit . . . . .	69
33	80% Absaloka–20% wheat straw fouling deposit . . . . .	69
34	80% Absaloka–20% alfalfa stem fouling deposit . . . . .	70
35	80% Absaloka–20% hybrid poplar fouling deposit . . . . .	70
36	80% Illinois No. 6–20% wheat straw slagging deposit . . . . .	71
37	Comparison of 80% Illinois No. 6–20% wheat straw deposit and fly ash chemistry . . . . .	76
38	Illinois No. 6 and wheat straw fuel and fly ash mineral particle-size distribution . . . . .	83
39	Absaloka and wheat straw fuel and fly ash mineral particle-size distribution . . . . .	83

Continued . . .

## LIST OF FIGURES (Continued)

40	Illinois No. 6 and alfalfa stem fuel and fly ash mineral particle-size distribution . . . . .	84
41	Absaloka and alfalfa stem fuel and fly ash mineral particle-size distribution . . . . .	84
42	Illinois No. 6 and hybrid poplar fuel and fly ash mineral particle-size distribution . . . . .	85
43	Absaloka and hybrid poplar fuel and fly ash mineral particle-size distribution . . . . .	85
44	On-line APS–SMPS particle-size distributions . . . . .	87
45	80% Illinois No. 6–20% wheat straw fly ash . . . . .	89
46	Wheat straw fly ash . . . . .	90
47	TraceTran program flow diagram . . . . .	94
48	TraceTran program interface . . . . .	95
49	Results from the TraceTran model calculations compared to measured particle-size distribution of baghouse ash from CEPS combustion tests . . . . .	98
50	Illustration of the assumed plug flow and the descretized size distribution . . . . .	101
51	Conceptual flow diagram for an aerosol calculation model using TraceTran input data . . . . .	104

## LIST OF TABLES

1	Typical Ash Composition of Alfalfa, Hybrid Poplar, Rice Straw, Switchgrass, Wheat Straw, and Wheat Stems . . . . .	14
2	Element Structures in Biomass . . . . .	15
3	Elements in Biomass . . . . .	16
4	Nutrient Deficiencies of Soil Types . . . . .	28
5	Summary of Switchgrass Sample Data . . . . .	32
6	Wood Energy Equipment Vendors Found on the Internet . . . . .	46
7	Bulk Density Values for Wheat Straw, Hybrid Poplar, and Alfalfa . . . . .	50
8	CCSEM Mineral Content of the Fuels . . . . .	52
9	CHF Analysis of Fuels . . . . .	54
10	Proximate and Ultimate Analysis of the Fuels . . . . .	55
11	Bulk Ash Chemistry of the Fuels . . . . .	56
12	Combustion Conditions for Deposit Testing . . . . .	62
13	Gas Analysis for Deposit Testing . . . . .	63
14	Deposit Strengths and Growth Rates . . . . .	64
15	Fouling Deposit Mineral Species . . . . .	73
16	Fouling Deposit Bulk Chemistry . . . . .	74
17	Illinois No. 6 Deposit and Ash Mineral Species . . . . .	75
18	Illinois No. 6 Deposit and Ash Chemistry . . . . .	75
19	CCSEM Fly Ash Analysis . . . . .	77
20	Average CCSEM Chemical Composition of Fly Ash . . . . .	78

Continued . . .

## LIST OF TABLES (Continued)

21	Average CCSEM Chemical Composition of Fly Ash with “Unknown” Mineral Composition .....	79
22	Differences Between Fuel and Deposit and Fly Ash Chemistry .....	81
23	Average Potassium Concentration of Illinois No. 6 and Blend Fly Ash .....	88
24	Summary of the TraceTran Source Code Files .....	92
25	Format of the CCSEM Analysis Files .....	93
26	Fragmentation and Coalescence Constants in TraceTran .....	96
27	EERC Identification Numbers for Data Used in the TraceTran Calculations .....	99
28	Predominant Minerals in the Fuels Investigated .....	100

## TASK 3.4 – IMPACTS OF COFIRING BIOMASS WITH FOSSIL FUELS

### EXECUTIVE SUMMARY

With a major worldwide effort now ongoing to reduce greenhouse gas emissions, cofiring of renewable biomass fuels at conventional coal-fired utilities is seen as one of the lower-cost options to achieve such reductions. The Energy & Environmental Research Center has undertaken a fundamental study to address the viability of cofiring biomass with coal in a pulverized coal (pc)-fired boiler for power production.

Wheat straw, alfalfa stems, and hybrid poplar were selected as candidate biomass materials for blending at a 20 wt% level with an Illinois bituminous coal and an Absaloka subbituminous coal. The biomass materials were found to be easily processed by shredding and pulverizing to a size suitable for cofiring with pc in a bench-scale downfired furnace.

A literature investigation was undertaken on mineral uptake and storage by plants considered for biomass cofiring in order to understand the modes of occurrence of inorganic elements in plant matter. Sixteen essential elements, C, H, O, N, P, K, Ca, Mg, S, Zn, Cu, Fe, Mn, B, Mo, and Cl, are found throughout plants. The predominant inorganic elements are K and Ca, which are essential to the function of all plant cells and will, therefore, be evenly distributed throughout the nonreproductive, aerial portions of herbaceous biomass. Some inorganic constituents, e.g., N, P, Ca, and Cl, are organically associated and incorporated into the structure of the plant. Cell vacuoles are the repository for excess ions in the plant. Minerals deposited in these ubiquitous organelles are expected to be most easily leached from dry material. Other elements may not have specific functions within the plant, but are nevertheless absorbed and fill a need, such as silica. Other elements, such as Na, are nonessential, but are deposited throughout the plant. Their concentration will depend entirely on extrinsic factors regulating their availability in the soil solution, i.e., moisture and soil content. Similarly, Cl content is determined less by the needs of the plant than by the availability in the soil solution; in addition to occurring naturally, Cl is present in excess as the anion complement in K fertilizer applications.

An analysis was performed on existing data for switchgrass samples from ten different farms in the south-central portion of Iowa, with the goal of determining correlations between switchgrass elemental composition and geographical and seasonal changes so as to identify factors that influence the elemental composition of biomass. The most important factors in determining levels of various chemical compounds were found to be seasonal and geographical differences related to soil conditions.

Combustion testing was performed to obtain deposits typical of boiler fouling and slagging conditions as well as fly ash. Analysis methods using computer-controlled scanning electron microscopy and chemical fractionation were applied to determine the composition and association of inorganic materials in the biomass samples. Modified sample preparation techniques and mineral quantification procedures using cluster analysis were developed to characterize the inorganic material in these samples. Each of the biomass types exhibited different inorganic associations in the fuel as well as in the deposits and fly ash.

Morphological analyses of the wheat straw show elongated 10–30- $\mu\text{m}$  amorphous silica particles or phytoliths in the wheat straw structure. Alkali such as potassium, calcium, and sodium is organically bound and dispersed in the organic structure of the biomass materials. Combustion test results showed that the blends fed quite evenly, with good burnout. Significant slag deposit formation was observed for the 100% wheat straw, compared to bituminous and subbituminous coals burned under similar conditions. Although growing rapidly, the fouling deposits of the biomass and coal–biomass blends were significantly weaker than those of the coals. Fouling was only slightly worse for the 100% wheat straw fuel compared to the coals. The wheat straw ash was found to show the greatest similarity from the fuel to the ash analyzed. A high percentage of particles from both fuel and ash samples contained both Si and K. While Cl was a significant component in the fuel, very little was detected in the ash sample. In contrast, both the hybrid poplar and alfalfa stems fuel show little Cl, while the ash contains quite high levels of Cl. These fuels exhibit a significant rearrangement of elements during combustion which can at least in part be contributed to the particle size being small.

The TraceTran model was examined and shows promise for use as an ash transformation model for biomass combustion. Modifications that would be required include 1) implementation of chemical equilibrium calculations to estimate the critical biomass species present and their quantity, 2) modifying the code to represent the majority of biomass-derived ash particles as irregular agglomerates and not as spheres, 3) generating additional experimental and empirical data to better determine constants suitable for biomass for use in the program algorithms, and 4) making a series of code changes that will make the model more flexible, and 5) adding key biomass elemental constituents such as chlorine and zinc to the input files.

## TASK 3.4 – IMPACTS OF COFIRING BIOMASS WITH FOSSIL FUELS

### INTRODUCTION

Well over half of the electric generation in the United States is derived from coal, and over two-thirds of the coal-fired boilers are configured as pulverized coal (pc)-fired units. More and more electric utilities that use coal for power generation are considering the use of renewable fuels such as waste products or energy crop-derived biomass fuels as a lowest-cost option for reducing greenhouse gas emissions. Calculations by the National Renewable Energy Laboratory (NREL) show that cofiring 15% and 5% by heat input of urban waste biomass with Illinois No. 6 coal reduces greenhouse gas emissions by 22% and 7%, on a CO<sub>2</sub>-equivalent basis per unit of electricity produced (1). Therefore, significant reductions of greenhouse gases can be achieved by coal-fired plants. However, questions arise as to the availability of biomass resources, modifications that may be necessary for existing plants, and the global greenhouse gas inventory.

Some experts are estimating that 14%–15% of total world energy consumption is already accounted for by biomass (2). Energy production from biomass fuel sources such as wood wastes, municipal wastes, agricultural wastes, and landfill or digester gases is currently only about 1% of the total U.S. output (3). However, recent projections show that production capacity could rise to 10% of the total U.S. output by the year 2010 (4), if more utilities take on cofiring strategies and if dedicated sources of energy crops are produced (5). The European Union (EU), after Kyoto, committed to reduce greenhouse gas emissions between 2008 and 2012 by 8% compared to 1990 levels. EU statistics show that currently about 2%–8% more CO<sub>2</sub> would be emitted within the EU without the current use of biomass (6). Estimates of remaining available solid biomass fuel potential indicate that further reduction of CO<sub>2</sub> emissions of 7%–28% could be achieved.

The global inventory of greenhouse gas emissions remains a serious problem since many countries have little incentive to reduce greenhouse gas emissions. Treaties such as that at Kyoto will hopefully create incentives. In the Netherlands, an additional incentive for the use of biomass wastes is the governmental policy aimed at a strong increase in renewable energy use (10% of the primary energy consumption in 2020, 4% from biomass and biomass wastes). Cofiring biomass and biomass waste streams with fossil fuels in large-scale power plants is considered to be an attractive option, since it benefits from the economy of scale and can potentially be realized at a relatively low investment cost (7). In the United States, it is perceived that more utilities will follow suit as in Europe and develop more use of biomass, which could have a significant impact on the global greenhouse gas pool.

Biomass types available for use as a cofiring fuel with coal in pc-fired boilers fall into two major categories: biomass wastes and biomass energy crops. Waste products include wood wastes such as wooden pallets, telephone poles, sawdust, and manufacturing scraps and municipal solid wastes or sludges. Agricultural wastes may include peach pits, rice hulls, and straws of wheat, alfalfa, rape, timothy, and barley. Energy crops include fast-growing switchgrass and hybrid trees such as poplar and willow. European research into direct firing and cofiring biomass with coal for power generation has been fairly

extensive with various agricultural biomass fuels such as wheat straw and wood waste product fuels (8–13). In the United States, research has focused primarily on cofiring arrangements for wood (14–21), and more localized agricultural waste biomass fuels have been studied less intensely (22–26). Figure 1 shows the types of biomass that could be expected to be available for power production in various regions of the United States. A recent synopsis of biomass for energy production, written by European researchers, discussed issues and barriers to using biomass such as wood for energy production (27). In Europe, biomass has been implemented for energy production much more so than in the United States. Biomass combustion is summarized as having the following impacts: it is excellent at reducing greenhouse gases, decreases  $\text{NO}_x$ , destroys polychlorinated biphenyls, decreases smog, increases volatile organic compounds (greatly dependent upon combustion process), decreases  $\text{CO}$ , stimulates landscape and forest conservation, and reduces soil erosion if the wood source is from dedicated resources such as tree farms (27, 28). Blending of this supplemental fuel would hopefully lower coal fuel costs (28) and provide a service to the community surrounding the power plant by creating business opportunities and economic development and by posing a solution to a potential biowaste disposal problem from tree harvesting.

Biomass utilization by conventional coal-fired utilities will create some technical challenges. Design limitations of conventional pc-fired boilers may also preclude the use of biomass beyond certain weight fractions of total fuel feed. Such limitations may include physical processing of the biomass for proper injection or feeding into the boiler. Other limitations include fireside performance of the biomass, including its impact on flame stability, boiler heat exchanger surface fouling or slagging, and corrosion. With respect to processing and feeding biomass, various utilities in Europe and the United States have either developed size-reducing methods that work for injecting the usually more fibrous and pliable biomass fuel into the boiler or, in many cases, separate injection ports have been installed (8–9). Ash deposition and boiler tube corrosion can be an issue because biomass can contain considerable alkali and alkaline-earth elements

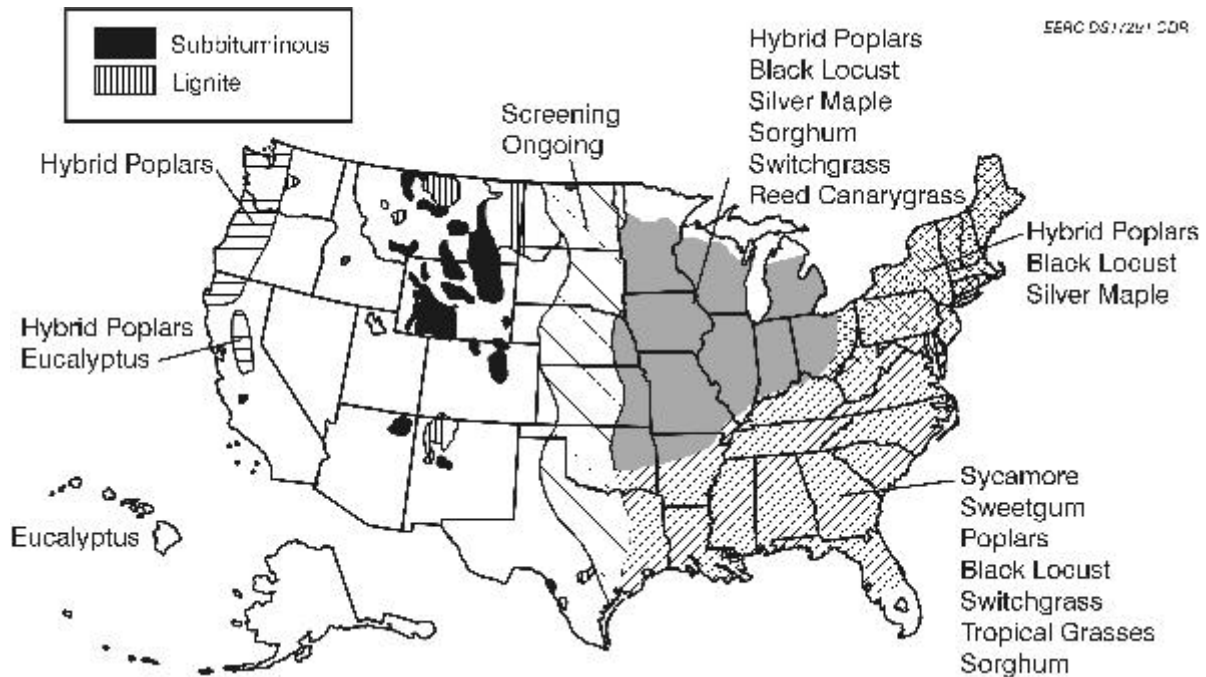


Figure 1. Biomass availability by region.

and chlorine which, when mixed with other gas components derived from coal such as sulfur compounds, promote a different array of vapor and fine particulate deposition in a coal-fired boiler (8–10, 13, 24). Biomass can also contain organically deposited minerals such as amorphous silica phytoliths (29) which are difficult to characterize with standard coal analysis methods and which also behave differently than mineral silica forms such as quartz in coal.

In most U.S. locations, the availability of biomass as a fuel feedstock for a pc-fired system is not reliable beyond 20% of what is a normal firing rate for coal. Cofiring biomass up to 20%, therefore, is a practical application for incorporating a renewable energy fuel into the pc-fired power plant for electrical generation.

By contrast, in Austria the main focus on biomass combustion is in hot-water-producing combustion plants for district heating purposes. These units are mainly grate fired, and the dominant biomass fuel is bark. However, other biomass fuels such as waste wood and agricultural residues such as straw are used as well. Because of the small scale of these plants (typically 3–10 MW) flue gas particle control devices represent a major investment cost for these plants. However, because of increased awareness of the hazardous effects of particle emissions, the regulatory limits of particulate emissions are being steadily decreased for these plants, making installation of expensive particle control units a necessity.

The research group at the Technical University of Graz is continuously collecting experimental data from Austrian biomass combustion plants, but by being able to model factors influencing the particle-size distribution during biomass combustion, new ideas and methods can be qualitatively tested prior to expensive full-scale test runs.

Part of the research of this project involved a collaboration with Dr. Jonas Dahl of the Technical University of Graz, Austria, who worked in a postdoctoral position at the Energy & Environmental Research Center (EERC) for 9 months during the year 2000. The objective of Dr. Dahl's work was to investigate the possibility of modifying and using a computer code developed for predicting ash transformation in coal combustion to model fly ash and aerosol formation in biomass combustion processes.

## **GOAL AND OBJECTIVES**

The goal of this project was to perform fundamental scientific investigations related to biomass cofiring with coal for power production. Specific objectives to attain this goal included:

- Determining cost-effective processing strategies for feeding different biomass types into pc-fired systems.
- Refining characterization methods for biomass feedstocks, especially to develop new computer-controlled scanning electron microscopy (CCSEM) mineral categories and classification algorithms for minerals specific to biomass fuel and combustion ash; improve

SEM automation and classification of amorphous elongate silica grains; and collaborate with biologists to better characterize organically associated elements and silica phytoliths.

- Evaluating mechanisms of fouling and slagging deposit formation for biomass and biomass–coal blends.
- Assessing the particle-size and composition distribution for biomass and biomass–coal blend entrained ash by cofiring biomass fuels with two types of coals, both individually and as blends to evaluate the interactions of coal clays with K–Ca-rich silicates from biomass in high-temperature combustion regimes; to determine the role of phosphorus in the inner deposit layer; and to assess the particle-size and composition distribution for biomass and biomass–coal blend entrained ash, with special attention on alkali sulfates and chlorides and fine silica.
- Collaborating with an international research group on the modeling of fine particulate and aerosol generation during combustion of biomass and biomass–coal blends to investigate the possibility of modifying and using a computer code developed for predicting ash transformation in coal combustion to model fly ash and aerosol formation in biomass combustion processes.

## **EXPERIMENTAL**

### **Biomass Processing**

Wheat straw, alfalfa stems, hybrid poplar wood, and switchgrass were selected as candidate biomass materials for blending at a 20 wt% level with an Illinois bituminous coal and with a Montana subbituminous coal. Only the wheat straw, alfalfa stems, and hybrid poplar were selected for detailed analysis and combustion testing. These biomass fuels were selected because of the potentially large quantities available as cofiring fuels in the Midwest and because of the limited amount of analytical and combustion data.

In the early 1990s, the EERC investigated hybrid poplar for two applications: catalytic fluid-bed gasification to produce  $H_2$ –CO and hydrothermal (hot-water drying) conversion to produce a pumpable slurry fuel (30). In this current study, hybrid poplar was again considered for experimental work as a short-rotation intensive cultivation biomass fuel source for cofiring with coal.

With assistance from Professor Wendell Johnson of the University of Minnesota, Crookston, the EERC selected two hybrid poplar trees from a test plot located in Section 30 of Sundal Township in Norman County, Minnesota, near the city of Fertile, Minnesota. The trees were approximately 10 years of age and were growing on 3.7-m (12-foot) spaced rows with 1.2 m (4 feet) between trees within a row. This particular hybrid poplar was a *deltoides-nigra* (DN) clone variety having *Populus deltoides* (native Cottonwood) and *Populus nigra* heritage. The DN clone typically has one main stem, with small side branches. Local growing conditions were represented by a poorly drained, sandy,

loamy soil with a pH of about 8. These trees typically have a moisture content of 40 wt% or greater and are considered very hardy and the most suitable of different tree varieties as a fuel source.

The trees were felled and delimbed with a bow saw, with the main stems cut to nominally 76-cm (30-in.) lengths using a chainsaw. All cut main stems and branches (with leaves) were transported and stored in 208-L (55-gallon) barrels. Approximately 261 kg (575 lb) of main stem and 79 kg (175 lb) of branches were recovered.

The wheat straw and alfalfa were procured in bale form from local farms. The alfalfa was deleafed prior to shredding in order to obtain a material consistent with the stem by-product resulting from the processing used to obtain high-protein leaf pellets for animal feed. The alfalfa was air-dried and manually agitated on a mesh screen with 1.3-cm (½-in.)-square openings to separate the dried leaves from the stems. The leaves and short stems passed the screen as refuse; the longer stems were retained as product. Size reduction of wheat straw, alfalfa stems, and hybrid poplar for combustion testing was performed using a laboratory-scale Nelmor knife shredder (Model G810P1). The shredder was equipped with changeable round-opening grinding screens of 6.3, 3.2, and 1.6 mm (¼, ⅛, and 1/16 in.), two replaceable stationary knives, and three replaceable knives on the rotor. The knife shredder has proven suitable for size reduction of other low-density materials such as wood chips and shavings, refuse-derived fuel, and plastic. Preliminary shredding tests were performed on wheat straw using each of the three grinding screens. The 1.6-mm (1/16-in.) screen was determined to produce suitably sized material for combustion testing.

Bulk densities were determined for whole bales of wheat straw and alfalfa, wheat straw and alfalfa with leaves, alfalfa stems and hybrid poplar, and 1.6-mm (1/16-in.) shredded wheat straw, alfalfa stems, and hybrid poplar. Whole-bale bulk density was determined from bale dimensions and weight. The bulk density of wheat straw and alfalfa (with leaves), alfalfa stems, and hybrid poplar was determined for a 0.028-cubic-meter (1-cubic-foot) volume of loosely packed material, and the bulk density of 1.6-mm (1/16-in.) shredded wheat straw, alfalfa stems, and hybrid poplar was determined by a similar procedure using a smaller 70-mL container.

### **Combustion Testing**

Combustion testing of the biomass and coal–biomass blends was performed in the conversion and environmental process simulator (CEPS). The CEPS, shown in Figure 2, is an intermediate-scale downfired combustor that effectively operates firing 0.5–2.0 kg (1–5 lb) of fuel per hour (31, 32). The CEPS is an extremely versatile system that simulates conditions of both the radiant and convective sections of a full-scale utility boiler and can generate realistic combustion test results for a variety of fuels and combustion conditions. The intermediate size of the system and its relatively simple operation ensure adequate quantities of actual flue gas and ash for analysis in a relatively short period of time. Control of gas temperatures and composition throughout the CEPS furnace is possible, independent of the heat capacity of the fuel, because of the external heating capacity of the CEPS. Heating elements line the main furnace, convective pass section, and baghouse chambers. Temperatures of the flue gas (approximately 0.085–0.200 standard m<sup>3</sup>/min [3–7 scfm]) can reach a maximum of 1500°C (2732°F) in the radiant section and can be maintained at 500–1200°C (932–2200°F) in the convective pass section and 120–250°C (248–482°F) in the baghouse.

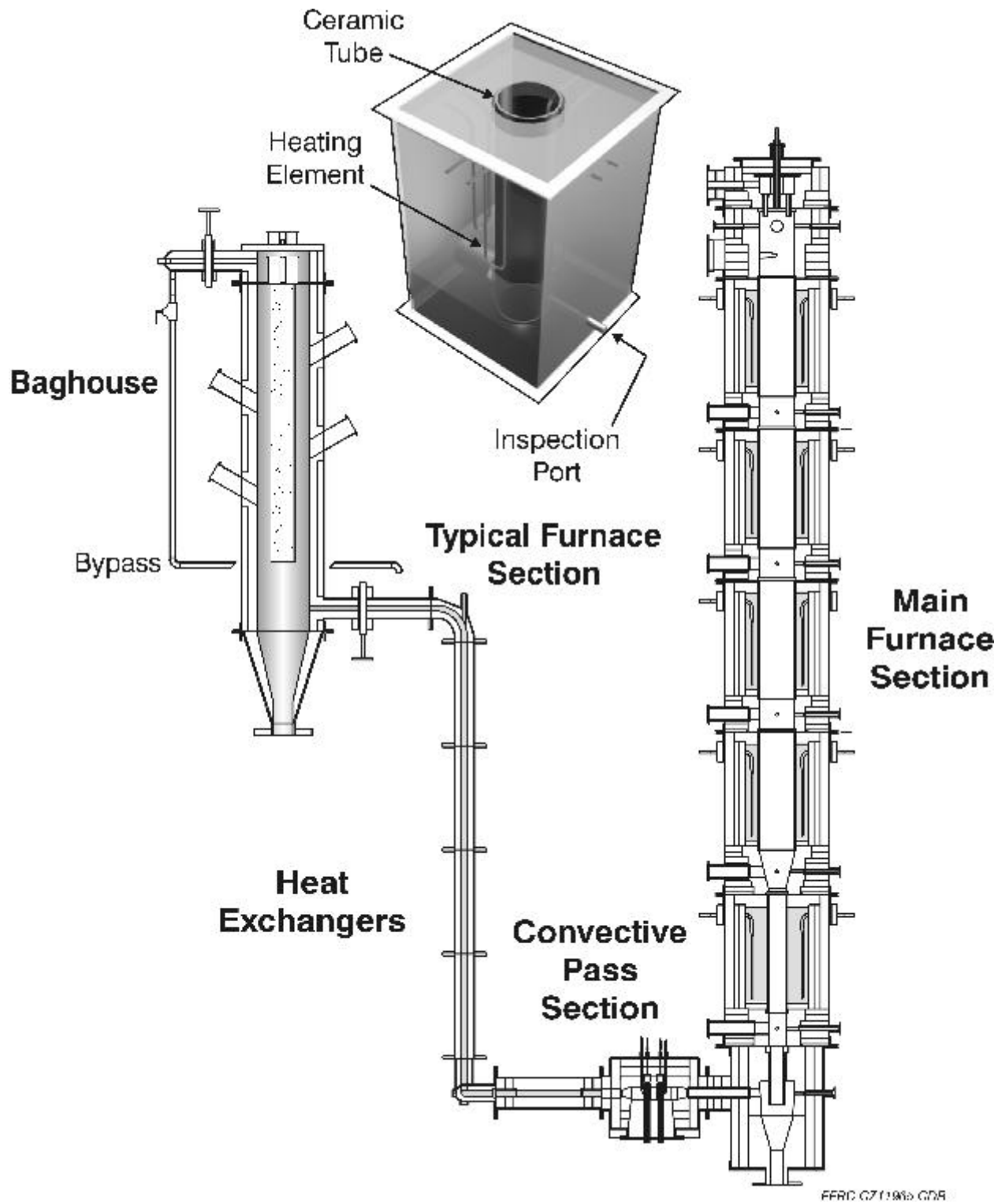


Figure 2. Conversion and environmental process simulator.

There is ample access for sampling, observation, and optical diagnostics through access ports located throughout the CEPS. A personal computer displays and records temperatures, gas flows, feed rates, and flue gas compositions. Flue gas ( $O_2$ ,  $CO_2$ ,  $CO$ ,  $SO_2$ , and  $NO_x$ ) compositions are sampled from ports in the radiant section and after the collection device.

Ash deposits were grown under fouling conditions at a gas temperature of  $1200^\circ C$  ( $2200^\circ F$ ), with a probe surface temperature of  $540^\circ C$  ( $1004^\circ F$ ). Estimates of deposition rates were obtained and the deposits removed for subsequent determination of deposit strength and chemical analysis. Entrained ash samples were also collected for analysis with a three-stage multicyclone and on a bulk filter, along with ash samples obtained from the convective pass and baghouse. Three deposits were obtained for the 80%–20% Illinois No. 6–wheat straw blends, with a second deposit grown under simulated slagging conditions at a gas temperature of  $1500^\circ C$  ( $2732^\circ F$ ) on a cooled slagging probe with a surface temperature of  $370^\circ C$  ( $698^\circ F$ ) and a third low-temperature fouling deposit collected at a gas temperature of  $600^\circ C$  ( $1112^\circ F$ ) in the CEPS convective pass.

It is known that biomass combustion typically results in a large submicron particle fraction because of condensation of volatilized minerals, primarily potassium and sodium sulfates and chlorides. The amount of submicron particulate generated is an important issue. As part of the CEPS combustion testing with hybrid poplar, Absaloka coal, and an 80%–20% Absaloka–hybrid poplar blend, on-line measurements were made using an aerodynamic particle sizer (APS) and a scanning mobility particle sizer (SMPS) to characterize the fine submicron particulates produced.

### **Fuel, Fly Ash, and Ash Deposit Analyses**

Biomass and coal materials were analyzed using conventional and advanced techniques. Fuels were analyzed for proximate–ultimate and heating values, and mineral oxides in the fuels were determined using x-ray fluorescence (XRF). The fuels were analyzed using chemical fractionation (CHF) and CCSEM to determine near-total inorganic quantification. Advanced analysis methods have previously been used along with conventional analyses to successfully predict fouling and slagging behavior of coals (33, 34). Chemical fractionation is used to quantitatively determine the modes of occurrence of the inorganic elements in coal, based on the extractability of the elements in solutions of water, 1 molar ammonium acetate, and 1 molar hydrochloric acid (35). The filtered residues or solvent are analyzed after each leaching using XRF to determine the percentage of each element remaining. The nonextractable elements are associated in the coal as silicates, aluminosilicates, sulfides, and insoluble oxides.

CCSEM determines the size and composition of mineral grains in the fuels (36, 37). The CCSEM system uses a computer to control the operation of the SEM in order to determine the size, quantity, distribution, and association of mineral grains and other particulate matter by analyzing the major chemical elements present in individual mineral grains  $>1 \mu m$  in size. The method is analogous to XRF analysis of the bulk coal ash. Mineral species present are inferred from the elemental chemistry of each mineral grain. CCSEM quantifies the different mineral species in a fuel fairly rigorously and also determines the size distribution of the minerals. Two fuels can have similar bulk elemental compositions, but have widely differing mineral contents. Image analysis is performed at the same time as the CCSEM data are collected

to determine whether each discrete mineral grain is locked within or liberated (i.e., included or excluded) from the fuel particles. Both the size and association of mineral matter can have a significant effect on subsequent ash deposition behavior. CCSEM output data, along with conventional analytical data, are used for predictive fouling and slagging models that have been developed (33, 34).

Chemical compositions of fly ash samples were determined by means of CCSEM analysis, and ash deposits were analyzed using a scanning electron microscopy point count (SEMPC) technique which quantifies the mineral and amorphous phases present in a deposit (38). SEMPC provides chemical analysis of points as small as 1 $\mu$ m in size. The system is automated and computer-controlled, which increases data manipulation and data storage capabilities. The SEMPC technique was developed at the EERC to systematically and quantitatively determine the distribution of phases in ash deposits and fly ash. Crystalline components are readily identified as minerals based on chemical composition and molar ratios. Amorphous components are classified as either derived phases or unclassified material. Derived phases resemble their coal mineral precursors. Unclassified material has no crystalline structure and shows no molar ratios that conform to mineral formulas stored in the SEMPC program. The SEMPC technique provides information on the degree of interaction and melting of the deposited ash components and the abundance of crystalline, amorphous, and unreacted ash particles. The data obtained from the technique are critical in identifying the components in ash deposits that are responsible for deposit growth and strength development. In addition, viscosity distribution profiles can be calculated for the amorphous or liquid phases using SEMPC data. This information provides insight into the propensity of a particular ash to form a strong deposit.

Work in this project involved making improvement to CCSEM and chemical fractionation. This work focused primarily on refining the classification and sizing schemes for the CCSEM mineral categorization procedure. Algorithms needed to be redefined to add biomass-specific minerals and biomass combustion ash minerals and phases. As part of this improvement, collaboration with biologists and a literature survey were undertaken to better understand the mode of occurrence of inorganic species in the biomass fuels being tested. Work was also done to better employ the chemical fractionation technique for biomass fuels.

## **RESULTS**

Results are presented according to selection and processing results, analytical technique development and fuel characterization, and fundamental fuel quality impacts on ash formation and deposition.

### **Background on Processing of Biomass Fuel Types**

A literature search was performed to identify 1) information on the types of inorganic structures present in biomass as well as the effects of these structures on cofiring of biomass with coal; 2) the effects of harvesting, transport, storage, and processing on biomass quality; 3) equipment used to prepare and inject the biomass into a pc-fired boiler; and 4) difficulties associated with cofiring biomass with coal. The results of the literature search are summarized in the following subsections, while a bibliography of the literature found during the search is organized by subject and presented in Appendix A.

## **The Effects of Plant Cell Chemistry on Cofiring Biomass with Coal**

Several mineral elements are essential for plant growth, including nitrogen, phosphorus, potassium, calcium, magnesium, sulfur, boron, chlorine, iron, manganese, zinc, copper, molybdenum, and nickel. Beneficial mineral elements that promote plant growth but are not absolutely necessary for completion of the plant life cycle include silica, sodium, cobalt, and selenium (39). Many of these elements can cause difficulties during firing of coal or biomass in utility boilers. Nitrogen in the biomass can increase NO<sub>x</sub> levels, depending on the nitrogen content and the stoichiometry of the system. Silicon, potassium, chlorine, and alkali metals can all contribute to ash deposition, while chlorine and alkali metals can also corrode the boiler system (40). Herbaceous biomass contains stomata on the undersurface of leaves as well as on the stems. The stomata are the main pathway for water loss from leaves and for carbon dioxide uptake by the leaves. Potassium is vital for cell membrane excitability. It helps the stomata serve as conduits for water and carbon dioxide. The relative enrichment of potassium in the stomata increases the availability of organically bound potassium in a vaporized form during combustion, thereby increasing the likelihood of fouling and slagging problems (41).

### ***Introduction***

Mineral uptake and storage by plants commonly considered for biomass cofiring were investigated. Information gathered pertained to plants in general and to biomass species of wheat (*Triticum aestivum*), rice (*Oryza sativa*), switchgrass (*Panicum virgatum*), hybrid poplar (*Populus tremuloides*), and alfalfa (*Medicago sativa*). These specific crops were chosen because they are relatively fast growing, are readily available or can be mass-produced, and provide large quantities of material for cofiring. A list of literature references examined is included in Appendix B and a glossary of biological terms is included as Appendix C.

For this summary, uptake and deposition factors have been divided into intrinsic properties and extrinsic influences. Intrinsic factors include a discussion of plant physiology, element activity and deposition, and silica body formation. Based on the assumption that the herbaceous biomass will be limited to plant parts left over after marketable materials have been removed, elemental deposition involving the reproductive parts of the plant will not be discussed. The reader should be aware, however, that there is elemental deposition specific to reproductive parts and seed production.

### ***Intrinsic Properties of Biomass***

Intrinsic properties are internal factors that may affect plant growth, uptake of nutrients, and mineral deposition in the biomass of interest. A brief discussion of plant physiology introduces how plants absorb nutrients. Elements essential to plants and those of interest from the perspective of biomass cofiring are provided as background knowledge for the rest of the report. Information specific to genera of biomass material is presented under each plant type, providing detailed information on the effects of elements found within the plant. Information on the development of silica bodies within plants is presented separately because of its relevance across several plant types.

## *Plant Physiology*

Plants possess two unique fundamental properties: the ability to fix carbon dioxide by photosynthesis and the production of a rigid cell wall. The former gives plants an internal source of carbon compounds to use for growth and in metabolism, and the latter provides a protective home for the cell within (42). All plants of interest for biomass cofiring are angiosperms—vascular seed-bearing fruiting plants. They include both monocots (wheat, switchgrass, and rice) and dicots (hybrid poplar and alfalfa). A cotyledon is the seed leaf within the embryo of a seed. If one leaf is present, the plant is a monocot; if there are two leaves present, the plant is a dicot.

A young flowering plant possesses three main types of organs—leaves, stems, and roots. Each organ is made up of three tissues—vascular, dermal, and ground. Vascular tissues move water and solutes between organs and provide mechanical support; the phloem transports organic solutes, and the xylem carries water and dissolved ions from the roots throughout the plant. Interconnection of all plant parts is achieved through the network of vascular bundles containing the phloem and xylem. Dermal tissue is the plant's protective outer covering in contact with its environment. In roots, it facilitates water and ion uptake. In leaves and stems, it regulates gas exchange. Cells of the epidermis are modified to form stomata—openings in the epidermis mainly on the lower surface of the leaf. They comprise a pore and two guard cells and regulate gas exchange in the plant by adjusting the diameter of the pore. Stomata are distributed in a specific pattern within each plant species' epidermis. Ground tissue is the packing and supportive tissue and makes up the bulk of the plant. Ground tissue comprises three cell types, including collenchyma, living cells that provide mechanical support; sclerenchyma, dead cells with strengthening and supporting functions; and parenchyma, which function in food manufacture and storage. Examples of parenchyma are the photosynthetic cells of the leaf and stem, and the meristematic cells of shoots and roots provide new cells required for growth (42).

Higher plants consist of large numbers of cells held together by the rigid cell walls that surround them. The size and shape of the cell wall depends on the specialized function of the cell it contains. However, the underlying structure of all cell walls comprises tough fibers of cellulose embedded in a cross-linked matrix of polysaccharides. The presence of cell walls makes possible turgor pressure, the driving force for cell expansion during growth and the mechanism for mechanical rigidity of living plant tissues. Turgor pressure is caused by the osmotic imbalance between its intracellular and extracellular fluids (42). A schematic diagram of a mesophyll cell including the cell wall is illustrated in Figure 3. The plasmodesmata penetrating the cell walls connect the cytoplasm of cells in the plant. In addition to the components typical to all eukaryotic cells, plant cells contain plastids, of which chloroplasts are the most well known member, and vacuoles (42).

Vacuoles are an important component of the cell for several reasons. As the plant cell expands, provacuoles fuse to form the central vacuole, which can occupy up to 90% of the cell volume. Its

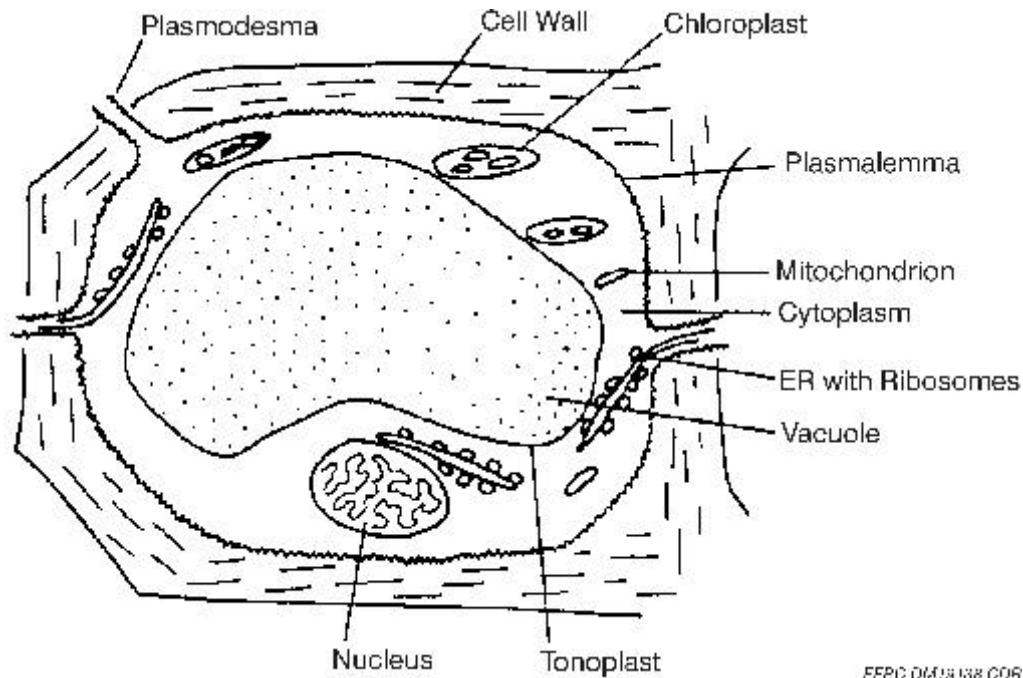


Figure 3. Simplified scheme of a mesophyll cell (43).

role is to increase cell size (ten- to twentyfold), and it accomplishes this task through water uptake, allowing the cell cytoplasm to maintain a narrow range of pH and solute concentrations. Other functions of the vacuole include:

1. Storage of compounds (e.g., sugars, polysaccharides, and proteins) needed for metabolic processes.
2. Toxic avoidance, a micro-kidney filtering and sequestering heavy metals and potentially toxic ions from the cytosol.
3. pH and ionic homeostasis—proton pumps on the tonoplast (vacuole membrane) regulate the pH and ionic content of the cytosol by pumping excess protons and ions into the vacuole against gradients.
4. Defense against microbial pathogens and herbivores.
5. Pigmentation.
6. Lysosomes (44).

The vacuole is the key to turgor pressure in plant cells, because the major increase in cell volume comes by enlargement of the vacuole rather than of the cytoplasm. In order to maintain the turgor pressure

required for continued cell expansion, solutes must be actively accumulated in the growing vacuole to maintain its osmolarity (42). Vacuolar sap contains the bulk of the cell's  $K^+$ ,  $Ca^{2+}$ , sugar, organic acids, and other solutes (44). The connection between mineral deposition and the first three roles of the vacuole listed is discussed below.

Photosynthetic cells contain chloroplasts and are sources of carbon-containing compounds and require light. Photosynthesis requires close regulation of humidity and carbon dioxide supply performed by the turgor in guard cells in the stomatal pores. Absorptive cells take up mineral nutrients from the environment, generally in the soil. They require a large surface area provided by the roots and membrane transport systems (42).

Plant development and maintenance depend on the chemical substance absorbed and transported via the roots (45). Nutrient supply to the roots is dependent on nutrient concentrations in the soil solution, soil moisture status (described in the Extrinsic Factors section), the plants' absorption capacity, and the nature of the nutrients. Nutrients move to plant roots by mass flow, diffusion, and root interception (43). Mass flow is the passive transport of nutrients in soil water by plants. The amount of nutrients is dependent upon the concentration of nutrients in solution and the rate of transport to and into the roots. Diffusion is defined as the movement of molecules from a region of high concentration to a region of low concentration. Diffusion develops when the supply of nutrients to the root vicinity is not sufficient to satisfy the plant demand by mass flow and root interception. The roots develop a concentration gradient, and nutrients then move by diffusion. Root interception occurs as the result of root growth in the soil. The roots push soil aside, and root surfaces come into contact with the particles and nutrients found in soil. The actual interception depends on specific variables such as soil volume occupied by roots, root morphology, and the concentration of nutrients in the root-occupied soil volume.

Peel found that the bulk of solutes, which are transported across the root system, are on their way to the leaves and other aerial portions of the plant (46). Nutrient uptake, as illustrated in the schematic diagram in Figure 4, occurs after ions have reached the plant roots and are absorbed by the root hairs. Ions enter the root cells; move through the epidermis, cortex, and endodermis; and are excreted into xylem vessels. Through the xylem, the ions are translocated to the shoot. Figure 5 shows a cross section of a typical root through which the ion uptake path can be traced.

Ion transport across all biological membranes is highly selective, which allows electrochemical potentials to be generated. These electrochemical potentials depend on the potassium gradient, which remains active for long periods of time. Such gradients are necessary for long-term cell functions such as nutrition, elongation, turgor, and water regulation (43).

### ***Elements of Interest***

Dr. B.J. Alloway states that there are three criteria for establishing whether or not a trace element is essential for the healthy growth of plants and/or animals: 1) The organism can neither grow nor complete its life cycle without an adequate supply of the element, 2) the element cannot be wholly replaced by any other element, and 3) the element has a direct influence on the organism

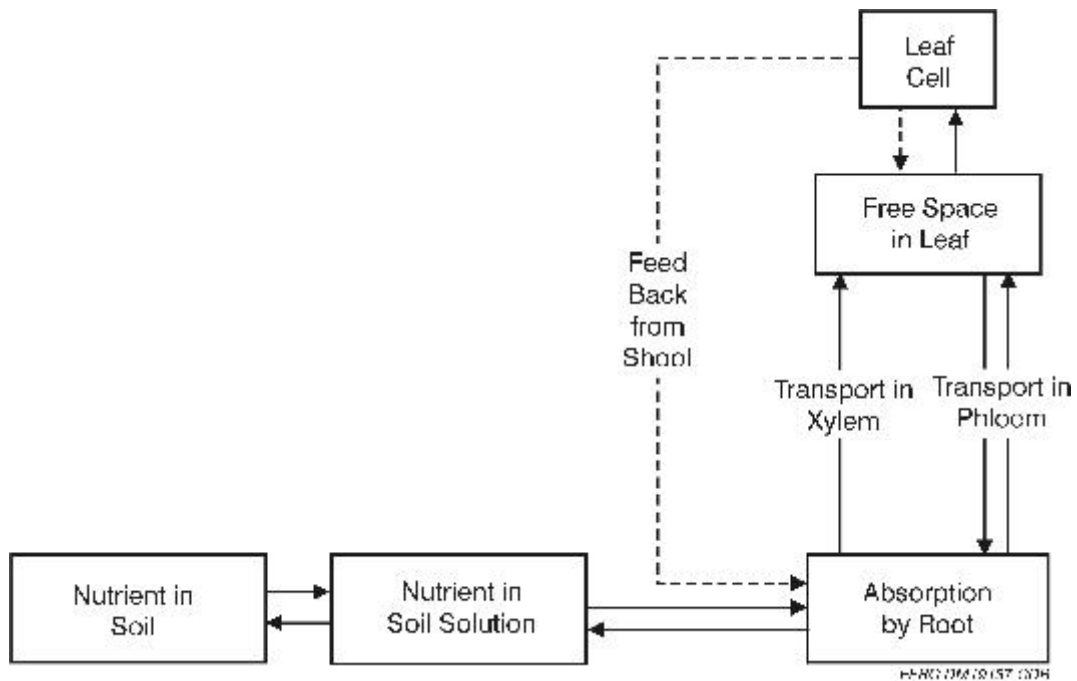


Figure 4. Process of nutrient uptake in soil-plant system (43).

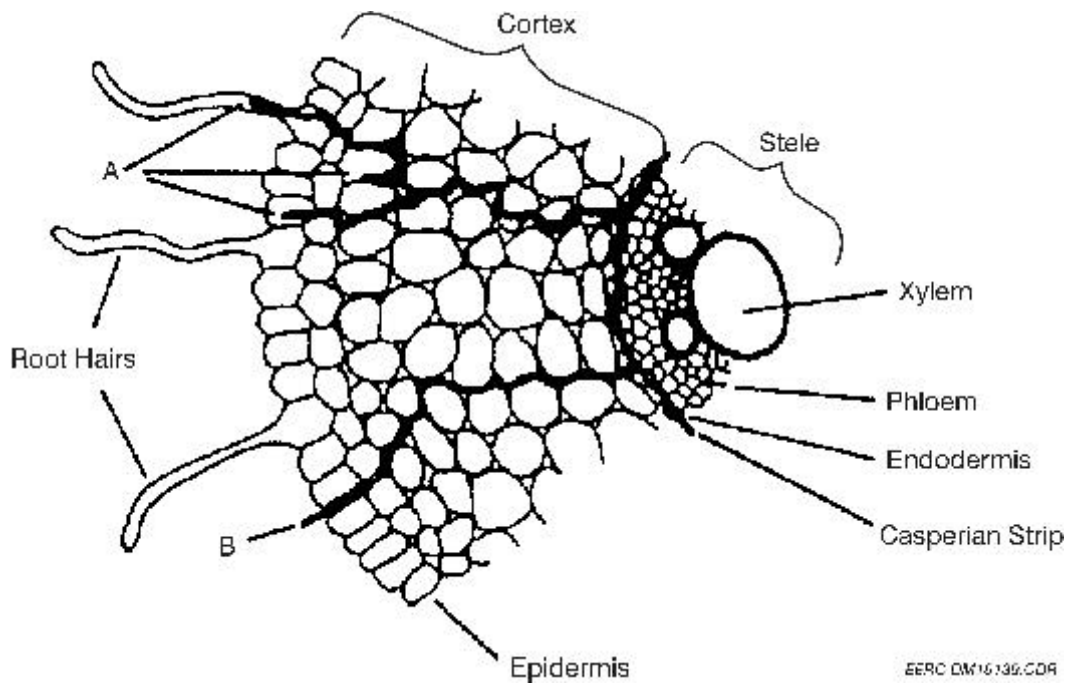


Figure 5. Transverse section of corn root showing the symplastic (A) and apoplastic (B) pathways of ion transport across the root (43).

There are 16 essential elements for plant growth: C, H, O, N, P, K, Ca, Mg, S, Zn, Cu, Fe, Mn, B, Mo, and Cl. The first three (C, H, O) make up about 95% of plant dry weight and are supplied to plants by air and water. Chlorine is also supplied through the atmosphere (43). Epstein states that K and Ca are the fourth and fifth most abundant elements in plants (48). Dr. Edward Deckard of North Dakota State University states that essential elements are found throughout the plant, that there is no specific place where they are deposited, and that essential elements must to be readily accessible where they are to be used (49).

Table 1 lists the elements of interest and includes the chemical form, principal form of uptake, and brief function description of each element. Table 2 lists structural examples of the elements in plants.

### *Elemental Occurrence in Biomass*

The ash composition of alfalfa, hybrid poplar, rice straw, switchgrass, and wheat straw and stem, as reported in the Phyllis database (50), is shown in Table 3. These data indicate that silica is the major ash constituent by weight percentage in rice straw, switchgrass, and wheat straw and stem. Calcium has the highest weight percentage for hybrid poplar and alfalfa stems. These data address only the elemental content of the ash, not the distribution or associations of elements in the living or dry plant tissues. Following is information specific to biomass families and genera. Information on mineral deposition for plants in general was obtained during the course of biomass investigation. The relevancy of this information warrants its inclusion in the discussion, especially in light of the limited data specific to genera of interest.

TABLE 1

Typical Ash Composition of Alfalfa, Hybrid Poplar, Rice Straw, Switchgrass, Wheat Straw, and Wheat Stems

Elemental Oxide, wt%	Alfalfa Stems	Hybrid Poplar	Rice Straw	Switchgrass	Wheat Straw	Wheat Stem
CO <sub>2</sub>	14.8	8.2	ND <sup>1</sup>	ND	ND	ND
SO <sub>3</sub>	1.9	2	ND	1.1	ND	ND
Cl	ND	ND	ND	ND	ND	ND
P <sub>2</sub> O <sub>5</sub>	7.6	1.3	1.7	3.6	1.3	2.8
SiO <sub>2</sub>	5.8	5.9	80.7	61.2	65.5	57.8
Fe <sub>2</sub> O <sub>3</sub>	0.3	1.4	0.9	0.8	1	0.6
Al <sub>2</sub> O <sub>3</sub>	0.1	0.8	1.5	0.6	1.9	0.4
CaO	18.3	49.9	2	12.1	2.8	7.6
MgO	10.4	18.4	2.1	5.4	2.6	1.7
Na <sub>2</sub> O	1.1	0.1	0.7	0.4	1.9	0.7
K <sub>2</sub> O	28.1	9.6	5.7	7.6	11.4	11.7
TiO <sub>2</sub>	0	0.3	ND	0.4	ND	ND

<sup>1</sup> Not determined.

TABLE 2

Element Structures in Biomass			
Element	Chemical Symbol	Principal Form of Uptake	Function
Carbon	C	CO <sub>2</sub>	Basic molecular component of carbohydrates, proteins, lipids, and nucleic acids.
Hydrogen	H	H <sub>2</sub> O	Plays a central role in plant metabolism; important in ionic balance; main reducing agent; has a key role in energy relations of cells.
Oxygen	O	H <sub>2</sub> O, O <sub>2</sub>	Occurs in organic compounds of living organisms.
Nitrogen	N	NH <sub>4</sub> <sup>+</sup> , NO <sub>3</sub> <sup>-</sup>	Component of many organic compounds, ranging from proteins to nucleic acids.
Phosphorus	P	H <sub>2</sub> PO <sub>4</sub> <sup>-</sup> , HPO <sub>4</sub> <sup>2-</sup>	Essential for all plant growth; plays central role in plants in energy transfer and protein metabolism.
Potassium	K	KCl, NaCl	Aids in osmotic and ionic regulation; functions as a cofactor or activator of many enzymes of carbohydrate and protein metabolism; the major ion inside every living plant and animal cell.
Calcium	Ca	Ca <sup>2+</sup>	Is required for structural, osmotic, and signaling purposes.
Magnesium	Mg	Mg <sup>2+</sup>	Component of chlorophyll; a cofactor for many enzymatic reactions.
Sulfur	S	SO <sub>4</sub> <sup>2-</sup> , SO <sub>2</sub>	Involved in plant cell energetics.
Iron	Fe	Fe <sup>2+</sup> , Fe <sup>3+</sup>	Involved in N fixation, photosynthesis, and electron transfer; plant needs continuous supply to maintain proper growth.
Manganese	Mn	Mn <sup>2+</sup>	Involved in photosynthesis; a component of enzymes arginase and phosphotransferase.
Boron	B	H <sub>3</sub> BO <sub>3</sub>	Essential for normal plant growth.
Zinc	Zn	Zn <sup>2+</sup>	Essential component of several dehydrogenases, proteinases, and peptidases.
Copper	Cu	Cu <sup>2+</sup> Cu(H <sub>2</sub> O) <sub>6</sub> <sup>2+</sup> , Cu(OH) <sub>2</sub>	Constituent of several enzymes; forms other compounds; relatively immobile element; important in plants' reproductive growth stage.
Molybdenum	Mo	MoO <sub>4</sub> <sup>2-</sup>	Required for assimilation of N in plants; an essential component of N <sub>2</sub> fixation enzymes.
Chlorine	Cl	KCl	Essential for photosynthesis; functions in osmoregulation of plants growing on saline soils.
Silica	Si	H <sub>2</sub> SiO <sub>3</sub> , Si(OH) <sub>4</sub>	A structural component of some plant species; plays a role in disease resistance in crop plants.
Sodium	Na	NaCl	Cell wall structure component.
Aluminum	Al	Al <sup>3+</sup>	Toxicity of Al decreases the uptake and distribution of other elements.
Selenium	Se	SeO <sub>4</sub> <sup>2-</sup>	Forms seleno–amino acids, selenosysteine, and selenomethionine; translocated from roots to all parts of the plant including the seed; found in newly formed leaves of alfalfa, rather than older leaves.

TABLE 3

Elements in Biomass				
Element	Chemical Symbol	Principal Form of Uptake	Structural Examples in Plants	Dried Form
Carbon	C	CO <sub>2</sub>	CO <sub>2</sub> , CH <sub>3</sub> -	
Hydrogen	H	H <sub>2</sub> O	OH <sup>?</sup> , H <sup>+</sup> , NH <sub>4</sub> OH	
Oxygen	O	H <sub>2</sub> O, O <sub>2</sub>	OH <sup>?</sup>	
Nitrogen	N	NH <sub>4</sub> <sup>+</sup> , NO <sub>3</sub> <sup>?</sup>	NO <sub>2</sub> <sup>?</sup> , NO <sub>3</sub> <sup>?</sup> , NH <sub>4</sub> <sup>+</sup>	
Phosphorus	P	H <sub>2</sub> PO <sub>4</sub> <sup>?</sup> , HPO <sub>4</sub> <sup>2?</sup>	P, ADP, ATP, R(PO <sub>4</sub> ) <sub>2</sub>	
Potassium	K	KCl	K <sup>+</sup>	
Calcium	Ca	Ca <sup>2+</sup>	CaC <sub>2</sub> O <sub>4</sub> , Ca <sup>2+</sup>	
Magnesium	Mg	Mg <sup>2+</sup>	Mg <sup>2+</sup>	
Sulfur	S	SO <sub>4</sub> <sup>2?</sup> , SO <sub>2</sub>	SO <sub>4</sub> <sup>2?</sup> , S	
Iron	Fe	Fe <sup>2+</sup> , Fe <sup>3+</sup>	Fe <sup>2+</sup>	
Manganese	Mn	Mn <sup>2+</sup>	Mn <sup>2+</sup>	
Boron	B	H <sub>3</sub> BO <sub>3</sub>	ND <sup>1</sup>	
Zinc	Zn	Zn <sup>2+</sup>	Zn <sup>2+</sup>	
Copper	Cu	Cu <sup>2+</sup> Cu(H <sub>2</sub> O) <sub>6</sub> <sup>2+</sup> , Cu(OH) <sub>2</sub>	Cu <sup>2+</sup> Cu(H <sub>2</sub> O) <sub>6</sub> <sup>2+</sup> , Cu(OH) <sub>2</sub>	
Molybdenum	Mo	MoO <sub>2</sub> <sup>?</sup>	MoO <sub>2</sub> <sup>?</sup>	
Chlorine	Cl	KCl, Cl <sup>?</sup>	Cl-	
Silica	Si	H <sub>2</sub> SiO <sub>3</sub> , Si(OH) <sub>4</sub>	SiO <sub>2</sub> ?nH <sub>2</sub> O	SiO <sub>2</sub>
Sodium	Na	NaCl	NaCl	
Aluminum	Al	Al <sup>3+</sup>	Al <sup>3+</sup>	
Selenium	Se	SeO <sub>4</sub> <sup>?</sup>	Seleno-amino acids	

<sup>1</sup> Not detected.

#### *Potassium, Calcium, Phosphorus, Chlorine, and Sodium*

Potassium is present mainly in the cytoplasm of cells because it is important in metabolism, charge balance, and sugar transport. Some K may be stored in the vacuole, depending on K supply to the plant. Very little K is found in structural components (51). Guard cell vacuoles accumulate large amounts of K (up to 500 mmol/L) during turgor regulation (44).

Calcium is generally used or sequestered locally in plant tissues. Most Ca is found in cell walls and the vacuole. It is believed that chelated Ca in the cell walls is used for strength by cross-linking the carboxyl groups of pectic polymers. Its concentration has been measured at 10–100  $\mu$ m. Most plant physiologists believe that the outer surface of the plasma membrane requires high Ca concentrations to maintain structural and functional integrity. In the vacuole, Ca is mostly associated with oxalic, phosphoric, and phytic acid salts. Ca<sup>2+</sup> concentrations in the vacuole have been measured at mM levels (48), whereas cytosolic Ca<sup>2+</sup> concentration is  $1 \times 10^{27}$  mol/L (44).

A constant supply of  $\text{Ca}^{2+}$  around 1–10 mM for the whole plant is required for normal growth and development. Removal of Ca supply yields rapid death to the apical meristem cells and cessation of plant growth. Although this phenomenon is not well understood, Gilroy and coworkers hypothesize that, “the low mobility of Ca within the plant body must be at least partially responsible” (48). This is attributed to the low  $\text{Ca}^{2+}$  concentration in the cytosol of transporting cells (100–200 nM).

One quantitative reference to P was located in Taiz who reported pyrophosphate concentration in the cytosol at 0.1–0.25 mM (44).

Chlorine is found in more than 130 chlorinated compounds in plants, is required for photosystem II, and is used as an osmoticum to regulate stomata and turgor pressure. It may be important in suppressing certain diseases, such as leaf spot. Optimal Cl concentrations are only in the range of 0.2 to 0.4 mg Cl per g of dry tissue, whereas fertilizers (like KCl), irrigation water, and soil Cl increase concentrations in most herbaceous crops by 10- to 100-fold and most of this extra Cl is stored in vacuoles within living cells (51).

Plants have developed high selectivity regarding Na absorption, since it is relatively highly available in soils but is essential only in some C4 plants (like amaranth and lambsquarters, but not corn or sorghum) and is needed by some halophytes for osmotic control. Like Cl, Na accumulates in the vacuoles (51). Accumulation of sodium in the vacuole is one of way in which salt-tolerant plants avoid the negative effects of salinity. The other is secondary active transport of sodium out of the cell through a  $\text{Na}^+/\text{H}^+$  antiporter on the plasma membrane (44). Dr. Russelle also indicated that storage of these nutrients in the cell vacuole or cytoplasm indicates high availability for leaching (51).

### ***Wheat***

*Triticum aestivum*, a cereal grass in the Gramineae (also known as Poaceae) family, is one of the oldest and most important of the cereal crops. Nitrogen and phosphorus are two of the most important nutrients related to cereal production. Their availability strongly determines the rate of crop growth and the final grain yield, but also their relative contribution to grain dry matter (52). Cramer and Lewis studied the effect of ammonium and nitrate assimilation on the gas exchange characteristics of the roots of wheat and maize. They found that the ammonium-treated plants had higher shoot–root ratios of N, and root oxygen consumption was greater than that of nitrate-treated plants (53). It was also found that the uptake and partial assimilation of ammonium required more energy than the uptake, reduction, and assimilation of nitrate within the root (54).

Phosphorus has a low diffusion coefficient and is the least mobile of the major nutrients. In rapidly growing plants, the P influx is higher than the rate of nutrient transport towards the root surface, resulting in a depletion zone around the roots (55). And under conditions of decreasing P availability the phosphorus-absorbing root surface becomes more and more important (56). Clarke and coworkers, through a study of N and P uptake, found that N and P uptake declined with reduced water availability and that the greatest grain yield occurred for an irrigated crop (57). From 67% to 102% of total plant N and 64% to 100% of total plant P present at harvest had been accumulated by anthesis, and 59%–79% of total N and 75%–87% of total P present in vegetative tissues at anthesis were translocated to the grain. Also,

the proportion of total N and P in the leaf declined with plant age, while stem N increased to anthesis and stem P increased to ligule of last leaf visible before declining (57). Frank and coworkers found similar results of N and P concentrations decreasing in leaf and stem as plants developed morphologically (58).

Frank and coworkers studied the concentrations of carbohydrates, N, and P of spring wheat leaves and stem. They found that water-soluble carbohydrate concentrations were greater in stems than in leaves for all samples, with concentrations in stems increasing rapidly as plants developed, while concentrations of the leaf tissue changed only slightly as the plant developed. It was also stated in this paper that numerous reports have related grain yields to N and P concentration and the accumulation of nonstructural carbohydrates in leaves and stems of wheat as a source of reserves for translocation to developing grain (58).

Elliot and coworkers hypothesized four possible factors linked to P criteria decreasing with advancing plant age (59). Firstly, a higher functional P requirement, the amount of phosphorus needed for plants to function, is necessary for young plants than for older plants. There may be a link between the high P requirement for growth in the first few weeks of growth and the high rate of P absorption by young plants. Secondly, competition for P circulating within the plant intensifies substantially with the initiation and emergence of new tillers and reproductive organs. Thirdly, the size and dry weight of each leaf blade increases as plants age. The blade at higher insertions in the main culm would be larger, have a higher cellulose content, and be more lignified. As a result, the proportion of P is diminished by increased cellulose content and lignification of the leaf tissue. Fourthly, the difference in the spatial distribution of applied P fertilizer in phosphorus-deficient soils may influence acquisition of P for translocation from roots to shoots. Elliot also found that soil moisture stress did reduce concentrations of inorganic and total P in wheat (59).

Sulfur is found in plant cell energetics, meaning it is involved in extracellular–intracellular interactions. Sulfur is similar to P in that it has also been shown to decrease with increased plant age. Sulfur deficiency results in reduced yields and inferior grain quality (60). Goodroad and coworkers found that increased concentrations of N, Mg, Fe, and Cu coincided with increased S concentrations in the plant. Concentrations of Ca, Mn, and Zn decreased with the increase of S concentrations in the plant, but it seems these decreased concentrations were more consistent with the increased growth of the plant. The sulfur deficiencies appear first in young leaves, while older leaves remain green, suggesting that S is relatively immobile in mature leaves (61). Also, insoluble sulfur (S bonded to a protein) in mature leaves is immobile even under conditions of S deficiency. Mobility is enhanced by N deficiency. Sulphate stored in mesophyll vacuoles is also relatively immobile (61).

During generative growth, rain-fed wheat must provide N and S to developing grains from reserves accumulated in the vegetative tissues before anthesis, whereas irrigated generative wheat can acquire available mineral forms of N and S directly from the soil. Fitzgerald and coworkers also found that the S that plants acquire during generative growth is a major source of S for grain growth and arrests redistribution of endogenous sources of both soluble and insoluble S (62).

Calcium is a major essential nutrient for plants. Calcium ions are universal second messengers in plant and animal cells. They mediate various signaling pathways, from signal perception to gene expression (63).

Net  $\text{Ca}^{2+}$  uptake into the root is greatest at the apical zones, less than 5mm from the root tip.  $\text{Ca}^{2+}$  is required for structural roles, in the vacuole as a counter cation for inorganic and organic signaling purposes as a cytoplasmic secondary messenger. Calcium can accumulate considerably in mature tissues of the plant, due to the immobility of calcium in phloem. The growth of developing parts of the plant is dependent upon the concurrent uptake of calcium (64).

Calcium must be acquired by the root from the soil solution and delivered to the xylem at rates sufficient for shoot growth. In a cereal seedling, calcium needs to be translocated at rates of  $40 \text{ nmol h}^{-1} \text{ g}^{-1} \text{ f.wt. root}$  to maintain minimal shoot calcium content of 0.1% dry weight (64). The root is composed of many different cell types, each specialized to a specific task. White stated that it may be possible to predict the characteristics of Ca channels in certain cell types on the basis of their physiology (64). Calcium channels involved in supplying the shoot with calcium are expected to be located primarily in the plasma membrane of root endodermal cells as long as the pathway of Ca movement occurs through the root to the xylem.

One very important role of calcium is in the chilling resistance of plants to grow at low temperatures. It is thought to be initiated by Ca influx across the plasma membrane and mediated by the consequent increase in calcium. Rapid cooling of plant roots to low nonfreezing temperatures evokes an initial increase in plant calcium followed by its restoration (64).

Zinc is an essential component of several enzymes, such as dehydrogenases, proteinases, and peptidases (43). These enzymes will be found throughout the plant. Zinc is also found to have an effect on P accumulation in old leaves of wheat plants. Webb and Loneragan have opposed the idea that Zn deficiency enhanced P accumulation to toxic concentrations by enhancing the rate of P absorption. In leaves with adequate Zn concentration, they suggest that low Zn combined with high P in solution may enhance accumulation of P in old leaves to concentrations which are toxic, thereby inducing symptoms of P toxicity which have been mistakenly identified as symptoms of Zn deficiency (65). They found that mild Zn deficiency had only a transient effect in enhancing inorganic P ( $\text{P}_i$ ) absorption rate, and severe Zn deficiency substantially depressed  $\text{P}_i$  absorption. Zinc deficiency enhanced P concentrations to toxic levels in old leaves through cumulative effects (65).

Aluminum is absorbed by plant material, although the actual necessity of Al is still unclear. Aluminum toxicity affects the uptake of essential nutrients. The presence of Al in the nutrient solution reduced the dry weight of all cultivars tested in the research of Mugwira and coworkers. They found that Al increased concentrations of P and K in the roots and K in the tops of most cultivars, while it reduced concentrations of Ca, Mg, and P in tops of wheat (66). Johnson and Jackson focused on the effect Al has on the uptake of Ca. They studied the uptake and distribution of Ca on excised roots and intact seedlings of wheat. It was found that Al treatments reduced both the absorption and accumulation phases of Ca uptake. The reduction in accumulation could not be overcome by increased amounts of Ca. Transport of Ca to shoots of intact seedlings was also restricted by Al, although some transport still occurred when root uptake was inhibited completely (67).

Fleming found that the ammonium in the presence of Al reduced the nitrate absorption, lowered the pH, and reduced root yield. Ammonium without Al did not cause a general decrease in the vegetative yield of the cultivars. In fact, the top growth was significantly increased by ammonia treatments and exceeded yields of other cultivars. Root yields, however, did not show a similar relationship (68).

When plants are grown under saline conditions, they respond with a variety of integrated changes in the distribution of ions, cell water relations, biochemical functions, and morphology (69). Research by Harvey and Thorpe measured the effects of sodium chloride on wheat. The seeds were planted in a NaCl solution. The NaCl concentration in the solution was increased over the growing period and reached a NaCl solution of 100 mol-m<sup>3</sup>. They found that although plants grew less well under the saline conditions than in the absence of NaCl, the leaves examined did not appear to show anatomical damage or damage to the leaf cells. The cells of wheat are unable to store sodium and chlorine in any way, which would minimize the toxic effects of the ions in the cytoplasm. The presence of substantial ion concentrations in the intercellular spaces denotes the presence of water and, hence, probably deleterious effects on gas exchange within the leaves (69).

The distribution of eight essential nutrients is illustrated in Figure 6. Based on the figure, one would expect to retain most of the Ca and K and some of the Mg and Mn in the portion of the plant available for biomass cofiring. Proportionately small amounts of P, Zn, Fe, and Cu will be retained.

### ***Rice***

*Oryza sativa* is an annual grass of the Gramineae family. It can be grown on a wide variety of soils, but slowly permeable clay soils are usually more suitable than soils without water-holding capacity, especially those soils that drain rapidly. Beyrouthy and coworkers stated that in the United States rice subjected to normal flooding consistently responded with the highest nutrient uptake. They found that some nutrients not readily available in an upland environment are often available under submerged conditions. Examples are ferrous phosphate, K, and Mn. Zinc, Fe, and Mn become more soluble under flooded conditions, and deficiencies are seldom observed. Unlike these other elements, N is subject to leaching in the nitrate form, and soil levels of plants available N may be severely reduced because of flooding (70).

Sulfur deficiency has been recognized as an important growth-limiting factor. In rice, sulfur deficiency results in a severe reduction in tiller number and plants become yellow and have thin erect leaves. The critical total sulfur limits were 0.11% in the shoot, .055% in the straw at maturity, and .065% in the grain (71). Samosir and Blair studied rice that was fertilized with sulfur-coated urea (SCU). They found that plants fertilized with SCU exhibited good growth in the first 2 weeks after transplanting, but after that, their growth rate slowed and plants showed signs of sulfur deficiency. The one positive of SCU was that the N efficiency increased (72).

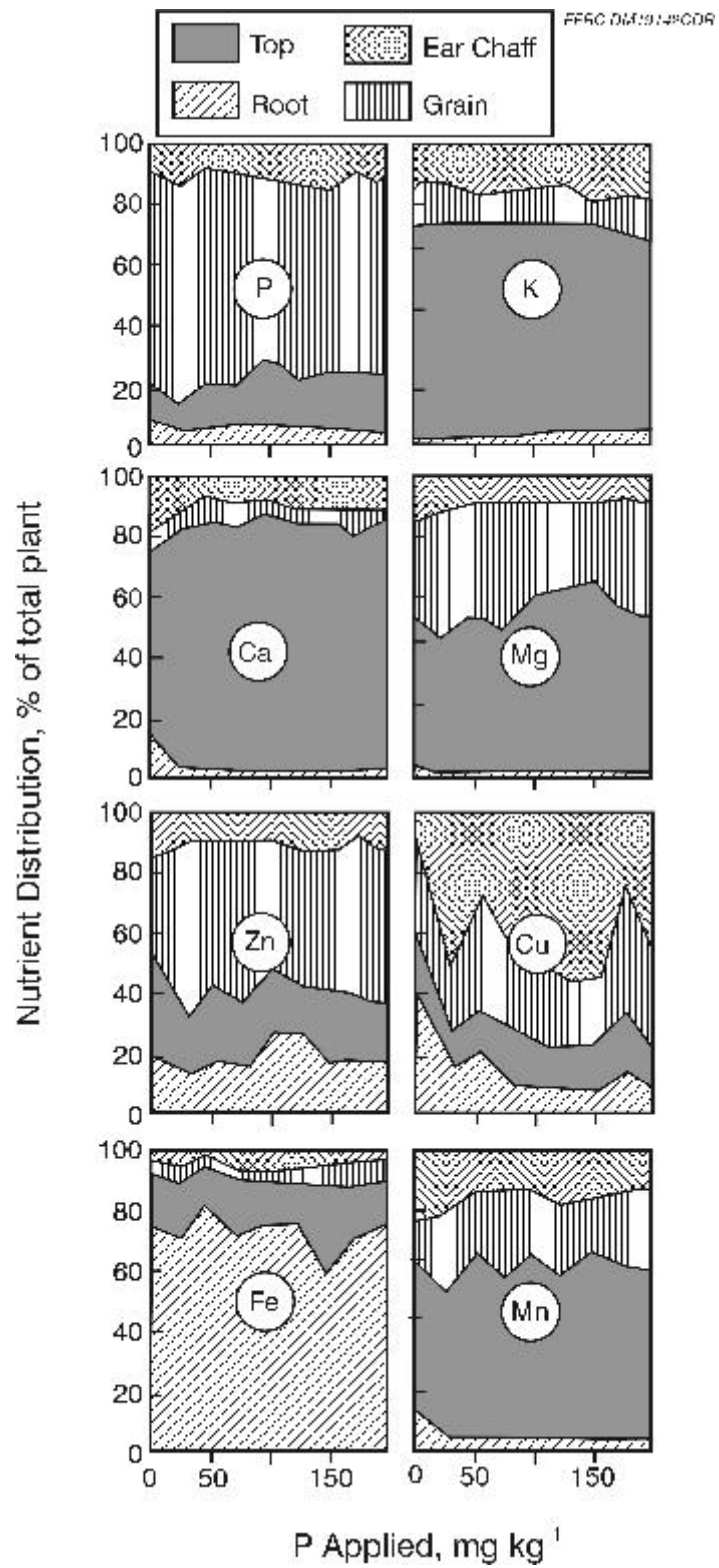


Figure 6. Distribution of nutrients in different plant parts of wheat (43).

The distribution of N, P, and K in two upland rice cultivars is illustrated in Figure 7. Based on the figure, one would expect to retain most of the K (80%–90%) and some of the N and P (30%–50%) in the portion of the plant available for biomass cofiring. Little other mineral information specific to rice was obtained. Silica associations in rice are described in that section.

### ***Switchgrass***

*Panicum virgatum* is an American native prairie grass ideally adapted to the eastern United States. It is highly productive, requires little fertilization and herbicide, and can be grown on marginal land. Nitrogen fertilizers along with higher soil water availability and adequate temperatures increased biomass accumulation (73, 74). It can be harvested twice a year with existing farm equipment. Grown by farmers on marginal land, switchgrass could offer a cash crop and a boost to the farm economy (75). Boylan and coworkers studied switchgrass efficiency for cofiring with coal. They found that the 10% switchgrass–90% coal mixture burned well in the pilot combustor blends with both eastern and western coals. No degradation in unburned carbon was observed, and no problems with slagging or fouling associated with grass were seen. In the combustor tests, NO<sub>x</sub> emissions were reduced firing eastern bituminous coal when 10% switchgrass was included. One negative illuminated by this project was the amount of dust produced. Therefore, an approach to pelletizing the switchgrass or forming a switchgrass–coal mixture is being studied to decrease the amount of dust (75).

Calcium oxalate crystal deposition is not common in Poaceae but can be found in *Panicum*. Crystals normally form intracellularly within vacuoles of actively growing cells and are usually associated with membrane chambers. The presence of extracellular crystals has been reported (76). Since these crystals have a covering of fibrous material, one hypothesis suggests intracellular initiation. The actual value of calcium oxalate crystals to normal plant growth and development is largely unknown and probably varies in plants. Prychid and Rudall suggest the crystals may represent storage forms of calcium and oxalic acid, and there has been some evidence of calcium oxalate resorption in times of calcium depletion. They may also act as simple depositories for metabolic wastes, which would otherwise be toxic to the cell or tissue. The crystals may be present in almost every part of both vegetative and reproductive organs, often in crystal idioblasts near veins, possibly due to calcium being transported through the xylem (76).

It has been postulated that an initial random distribution of dissolved calcium and oxalate ions in the crystal chamber may come together to form a crystalline configuration or “cluster.” These clusters break up and reform easily. As the concentration of the dissolved ions increases, the cluster may grow in size rather than break up. This increase in concentration to the point of saturation is controlled by plant metabolism. The crystal nuclei redissolve unless they reach a stable “critical size,” when their free energy is lower than that of the solution (76).

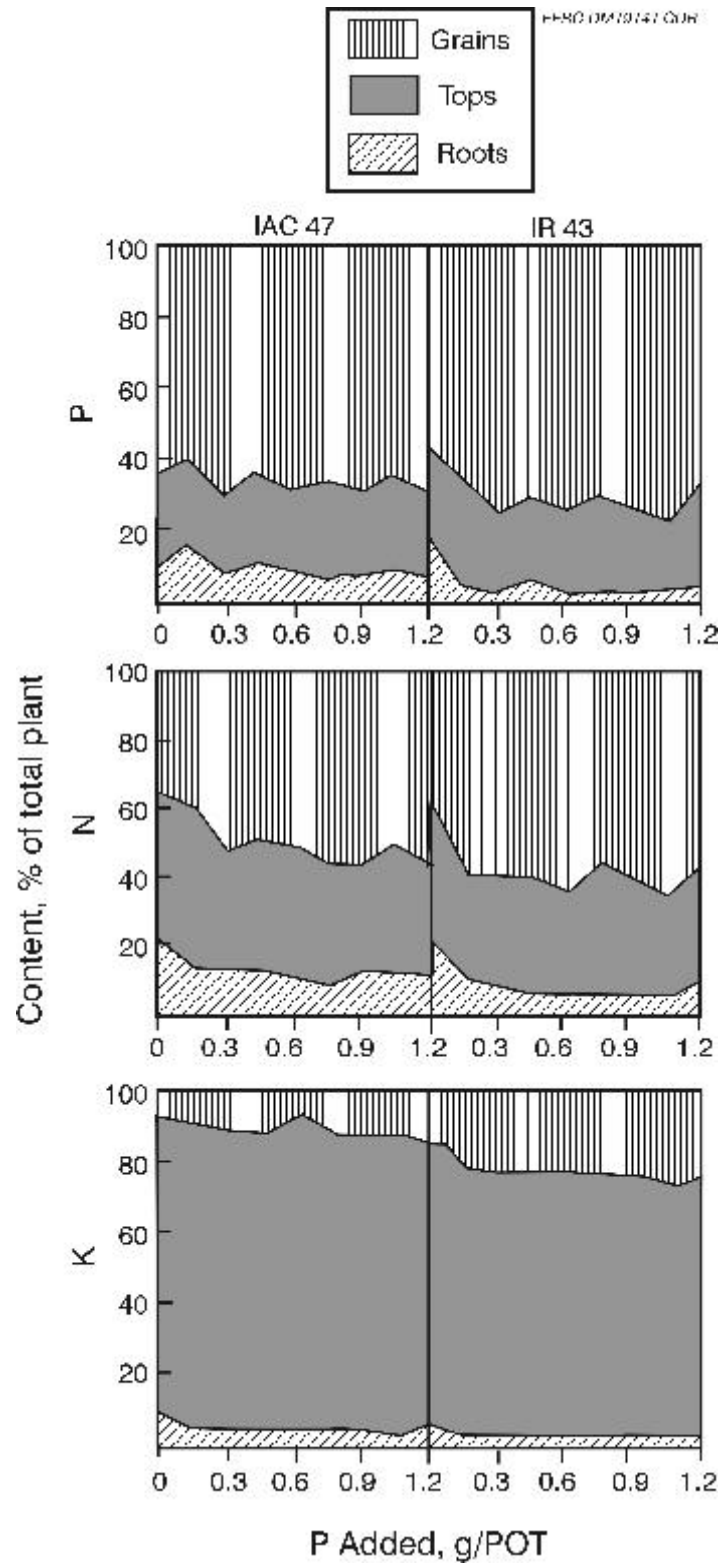


Figure 7. Distributions of N, P, and K in roots, tops, and grains of two upland rice cultivars (43).

### ***Hybrid Poplar***

*Populus tremuloides* contains calcium oxalate crystals in the bark of the tree. Trockenbrodt found that solitary crystals and chambered crystal-containing cells were present in a similar way in the bark of oak and poplar (77). In poplar, druses (multiple crystals that are thought to have formed around a nucleation site to form a crystal conglomerate) were frequently present in the secondary phloem and the cortex (76). They were relatively scarce in the chambered cells in the vicinity of the cambium, but common in the spherical cells of the secondary phloem and in the cortex (77).

### ***Alfalfa***

*Medicago sativa* is a perennial, leguminous plant of the Fabaceae family, which is known for its tolerance of drought, heat, and cold; for the productivity and quality of herbage; and for its value in soil improvement (78). Alfalfa has a remarkable capacity for rapid and abundant regeneration of dense growths of new stems and leaves following cutting, which makes it possible to have up to 13 crops of hay in one growing season (78).

Information on the influence of soil moisture on mineral concentrations, is limited in alfalfa. Kidambi and coworkers found that water stress may result in higher levels of Ca, Mg, Zn, and P in alfalfa. Their results indicated that soil moisture level affected the mineral concentrations but not the relationships among minerals in the forage of alfalfa. The focus of the article was nutritional needs of beef cattle (79).

Smith and Struckmeyer studied the effects of chlorine in alfalfa shoots because potassium chloride (KCl) is the most common source of K for fertilizing alfalfa. A high level of K is required for optimum growth and productivity of alfalfa, but Cl could be absorbed in amounts damaging to the plants (80). Research has shown that high application rates of KCl can cause burning of leaflets and death of shoots on alfalfa plants, presumably from Cl. Their study showed that the highest percentage of Cl was found in the petioles as compared to the leaflets and internodes. It was highest in the bottom leaflet and decreased toward the top leaflet. The bottom petiole had the highest percentage of Cl. The highest percentage of Cl was found at the top of the shoots. Cl accumulates largely in the bottom leaflets and in the upper internodes of alfalfa shoots. High KCl concentrations in the plant appear as yellowing and deforming plant parts (80).

Selenium is translocated from the roots to all parts of the plant including the seed. A study by Wilson and coworkers showed the presence of selenium in alfalfa. Alfalfa samples were collected in order to observe any relationships between the selenium content of soils and plants. The portions of the plant that were sampled were any amounts 3 inches above the soil; the purpose was to minimize soil contamination. The amount of selenium that was detected was in ppb range and the mean Se concentrations were 2400, 1400, and 950 ppb (81).

### ***Silica***

The vast abundance of Si is reflected by the concentrations seen in the plants' ash content in Table 3. Silica is not considered an essential element in plants; it nevertheless has secondary effects. Some plants

seem to use Si in the form of silica for building parts of the skeletal structure, and others take up silica from the soil even though the silica has no apparent function (82). Silica has been found to be present in abundance in plants of Gramineae, constituting 50% to 70% of the ash (83).

Soluble silica is mainly derived from the weathering of silicate minerals such as quartz and feldspar. It is constantly dissolving and precipitating over a large part of the earth's surface. The weathering depends on factors such as climate, topography, bedrock character, and the amount of water passing through the soil (29).

Plants absorb silica through their roots and carry it upward to the aerial organs in the transpiration stream via the water-conducting tissue called xylem. Silica is taken up as monosilicic acid,  $\text{Si}(\text{OH})_4$ , between soil pH values of 2 and 9. The levels of monosilicic acid in soils are affected by pH in a manner that is independent of the presence of iron and aluminum. The capacity of soil particles to absorb soluble silica changes as pH changes, and the concentration of monosilicic acid has been found to increase on either side of minimum between a pH of 8 and 9. Thus acidic soil environments have more free silica available to enter plants (29). The relative rates at which silica and water entered shoots were largely controlled by metabolic processes in the root. It was also indicated that under conditions of high humidity, silica appeared to be entering the shoots against a concentration gradient in plants with living roots.

Deposits of silica, as well as other types of plant mineral deposits, are called phytoliths, literally meaning plant rocks (84). There are two proposed mechanisms of silica uptake: active transport by metabolic processes and passive transport. The hypothesis of active transport was backed up by the finding of silicic acid entering the xylem sap of rice shoots against a concentration gradient. The passive transport hypothesis is supported by a well-established fact that the amount of silica in some laboratory-grown, silicon-accumulating plants is directly proportional to the amount of dissolved silica in soils. It has also been shown that a prediction could be made about knowing the Si contents in oats, simply by knowing the concentration of silicic acid and the amount of water transpired. It is known that angiosperm roots may exhibit an active or passive absorption, depending on the species and that in some taxa both processes are involved, each operating in different locations of the plant (29).

Once monosilicic acid enters plant tissues, a process of polymerization begins with the result that some of it is amorphous and forms silicon dioxide ( $\text{SiO}_2$ ) in and around plant cells. In plant tissues, there are three loci of silica deposition: 1) cell wall deposits, often called membrane silicification; 2) infillings of the cell lumen; and 3) in the intercellular spaces of the cortex. Stored in the plant as a solid hydrated form,  $\text{SiO}_2 \cdot n\text{H}_2\text{O}$  is known as "opal" or "opaline silica" (85). Patterns of localization are similar in species and whole families of plants (29). Many studies of silica deposition have been focused on the aerial organs of grasses, because this is where transpiration and water loss have been implicated as a major contributing factor. In active transpiring cells, a supersaturated solution of silicic acid may develop, leading to the precipitation of silica. In areas of the plant where water loss is highest, such as the flag or uppermost leaf and floral bracts of grasses, substantially more silica is deposited than in other areas. Piperno observed that few cells are silicified in intercostal areas (between veins), where transpiration occurs (29).

Typical silicification in grass leaves in the costal (over the vein) areas forms dumbbell, saddle, and cross-shaped bodies. An atypical silicification takes place intercostally in cells not primarily associated with deposition, such as stomatal complexes and long or fundamental cells, and is more random and sporadic in occurrence. Atypical deposition is usually found in older plants, suggesting formation from an excess supply of soluble silica (29). The Gramineae is the family best-known for depositing silica; the deposition takes place in both cell walls and cell lumina (83, 86). It is characteristic of the Gramineae family that most of the silica absorbed is deposited as opaline silica bodies in epidermal cells, and it is evident that specific shapes of silica bodies are formed, depending on the shape of the cell in which the silica is deposited (87, 88). In the genus *Oryza*, of the Gramineae family, most silica bodies form in the epidermal long cells of leaf veins. They often occur in rows (89).

Paleobotanists and archeologists lead the effort to categorize silica phytoliths. Whang and coworkers state that one of the main obstacles in phytolith systematics is variation in silica body morphology from tissue to tissue and within specific tissues. Factors that may influence variation include the following (89):

- Stage of plant maturity
- Intraspecific variation within plant taxa
- Amount of soluble silica in groundwater
- Rate of leaf transpiration
- Tissue within which the phytoliths form
- Location of phytoliths in leaf blades
- Genetic variation among plants
- Geographic location where the plants grew

The rate and time of maturation of the tissues are important in silica deposition, whether the mechanism of deposition is active or passive, as maturation brings about the crucial change in the cellular environment required to cause silica deposition. It seems that environmental factors affect silica deposition indirectly through the maturity induced in the plant cells and plant tissues (90). Although much effort has been expended on cataloguing phytolith morphology, literature review and conversations with staff at the University of Minnesota–Duluth Archeometry Laboratory revealed an absence of elemental analysis of phytoliths. It is, therefore, unknown at this time whether phytoliths incorporate other elements into their structure.

Investigations concerning the role of Si in higher plant growth have yielded conflicting results. There have been arguments about whether Si can be considered an essential element based on the lack of evidence that silica plays a direct role in the metabolism of grasses or in other plants that accumulate it in considerable quantities. Some plants have growth and reproduction benefits due to the presence of silica. In rice, Si enhances resistance to fungus disease and increases grain yield. Rice leaf blades are more erect when silica slags are applied, which allows more light to reach the lower leaves and results in increased photosynthesis activity. And all awns of rice contained silica bodies such as prickle hairs, microhairs, and stomata (91). Also, it has been proven that rice plants showed retardation of their vegetative growth and decrease of degree of seed setting when their silicon content was extremely low (92). It could then be concluded that silicon must be essential for rice. Grass shoots have shown resistance to predation by

chewing insects and mammalian herbivores, presumably as a result of their high phytolith content (29). Because phytoliths are mineral, they resist decomposition. Thus when the plant material decomposes, the phytoliths maintain their morphological integrity, even if they are burned, buried, or ingested (84).

## **Extrinsic Properties of Biomass**

### ***Environmental Factors***

The environment of a plant may be defined as the sum of all external forces and substances affecting the growth, structure, and reproduction of the plant. Climatic and geologic factors with an important role in crop production are temperature, solar radiation, moisture supply, and soil (43).

Optimal conditions for plant growth are difficult to define because they vary with plant species, type of soil, and geographic region. The climate of an area determines which vegetation should be grown. Rice, for example, should not be grown in climates that have an average temperature lower than 25°C or higher than 30°C for optimal crop yield. Soil and air temperatures are important because these temperatures will determine the growing season. The soil temperature affects the root temperature. It determines the ability of the plant to uptake nutrients and which nutrients are absorbed.

The solar radiation of the region also influences plant growth and development and coincides with the climate that is going to be best chosen for the crop. Solar radiation affects photosynthesis and, thus, crop productivity. Also, the lengthening and shortening of daylight is an environmental trigger that leads to life-stage responses in plants.

Moisture availability is one of the most important factors determining crop production. The distribution of vegetation in a region is controlled more by availability of water than by any other factor. Water is required by plants for the translocation of mineral elements, manufacture of carbohydrates, and maintenance of hydration of protoplasm. Most field crops are more sensitive to water stress during reproduction and grain-filling stages than the vegetative stage. In cereals, the most sensitive growth stage for water deficiency is around flowering (43, 93). The Clarke and coworkers study described in the wheat section illustrates the importance of moisture availability to the growth of a crop (57). Obviously, for some crops, flooding will be detrimental, while others, such as wetland rice, will need flooding to obtain many nutrients that are not available for uptake through the dry soil.

Soil is the unconsolidated mineral material on the immediate surface of the earth that serves as a natural medium for plant growth. Inadequate nutrient supply restricts plant growth and yield. The deficiencies in soils are related to the parent material, weathering, cultivation, and erosion. Nutrient deficiencies vary among soils and areas. Table 4 summarizes the nutrient deficiencies associated with major soil types. Temperate and tropical soils around the world are most often deficient in nitrogen and phosphorus. Nutrient deficiencies can be alleviated through application of fertilizers and amendments and selection of appropriate cultivars. Ultimately, the plant is dependent on the combination of mineral content in the soil and moisture availability because its roots pull nutrients from the soil solution. Without moisture

in the soil, nutrients will be held in organic matter in the soil, precipitate as inorganic solids, or adsorb on soil surfaces. It is the mineralization, dissolution, and desorption of the nutrients by moisture that render their bioavailability (43).

TABLE 4

Nutrient Deficiencies of Soil Types		
Soil Group	Deficiency	Toxicity
Acrisols and Nitosols	N, P, and most other elements	Al, Mn, Fe
Andosols	P, Ca, B, Mo	Al
Chreozems and Greyzems	Zn, Mn, Fe	Unknown
Fluvisols	Unknown	Al, Mn, Fe
Gleysols	Mn	Fe, Mo
Histosols	Cu	Unknown
Phaeozem	Unknown	Mo (if poorly drained)
Podzols	N, P, K, and micronutrients	Al
Planosols	Most nutrients	Al
Lithosols, Rendzinas, and Rankers	P, Mn, Zn, Fe	Unknown
Solonchaks and Solonetztes	N, P, K, Cu, Zn, Mn, Fe	Na, B, Cl
Vertisols	N, P	S (sulfide)
Xerosols and Kastanozems	P, K, Mg, Zn, Fe, Mn, Cu	Na
Yermosols	P, K, Mg, Zn, Fe	Unknown

### *Toxicities*

The toxicities most commonly found in food crops are Al, Mn, and Fe. Aluminum and Mn toxicities are most common in acid soils, whereas Fe toxicity occurs in flooded rice under reduced soil conditions. Metal toxicity can be expressed as direct and indirect toxicity. Direct toxicity occurs when the excess of the element is absorbed and becomes lethal to the plant cell. Indirect toxicity can be related to nutritional imbalance. Aluminum, Mn, and Fe in the growth medium induce nutritional deficiency by inhibiting the uptake, transport, and utilization of many other nutrients (43). Table 4 also lists toxicities of major soil types around the world.

Increased Al concentrations in the soil inhibit the concentrations of N, P, K, Ca, Mg, Zn, Fe, Mn, and Cu in the plant tops. Fageria lists the hypotheses formed by other authors that may explain why aluminum affects the concentrations of the other nutrients (43):

- Aluminum inhibits root growth, thereby causing the uptake of these nutrients to be reduced.
- Aluminum reduces cellular respiration in plants, inhibiting the uptake of ions.

- Aluminum increases the viscosity of the protoplasm in plant root cells and decreases overall permeability to salts.
- Aluminum blocks, neutralizes, or reverses the negative charges on the pores of the free space and thereby reduces the abilities of such pores to bind Ca.
- Aluminum may compete for common binding sites at or near the root surface and thereby reduce uptake of K, Ca, Mg, and Cu.
- Aluminum reduces Ca uptake by completely inactivating part of the Ca accumulation mechanism.
- In general, Al interferes with cell division in plant roots, decreases root respiration, interferes with certain enzymes governing the deposition of polysaccharides in cell walls, increases cell wall rigidity, and interferes with the uptake, transport, and use of several elements such as K, Ca, and Mg.
- Aluminum injures plant roots and reduces Ca uptake.
- Aluminum decreases the sugar content, increases the ratio of nonprotein to protein N, and decreases the P contents of leaves from several plants grown on acid soils.

Similarly, high Fe concentrations in the growth medium reduce uptake of nutrients. Among macronutrients, the uptake of P, K, and N is affected. Among micronutrients, absorption of Mn and Zn is most affected. These results show that when there is a toxicity of Fe, especially in lowland or flooded rice, an increase in P, K, and Zn should be supplied through fertilization (43).

### ***pH***

Soil pH is a very important chemical factor with regard to crop yield. The pH of soil indicates whether it is acid, neutral, or alkaline. The critical pH standards should be known for both the soil and crop to be planted. This will help maximize the crop yield. Most crops are tolerant to pH levels of 5.0–6.5 (43).

### **Summary**

Investigations into mineral uptake and storage by plants that are considered for biomass cofiring revealed the form and concentration of inorganic elements in plant matter. Sixteen essential elements, C, H, O, N, P, K, Ca, Mg, S, Zn, Cu, Fe, Mn, B, Mo, and Cl, are found throughout plants. Aside from H and O, the predominant inorganic elements are K and Ca, which are essential for the function of all plant cells and will, therefore, be evenly distributed throughout the nonreproductive, aerial portions of herbaceous biomass.

Some inorganic constituents, e.g., N, P, Ca, and Cl, are organically associated and incorporated into the structure of the plant. Cell vacuoles are the repository for excess ions in the plant. Minerals deposited in these ubiquitous organelles are expected to be most easily leached from dry material.

There are other elements obtained from soil interaction with roots, air interaction with aerial portions of the plants, and water interactions with both roots and aerial portions of plants. These elements may not have specific functions within the plant, but are nevertheless absorbed and fill a need. An example is Si, found in the form of monosilicic acid,  $\text{Si}(\text{OH})_4$ . In rice, it enhances resistance to fungus disease and increases grain yield. The leaf blades of rice are more erect when silica slags are applied, and it has also been proven that rice plants showed retardation of their vegetative growth and a decreased degree of seed setting when the Si content was extremely low.

Another common nonessential element, Na, is deposited throughout the plant despite its nonfunctional status. Its concentration will depend entirely on extrinsic factors regulating its availability in the soil solution, i.e., moisture and soil content. Similarly, Cl content is determined less by the needs of the plant than by availability in the soil solution; in addition to occurring naturally, Cl is present in excess as the anion complement in K fertilizer applications.

Overall plant development and maintenance depend on the chemical substances absorbed and transported by the roots. Nutrient supply to the roots is dependent on nutrient concentrations in the soil solution, the nature of nutrients, soil moisture status, and the plant's absorption capacity. The data suggest that although mineral content varies somewhat based on the needs of the plant, much is dependent on the availability of elements in the soil solution surrounding plant roots. This is most influenced by soil content, moisture availability, root uptake activity, and, in some cases, pH. Knowing the soil and moisture conditions, pH, and fertilizer history will provide insight into expected concentrations of elements in plants.

## **GEOGRAPHIC AND SEASONAL DIFFERENCES IN SWITCHGRASS ELEMENTAL COMPOSITION**

### **Background**

The section describing the extrinsic properties of biomass shows how the plant environment will affect the growth, structure, and reproduction of the plant. Climatic and geologic factors including temperature, solar radiation, moisture supply, and soil strongly influence plant growth. These factors also affect the elemental uptake of plants, which varies between plant species. Thus the plant environment will affect the inorganic content of biomass. This variability is of particular interest for elements that give rise to slagging, fouling, and particulate emission when the biomass is used as an energy source in combustion systems.

Switchgrass is being tested as a potential biomass energy crop. To better understand the extent to which environmental variables can alter the elemental composition, the EERC was supplied with data collected by the Chariton Valley Resource Conservation & Development (RCD) group, based in

Centerville, Iowa. Chariton Valley RCD collected soil and switchgrass samples from ten different farms in the south-central portion of Iowa. These samples were then analyzed by Hazen Research, Inc., based in Golden, Colorado. As part of this project, the supplied data were reduced, processed, and examined for correlations between switchgrass elemental composition and geographical and seasonal changes, with the goal of identifying factors that influence the elemental composition of biomass.

The examination of the data began with three main hypotheses as to why elemental concentrations would vary between switchgrass samples:

1. *Certain elements associate with one another because of their association in the plant matter:*

Certain elements and compounds naturally associate in aqueous suspension. In biomatter such as plants, this is even more true, because individual cells have different affinities for nutrients and elements.

2. *Geography due to its different soil, fertilizing, and drainage characteristics may impact elemental concentration:*

Each different soil type may have a surplus or deficit of elements required by the switchgrass as well as different drainage characteristics due to both soil type and topography. Even the most localized natural phenomenon will cause a variation in plant growth characteristics.

3. *Season of harvest may impact elemental concentrations caused by varied elemental uptake into plant structure:*

Unlike many other midwestern states, southern Iowa is warm enough to grow and harvest a crop for a majority of the year. For instance, the coldest temperature recorded by any farm in these data is 25°F on February 1, 2000. The very next day, the temperature was 38°F, and at no other time was a freezing temperature recorded. It is important to know which season will bring what form of moisture, since runoff and rainfall may have different effects. For example, spring may bring snow runoff, but unwanted elements may be transported in with the water; likewise, late summer may have only groundwater as a moisture source, but this water may carry elements up from the subsoil. Seasonal changes may also cause certain plants to go into a dormant state, which can change chemical and physical plant characteristics.

## **Analysis Results**

This study included ten farms located in three counties. Six farms returned a harvested crop between late October and mid-January, two farms returned unharvested crop samples all year around, and four farms were not labeled as either harvested or unharvested. However, these last four farms were sampled on March 21, 2000, and had sampling methods identical to those of unharvested farms, suggesting that they were most likely unharvested. Table 5 summarizes the location and harvest status of the samples. The proximate, ultimate, and ash chemistry of the samples are given in Appendix D.

TABLE 5

## Summary of Switchgrass Sample Data

County	Township	Farm	Status
Appanoose	Chariton	Lodge Land #1	Harvested
Appanoose	Chariton	Lodge Land #2	Harvested
Lucas	English	G. Peterson #1	Harvested
Lucas	English	G. Peterson #2	Harvested
Lucas	English	Schultz #1	Unharvested
Lucas	English	Schultz #3	Unharvested
Lucas	English	Schultz #5	Unharvested
Lucas	English	Schultz #7	Unharvested
Lucas	English	Schultz #9	Unharvested
Lucas	English	Schultz #11	Unharvested
Lucas	English	Schultz #13	Unharvested
Lucas	English	Schultz #15	Unharvested
Lucas	English	Schultz #17	Unharvested
Lucas	English	Van Patten #1	Harvested
Lucas	English	Van Patten #2	Harvested
Lucas	Liberty	Krutsinger #1	Harvested
Lucas	Liberty	Krutsinger #2	Harvested
Wayne	South Fork	Cross Farm #1	Harvested
Wayne	South Fork	Cross Farm #2	Harvested
Wayne	Union	Sellers #1	Harvested
Wayne	Union	Sellers #2	Harvested
Wayne	Union	Sellers #2	Unharvested
Wayne	Union	Sellers #4	Unharvested
Wayne	Union	Sellers #6	Unharvested
Wayne	Union	Sellers #8	Unharvested
Wayne	Union	Sellers #10	Unharvested
Wayne	Union	Sellers #12	Unharvested
Wayne	Union	Sellers #14	Unharvested
Wayne	Union	Sellers #16	Unharvested
Wayne	Union	Sellers #18	Unharvested
Wayne	Union	Sellers #21 Fescue	NA <sup>1</sup>
NA	NA	Bills Brome #20	NA
NA	NA	Cemensky #19	NA
NA	NA	Peck #22 Orchard	NA

<sup>1</sup> Not applicable.

Correlations were observed between the levels of  $K_2O$  and Cl. Concentrations of  $K_2O$  versus Cl are plotted in Figure 8 for harvested crops. A regression line is drawn through the data, and the correlation coefficient  $r^2$  is displayed as 0.4619.

Also in Figure 8 are lines labeled  $K_2O$  vs. Cl and  $Na_2O$  vs. Cl. These plots represent the ideal case of having only pure KCl and NaCl. In such a case, the ratio of  $K_2O$  to Cl would be 1.715, and the ratio of  $Na_2O$  to Cl would be 1.129. If  $K_2O$  and  $Na_2O$  were reacting completely with the chlorine in switchgrass, then the slopes of both oxides against chlorine would equal these ratios. However, neither  $K_2O$  nor  $Na_2O$  approach their ideal cases except at very low values.

For the harvested crop, the  $r^2$  value for  $K_2O$  versus Cl is only 0.4619, indicating a poor correlation. For other farms, the values are higher: Schultz  $r^2$  is 0.5682, Sellers is 0.9402, and the other (unknown harvested status) farms are 0.9344. However, despite some excellent correlation coefficients, none of the slopes are what would be predicted for a system of pure KCl. Sodium is a water-soluble alkali like potassium which seems to fluctuate with Cl. To see whether there is a correlation between  $Na_2O$  and Cl, sodium was plotted alongside  $K_2O$  on Figure 8. (Actually,  $K_2O$  and  $Na_2O$  are not found in uncombusted biomass in this strongly basic form, but as some form of carbonate [i.e.,  $K_2CO_3$ ,  $KHCO_3$ ] or as a cation attached to the organic plant structure. However, for simplicity, all potassium and sodium substances in ash will be referred to as  $K_2O$  or  $Na_2O$ ).

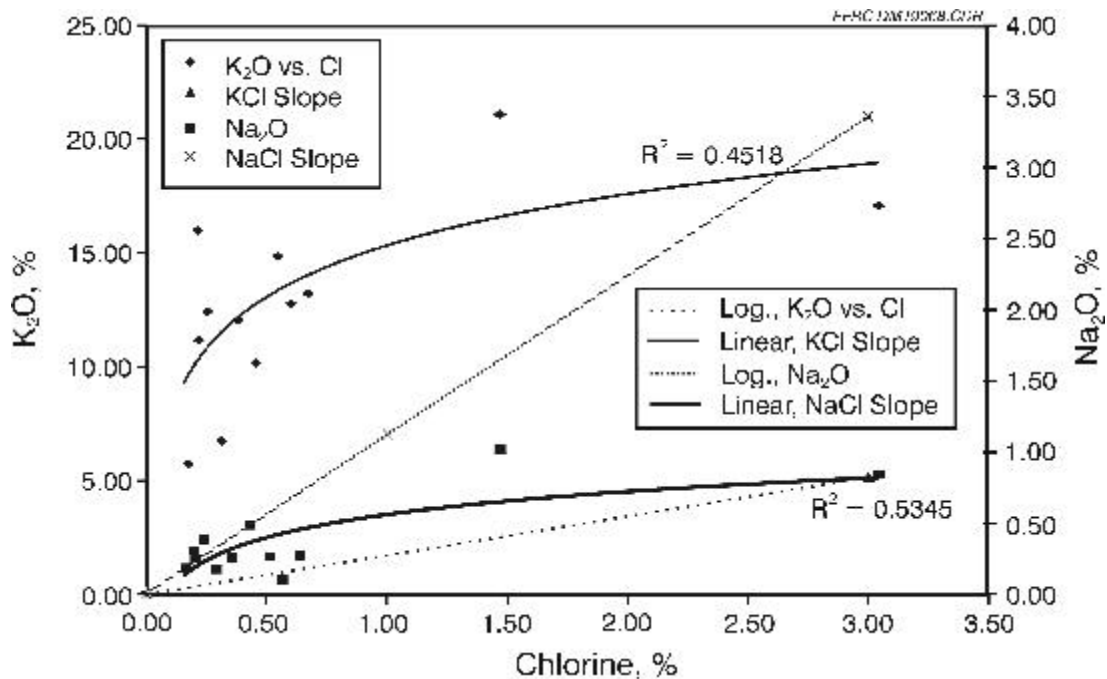


Figure 8.  $K_2O$  versus Cl in harvested switchgrass.

The  $r^2$  value is 0.5345 for harvested crops, so any hypothetical correlation is inconclusive. For all other farms, the  $r^2$  value is lower, suggesting that there is no association. Three out of four of the  $\text{Na}_2\text{O}$  trend lines share a common trait that is mirrored in Figure 8: They start out tangential to the pure  $\text{NaCl}$  line, then quickly fall away. This is to be expected, since sodium is stored with chlorine in the vacuoles. When more chlorine comes into the plant, it is automatically used (there are 130 vital compounds in the plant which contain chlorine). The sodium, by contrast, is always stored in the vacuoles. This suggests that the plant sodium concentration will reach an equilibrium with the amount of available sodium in the soil and cease to increase, while chlorine levels may continue to rise.

Figure 9, which plots water-soluble alkalis versus moisture, shows that sample moisture seems to have little or no relationship to  $\text{K}_2\text{O}$ . This is indicative of all graphs of water-soluble alkalis vs. moisture, including air-dried models and those not using moisture-free numbers. Since  $\text{Na}_2\text{O}$  is present in very small concentrations (most are less than .001%), it is multiplied by 100 in Figure 9. Sodium shows some local maximums, but only one of these coincides with  $\text{K}_2\text{O}$  maximums. There appears to be no relationship between sodium and sample moisture. Since sample moisture may be expected to be related to ambient moisture conditions in the fields, it appears that this has little effect on potassium and sodium concentrations.

### Geographical Variations by County and Township

The data were subdivided by county and then by township to see whether location played any role in elemental composition. Three counties (Appanoose, Lucas, and Wayne) had a total of six townships (Chariton in Appanoose; English, Liberty, and Warren in Lucas; South Fork and Union

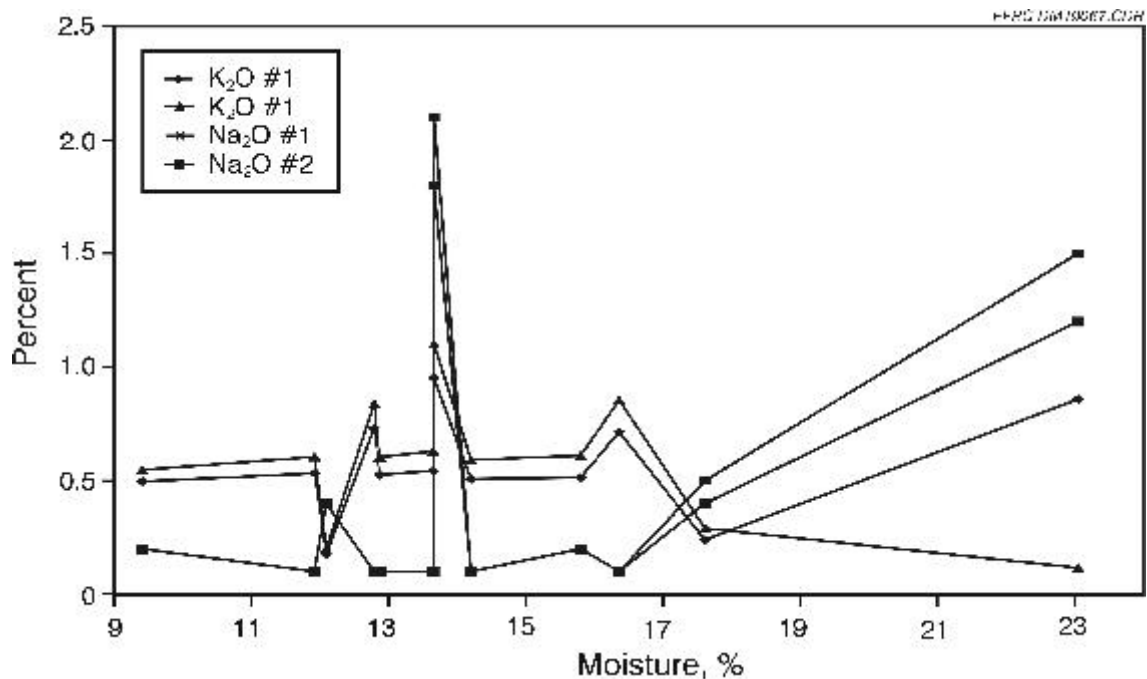


Figure 9. Water-soluble alkalis versus moisture in harvested switchgrass.

in Wayne) which were sampled. An on-line map (94) was used to determine the locations of counties, townships, as well as the approximate location of each farm. The townships form a single patch at the intersection of the three counties.

Moisture-free concentrations of each compound were calculated for each township, as were moisture-free Btu/lb measurements. These values were then averaged and plotted in Figure 10, which shows each element is associated with the others. For Chariton Township in Appanoose County, moisture accounts for 18.4% of the switchgrass samples' average weight, as opposed to about 13.5% average for the remainder. The same township also shows slightly lower concentrations of volatile compounds. Heat content averaged 6430 Btu/lb for Chariton (500 Btu/lb less than average), and maf Btu/lb was 6720 (about 500 maf Btu/lb less than average).

English Township in Wayne County has a recorded average moisture level of 15.3%, which, like Chariton in Appanoose, results in lower concentrations of volatile compounds. This results in Btu/lb values of 6760 and 7070 for higher heating value (HHV) and maf, respectively. These numbers are lower than average but not as low as Chariton Township's. This corresponds to Chariton's moisture level being higher than the others. Along with decreased volatile compounds and Btu/lb measurements, both Chariton and English Townships give slightly lower concentrations of carbon in their ultimate analysis. Note that these effects are seen even when the samples have been normalized on a moisture-free basis.

### **Seasonal Variations**

The hypothesis that changes in season affect the concentration of various elements and compounds was tested by selecting two farms and three separate dates. The data from the Schultz and Sellers unharvested samples were chosen for examination, since they showed identical collection dates and also had the earliest and the latest collection dates. The three dates chosen for analysis were August 7, 1999; January 8, 2000; and May 11, 2000, representing the earliest, latest, and approximate median collection times.  $K_2O$  and Cl were also averaged before and after the first freeze of the year for the Schultz and Sellers farms to test whether the onset of frost had an effect.

The values for these farms are plotted in Figures 11 and 12. There are many noticeable variations, but the most notable changes were those of the oxide concentrations.  $SiO_2$ ,  $Al_2O_3$ , and CaO all increased, while MgO,  $K_2O$ ,  $P_2O_5$ , and Cl all decreased at the same interval.  $Na_2O$  also decreased for the most part, although not as much as  $K_2O$ . Strangely,  $Fe_2O_3$  dropped noticeably in the winter, then increased to a value even higher than in the spring. Other oxides either did not change or underwent inconsistent changes.

Ash and fixed carbon made definite drops, as did chlorine by weight. Nitrogen seemed to drop significantly between summer and winter, although the final stage was less severe and perhaps questionable. Maf Btu/lb measurements drop from season to season for Sellers unharvested, but Schultz shows a rise in January before dropping significantly in May. Moisture levels in both farms fall and then rise in the spring as expected, as does carbon by weight, although the carbon results are less decisive. Volatile compounds and Btu/lb (HHV) both rise in the winter and drop in the spring. Other elements show little or no change.

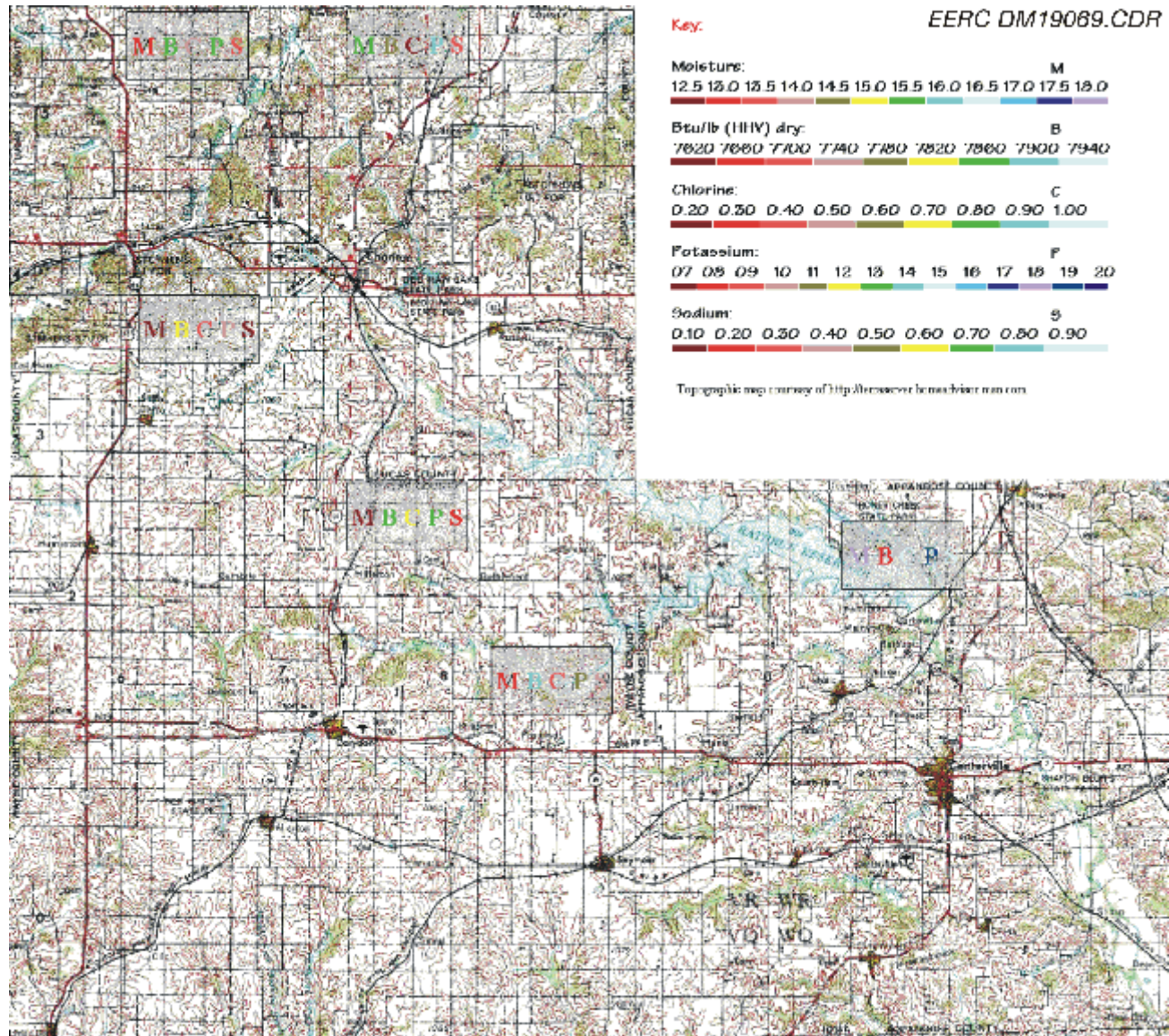


Figure 10. Switchgrass dry-basis county averages for October and November 1999.

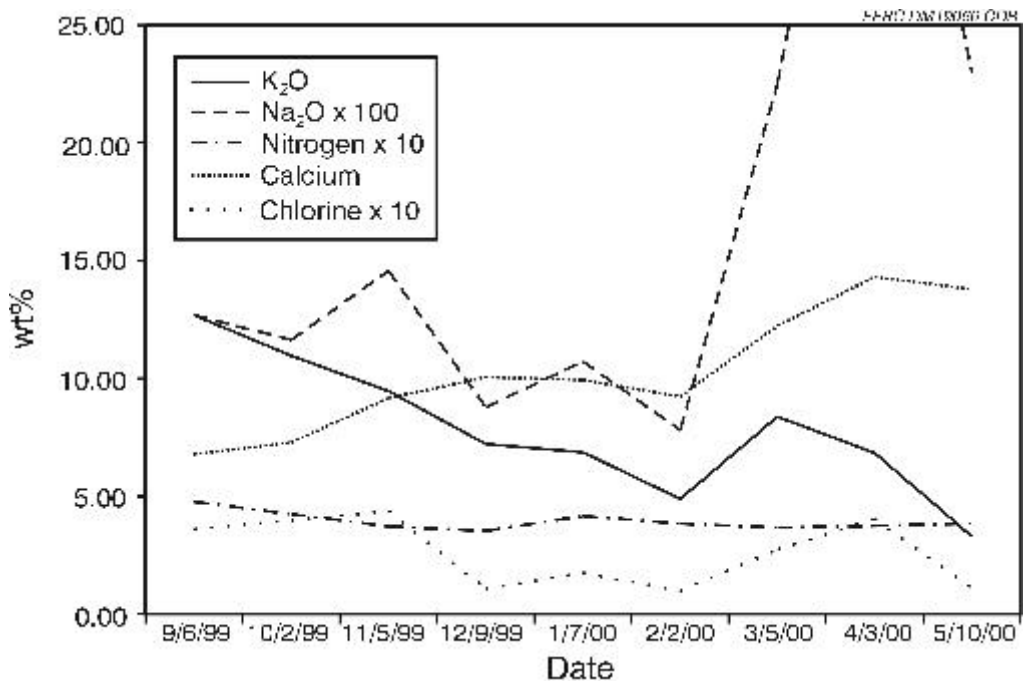


Figure 11. Seasonal changes of unharvested switchgrass from the Schultz farm.

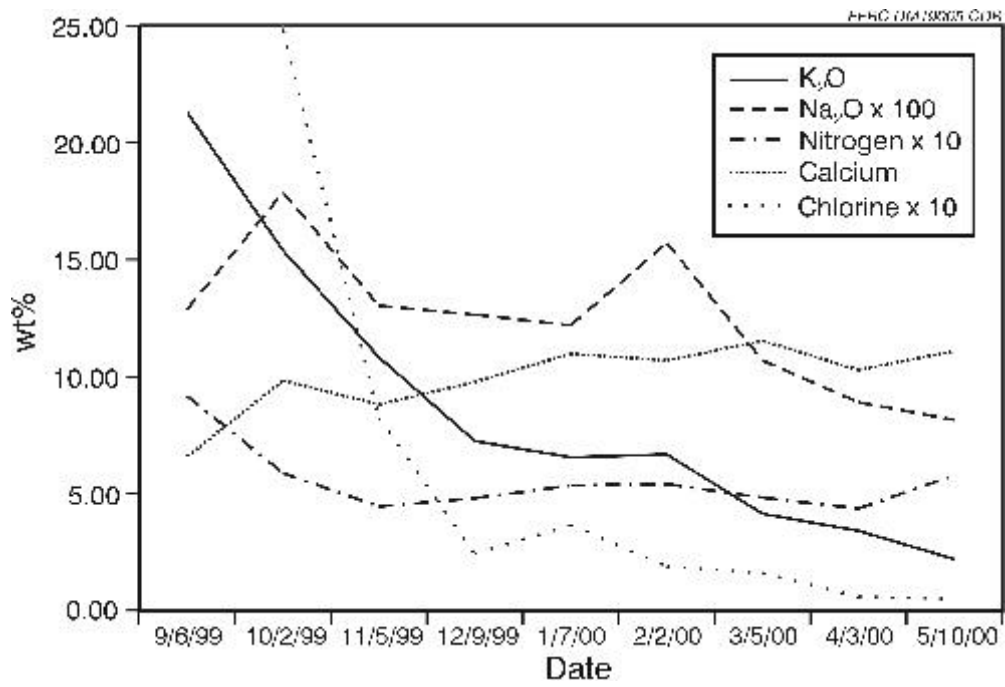


Figure 12. Seasonal changes of unharvested switchgrass from the Sellers farm.

The first freeze of 1999 in southern Iowa occurred at the end of November. Three samples were taken from each farm before the freeze, and three samples were taken from each farm before temperatures reached 70°F in March. Before the first freeze, the average CI level was 0.41% for Schultz and 2.81% for Sellers. It should be noted that the first Sellers reading was 5.1%, so the average is probably shifted too high by erroneous data. After the freeze, the average CI level for Schultz was 0.13%; the average for Sellers was 0.26%. This marks a sharp drop in CI during the time when switchgrass goes into dormancy.

For K<sub>2</sub>O, Schultz recorded a 0.619% average prior to the first frost. Sellers recorded 0.830%. From December to February, the average K<sub>2</sub>O level for Schultz was 0.280%, and the average for Sellers was 0.239%. This drop is caused by switchgrass dormancy, during which time compounds such as K<sub>2</sub>O and CI leave the top of the switchgrass crop and move into the roots.

Figure 13 illustrates the effects of time on ash and alkali content. For some time, switchgrass was considered unusable as an energy crop because of high concentrations of both of these variables. This graph clearly shows that this is the case in August and early September, but by middle to late fall, the levels are much lower. The generally accepted “low” region is from 0.0 to 4.0% for ash, the “middle” region is 4.0 to 8.0%, and any concentration greater than eight is considered high. For alkali, these values are one-tenth those of ash.

### Combustion Characteristics

The presence of alkali and alkaline-earth elements in biomass will have a significant effect on ash viscosity. In switchgrass, elements such as sodium and potassium will be present in a highly

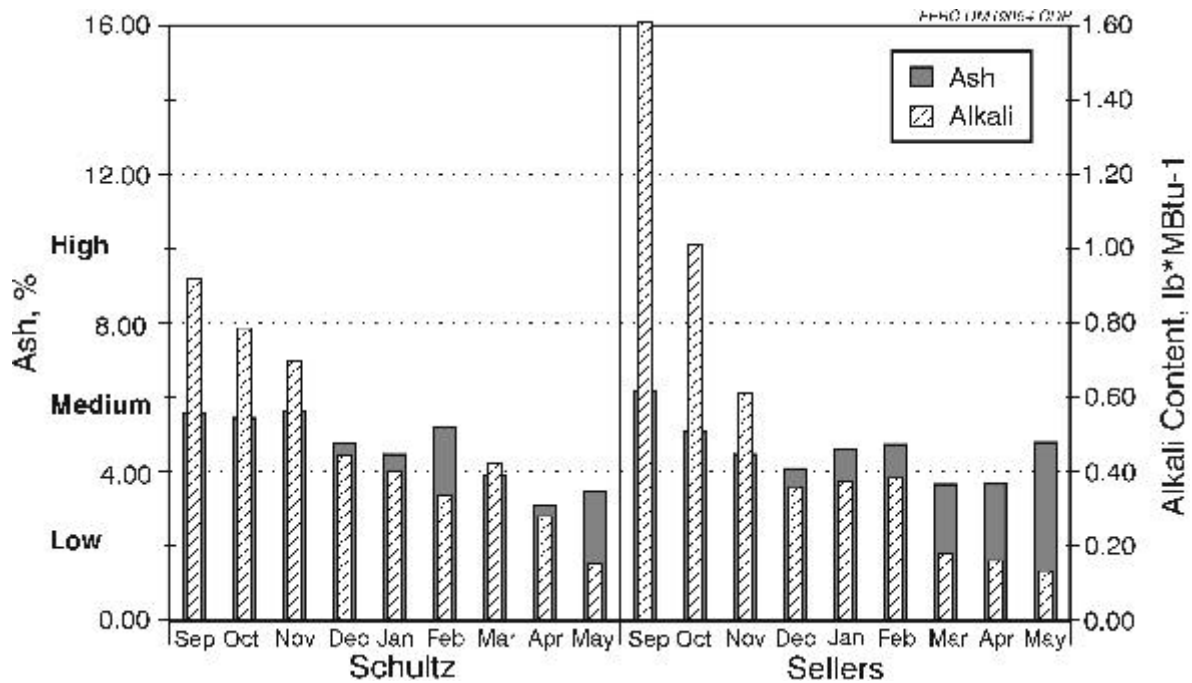


Figure 13. Ash and alkali content for unharvested switchgrass.

dispersed ionized form in the moisture in the internal plant structure. Bulk elemental analysis data for the switchgrass samples and typical combustion temperatures were input into a model that predicts the viscosity of molten ash. Lower-viscosity liquid phases in boiler ash deposits are generally more problematic because they form stickier and harder-to-remove fouling deposits that cover heat-transfer surfaces and degrade boiler performance. Using a number of switchgrass collection dates, Figure 14 shows the time of year when the ash has the lowest and highest viscosity.

At 1200°C, which is a typical fouling temperature, viscosity is a low 2.14 on a log<sub>10</sub> poise basis for September samples. During the late fall and winter months, the viscosities become higher. The first frost in southern Iowa during 1999 occurred at the end of November. This corresponds to a peak in the viscosity before the slope becomes temporarily negative. Soon, the upward trend resumes, and by May, the viscosity increases to 4.26.

## Discussion

### *K<sub>2</sub>O, Na<sub>2</sub>O, and Cl Correlations*

The correlation coefficient for K<sub>2</sub>O vs. Cl is very high for Sellers unharvested and unknown status farms, while it is lower for harvested and Schultz unharvested farms. It should be noted that the harvested farms are lumped together as one, rather than being analyzed county by county or season by season. Since the analysis is based on the hypothesis that weather and geography might affect levels of various chemicals, it seems likely that the r<sup>2</sup> value is just experimental error (six different farms from six different locations were harvested over a period of almost three months).

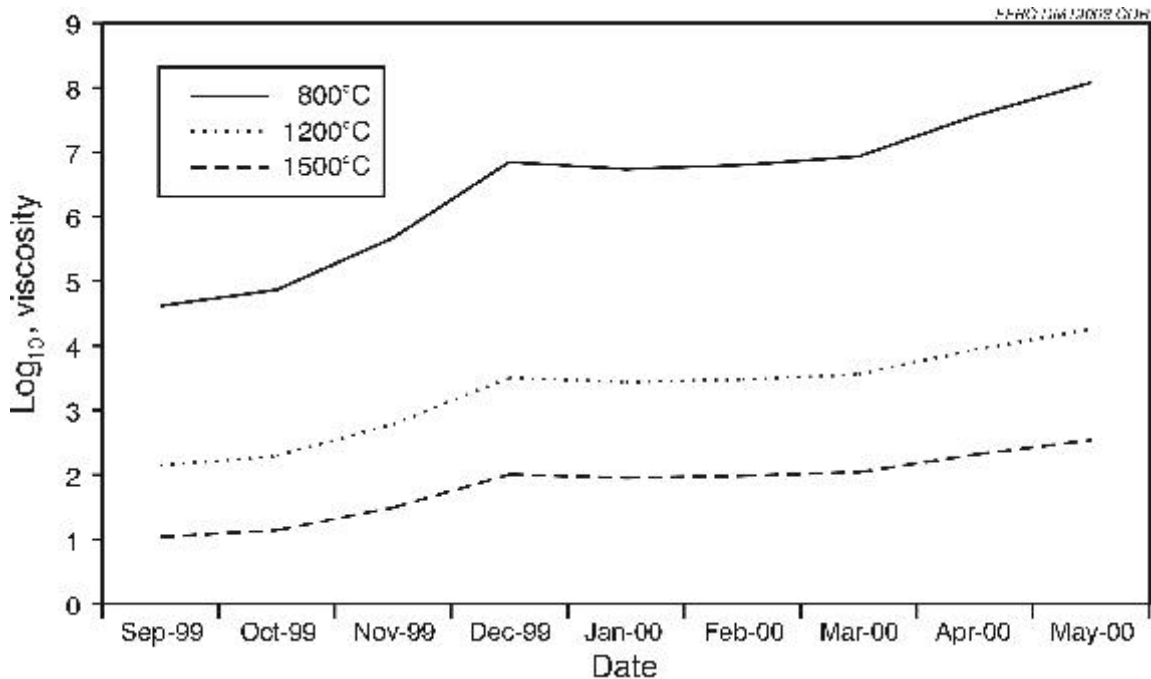


Figure 14. Sellers farm switchgrass ash viscosity by season.

If the harvested data are rejected as erroneous, or at least inconclusive, then two sets of data remain which correlate strongly and one set which does not. This suggests that the correlation between  $K_2O$  and Cl is fairly strong. However, Cl is found mostly in the soil and is used only moderately by plants; experiments have shown that completely removing it from soil will not harm many plants, since the quantity needed can be drawn in from the air (95). Potassium, on the other hand, is highly essential to plant growth and may be unevenly distributed throughout the plant. If the data are not just coincidental, then the association is probably indirect and the switchgrass may be drawing chlorine up through its roots in the form of a potassium compound. Since the plant requires potassium for survival, and since chlorine is neither extremely necessary nor extremely deadly in its ionic state, then potassium will be stored up in the plant's cytoplasm while chlorine is stored into vacuoles for later use.

### ***Geographical Variations***

The data were examined by location and season. According to the Chariton Valley RCD, the samples were taken from six different townships in three different Iowa counties: Appanoose, Lucas, and Wayne. These three counties are adjacent at a common corner, so the geographical differences are not likely to be significant. However, one township in particular did stand out from the rest: Chariton Township, in Appanoose County, gives an average moisture level of 18.4% in Figure 3, where percent is according to weight. This is roughly 50% higher than levels recorded in most other townships and may be due to the presence of a large reservoir in Chariton Township. The only other township with greater than 13% average moisture levels is English Township, in Lucas County, which shows an average moisture level of 15.3%.

Chariton Township and English Township both show fairly high average moisture levels. They also show slightly lower concentrations of  $SiO_2$ , while  $K_2O$  is higher than normal for both townships. These differences seem to match the variations in moisture levels for both townships, suggesting that there may be a connection between water content and the presence of certain oxides.

For some reason, Cl did not correlate with  $K_2O$  according to geography. Chariton Township recorded Cl levels of 2.27%—five times the average value for all the other farms. No other township comes close to matching this number, so it may be a statistical error. English Township, which had the highest moisture level after Chariton, did not show a high chlorine concentration. Geography appeared to have the greatest effect on moisture, Btu/lb, and  $K_2O$ .

### ***Seasonal Variations***

Although the Sellers farm and Schultz farm are in different counties, they have identical sample collection dates and were collected over a period of 9 months. To help normalize any errors, a sample from each month between September and May was chosen and data were examined individually, rather than as an average of the two farms.

Like the geographic differences, seasonal differences seem very clear-cut. The samples from the late spring have high moisture contents and also have the highest calcium levels. Although not shown, the Sellers farm samples taken in September and January both show only 0.01%  $Al_2O_3$ , but the May sample jumps

to 1.35%. A similar increase occurs for the Schultz farm, with an increase from 0.08% to 1.25%  $\text{Al}_2\text{O}_3$ . Unless there are other unknown factors, there appears to be a correlation between the extra spring moisture and the increase in  $\text{Al}_2\text{O}_3$ . This does not occur for the other elements, and its only real significance is that a combination of high potassium and aluminum will result in worse slagging and fouling. However, since  $\text{K}_2\text{O}$  is lowest in the spring, this will tend to offset the high aluminum content, as is shown by the viscosity plot of Figure 14.

Other bulk element readings, such as nitrogen, showed no good correlation between season and concentration, despite the expectation that the first frost of winter would flush out such elements. The  $\text{K}_2\text{O}$  concentration does follow the seasons, as it decreases almost continuously from early autumn to the middle of spring. Since no analyses are available for the following summer months, it is not known whether  $\text{K}_2\text{O}$  will be assimilated back into the year-old switchgrass.  $\text{Na}_2\text{O}$  does not drop as continuously as expected, although Cl does. Note that chlorine seems to follow sodium to some extent for the Sellers but not for the Schultz farm; this is probably an effect of soil composition, assuming NaCl is present in Sellers farmland, and KCl is more abundant at the Schultz farm.

For water-soluble alkalis, the presence of  $\text{K}_2\text{O}$  and Cl is significantly higher in late summer than in the winter or spring.  $\text{K}_2\text{O}$  is about three times as abundant in the fall as it is in the winter and about nine times as abundant again in the late spring. Chlorine levels for the Sellers farm in August are almost certainly skewed (5.1%, as opposed to 0.38% in the next trimester), but the Schultz farm also shows a sharp decrease in Cl (0.37% to 0.18% between August and January). Like  $\text{K}_2\text{O}$ , these values drop even more in the spring, so it seems that an indirect relationship between  $\text{K}_2\text{O}$  and Cl may exist according to seasonal differences.

Finally, the Btu/lb readings show that March seems to have the highest moisture-free burning value, with the Schultz farm giving 7973 Btu/lb and the Sellers farm giving 7926 (Btu/lb for Sellers was slightly higher in January, but the difference is negligible). February showed only 7686 Btu/lb for Schultz and 7783 Btu/lb for Sellers, but April showed moisture-free Btu/lb values within 45 units of those in March. Since this trend is displayed in both sets of data, the best time to harvest switchgrass in this area of southern Iowa is in late March. A February harvest would result in lower moisture-free Btu/lb values.

## **Conclusions**

Switchgrass can be an acceptable energy fuel showing low–moderate ash content, low sulfur, relatively low moisture, and acceptable heat contents. The most important factors in determining levels of various chemical compounds appear to be seasonal and geographical differences. From a standpoint concerned only with the amount of energy present in each sample, early spring is the best harvest time in southern Iowa. From a standpoint of purely environmental views, the time with the lowest concentration of ash and various chemical compounds is probably April or May, although some oxides actually peak in the spring and are less abundant in the early fall. The best time in general to harvest a crop is probably in late March or early April when the crops are coming out of dormancy. At this point, viscosity of liquid phases formed during combustion would be higher because of a lack of alkali and chlorine, and boiler performance would be better. Moisture-free heat content is also high, and even the air-dried switchgrass

readings (for which moisture is still present) show relatively high Btu/lb ratings. This is significant because of the energy requirements needed to dry the harvested switchgrass.

Geographically, the highest, driest areas generally produce more Btu/lb and less  $K_2O$  than do low-lying wetlands. Growing at high elevations means less time air-drying and more heat content per pound, as well as lower  $K_2O$  concentrations, which will reduce the contribution of  $K_2O$  in forming fouling deposits in a boiler.

## **BIOMASS CHARACTERISTICS**

### **Effects of Chemical Composition on Power-Generating Equipment**

Coal and biomass are very different fuels in terms of composition, in particular the inorganic content. In general, biomass contains less sulfur, fixed carbon, and fuel-bound nitrogen and more oxygen than coal. Biomass usually has less ash than coal, and the composition of its ash tends to reflect the inorganic material required for plant growth, while coal ash tends to be composed of mineralogical material. As a result, the alkali metals in coal tend to be less volatile than those found in biomass, meaning that biomass combustion can result in significant deposit formation. Woody biomass tends to have very low chlorine and low alkali metal contents; herbaceous biomass (i.e., grasses and straws) contains more alkali metal and chlorine (96). Appendix E compares the as-received analytical characterizations of 23 different biomass samples ranging from woody biomass and consumer–construction waste to switchgrass and agricultural crops. When these analyses are converted to moisture-free values, woody biomass contains the least ash, silicates, alkali metals, and chlorine, indicating that it should cause fewer operational difficulties than any of the other types of biomass. Nutshells–hulls and waste wood and paper have the potential to cause some slagging, fouling, and corrosion problems, while herbaceous biomass probably poses the greatest potential to form deposits in the boiler.

Studies have been performed on the variability of short rotation woody feedstocks (such as hybrid poplar or willow) and have found minimal compositional variation due to clonal, geographical, and environmental factors, indicating that they are a consistent and stable feedstock for biofuels production (97). Compositional variability has also been assessed for herbaceous energy crops. In this case, large differences in composition were found between stems and leaves, with leaves containing much higher concentrations of nonstructural components. The geographic location of where the plants were grown was found to affect the composition even more than differences between varieties (98). Switchgrass was singled out for study of its suitability for conversion into fuel or as a source of energy when combusted. The results indicated that it would be a versatile bioenergy feedstock. Switchgrass's energy content is comparable to that of wood but with a significantly lower initial moisture content. Extensive analysis of ash and alkali content shows that switchgrass should have a low slagging potential in coal-fired combustion systems (99).

## **Effects of Physical Characteristics on Process Design and Equipment**

Biomass resources that are used during fuel, chemical, and electric power production vary over a wide range, and each type has unique characteristics that should be taken into account when applying them to unconventional uses. Examples of biomass resources include postconsumer wastes such as construction–demolition wood, yard waste, waste newsprint, waste writing paper, corrugated cardboard, and kraft paper; agriculture residues such as wheat straw and husks, corn stoker, cobs, and husks, rice stoker and hulls, bagasse, and edible nut processing wastes; forest residues, including waste wood from processing or in-forest residue; dedicated short-rotation woods, including hybrid poplars, willows, black locust, and eucalyptus; herbaceous crops such as switchgrass and reed canary grass; and oil seeds such as soybean, sunflower, and rapeseed (100). A number of added chemical constituents can be found in the postconsumer wastes. The harvest of agricultural residues usually takes place within a short span of time (usually once a year), requiring the availability of ample storage space. Agricultural residues that are collected and centralized because of processing are particularly attractive and have an innate advantage resulting from their chemical composition in that they are easily delignified. On the other hand, softwoods such as are found in wood processing are difficult to delignify. Short-rotation woody crops are mostly hardwoods and are relatively easy to delignify, but because these trees are of smaller diameter than those from conventional forestry, cost-effective harvesting methods must still be developed. Herbaceous energy crops can be planted, harvested, and stored using conventional farming equipment (100).

## **Biomass Production, Harvesting, Transport, and Storage Issues**

The U.S. Department of Energy (DOE) has developed strategies relating to the improved production of short-rotation woody crops for fiber and energy uses for four major geographical regions in the United States (101). Integrated research and industry participation have contributed to woody crop development in the Pacific Northwest, and the lessons learned are contributing to further development in the other three regions. Among the projects included in the work performed by DOE is an estimation of the cost of producing dedicated energy crops for several regions of the United States. Switchgrass and hybrid poplar were chosen as representative herbaceous and woody crop species for the estimation. Out-of-pocket cash expenses (fertilizer, seed, etc.), fixed costs (taxes, overhead), and the costs of owned resources (equipment depreciation, land values, etc.) were all included in the estimation. The competitiveness of energy crops with conventional crops varied by region. Break-even prices for poplar were found to be higher than for switchgrass in all regions because of the higher cost of producing poplars (102). The potential production of biomass wood and grass crops in the United States in 1995 was estimated to be 34 million acres for switchgrass and 20 million acres for wood crops including poplar or willows (103).

The feasibility of using urban wood waste such as creosote-, pentachlorophenol-, and chromated copper arsenate-treated wood; particleboard–plywood; and construction–demolition debris has also been examined. Regulatory concerns will probably affect the extent of the use of treated wood and construction–demolition debris. Regulatory issues, the quantity of waste generated, and the need for fuel for electricity-generating facilities and other end markets are interdependent and affect the demand for and prices and supply of urban wood waste in complex ways (104). The complexity of utilizing urban wood

waste as a biomass energy source may hinder its development relative to dedicated crops such as hybrid poplars or switchgrass.

The economics and the physical and chemical makeup of crops that are grown as dedicated biomass feedstocks are significantly affected by harvesting, transport, and storage practices. The high yields of switchgrass that can be expected when grown as an energy crop can cause problems during baling operations that range from occasional jamming of smaller balers to considerable difficulty with larger balers (105). Changes in the design and operation (or both) of commercial mowing and baling equipment may be required if it is to be used to harvest herbaceous energy crops.

When thick-stemmed species such as forage sorghum and Napier grass are harvested for biomass uses, their relatively high moisture content (up to 60% to 70%) necessitates that they be handled and stored as silage rather than in bales. The cost of harvesting and transporting the heavier silage has been estimated to range from \$2.81 to \$10.83/dry ton (106).

A study has found that weathering of switchgrass bales because of outdoor storage results in changes in switchgrass composition, especially in the cellulose, hemicellulose, extractive, and ash contents. Loss of carbohydrates and extractives obviously has a greater impact on the use of switchgrass as a feedstock for the production of ethanol than on its use in power generation by cofiring with coal (107). However, changes in ash composition can affect its behavior during cofiring. Ten biomass feedstocks were exposed to weathering because of open storage during another study. Four of the biomass feedstocks were woody, and six were herbaceous. Among the woody samples, only hybrid poplar ash content tended to increase during weathered storage. Ash levels increased for most of the herbaceous feedstocks during storage (108).

## **Biomass Grinding and Feeding Methods and Equipment**

### ***Chipping and Grinding***

Preparation of biomass for cofiring in a boiler requires reducing the material to a fairly uniform, small size. In the case of short-rotation woody crops such as hybrid poplar, the comminution can take place in the field just after felling the trees. Virtually all chippers produce wood chips that are acceptable for the direct combustion energy market. The highest-quality chips are produced by large, stationary disk chippers. The blade and anvil on disk chippers can be set to control chip thickness, and the larger size results in more uniform speeds and, therefore, more uniform wood chips. Drum chippers can process larger, less uniform material than an equivalently sized disk chipper. Drum chipper knives can be sharpened many times without removing them, making them attractive for use in the production of biomass fuel (109).

Small-diameter woody crops are not easily harvested with equipment designed for the substantially larger trees that are normally processed in the timber industry. Whole trees cannot be as efficiently packed as wood chips, resulting in higher transportation costs for whole trees. One way to reduce transport cost (one of the main costs associated with biomass production) is to chip the wood at the harvesting site and transport only the chips. Special equipment has been designed and tested that combines the harvesting and

comminution of woody biomass, including cut-and-chip harvesters, cut-only harvesters, and cut-and-forward harvesters (109). Cut-and-chip harvesters chip the material immediately after felling and debarking. Some models of cut-and-chip harvesters are Salix Maskiner Harvester, Texas A&M Harvester, Austoft sugar cane harvester, Claas Jaguar, John Deere 6910 harvester, and New Holland 719 harvester. Cut-only harvesters fell the trees and crush or bundle the wood trunks. Examples of cut-only harvesters include Frobbesta Harvester, Empire 2000, Nicholson Harvester, and Energiskogsmaskiner AB Harvester. The cut-and-forward harvesters fell and transport large quantities of trees from the harvest site to the highway trucks or railcars; an example is the Brunn AIB SRICB Harvester (109).

Many of these multiple-function machines were not effective during field testing, but the continuous-travel feller–chippers (such as the Class Jaguar) are the best multipurpose machines tested to date. Production rates can be quite impressive. The chips are blown into chip bins and transported to the power plant or other final destination, minimizing the amount of handling and equipment needed (109).

It is not necessary to size herbaceous biomass in the field as a step in the harvesting process. Rather, the biomass is usually baled and transported to the site at which it will be used. Size reduction at that site is usually accomplished by hand-fed brush chippers (110), hammermills, horizontal or tub grinders, or augers. Augers such as the Komar Tri-Auger can provide primary and secondary shredding of many types of materials. The shredded material is thoroughly blended before injection into a boiler (111). Occasionally, herbaceous biomass is briquetted prior to feeding, with the briquettes providing a more uniform feed. Common densification machines include screw presses, pelletizing presses, roll presses, and cubing machines (112). Biomass charcoal has been produced from eucalyptus, kiawe, leucaena wood, and kiki, macadamia, and palm nutshells. Cofiring of the charcoal does not require a separate biomass feed system.

Table 6 lists some Internet Web sites at which many vendors offering equipment needed in the wood energy industry can be identified and contacted. Some vendors provide chipping and grinding equipment, and others can provide fuel-metering and feeding equipment.

### ***Feeding Biomass to a Combustor***

The most common method of feeding biomass to a combustor is by injection of powdered fuel. One of the most important requirements of fuel feeding is a very homogeneous mass flow. A constant mass flow rate can be difficult to achieve, but one method that has been found to work is a pneumatic feeding system that incorporates a screw feeder with a vibrating conveyor to homogenize the flow rate (113).

As noted, fuel properties play a critical role in handling and feeding wood and wood–coal blends. When a tub grinder is used to comminute the wood, the amount of fines is increased. Fines can affect the fuel flow characteristics by changing the slumping behavior that assists fuel flow into the chutes and by forming “plugs” of fines within the bins. When the plugs pass down the chute and onto the grate—into the boiler, they adversely affect the consistency of the fuel mixture’s burning characteristics (114). Bridging of biomass in storage bins can also be a problem, although one that

TABLE 6

## Wood Energy Equipment Vendors Found on the Internet

Web Site Name	Web Site Address	Type(s) of Equipment Mentioned
Directories of Wood Energy Equipment Vendors and of Wood Chip Suppliers and Brokers in the Northeast	<a href="http://rredc.nrel.gov/biomass/doe/rbep/equip_vend/index.html">http://rredc.nrel.gov/biomass/doe/rbep/equip_vend/index.html</a>	A listing of 76 vendors offering wood chippers and classifiers, transport systems, and feeders
Keith Walking Floor	<a href="http://www.keithwalkingfloor.com">http://www.keithwalkingfloor.com</a>	Conveying and unloading systems
Wisconsin's Renewable Energy Yellow Pages – Wood Energy Equipment & Services	<a href="http://www.mailbag.com/users/mjvrenew/wood.html">http://www.mailbag.com/users/mjvrenew/wood.html</a>	A listing of 16 vendors of industrial heating equipment, fuel-handling systems, burners, and boilers
Chemco Equipment	<a href="http://www.chemcoequipment.com">http://www.chemcoequipment.com</a>	Grinding and feed systems
Primenergy, Inc.	<a href="http://primenergy.com">http://primenergy.com</a>	Biomass energy conversion systems

can be addressed by changing the geometry of the bin and design of the discharge feeder. Most screw feeders tend to draw material primarily from the rear of the bin and pack material against the front wall, often resulting in severe plugging. A nonconsolidating “moving hole” feeder averts these problems by avoiding packing of the material in the bin and permitting reliable, first-in, first-out flow for the fuel. The moving hole feeder consists of one or more slots that traverse back and forth without any friction between the stored material and the feeder deck. The feeder relies entirely on gravity for material discharge (115).

HiMicro Incorporated is developing specialized mills for pulverizing–micronizing coal and biomass solid fuels. In cofiring applications, there are essentially two modes of biomass processing–size reduction and handling: separate biomass grinders and feeders and copulverization and feeding of coal and biomass. Copulverization options include processing using existing coal pulverizers or through specialized mills that

bypass and/or replace the existing coal pulverizers. The fibrous nature of biomass results in relatively coarse material when conventional size-reduction equipment such as tub grinders, hoggers, and hammer mills are used. Pine bark and switchgrass that were ground using the HiMicro mills were in the size range of pc particles, or 40–60  $\mu\text{m}$  in diameter. This is more than ten times smaller than is typical for other types of grinders. No transport or feeding difficulties were noted during pilot-scale cofiring combustion tests conducted in DOE's Combustion and Environmental Research Facility (116).

### **Results of Biomass–Coal Cofiring Studies**

Successful biomass cofiring has been tested in pc boilers (both wall- and tangentially fired), cyclone boilers, fluidized-bed boilers, and spreader stokers. The tests have shown that effective substitutions of biomass for coal can be accomplished with modifications to only the feed intake system and burners of existing power stations (14–18, 24, 25).

Parametric cofiring tests have shown that separate feeding of biomass and coal was more appropriate than feeding a biomass–coal mixture. When biomass and coal are pulverized and fed as a mixture, the percentage of biofuel is limited to about 5 wt% of the total fuel to the boiler, the power required to operate the mill increases, and sieve analysis can degrade. Favorable results were obtained when wood waste of 0.25-in. top size was pneumatically transported to the boiler, introduced down the centerpipe of the pc burners, and diffused into the coal flame by means of an inverted diffuser cone installed at the centerpipe exit (18).

Low-percentage cofiring using sawdust waste wood has been commercialized by the Tennessee Valley Authority. During the commercialization process, a low-cost, highly effective materials-handling system was implemented for the cofiring of waste wood with coal in a wall-fired pc boiler. A trommel screen was used to size the sawdust to  $\frac{3}{4}$  in. The sized sawdust was ejected from the trommel screen directly onto a conveyor and transported to a feeder where it was metered into the reclaim hopper. The reclaim hopper feeders were vibrated to permit good sawdust flow, even during periods of light rain (117).

Herbaceous biomass generally contains more silicon, potassium, and chlorine than other biomass fuels, indicating that it could cause potentially severe ash deposition problems. The potassium that is present in biomass is predominantly biologically occurring material and is, therefore, quite mobile and available for deposit-forming reactions. Chlorine can play a major role in deposit formation by facilitating the mobility of inorganic potassium compounds as well. Fuels with less alkali, chlorine, silica, and total ash-forming material and higher calcium contents resulted in the most manageable ash deposits during extensive pilot-scale studies conducted in biomass boilers (25).

Switchgrass has been successfully cofired with coal in a 50-MW, wall-fired, pc utility boiler. A tub grinder was used to reduce the switchgrass size to 90% less than 10 cm in length with stems shattered. A hammer mill gave better size reduction, but it was difficult to feed. The coarser particles produced by the tub grinder increased the quantity of unburned carbon in the bottom and cyclone ashes. It was noted that dust from switchgrass shredding can be a major problem and that pulverizing switchgrass requires a good dust control system. Switchgrass cofiring did not adversely affect boiler operation, and in fact, nitrogen

oxide emissions were reduced 31%, and opacity was reduced 62% when cofiring. Neither slagging and fouling of the boiler or degradation of the electrostatic precipitator was observed (25).

A study conducted by researchers at Sandia National Laboratories, Combustion Research Facility in Livermore, California; the National Energy Technology Laboratory in Pittsburgh, Pennsylvania; and NREL in Golden, Colorado, focused on four critical fireside issues associated with cofiring: ash deposition, NO<sub>x</sub> production, corrosion, and carbon burnout. Pilot-scale data indicate that ash deposition rates and NO<sub>x</sub> emissions can either exceed or be less than those of coal, depending upon the type of biomass. The potential for chlorine-based corrosion is seen to be less significant when blends are cofired than when pure biomass is fired, but it is not always negligible. Diameters larger than 0.125 in. increase the chance of incomplete combustion of the biomass. Fireside problems can be minimized by careful selection of fuels, boiler design, and boiler operation. Less prudent choices could lead to significant boiler damage and operational costs. Guidelines that were developed based upon the results of this study can be summarized as follows (40):

- NO<sub>x</sub> emissions
  - Chemical interaction between the offgases from biomass and coal that would alter NO<sub>x</sub> emissions is insignificant.
  - NO<sub>x</sub> emissions from wood residues are generally lower than those from coal, leading to some overall NO<sub>x</sub> reduction relative to coal during cofiring.
  - The large volatile yield from biomass can be used to lower NO<sub>x</sub> cofiring through well-established, stoichiometric-driven means.
  
- Ash deposition
  - Deposition rates should decline when cofiring wood or similar low-ash, low-alkali, low-chlorine fuels.
  - Deposition rates should increase when cofiring high-ash, high-alkali, high-chlorine fuels such as many herbaceous materials.
  - Deposition rates depend strongly on interactions between the cofired fuels as well as on individual fuel properties.
  
- Carbon conversion
  - Biomass prepared with top sizes greater than 0.125 in. will experience increasing difficulty in achieving burnout, with significant residual carbon expected at sizes greater than 0.25 in.
  - Biomass fuels having moisture contents in excess of 40% must be further reduced in size to achieve burnout.
  - Biomass char-burning rates are controlled by geometry and size, not kinetics, making burning rates essentially fuel-independent if size, shape, density, and moisture contents are the same.
  
- Corrosion
  - Fuel chlorine should be minimized in all cases.
  - Tube surface temperatures should be kept as low as possible.
  - Less chlorine is present in the deposits when sulfur is also present.

## Summary of Literature and Background on Biomass Processing

Biomass can be successfully cofired with coal in both wall- and tangentially fired pc boilers, cyclone boilers, fluidized-bed boilers, and spreader stokers. Woody biomass is the preferred cofire fuel because it contains less ash, silicates, potassium, and chlorine that could stimulate deposit formation. Herbaceous biomass (such as switchgrass and straw) contain more of the chlorine, silicates, and alkali metals that facilitate deposition, but they can be used if care is taken during selection and fuel preparation. Deposition rates have been found to depend strongly on interactions between the cofired fuels as well as on individual fuel properties. Biomass should not be stored outdoors for long periods of time as the material tends to degrade during storage.

Proper fuel preparation is an important factor in successful cofiring. The biomass should be uniformly pulverized to at least  $\frac{1}{4}$  in. diameter (preferably  $\frac{1}{2}$  in.). Drum chippers work well for woody biomass comminution, while hammer mills are the most effective for pulverizing herbaceous biomass. Wet biomass should be pulverized to a smaller size to minimize residual carbon in the ash. The biomass should be fed to the boiler separately from the coal. Transport of the biomass can be made more consistent by adding vibration to the conveyors and bins.

$\text{NO}_x$  emissions are not adversely affected by the addition of biomass. In fact, when woody biomass is cofired with coal, the overall  $\text{NO}_x$  emissions are often reduced. Corrosion can be minimized by keeping the tube surface temperatures as low as possible and by firing higher-sulfur-content coal with higher-chlorine-containing biomass since less chlorine is present in deposits when sulfur is also present in the system.

## Biomass Processing Data Results

Table 7 shows size reduction and processing data for the raw wheat straw, alfalfa stem, and hybrid poplar biomass. The average bulk densities for baled wheat straw, alfalfa, and hybrid poplar were 89.7 kg-cu-m (5.6 lb-cu-ft), 147.4 kg-cu-m (9.2 lb-cu-ft), and 259.0 kg-cu-m (16.169 lb-cu-ft), respectively. The average bulk density of wheat straw was 11.77 kg-cu-m (0.74 lb-cu-ft), and the average bulk densities of alfalfa (with leaves) and alfalfa stems were 13.3 kg-cu-m (0.83 lb-cu-ft) and 18.58 kg-cu-m (1.16 lb-cu-ft), respectively. The bulk densities of shredded wheat straw, alfalfa stems, and hybrid poplar were 189.0 kg-cu-m (11.8 lb-cu-ft), 198.6 kg-cu-m (12.4 lb-cu-ft), and 388.0 kg-cu-m (24.2 lb-cu-ft), respectively.

Approximately 9.1 kg (20 lb) each of shredded wheat straw, alfalfa stems, and hybrid poplar were subsequently produced for combustion testing. The typical appearance of the shredded material is shown in Figure 15. The shredded biomass material itself, as well as 20% blends with the coals, was found to feed quite evenly, even though two quite dissimilar materials were mixed. Good burnout was achieved with the pure biomass, although some unburned char was produced with the alfalfa stem blends.

TABLE 7

Bulk Density Values for Wheat Straw, Hybrid Poplar, and Alfalfa, lb/cu-ft				
Material	Test 1	Test 2	Test 3	Average
Wheat Straw Bale	5.2	6.0	NA <sup>1</sup>	5.6
Alfalfa Bale	9.5	8.9	NA	9.2
Wheat Straw	0.641	0.765	0.800	0.735
Alfalfa (with leaves)	0.934	0.757	0.790	0.827
Alfalfa Stems	1.19	1.20	1.08	1.16
Chipped Hybrid Poplar	16.0	16.4	—	16.2
Shredded Wheat Straw	11.8	11.6	12.0	11.8
Shredded Alfalfa Stems	12.5	12.2	12.5	12.4
Shredded Poplar	24.5	24.0	—	24.2

<sup>1</sup> Not available.



Figure 15. Wheat straw and alfalfa stems before and after shredding.

Two hybrid poplar trees from a tree farm test plot located in northwestern Minnesota were felled and delimbed, creating approximately 261 kg (575 lb) of main stem and 79 kg (175 lb) of branches (Figure 16). Coarse size reduction of the main stem was successful using an industrial, portable chipper. The chipper accepted the 76-cm (30-in.) cut length stems, some up to 25.4-cm (10-in.) diameter, without prior splitting. The chipper produced relatively flat strips of wood ranging up to 15 cm (6 in.) in length and 2.5 cm (1 in.) in width. All of the main trunks and stems were processed through the chipper. Smaller leafy branches were not processed as they showed somewhat advanced mold growth even after a few days' storage in the closed barrels. A single barrel of chipped stems was placed in frozen storage for future CEPS combustion tests, and a second barrel of material was selected for subsequent processing in the Nelmor knife shredder.

The as-received chipped stems were too moist initially, and the Nelmor shredder would not process the chips to pass through a 1/16 screen. After the chips were floor-dried for 2 days to reduce moisture, they were successfully shredded, and the final product was sealed in plastic-lined drums for further processing and combustion testing. Commercial use of hybrid poplar in combustion systems will require some degree of drying and processing because of its pliability and high moisture content.

## BIOMASS CHARACTERIZATION

Part of the characterization task of the biomass work involved modifying techniques for effective characterization of biomass. Pulverized-coal samples are prepared for CCSEM analysis by

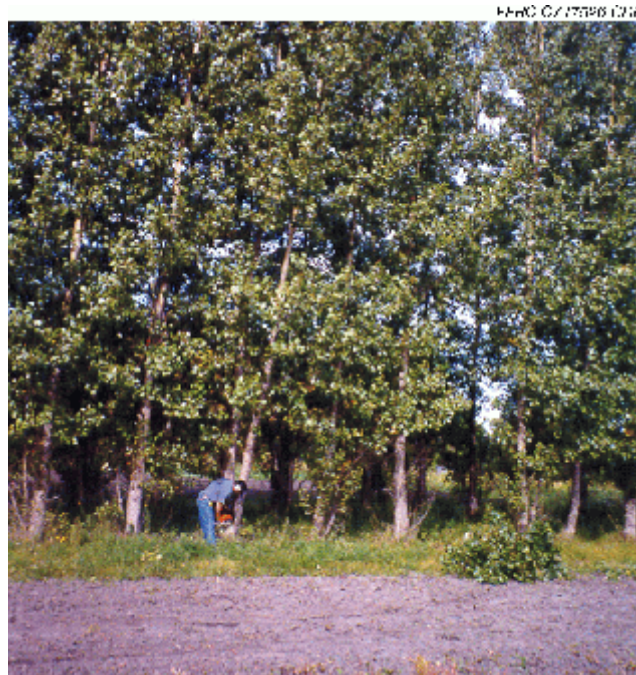


Figure 16. Hybrid poplar tree being harvested from an experimental tree farm in northwestern Minnesota.

mounting in carnauba wax, cross-sectioning, polishing, and coating with a 20-nm layer of carbon to provide a flat, highly conductive surface. This preparation method was found to be completely unsuitable for biomass material because of the inability to polish the specimen and severe charging in the SEM. A method was adopted using light element binders and high pressures to press a sample against a highly polished surface. Carbon powder is mixed with the sample and binder to improve conductivity between particles and a very fine wire pressed into the sample to increase conductivity and reduce particle charging. A modified CCSEM technique was used to collect data on particle size and chemistry of the inorganic constituents in wheat straw, alfalfa stems, and hybrid poplar. Major mineral species for the coals and for the biomass samples as determined by CCSEM are given in Table 8. The majority of the larger inorganic material in these biomass samples is in the form of thin amorphous silicate structures or phytoliths. Figure 17 shows these structures after the surrounding organic material has been removed by a chemical oxidation procedure (29). The physical form of this silica may result in deposition behavior quite different from silica in quartz or clays found in coals.

### Analytical Technique Development and Fuel Characterization Results

Methods for accurately quantifying organically bound elements in biomass fuels using chemical fractionation were developed. Cold chemical digestion using concentrated nitric acid followed by inductively coupled plasma (ICP) analysis of the elemental chemistry of biomass fuels was determined to be giving erroneous numbers for silica in the chemical fractionation leaching extracts for wheat straw, alfalfa, and other biomass types that were investigated. The silicon concentrations determined by this method were below detection in some cases using ICP, while in comparison, XRF analysis showed 10%–20% silicon in the bulk ash. It was determined that nearly

TABLE 8

CCSEM Mineral Content of the Fuels					
	Absaloka				
	Illinois No. 6	Coal	Wheat Straw	Alfalfa	
	Coal	Sample 1	Biomass	Biomass	Hybrid Poplar
Mineral Fraction:	19.442	8.449	0.855	2.412	2.299
Mineral, wt%	Total	Total	Total	Total	Total
Quartz	15.3	17.7	26.1	34.3	1.9
Iron Oxide	1.1	4.2	1.5	0.3	9.1
Calcite	3.5	11.5	4.5	37.7	68.6
Kaolinite	8.2	30.9	0.0	0.0	0.9
K Al-Silicate	7.5	3.3	0.0	0.5	0.6
Pyrrhotite	46.3	8.6	0.0	0.0	0.7
Si-Rich	2.4	1.1	11.4	5.1	0.4
Unknown	8.2	8.7	55.3	18.6	9.3
Other	7.5	14	1.2	3.5	8.5

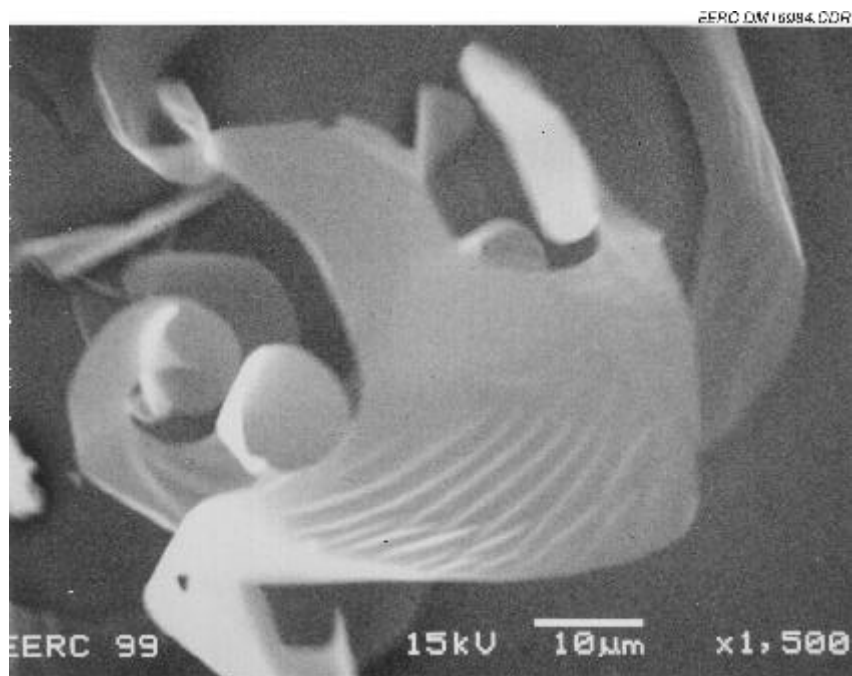


Figure 17. Phytolith structures of wheat straw.

all the silicon present was not solubilized during the ICP pretreatment, and an alternate lithium metaborate ash fusion method is required for silicon determination. The ability to use ICP is of importance for the analysis of low-ash-content biomass materials, requiring much less sample to be processed in the CHF analysis procedure than does analysis by ashing and XRF analysis. The CHF analyses are given in Table 9.

The proximate and ultimate analyses of the coals and the biomass materials are given in Table 10 and the ash chemistry analysis in Table 11. Because of the high level of volatile potassium and other inorganic material in the biomass samples, ashing was performed at a lower temperature than that for coal procedures (575°C; 1067°F) following American Society for Testing and Materials (ASTM) Procedure E 1755-95 (118). A second sample of the Absaloka subbituminous coal with slightly different analyses was used for the combustion tests with the hybrid poplar blends. Proximate–ultimate and ash chemistry of the blends were not analyzed, but calculated based on the analyses of the parent fuels.

The biomass samples have a lower heating value and are characterized by much higher volatile matter and oxygen content and lower sulfur than the coals. The wheat straw ash level is similar to that of the Absaloka coal, with the alfalfa stems and hybrid poplar having a much lower ash content than the coals. Although the ash content is lower, each of the three biomass materials has a distinctly different ash chemistry. The wheat straw ash contains primarily silica along with significant potassium, while the alfalfa stems contain nearly equal amounts of silica, calcium, and potassium along with significant phosphorus. Both have very high chlorine content. In contrast, the hybrid poplar ash is comprised mostly of calcium and potassium, again with significant phosphorus present. The presence of significant, potentially

TABLE 9  
CHF Analysis of Fuels, wt%

	Element	Removed by Water	Removed by NH <sub>4</sub> OAc	Removed by HCl	Remaining
Illinois No. 6	Si	0	0	0	100
	Al	0	0	0	100
	Fe	9	0	0	91
	Ti	0	0	2	98
	P	0	0	0	100
	Ca	19	74	0	7
	Mg	3	6	0	91
	Na	47	17	3	33
	K	2	2	2	94
Absaloka	Si	0	0	0	100
	Al	0	0	18	82
	Fe	8	5	28	59
	Ti	0	6	6	88
	P	0	3	91	6
	Ca	0	70	30	0
	Mg	0	68	17	15
	Na	58	42	0	0
	K	2	8	7	83
Wheat Straw	Si	2	16	3	79
	Al	12	44	44	0
	Fe	3	2	16	79
	Ti	0	1	1	98
	P	100	0	0	0
	Ca	14	51	19	16
	Mg	55	45	0	0
	Na	71	20	1	8
	K	88	12	0	0
Alfalfa Stems	Si	31	69	0	0
	Al	18	57	24	1
	Fe	2	4	19	75
	Ti	5	16	10	69
	P	79	14	0	7
	Ca	14	44	26	16
	Mg	46	42	0	12
	Na	68	25	4	3
	K	72	21	0	7
Hybrid Poplar	Si	19	41	16	24
	Al	16	34	1	49
	Fe	15	25	56	5
	Ti	23	40	21	16
	P	50	43	5	2
	Ca	8	69	23	0
	Mg	21	76	2	1
	Na	51	30	12	7
	K	62	38	0	0

TABLE 10

## Proximate and Ultimate Analysis of the Fuels

Fuel	Absaloka		Wheat Straw	Illinois No. 6			Absaloka		Illinois No. 6		Absaloka	
	Coal	Sample 1		Coal	Sample 1	Wheat Straw	Wheat Straw	Alfalfa	Alfalfa	Hybrid	Hybrid	Sample 2
	Coal	Sample 1	Sample 2	Biomass	80%–20% Blend (calculated)	80%–20% Blend (calculated)	Alfalfa	80%–20% Blend (calculated)	80%–20% Blend (calculated)	Poplar	80%–20% Blend (calculated)	80%–20% Blend (calculated)
Proximate Analysis, as received wt%												
Moisture	3.31	22.00	21.00	9.60	4.57	19.52	7.80	4.21	19.16	5.20	3.69	17.84
Volatile Matter	33.27	33.71	36.25	74.40	41.50	41.85	82.92	43.20	43.55	78.85	42.39	44.77
Fixed Carbon	53.16	36.39	33.40	8.38	44.20	30.79	5.35	43.60	30.18	14.82	45.49	29.68
Ash	10.26	7.90	9.34	7.62	9.73	7.84	3.93	8.99	7.11	1.13	8.43	7.70
Ultimate Analysis, as received wt%												
Hydrogen	5.13	6.33	5.61	5.91	5.29	6.25	6.11	5.33	6.29	6.13	5.33	5.71
Carbon	67.70	52.82	49.44	38.29	61.82	49.91	41.83	62.53	50.62	45.04	63.17	48.56
Nitrogen	1.18	0.65	1.07	0.76	1.10	0.67	1.64	1.27	0.85	0.82	1.11	1.02
Sulfur	3.60	0.57	0.78	0.23	2.93	0.50	0.12	2.90	0.48	0.25	2.93	0.67
Oxygen	12.13	31.73	33.74	47.18	19.14	34.82	46.37	18.98	34.66	46.63	19.03	36.32
Ash	10.26	7.90	9.34	7.62	9.73	7.84	3.93	8.99	7.11	1.13	8.43	7.70
Heating Value, Btu/lb	11,500	8981	8720	6462	10,492	8477	7112	10,622	8607	7641	10,728	8504
Chlorine, μg–g dry basis	340	50	50	2120	696	464	2340	740	508	93	291	59

TABLE 11

## Bulk Ash Chemistry of the Fuels, wt%

Fuel	Illinois No.	Absalok	Absalok	Wheat Straw Biomass	Illinois No.	Absaloka	Illinois No. 6 Alfalfa Blend	Absaloka	Illinois No. 6 Hybrid Poplar Blend	Absaloka	Illinois No. 6 Hybrid Poplar Blend	Absaloka
	6	a	a		6	Sample 1		Sample 1		6		Sample 2
	Coal	Coal	Coal		Wheat 80%–20% Blend (calculated)	Wheat 80%–20% Blend (calculated)	Alfalfa Biomass	Alfalfa Blend (calculated)	Alfalfa Blend (calculated)	Hybrid Poplar Biomass	Hybrid Poplar Blend (calculated)	Hybrid Poplar Blend (calculated)
SiO <sub>2</sub>	53.1	32.8	24.9	63.9	54.8	38.8	30.0	51.1	32.5	4.6	51.8	31.8
Al <sub>2</sub> O <sub>3</sub>	20.3	18.9	16.7	0.0	17.1	15.2	0.5	18.6	16.9	1.5	19.8	18.3
Fe <sub>2</sub> O <sub>3</sub>	14.2	4.8	5.1	0.4	12.0	3.9	0.7	13.0	4.3	2.0	13.9	4.7
TiO <sub>2</sub>	0.9	0.9	0.8	0.1	0.8	0.7	0.1	0.8	0.8	0.1	0.9	0.9
P <sub>2</sub> O <sub>5</sub>	0.2	0.4	0.3	1.3	0.4	0.6	8.7	0.9	1.3	7.8	0.4	0.7
CaO	3.4	20.2	30.0	3.4	3.4	16.9	25.1	5.3	20.7	49.0	4.6	21.2
MgO	1.6	5.4	3.2	1.7	1.6	4.7	4.3	1.8	5.3	8.5	1.8	5.5
Na <sub>2</sub> O	1.3	0.7	1.4	2.7	1.5	1.1	1.5	1.3	0.8	0.4	1.3	0.7
K <sub>2</sub> O	2.1	0.5	0.5	22.6	5.3	4.8	27.9	4.4	3.5	24.9	2.7	1.3
SO <sub>3</sub>	2.9	15.6	17.1	4.0	3.1	13.3	1.2	2.8	14.0	1.2	2.9	15.1

volatile potassium can be expected to contribute to increased ash deposition during combustion. The chlorine level in the two herbaceous biomass samples is also nearly an order of magnitude higher than in the Illinois No. 6 coal and 40 times higher than in the Absaloka subbituminous coal, indicating that corrosion on metal heat exchange surfaces may be an issue. The effect of the biomass ash composition on the blends is not as pronounced as would be expected, since the 80% coal–20% biomass are prepared by weight on an as-received basis. The higher moisture and ash content of the coals tend to dominate and mask the calcium, potassium, and phosphorus contribution of the biomass.

The CCSEM analysis summary of Table 8 identifies significant calcite material in the alfalfa stems and the hybrid poplar. Both the wheat straw and the alfalfa stems have significant amounts of material classified as quartz, which is the amorphous silica-based phytoliths. SEM BEI (backscattered electron imaging) images of the wheat straw, alfalfa stems, hybrid poplar and Illinois No. 6 and Absaloka coals are shown in Figures 18–22, illustrating the contrast in the shape and size of the mineral matter present between the coal and biomass. The wheat straw is also silica-rich and has a large amount of material classified as unknown. This unknown material is a potassium–calcium-rich silicate also probably phytolithic, for which there is no corresponding coal mineral type. In contrast, nearly half the mineral content of the Illinois No. 6 coal is pyritic, with only moderate amounts of quartz, kaolinite clay, potassium aluminosilicate, and minor amounts of other minerals. The Absaloka subbituminous coal minerals are predominantly quartz, kaolinite clays, and calcite. The particle-size distribution indicates that the combined quartz and Si-rich mineral matter for the wheat straw and alfalfa stems is significantly larger than for the Illinois No. 6 coal and comparable to the Absaloka coal, as shown in Figure 23. This may have an important effect on the deposition behavior. The complete CCSEM analyses of the coals and biomass materials (using coal analysis mineral criteria) are given in Tables F1–F5 of Appendix F.

Because the CCSEM classification scheme was designed for mineral phases in coal and the biomass material is phytolithic in origin, most of the chemical point analyses are unclassified by the CCSEM data reduction program. Cluster analyses were performed on these unknowns using Minitab Release 13 for the multivariate analyses. Clusters were defined by their average composition. A graphic representation of the five most abundant clusters for each of the biomass fuels can be found in Appendix G, Figure G37 for the hybrid poplar, Figure G39 for the alfalfa stems, and Figure G41 for the wheat straw. Each of these figures are accompanied by a pie chart representing the frequency of each of the clusters. For the hybrid poplar, the Ca-rich cluster represents 68% of the particles analyzed. The alfalfa stems and wheat straw both showed a Si–K cluster as the dominant chemical group.

The chemical fractionation results for the Illinois No. 6 coal, given in Table 10, show significant solubility of calcium and sodium only with water and ammonium acetate extraction, although very little of these elements is present. The results for the Absaloka coal are typical for a western subbituminous coal, with three quarters of the calcium and magnesium and all of the sodium in an ion-exchangable form. In contrast, all of the elements in the biomass samples show some solubility in water and ammonium acetate, particularly phosphorus, calcium, potassium, and magnesium. In a subbituminous coal, this would be indicative of organically bound cations; however, in the biomass, this may also be the result of water-soluble compounds.

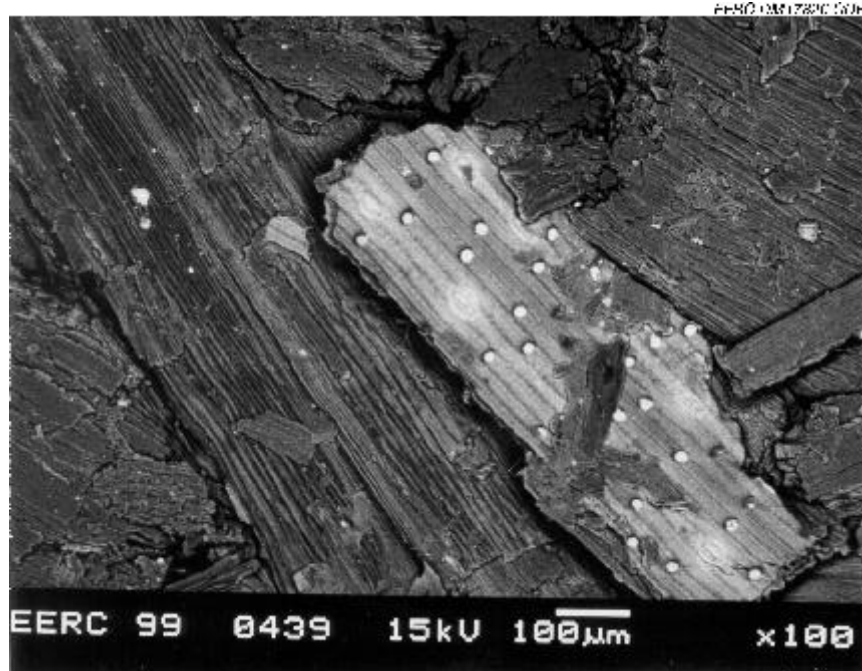


Figure 18. SEM BEI image of wheat straw.

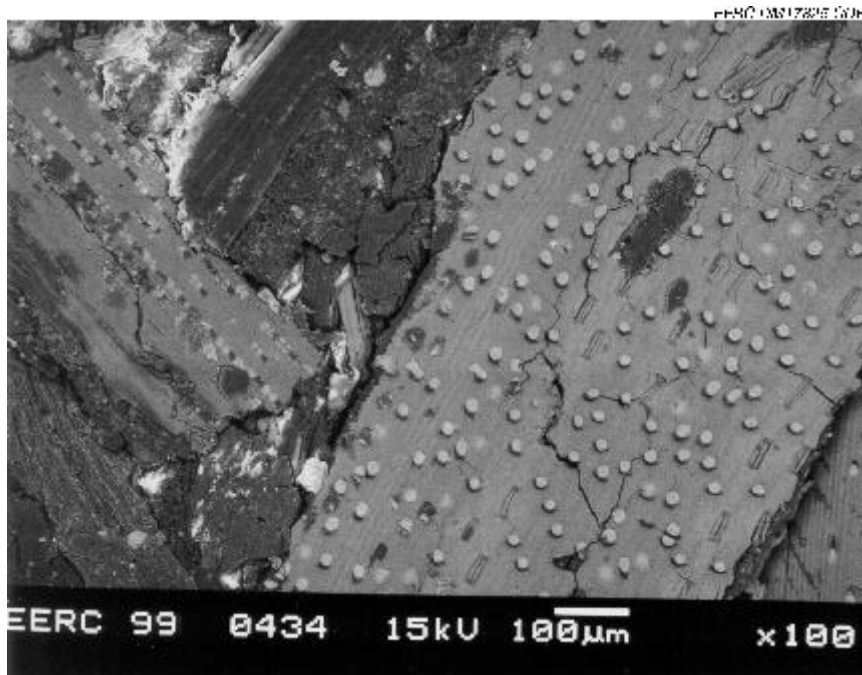


Figure 19. SEM BEI image of alfalfa stems.

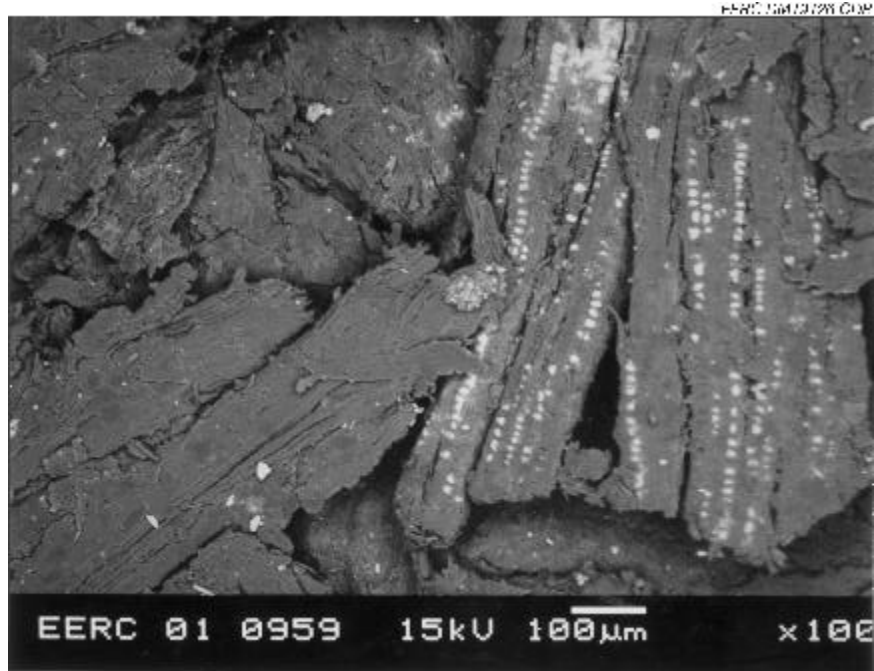


Figure 20. SEM BEI image of hybrid poplar.

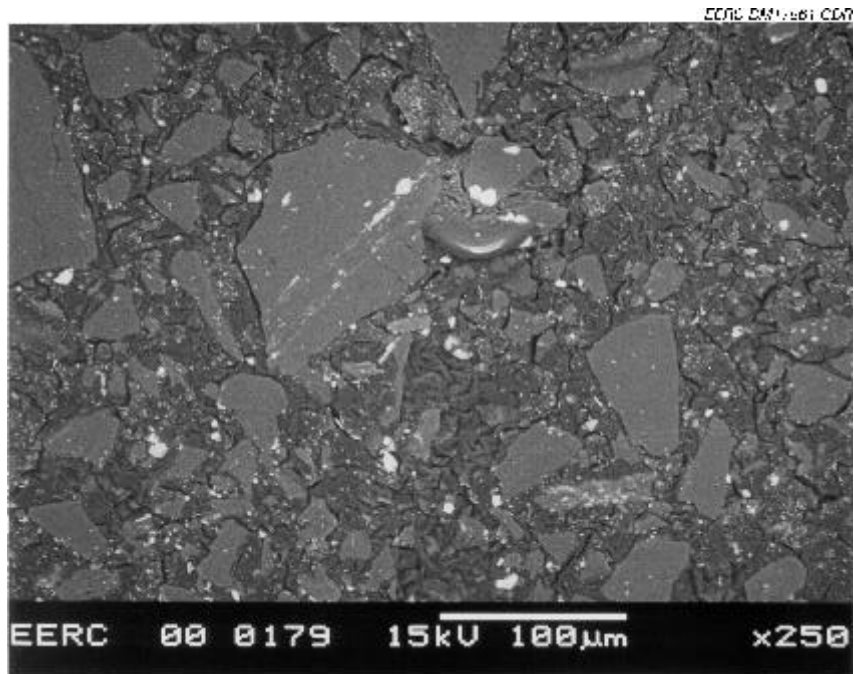


Figure 21. SEM BEI image of Illinois No. 6 coal.

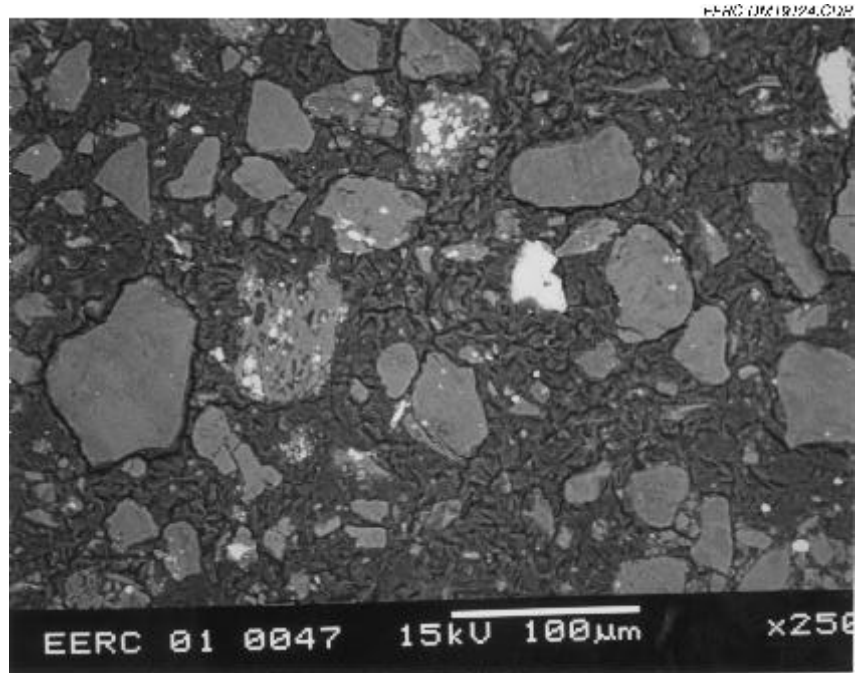


Figure 22. SEM BEI image of Absaloka coal.

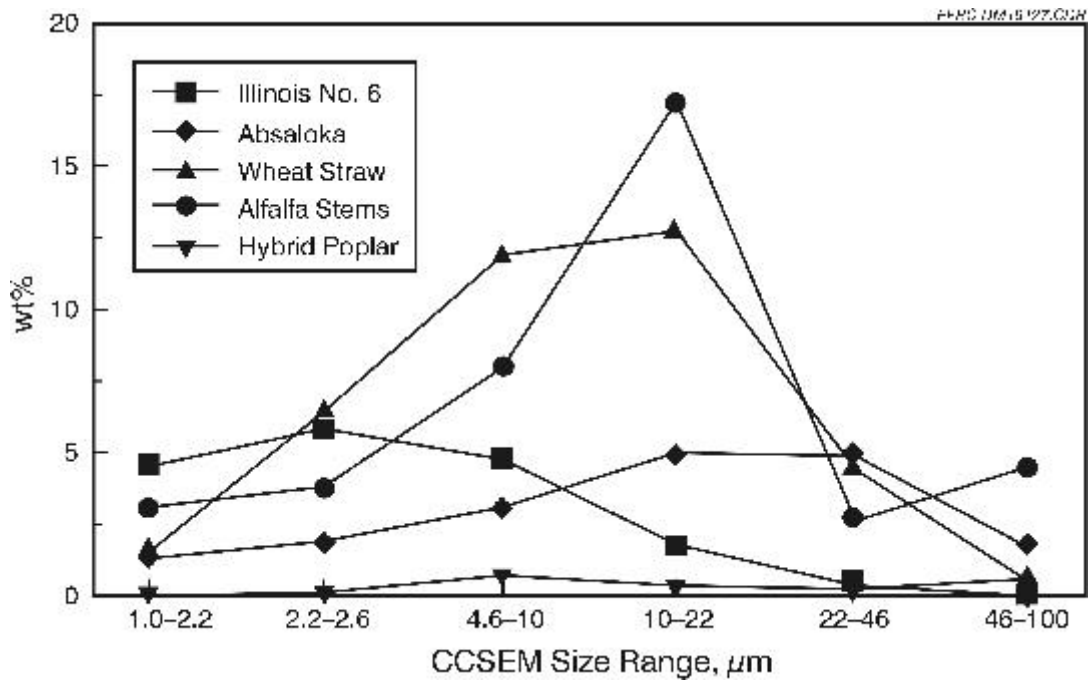


Figure 23. Particle-size distribution of quartz and silica-rich material.

## Combustion Testing and Biomass Cofiring Results

Entrained fly ash and fouling deposits were generated in the CEPS combustor for the parent coals and biomass materials and blends of 80% coal with 20% biomass. Slagging and low-temperature fouling deposits were also produced for the blend of 80% Illinois No. 6 coal with 20% wheat straw. The general combustion test conditions are given in Table 12. Slagging and fouling deposits were collected on a removable cooled probe for later analysis and determination of deposit strength, with gas composition monitored during the tests.

Table 13 gives the gas compositions for the CEPS combustion tests. The oxygen and CO<sub>2</sub> levels in the flue gas after combustion were approximately 3.2%–5.0% and 17.0%–18.7%, respectively. The CO levels for the blend were approximately twice that of the 100% Illinois No. 6 coal and three times that of the 100% wheat straw. The CO level for the pure alfalfa stems was approximately twice that for the coal–alfalfa stem blends, which were similar to those of the coals. The hybrid poplar gave the highest CO level at 183 ppm, about twice that of the coal hybrid poplar blends. A decrease in the blend SO<sub>2</sub> levels from that of the pure coals can be attributed to the blending with the very-low-sulfur-content wheat straw as well as possible sulfur capture by the alkali and alkaline-earth elements in the wheat straw ash. The NO<sub>x</sub> level for the coal–wheat straw blends is comparable to those of the parent coals in the blends. However, the 100% wheat straw and 100% hybrid poplar showed high NO<sub>x</sub> levels comparable to the 100% Absaloka coal. Blending these two biomass materials with Absaloka coal appeared to significantly reduce the NO<sub>x</sub> levels. The 100% alfalfa stems exhibited the highest NO<sub>x</sub> level. Again, blending with the coals reduced the NO<sub>x</sub> level to a value comparable to or lower than that of the pure coals.

Deposit growth rates and strengths are given in Table 14. Note that three deposit tests were performed with the 80% Illinois No. 6–20% wheat straw blend. Figure 24 summarizes the growth rates and crushing strengths of fouling deposits formed from the coals, biomass materials, and 80% coal–20% biomass blends. The wheat straw fouling deposits, although growing rapidly, had very little strength or indication of sintering. Coal–wheat straw blends, although growing more rapidly than the coal deposits, had effectively no strength. The rate of growth of the alfalfa and coal–alfalfa blends was similar, with the blend deposit strengths lower than that of the alfalfa and parent coals. Similar behavior is also seen for the hybrid poplar and coal–hybrid poplar blends. The blending of coal with biomass appears to dilute the coal minerals with the porous biomass ash, resulting in fouling deposits with lower strength and which are more easily removable. No strengths were obtained for several of the deposits because of their extreme weakness. A slagging deposit was produced only for the 80% Illinois No. 6 coal–20% wheat straw blend. Although the deposit deposition rate was lower than the corresponding blend fouling deposit, the slagging deposit is quite strong because of the higher formation temperature, allowing increased interaction of the deposit ash components. Photographs of the deposits produced are given in Figures 25–35.

### Slagging Deposit

The deposits were examined using SEMPC and CCSEM analysis performed on the entrained ash. The morphology of the 80% Illinois No. 6 coal–20% wheat straw blend slagging deposit showed distinct elongated silicate structures derived from the wheat straw plant material as well as

TABLE 12

## Combustion Conditions for Deposit Testing

Test	CEPS 101	CEPS 95	CEPS 102	CEPS 94-4	CEPS 94-2	CEPS 94-CP1	CEPS 116	CEPS 115	CEPS 113	CEPS 114	CEPS 111	CEPS 117	CEPS 112
Sample	Illinois No. 6 100% Coal	Absalok a 100% Coal	Wheat Straw 100% Biomass	Illinois No. 6 Wheat Straw 80%–20% Blend	Illinois No. 6 Wheat Straw 80%–20% Blend	Illinois No. 6 Wheat Straw 80%–20% Blend	Absaloka Wheat Straw 80%–20% Blend	Alfalfa 100% Biomass	Illinois No. 6 Alfalfa 80%–20% Blend	Absaloka Alfalfa 80%–20% Blend	Hybrid Poplar 100% Biomass	Illinois No. 6 Hybrid Poplar 80%–20% Blend	Absaloka Hybrid Poplar 80%–20% Blend
Deposit	Fouling	Fouling	Fouling	Slagging	Fouling	Convective Pass	Fouling	Fouling	Fouling	Fouling	Fouling	Fouling	Fouling
Gas Flows, lpm													
Primary Air	20	30	20	20	20	20	20	20	20	20	20	20	20
Secondary Air	77	137	77	77	77	77	77	77	77	77	77	77	77
Purge Air	3	3	3	3	3	3	3	3	3	3	3	3	3
Total Air In	100	170	100	100	100	100	100	100	100	100	100	100	100
Flue Gas Flow	111	180	112	110	111	111	120	115	111	120	111	111	112
Temperatures, °C													
Preheat Furnace	1000	1000	1000	1000	1000	1000	1000	1000	1000	1000	1000	1000	1000
Furnace No. 3	1500	1500	1500	1500	1500	1500	1500	1500	1500	1500	1500	1500	1500
Furnace No. 4	1500	1500	1500	1500	1500	1500	1500	1500	1500	1500	1500	1500	1500
Furnace No. 5	1400	1500	1400	1400	1400	1400	1400	1400	1400	1400	1400	1400	1400
Furnace No. 6	1300	1400	1300	1300	1300	1300	1300	1300	1300	1300	1300	1300	1300
Furnace No. 7	1200	1300	1200	1200	1200	1200	1200	1200	1200	1200	1200	1200	1200
Preheat Air	847	794	847	846	849	849	848	846	847	848	845	847	846
Secondary Air	724	645	727	686	713	713	705	689	681	701	688	709	683
Section 2	1242	1253	1176	1247	1279	1279	1224	1138	1228	1227	1137	1261	1206
Section 3	1297	1391	1227	1264	1267	1267	1245	1239	1224	1215	1221	1250	1226
Section 4	1306	1314	1326	1252	1291	1291	1311	1311	1291	1294	1324	1302	1306
Section 5	1307	1379	1313	1267 <sup>1</sup>	1311	1311	1310	1320	1303	1309	1330	1307	1311
Section 6	1235	1331	1237	1223	1244	1244	1219	1234	1233	1240	1259	1220	1239
Section 7	988 <sup>1</sup>	1089 <sup>1</sup>	1012 <sup>1</sup>	1005	981 <sup>1</sup>	981	1042 <sup>1</sup>	1025 <sup>1</sup>	995 <sup>1</sup>	1010 <sup>1</sup>	1006 <sup>1</sup>	987 <sup>1</sup>	1000 <sup>1</sup>
Section 8	780	900	805	837	788	788	854	864	748	788	799	742	768
Convective Pass Outlet	NA <sup>2</sup>	533	NA <sup>2</sup>	565	560	560 <sup>1</sup>	437	437	NA <sup>2</sup>	NA <sup>2</sup>	379	395	342
Heat Exchanger No. 1	232	399	262	207	221	221	NA <sup>2</sup>	NA <sup>2</sup>	NA <sup>2</sup>	NA <sup>2</sup>	274	NA <sup>2</sup>	266
Outlet													
Heat Exchanger No. 4	118	220	136	127	135	135	NA <sup>2</sup>	NA <sup>2</sup>	NA <sup>2</sup>	NA <sup>2</sup>	169	NA <sup>2</sup>	161
Outlet													
Baghouse Inlet	114	202	133	103	94	94	NA <sup>2</sup>	NA <sup>2</sup>	NA <sup>2</sup>	NA <sup>2</sup>	178	NA <sup>2</sup>	171
Baghouse Bottom	97	130	105	96	90	90	180	202	160	173	65	125	57
Baghouse Top	139	138	140	138	140	140	60	94	116	143	91	76	89
Deposit Probe	540	532	540	500	540	540	540	540	540	540	540	540	540
Centerline Gas	NA <sup>2</sup>	NA <sup>2</sup>	NA <sup>2</sup>	NA <sup>2</sup>	NA <sup>2</sup>	NA <sup>2</sup>	1034	1034	1034	1034	NA <sup>2</sup>	1034	1034
Temperature <sup>3</sup>													

<sup>1</sup> Location of deposit probe.<sup>2</sup> Not applicable.<sup>3</sup> At probe location.

TABLE 13

## Gas Analysis for Deposit Testing

	CEPS 101	CEPS 95	CEPS 102	CEPS 94-4	CEPS 94-2	CEPS 94-CPI	CEPS 116	CEPS 115	CEPS 113	CEPS 114	CEPS 111	CEPS 117	CEPS 112
	Illinois No. 6	Absaloka	Wheat Straw	Illinois No. 6 Wheat Straw	Illinois No. 6 Wheat Straw	Illinois No. 6 Wheat Straw	Absaloka Wheat Straw	Alfalfa	Illinois No. 6 Alfalfa	Absaloka Alfalfa	Hybrid Poplar	Illinois No. 6 Hybrid Poplar	Absaloka Hybrid Poplar
	100% Coal	100% Coal	100% Biomass	80%–20% Blend	80%–20% Blend	80%–20% Blend	80%–20% Blend	100% Biomass	80%–20% Blend	80%–20% % Blend	100% Biomass	80%–20% Blend	80%–20% Blend
	Fouling Deposit	Fouling Deposit	Fouling Deposit	Slagging Deposit	Fouling Deposit	Convective Pass Deposit	Fouling Deposit	Fouling Deposit	Fouling Deposit	Fouling Deposit	Fouling Deposit	Fouling Deposit	Fouling Deposit
O <sub>2</sub> , %	3.17	4.12	5.01	4.85	4.67	4.67	4.93	4.97	4.72	4.83	4.77	4.76	5.03
CO <sub>2</sub> , %	18.50	18.54	18.44	17.00	17.01	17.01	18.46	18.55	18.24	18.39	18.73	18.27	18.41
CO, ppm	24	28	24	86	74	74	32	43	21	28	183	71	102
SO <sub>2</sub> , ppm	2688	609	159	2135	2171	2171	467	61	2136	464	43	2089	553
NO <sub>x</sub> , ppm	1020	1577	1557	1120	1071	1071	1404	1942	1355	1514	1410	1142	1222

TABLE 14

## Deposit Strengths and Growth Rates

	CEPS 101	CEPS 95	CEPS 102	CEPS 94-4	CEPS 94-2	CEPS 94- CP1	CEPS 116	CEPS 115	CEPS 113	CEPS 114	CEPS 111	CEPS 117	CEPS 112
	Illinois No. 6	Absalok a	Wheat Straw	Illinois No. 6 Wheat Straw	Illinois No. 6 Wheat Straw	Illinois No. 6 Wheat Straw	Absaloka Wheat Straw	Alfalfa	Illinois No. 6 Alfalfa	Absaloka Alfalfa	Hybrid Poplar	Illinois No. 6 Hybrid Poplar	Absaloka Hybrid Poplar
	100% Coal	100% Coal	100% Biomass	80%–20% Blend	80%–20% Blend	80%–20% Blend	80%–20% Blend	100% Biomass	80%–20% Blend	80%–20% Blend	100% Biomass	80%–20% Blend	80%–20% Blend
	Convective												
	Fouling Deposit	Fouling Deposit	Fouling Deposit	Slagging Deposit	Fouling Deposit	Pass Deposit	Fouling Deposit	Fouling Deposit	Fouling Deposit	Fouling Deposit	Fouling Deposit	Fouling Deposit	Fouling Deposit
Fuel Fed, kg	0.77	2.83	0.15	0.77	0.47	0.88	0.34	2.10	1.03	1.36	4.60	1.41	2.65
Fuel Fed, lb	1.69	6.23	0.34	1.70	1.03	1.95	0.74	4.63	2.28	3.00	10.14	3.11	5.85
% Ash	10.26	7.84	7.62	9.73	9.73	9.73	7.84	3.93	8.99	7.11	1.13	8.43	7.70
Deposit Duration, min	60.0	120.0	7.0	60.0	35.0	70.0	20.0	102.0	80.0	80.0	244.0	111.0	150.0
Deposit Main Ash, g	1.3858	5.3267	2.4534	0.7937	1.6320	NA <sup>1</sup>	1.6305	3.8188	3.8905	2.5356	0.3716	0.7335	2.1238
Deposit White Ash, g	0.6330	0.4234	0.0560	0.0916	NA <sup>1</sup>	NA <sup>1</sup>	0.1329	1.3916	0.3011	0.3350	0.2519	0.5503	0.3925
Deposit Total Weight, g	2.0188	5.7501	2.5094	0.8853	1.6320	NA <sup>1</sup>	1.7634	5.2104	4.1916	2.8706	0.6235	1.2838	2.5163
g Deposit–kg Ash Fed	25.65	25.95	213.34	11.79	35.86	NA <sup>1</sup>	67.01	63.13	45.08	29.67	12.00	10.80	12.32
g Deposit–lb Ash Fed	11.64	11.77	96.86	5.35	16.28	NA <sup>1</sup>	30.40	28.64	20.45	13.46	5.44	4.90	5.59
Deposit Rate, g–min	0.0336	0.0479	0.3585	0.0148	0.0466	NA <sup>1</sup>	0.0882	0.0511	0.0524	0.0359	0.0026	0.0116	0.0168
Deposit Strength, kPa	1834.0	2820.0	220.6	3771.4	*	2220.1	*	1054.9	327.5	393.0	*	199.9	*
Deposit Strength, psi	266.0	409.0	32.0	547.0	*	322.0	*	153.0	47.5	57.0	*	29.0	*

<sup>1</sup> Not applicable.

\* Too weak to be measured.

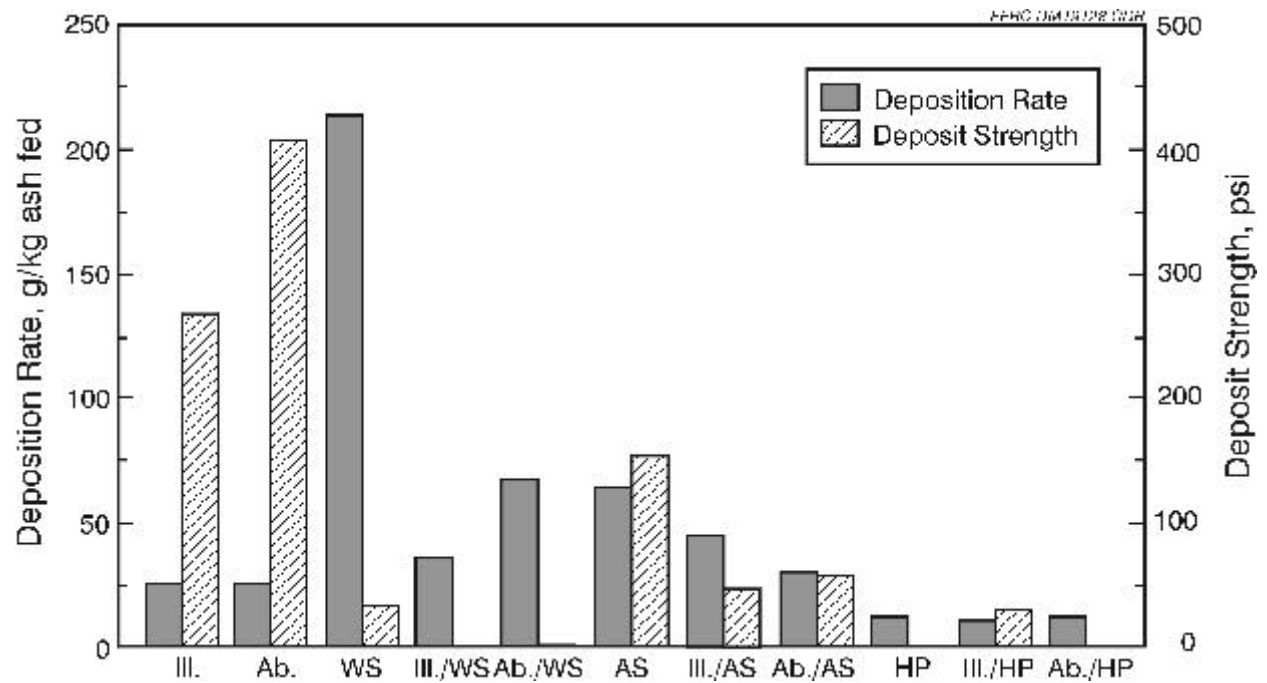


Figure 24. Comparison of deposit growth rates and crushing strengths.



Figure 25. Illinois No. 6 fouling deposit.



Figure 26. Absaloka fouling deposit.



Figure 27. Wheat straw fouling deposit.



Figure 28. Alfalfa stem fouling deposit.



Figure 29. Hybrid poplar fouling deposit.



Figure 30. 80% Illinois No. 6–20% wheat straw fouling deposit.



Figure 31. 80% Illinois No. 6–20% alfalfa stem fouling deposit.



Figure 32. 80% Illinois No. 6–20% hybrid poplar stem fouling deposit.



Figure 33. 80% Absaloka–20% wheat straw fouling deposit.



Figure 34. 80% Absaloka–20% alfalfa stem fouling deposit.



Figure 35. 80% Absaloka–20% hybrid poplar fouling deposit.

distinct angular mineral matter derived from the coal, both being assimilated into the potassium–iron aluminosilicate melt phase as shown in Figure 36. It appears that interaction of potassium occurs in the deposit and not with the entrained fly ash at this point in the combustion process. Although condensation may be occurring on the surface of the entrained ash, the angular shape and evidence of remnant plant structural features of the biomass-derived silica indicate that significant interaction and melting is not occurring until incorporated into the deposit. This may be due to additional potassium in the form of chlorides, hydroxides, and sulfates and, to a lesser degree, similar sodium species condensing onto the deposit as it forms. Phosphorus, which is also present in higher amounts in the blend and biomass deposits, may also be acting as a fluxing agent similar to sodium, potassium, and calcium. The CHF showed 100% removal of phosphorus by water and ammonium acetate from the biomass material, indicating that it is either organically bound or in a water-soluble form. If organically bound, the phosphorus would be expected to form either gas-phase species or very fine particulate with minimal interaction with other ash components during the combustion stage. However, at present, the form of entrained phosphorus and its role in deposit formation and sintering is not known. Examination of the fly ash CCSEM analysis indicates that particles containing high phosphorus concentrations generally also have high calcium concentrations, suggesting the formation of a calcium phosphate in the combustion process. The blend slagging deposit produced was hard and well sintered, with evidence of partial melting of the deposit material. In contrast to the slagging deposit, the blend fouling deposit, although growing rapidly, had very little strength or indication of sintering. This low strength may be the result of the large silica (amorphous silica) structure which did not entirely fuse and provides a physical weakening of the deposits. The blend low-temperature fouling deposit obtained from the CEPS convective pass similarly had very little strength.

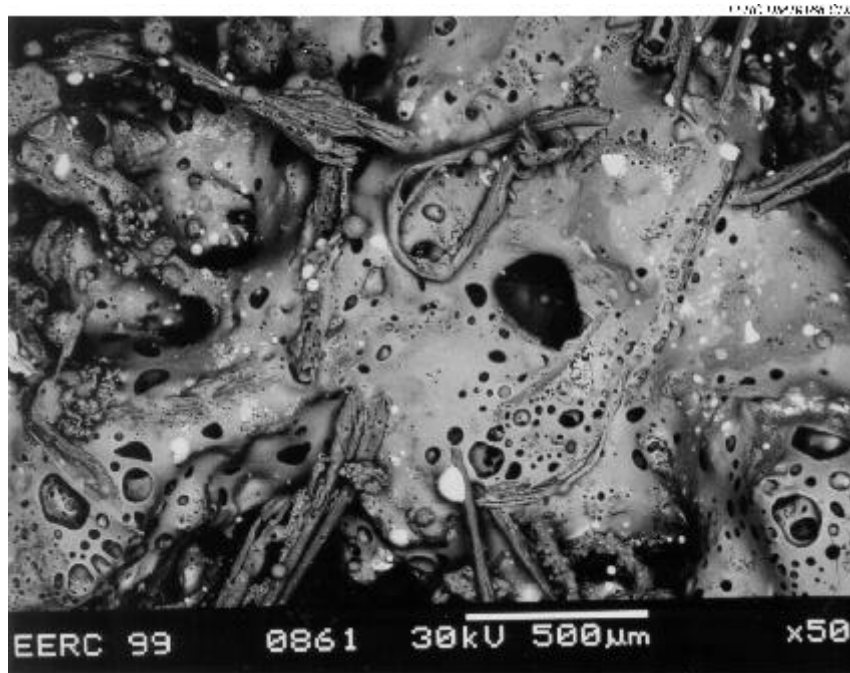


Figure 36. 80% Illinois No. 6–20% wheat straw slagging deposit.

Table 15 compares the SEMPC mineral species determined for the fouling deposits. The 100% Illinois No. 6 deposit is dominated by illite clay, mixed carbon-rich species, and mixed silica-rich species, with very little quartz. The Absaloka deposit is comprised of high-silica-content aluminosilicate material classified as “mixed-metal-rich,” along with anorthite, wollastonite, illite clay, and mixed silica-rich species. The 100% wheat straw fouling deposit mineral species are primarily quartz derived from the plant inorganic silica structures and mixed-silicon-rich material resulting from the reaction of the plant silica with calcium, potassium, and magnesium. The 80% Illinois No. 6–20% wheat straw blend fouling deposit reflects the high silica content of the blended wheat straw, with the majority of the material being mixed-silica-rich species. The 80% Absaloka–20% wheat straw blend also includes large amounts of quartz and silica-rich material, along with illite. The illite may be derived from the Absaloka coal, with the diluting effect of the high-silica-content wheat straw ash. Again, the material classified as quartz by the SEMPC analysis of the wheat straw is probably predominantly plant-derived amorphous silica. The alfalfa stems have a very high calcite content, along with mixed-silica-rich material. The 80% Illinois No. 6–20% alfalfa blend is primarily mixed-silica-rich material, along with some illite clays and iron oxide. It appears that iron has been assimilated into the blend deposit in amounts greater than in either the Illinois No. 6 or the alfalfa deposits. The 80% Absaloka–20% alfalfa blend also contains mostly mixed-silica-rich material, along with some quartz and clays.

The overall chemistry and the chemistry of the inner (tube side) and outer (gas side) portions of the deposits were obtained from the SEMPC analysis. No significant difference was seen in the deposit composition between the inner and outer portions. The overall deposit chemistry is given in Table 16. The chemistry of the deposits generally reflects the bulk ash chemistry of the parent coal, wheat straw, and blend.

Tables 17 and 18 give the SEMPC mineral species and chemistry for the 80% Illinois No. 6 coal slagging and fouling deposits, as well as a low-temperature deposit obtained from the CEPS convective pass and the CCSEM analysis of the blend fly ash. Reported as oxides, the results showed a decrease in  $\text{SiO}_2$  content, with a corresponding increase in  $\text{Al}_2\text{O}_3$  content from the slagging to fouling to low-temperature fouling deposit and entrained ash sample, as shown in Figure 37. The  $\text{Fe}_2\text{O}_3$  content of the fouling deposit is approximately half that of the slagging and low-temperature deposits, which are comparable. Sodium, potassium, and sulfur content is also significantly higher in the low-temperature deposit and in the entrained ash. The finer entrained ash which is  $<22\ \mu\text{m}$  is enriched in potassium in combination with silica, iron, and aluminum. Enrichment of chlorine and sulfur is also seen in the finest  $<2.2\ \mu\text{m}$  size fraction. This is consistent with a mechanism of condensation of gas-phase potassium species onto the entrained ash at lower temperatures. The weakness of the fouling and low-temperature fouling deposits indicates that little interaction of the potassium with the entrained ash occurs at lower temperature and that low-viscosity melts are not produced later in the combustion process, during the formation of Illinois No. 6 fly ash.

CCSEM analysis was performed on the fly ash of the coals and blends. A summary of these results is given in Table 19. The complete CCSEM analysis results are given in Tables H1–H11 of Appendix H. Although some quartz, clays, and aluminosilicates are identified, the great majority of the ash is classified as either unknown or silica-rich. Note that the 80% Illinois No. 6–20% wheat straw blend has a high level of iron oxide, similar to the fouling deposit. The mineral

TABLE 15

## Fouling Deposit Mineral Species

Test	CEPS 101	CEPS 95	CEPS 102	CEPS 94-4	CEPS 94-2	CEPS 94-CP1	CEPS 116	CEPS 115	CEPS 113	CEPS 114	CEPS 111	CEPS 117	CEPS 112
	Illinois No. 6	Absaloka a	Wheat Straw 100%	Illinois No. 6 Wheat Straw 80%–20%	Illinois No. 6 Wheat Straw 80%–20%	Illinois No. 6 Wheat Straw 80%–20%	Absaloka Wheat Straw 80%–20%	Absaloka Alfalfa 100%	Illinois No. 6 Alfalfa 80%–20%	Absaloka Alfalfa 80%–20%	Hybrid Poplar 100%	Illinois No. 6 Hybrid Poplar 80%–20%	Absaloka Hybrid Poplar 80%–20%
Sample	Coal	Coal	Biomass	Blend	Blend	Blend	Blend	Biomass	Blend	Blend	Biomass	Blend	Blend
Deposit Type	Fouling	Fouling	Fouling	Slagging	Fouling	Pass	Fouling	Fouling	Fouling	Fouling	Fouling	Fouling	Fouling
Calcium Oxide	0.8	0.0	0.4	0.0	0.4	0.0	4.0	7.6	0.0	2.8	17.2	0.0	6.8
Iron Oxide	0.8	0.8	0.0	0.4	1.2	5.2	0.8	0.0	10.8	2.0	1.6	5.2	2.8
Mixed-Oxide-Rich	0.0	0.4	0.0	0.0	0.0	0.4	0.0	1.2	0.0	0.4	12.4	0.8	0.4
Mixed-Sulfur-Rich	1.6	2.0	0.0	0.4	0.8	3.2	2.8	1.2	0.0	1.6	0.8	1.2	8.8
Apatite	0.4	0.0	0.0	0.0	0.0	0.0	0.0	7.2	0.4	0.0	0.4	0.0	0.0
Mixed-Phosphorus-Rich	0.0	0.0	3.2	0.4	2.4	0.8	2.0	42.8	3.2	0.8	16.0	0.0	0.0
Calcite	0.0	0.0	0.0	0.0	0.0	0.0	0.0	0.0	0.0	0.0	7.2	0.0	0.4
Mixed-Carbon-Rich	14.4	0.0	0.0	6.4	1.2	0.4	0.0	0.0	0.0	0.0	0.0	0.4	0.0
Mixed-Metal-Rich	0.0	22.4	0.0	0.0	0.4	0.0	0.4	0.8	0.0	0.0	0.0	0.0	0.0
Quartz	4.0	0.8	34.4	8.4	22.4	1.2	19.2	0.0	3.2	11.6	1.2	2.0	8.4
Anorthite	7.6	21.2	0.0	0.0	0.0	0.0	2.4	0.0	2.8	3.2	0.0	16.8	13.2
Altered Kaolinite	0.8	0.8	0.0	0.0	0.0	1.2	1.6	0.0	0.0	4.0	0.0	0.4	1.6
Illite	15.2	1.2	0.4	22.8	26.0	27.2	22.8	1.2	12.0	9.6	2.0	12.8	5.2
Montmorillonite	6.4	13.6	0.0	4.0	2.0	0.0	2.8	0.0	0.8	1.6	0.0	8.0	0.8
Wollastonite	0.4	14.4	0.0	0.4	1.2	0.0	0.8	0.0	0.4	0.4	0.0	0.4	0.0
Calcium Silicate	0.4	0.4	0.0	0.0	0.0	0.0	1.6	0.4	0.4	1.6	0.0	0.4	8.0
Gehlenite	0.0	0.8	0.0	0.0	0.0	0.0	0.4	0.0	0.4	7.2	0.0	0.0	4.8
Mixed-Silicon-Rich	45.2	14.8	61.6	51.2	39.2	57.2	32.8	29.2	63.6	44.0	4.8	48.8	30.4
Unknown	0.8	1.2	0.0	0.0	0.8	1.6	1.2	6.4	1.6	6.4	34.4	0.4	2.8
Other	1.2	5.2	0.0	5.6	2.0	1.6	4.4	2.0	0.4	2.8	2.0	2.4	5.6

TABLE 16

## Fouling Deposit Bulk Chemistry, wt%

Test	CEPS 101	CEPS 95	CEPS 102	CEPS 94-4	CEPS 94-2	CEPS 94-CP1	CEPS 116	CEPS 115	CEPS 113	CEPS 114	CEPS 111	CEPS 117	CEPS 112
	Illinois No. 6	Absalok a	Wheat Straw 100%	Illinois No. 6 Wheat Straw 80%–20%	Illinois No. 6 Wheat Straw 80%–20%	Illinois No. 6 Wheat Straw 80%–20%	Absaloka Wheat Straw 80%–20%	CEPS 115 Alfalfa 100%	Illinois No. 6 Alfalfa 80%–20%	Absaloka Alfalfa 80%–20%	Hybrid Poplar 100%	Illinois No. 6 Hybrid Poplar 80%–20%	Absaloka Hybrid Poplar 80%–20%
Sample	Coal	Coal	Biomass	Blend	Blend	Blend	Blend	Biomass	Blend	Blend	Biomass	Blend	Blend
Deposit Type	Fouling	Fouling	Fouling	Slagging	Fouling	Convective Pass	Fouling	Fouling	Fouling	Fouling	Fouling	Fouling	Fouling
SiO <sub>2</sub>	49.2	53.7	76.9	61.2	66.6	45.8	59.8	14.5	44.8	44.3	8.2	49.2	37.4
Al <sub>2</sub> O <sub>3</sub>	16.4	16.3	0.4	8.7	11.1	18.6	7.3	0.4	15.7	13.6	3.4	17.7	12.8
Fe <sub>2</sub> O <sub>3</sub>	21.6	7.3	0.3	13.8	6.7	13.0	2.4	0.3	18.5	4.6	2.6	16.2	5.9
TiO <sub>2</sub>	0.8	0.8	0.1	0.3	0.4	1.4	0.2	0.1	0.7	0.5	0.1	0.6	0.5
P <sub>2</sub> O <sub>5</sub>	0.3	0.3	2.3	1.3	1.4	0.8	1.6	20.2	2.5	4.0	9.5	1.0	1.0
CaO	6.4	16.3	5.6	5.9	5.6	2.1	17.7	38.9	8.9	22.5	52.1	9.6	31.6
MgO	0.6	1.7	2.8	2.5	2.1	0.8	1.9	7.1	1.5	2.6	8.9	1.6	2.0
Na <sub>2</sub> O	0.4	0.5	0.7	0.7	0.4	1.2	0.8	0.4	0.6	0.5	0.6	0.5	0.9
K <sub>2</sub> O	2.4	0.6	10.4	4.7	4.6	8.9	5.8	16.6	5.8	5.6	11.6	2.3	1.5
SO <sub>3</sub>	1.1	1.4	0.2	0.4	0.7	5.6	2.0	1.1	0.6	1.3	2.5	0.8	5.7
ClO	0.4	0.6	0.3	0.3	0.2	1.5	0.2	0.1	0.2	0.1	0.2	0.2	0.2
Cr <sub>2</sub> O <sub>3</sub>	0.1	0.2	0.1	0.1	0.1	0.1	0.1	0.1	0.1	0.1	0.1	0.1	0.1
BaO	0.2	0.4	0.1	0.1	0.1	0.3	0.2	0.1	0.2	0.3	0.2	0.2	0.4

TABLE 17

Illinois No. 6 Deposit and Ash Mineral Species, wt%					
SEMPC Mineral	Slagging Deposit	Fouling Deposit	Convective Pass Deposit	Bulk Filter	CCSEM Mineral
Calcium Oxide	0.0	0.4	0.0		
Iron Oxide	0.4	1.2	5.2	18.4	Iron oxide
Mixed Oxide	0.0	0.0	0.4		
Pyrite	0.0	0.0	1.2	0.1	Oxidized pyrrhotite
Mixed-Sulfur-Rich	0.4	0.8	3.2		
Mixed-Phosphorus-Rich	0.4	2.4	0.8		
Mixed-Carbon-Rich	6.4	1.2	0.4		
Mixed-Metal-Rich	0.0	0.4	0.0		
Quartz	8.4	22.4	1.2	4.8	Quartz
K Feldspar	0.4	0.8	0.4	4.2	K-Al-silicate
Altered Kaolin	0.0	0.0	1.2		
Illite	22.8	26.0	27.2		
Montmorillonite	4.0	2.0	0.0		
Pyroxene	0.8	1.2	0.0		
Wollastonite	0.4	1.2	0.0		
Mixed-Silicon-Rich	51.2	39.2	57.2	4.3	Si-rich
Al-Si-Ca-Rich	4.4	0.0	0.0	0.0	
Other	0.0	0.8	1.6	62.8	Unclassified (Si-rich)

TABLE 18

Illinois No. 6 Deposit and Ash Chemistry, wt%				
	Slagging Deposit	Fouling Deposit	Convective Pass Deposit	Bulk Filter
SiO <sub>2</sub>	61.2	66.6	45.8	46.8
Al <sub>2</sub> O <sub>3</sub>	8.7	11.1	18.6	15.9
Fe <sub>2</sub> O <sub>3</sub>	13.8	6.7	13.0	22.2
TiO <sub>2</sub>	0.3	0.4	1.4	1.0
P <sub>2</sub> O <sub>5</sub>	1.3	1.4	0.8	0.6
CaO	5.9	5.6	2.1	3.9
MgO	2.5	2.1	0.8	0.9
Na <sub>2</sub> O	0.7	0.4	1.2	1.0
K <sub>2</sub> O	4.7	4.6	8.9	5.9
SO <sub>3</sub>	0.4	0.7	5.6	1.5
ClO	0.3	0.2	1.5	0.0
Cr <sub>2</sub> O <sub>3</sub>	0.1	0.1	0.1	0.0
BaO	0.1	0.1	0.3	0.2

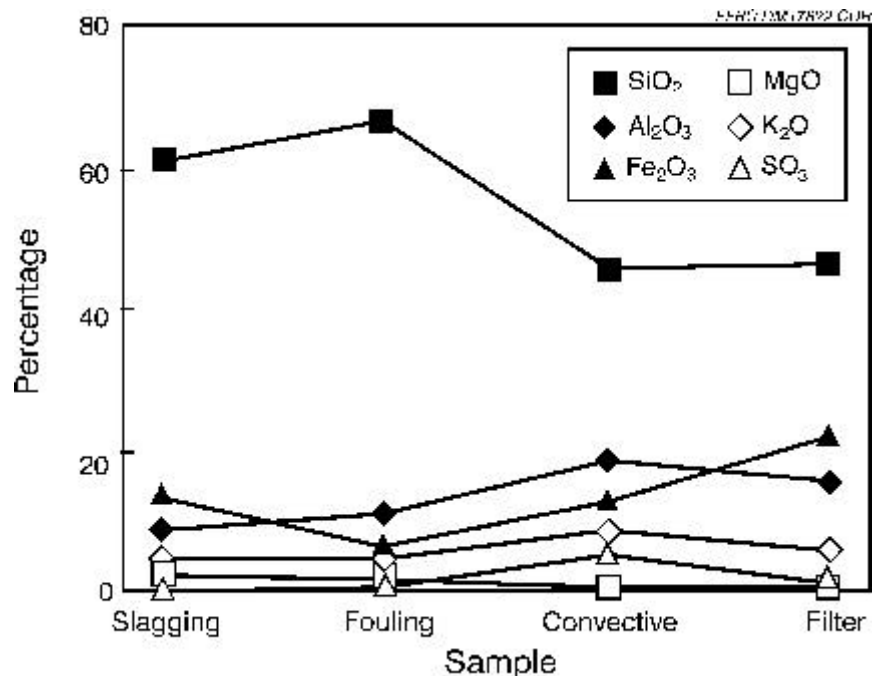


Figure 37. Comparison of 80% Illinois No. 6–20% wheat straw deposit and fly ash chemistry.

classifications provide little information about ash transformations and interactions, because of the large component of material classified as unknown. More information is provided by the average chemical composition of the fly ash given in Table 20. The majority of the material in the fly ash is in the unknown classification, with an average chemical composition given in Table 21.

Cluster analysis was performed on the CCSEM ash results because of the high number of unclassified particles resulting from the presence of inorganic matter arising from the biomass. These analyses were done in the same manner as with the fuel analyses. Results for the biomass ash samples can be found in Appendix G, Figures G1 through G12. For each biomass ash, there is a figure representing the average composition of the unknowns (Figures G1, G5, and G9), a figure representing the five most significant clusters (Figures G2, G6, and G10), a pie diagram showing the frequency distribution (Figures G3, G7, and G11), and a figure showing the particle-size distribution (Figures G4, G8, and G12). The wheat straw ash shows the greatest similarity from the fuel to the ash analyzed. A high percentage of analyses from both samples contained both Si and K. While Cl was a significant component in the fuel, very little was detected in the ash sample (Figure G5). In contrast, both the hybrid poplar and alfalfa stem fuels show little Cl, while the ash unknowns contain 10% and 28%, respectively. These fuels show a significant rearrangement of elements during combustion which can at least in part be contributed to the particle size being small (greater than 50% of the particles analyzed were below 10  $\mu\text{m}$  in diameter). Significant amounts of Ca and K tend to reduce the melting temperature of the Si-containing particles, allowing more components to be incorporated into the glassy matrix. SEM microprobe analyses cannot distinguish between any phases that may condense on the surface of the ash particle as it cools or the bulk of the particle. These samples were cut and polished cross sections of the ash particles, but significant

TABLE 19

## CCSEM Fly Ash Analysis, wt%

Test	CEPS 101	CEPS 95	CEPS 102	CEPS 94-2	CEPS 116	CEPS 115	CEPS 113	CEPS 114	CEPS 111	CEPS 117	CEPS 112	
				Absaloka								
	Illinois No. 6	Absaloka	Wheat Straw	Illinois No. 6 Wheat Straw	Wheat Straw	Alfalfa	Illinois No. 6 Alfalfa	Absaloka Alfalfa	Hybrid Poplar	Illinois No. 6 Hybrid Poplar	Absaloka Hybrid Poplar	
Sample	100% Coal	100% Coal	100% Biomass	80%–20% Blend	80%–20% Blend	100% Biomass	80%–20% Blend	80%–20% Blend	100% Biomass	80%–20% Blend	80%–20% Blend	
Deposit Type	Fouling	Fouling	Fouling	Fouling	Fouling	Fouling	Fouling	Fouling	Fouling	Fouling	Fouling	
Quartz	0.1	0.0	31.9	4.8	1.6	1.5	6.7	5.8	1.4	8.7	4.5	
Iron Oxide	1.7	1.2	0.0	18.4	1.2	1.8	7.1	2.9	9.0	4.5	1.5	
Calcite	0.2	3.2	1.2	0.3	3.2	0.3	0.1	0.7	7.9	0.3	7.0	
Dolomite	0.0	0.6	0.7	0.0	0.5	0.2	0.0	0.3	6.3	0.1	0.5	
Kaolinite	0.1	6.6	0.0	0.0	0.0	0.2	0.6	0.1	0.1	0.2	0.0	
K Al-Silicate	4.2	4.1	0.1	4.2	2.3	1.4	15.1	8.2	0.6	12.2	1.7	
Ca Al-Silicate	0.1	15.2	0.0	0.0	2.1	0.5	0.2	2.9	0.0	0.5	6.6	
Mixed Al-Silicate	13.2	6.2	0.0	2.1	0.0	0.2	0.9	0.1	0.7	5.0	4.1	
KCl	0.0	0.0	0.2	0.0	0.0	9.6	0.0	0.0	0.2	0.1	0.0	
Si-Rich	2.3	0.3	36.1	4.3	1.8	1.0	5.3	1.9	0.6	3.9	1.3	
Ca-Rich	1.5	1.4	0.5	1.7	1.7	0.2	0.3	1.0	6.1	1.1	2.8	
Unknown	74.1	51.4	27.4	62.8	80.0	82.2	62.0	72.4	57.2	60.2	63.6	
Other	2.5	9.8	1.9	1.4	5.6	0.9	1.7	3.7	9.9	3.2	6.4	

TABLE 20

## Average CCSEM Chemical Composition of Fly Ash, wt%

Test	CEPS 101	CEPS 95	CEPS 102	CEPS 94-2	CEPS 116	CEPS 115	CEPS 113	CEPS 114	CEPS 111	CEPS 117	CEPS 112
		Absalok	Wheat	Illinois No. 6	Wheat		Illinois No. 6	Absaloka		Illinois No. 6	Absaloka
	Illinois No. 6	a	Straw	Wheat Straw	Straw	Alfalfa	Alfalfa	Alfalfa	Hybrid Poplar	Hybrid Poplar	Hybrid
	100%	100%	100%	80%–20%	80%–20%	100%	80%–20%	80%–20%	100%	80%–20%	80%–20%
Sample	Coal	Coal	Biomass	Blend	Blend	Biomass	Blend	Blend	Biomass	Blend	Blend
Deposit Type	Fouling	Fouling	Fouling	Fouling	Fouling	Fouling	Fouling	Fouling	Fouling	Fouling	Fouling
SiO <sub>2</sub>	50.1	32.6	75.0	43.0	20.1	10.7	46.1	31.2	10.0	44.4	25.5
Al <sub>2</sub> O <sub>3</sub>	22.6	22.9	0.4	15.7	12.3	3.7	14.8	15.3	4.0	15.8	15.0
Fe <sub>2</sub> O <sub>3</sub>	10.9	5.8	0.4	24.5	3.7	5.7	13.1	5.0	16.2	9.7	3.8
TiO <sub>2</sub>	1.6	1.2	0.1	1.2	0.7	0.4	1.1	0.8	0.4	0.9	0.8
P <sub>2</sub> O <sub>5</sub>	0.8	0.7	2.0	0.9	1.8	4.4	1.0	1.5	7.1	1.0	0.9
CaO	4.1	26.7	8.1	3.5	23.1	7.8	3.1	21.0	30.3	8.2	26.4
MgO	0.9	4.4	2.9	0.9	2.5	1.6	0.7	3.6	5.5	1.2	2.4
Na <sub>2</sub> O	1.4	0.9	0.7	1.1	1.1	1.6	0.7	0.6	1.0	1.1	1.3
K <sub>2</sub> O	5.9	1.4	9.0	6.3	3.5	21.1	7.9	6.1	7.1	5.2	2.1
SO <sub>3</sub>	1.5	2.4	0.5	2.2	13.4	17.3	5.1	4.8	9.7	6.3	6.8
BaO	0.3	0.7	0.2	0.3	0.8	0.4	0.3	0.5	0.2	0.4	0.8
ClO	0.1	0.3	0.8	0.2	17.1	25.6	5.8	9.9	8.5	5.7	14.0

TABLE 21

## Average CCSEM Chemical Composition of Fly Ash with "Unknown" Mineral Composition, wt%

Test	CEPS 101	CEPS 95	CEPS 102	CEPS 94-2	CEPS 116	CEPS 115	CEPS 113	CEPS 114	CEPS 111	CEPS 117	CEPS 112
		Absalok	Wheat	Illinois No. 6	Absaloka	Wheat	Illinois No. 6	Absaloka		Illinois No. 6	Absaloka
	Illinois No. 6	a	Straw	Wheat Straw	Straw	Alfalfa	Alfalfa	Alfalfa	Hybrid Poplar	Hybrid Poplar	Hybrid
	100%	100%	100%	80%–20%	80%–20%	100%	80%–20%	80%–20%	100%	80%–20%	80%–20%
Sample	Coal	Coal	Biomass	Blend	Blend	Biomass	Blend	Blend	Biomass	Blend	Blend
Deposit Type	Fouling	Fouling	Fouling	Fouling	Fouling	Fouling	Fouling	Fouling	Fouling	Fouling	Fouling
SiO <sub>2</sub>	50.1	27.2	55.1	48.9	18.3	8.8	41.1	25.8	10.1	37.5	21.5
Al <sub>2</sub> O <sub>3</sub>	23.1	19.8	1.0	21.1	12.4	3.6	16.3	15.7	3.1	17.1	15.6
Fe <sub>2</sub> O <sub>3</sub>	10.4	6.5	0.7	11.0	2.9	4.7	8.9	2.7	9.3	7.7	2.8
TiO <sub>2</sub>	1.7	1.7	0.2	1.7	0.8	0.4	1.5	1.0	0.5	1.2	0.9
P <sub>2</sub> O <sub>5</sub>	0.8	1.1	4.8	1.0	1.9	4.9	1.4	1.7	8.5	1.3	1.0
CaO	3.2	32.1	13.7	2.8	19.5	7.9	3.9	23.2	24.8	9.5	21.1
MgO	0.9	6.1	6.0	1.1	2.5	1.8	0.9	4.3	6.0	1.5	2.6
Na <sub>2</sub> O	1.5	0.5	1.5	1.2	1.1	1.7	0.9	0.6	1.4	1.2	1.4
K <sub>2</sub> O	6.4	1.1	14.6	8.5	3.5	21.8	9.5	6.0	11.2	5.9	2.4
SO <sub>3</sub>	1.5	2.8	0.9	2.2	15.5	18.5	7.0	5.5	13.5	8.2	8.9
BaO	0.4	0.9	0.3	0.4	0.9	0.4	0.3	0.6	0.3	0.6	0.9
ClO	0.1	0.3	1.4	0.2	20.8	25.6	8.2	13.0	11.3	8.3	21.1

amount of Cl were found with the alfalfa stems ash (Figure G1) and a moderate amount of P was found with the hybrid poplar ash (Figure G9).

To form a clearer picture of the chemical interactions of the ash in the deposits and fly ash, Table 22 provides values of the difference between the deposit or fly ash chemical composition and that of the inorganic material in the fuel. A positive value indicates enrichment and a negative value depletion. Because of the variable amount of sulfur capture by the fly ash, the values given are on a sulfur-free basis and, for consistency with the fuel analysis, on a  $\text{Cr}_2\text{O}_3$ - and BaO-free basis as well.

The composition of the Illinois No. 6 ash is dominated by silica, alumina, and iron and the composition of the Absaloka ash by silica, alumina, and calcium. The wheat straw ash is predominantly silica, with 8% calcium and 9% potassium present. A small enrichment of iron occurs in the Illinois No. 6 deposit, while silica is enriched and calcium depleted in the Absaloka deposit relative to the chemistry of the parent coal inorganic material. There is also a slight depletion of calcium in the Absaloka fly ash. No enrichment or depletion of chlorine occurs for the deposits or fly ash for the coals. The wheat straw shows a depletion of potassium and enrichment of silica in the deposit. This would be expected because of the impaction of large silica phytoliths along with the formation of vapor-phase or fine particulate potassium species which would not be expected to deposit. The wheat straw fly ash is very close in composition to that expected from the inorganic chemistry of the fuel. The blends of wheat straw with the coals has the major chemical constituents corresponding to the parent fuels. The 80% Absaloka–20% wheat straw blend composition also includes a significant amount of sulfur captured by the coal-derived calcium and the wheat straw-derived potassium. Although the wheat straw contains appreciable chlorine, there is little in either the wheat straw fly ash or the 80% Illinois No. 6–20% wheat straw blend fly ash. However, chlorine is a significant component of the 80% Absaloka–20% wheat straw blend fly ash. This suggests that the chlorine in the wheat straw and Illinois–wheat straw blend remains in the gas phase (possibly as HCl) or as a very fine submicron aerosol (possibly as KCl) which is too small to be analyzed by the CCSEM technique. The presence of chlorine in the Absaloka–wheat straw ash indicates either condensation or agglomeration of chlorine compounds such as KCl onto larger ash particles or competition of Absaloka-derived calcium with the wheat straw-derived potassium for chlorine capture. Some enrichment of silica is seen in the Illinois No. 6–wheat straw and Absaloka–wheat straw deposits along with depletion of aluminum. The Absaloka–wheat straw fly ash also contained much less silica than would be expected and significantly more chlorine as well as some enrichment of calcium. The lack of silica in the fly ash may be due to deposition in the CEPS ducting prior to the baghouse where the sample was collected.

The alfalfa deposit shows enrichment of phosphorus and potassium, along with depletion of silica, potassium, and chlorine. The alfalfa fly ash chemistry is comprised of silica, calcium, and potassium, with a significant amount of captured sulfur. A very high amount, 25% of the ash weight, is chlorine. There is a depletion of calcium, possibly due to the formation of fine calcium species. The 80% Illinois No. 6–20% alfalfa and 80% Absaloka–20% alfalfa blend fly ashes have silica and alumina content similar to the wheat straw blend fly ashes. The Absaloka–alfalfa blend fly ash does not exhibit the high sulfur capture shown by the Absaloka–wheat straw blend or the alfalfa fly ash. Although the Absaloka–alfalfa fly ash does contain more chlorine than the Illinois No. 6–alfalfa fly

TABLE 22

## Differences Between Fuel and Deposit and Fly Ash Chemistry, wt%

Sample	Illinois No. 6 100% Coal		Absaloka 100%		Wheat Straw 100% Biomass		Illinois No. 6 Wheat Straw 80%–20% Blend		Absaloka Wheat Straw 80%–20% Blend		Alfalfa 100% Biomass	
	Deposit	Fly Ash	Deposit	Fly Ash	Deposit	Fly Ash	Deposit	Fly Ash	Deposit	Fly Ash	Deposit	Fly Ash
SiO <sub>2</sub>	?4	?3	25	4	13	?2	6	11	17	?38	?13	?15
Al <sub>2</sub> O <sub>3</sub>	?4	2	?4	4	0	0	?9	?6	?10	7	?0	4
Fe <sub>2</sub> O <sub>3</sub>	7	?3	1	?0	?0	0	2	?5	?2	2	?0	6
TiO <sub>2</sub>	?0	1	?0	0	0	0	?1	0	?1	1	0	0
P <sub>2</sub> O <sub>5</sub>	0	1	?0	0	1	?0	1	1	1	0	12	?3
CaO	3	1	?20	?9	2	3	2	2	?1	9	16	?14
MgO	?1	?1	?2	1	1	0	1	0	?3	1	3	?2
Na <sub>2</sub> O	?1	0	?1	?1	?2	0	?1	?1	0	0	?1	0
K <sub>2</sub> O	0	4	0	1	?12	?1	?1	?1	0	?2	?9	?1
ClO	?0	?0	1	0	?3	1	?1	?1	?1	20	?7	24

Sample	Illinois No. 6 Alfalfa 80%–20% Blend		Absaloka Alfalfa 80%–20% Blend		Hybrid Poplar 100% Biomass		Illinois No. 6 Hybrid Poplar 80%–20% Blend		Absaloka Hybrid Poplar 80%–20% Blend	
	Deposit	Fly Ash	Deposit	Fly Ash	Deposit	Fly Ash	Deposit	Fly Ash	Deposit	Fly Ash
SiO <sub>2</sub>	?7	?3	8	?4	4	7	?3	?5	3	?10
Al <sub>2</sub> O <sub>3</sub>	?3	?3	?6	?3	2	3	?2	?3	?8	?5
Fe <sub>2</sub> O <sub>3</sub>	5	1	0	0	1	16	2	?4	1	?1
TiO <sub>2</sub>	0	0	0	0	0	0	0	0	?1	0
P <sub>2</sub> O <sub>5</sub>	2	0	3	0	2	0	1	1	0	0
CaO	4	?2	?1	?2	5	?15	5	4	9	4
MgO	0	?1	?3	?2	1	?2	0	?1	?4	?4
Na <sub>2</sub> O	?1	?1	0	0	0	1	?1	0	0	1
K <sub>2</sub> O	1	4	2	2	?13	?17	0	3	0	1
ClO	?1	5	?1	9	?1	8	0	6	0	15

ash, it is approximately half that of the Absaloka–wheat straw blend, even though the chlorine content of the wheat straw and alfalfa are nearly the same. Indeed, there is only a small enrichment of chlorine (9%) in the Absaloka–alfalfa fly ash. As the coal–alfalfa blend deposits exhibited the highest strengths, this would suggest that interactions of the Absaloka and alfalfa minerals have occurred, with calcium now in a form less amiable to sulfur and chlorine capture.

The hybrid poplar deposit shows a depletion of potassium, with the fly ash showing depletion of both calcium and potassium and some iron enrichment. Despite this, the hybrid poplar fly ash contains significant calcium, along with silica, iron, 7% phosphorus, and 7% potassium. There is also moderate capture of sulfur and chlorine, moderately higher than would be expected from the fuel chlorine content. Because of the low ash content of the hybrid poplar, the effect on the coal–poplar blends is not as pronounced, although the Absaloka–poplar blend fly ash does show a fair degree of chlorine capture and the deposit some enrichment of calcium.

A comparison of the overall CCSEM mineral particle-size distributions of the coals and biomass fuels and fly ashes is shown in Figures 38–43. The Illinois No. 6 coal is dominated by large pyritic mineral particles (pyrite and pyrrhotite) as is the calculated mineral-size distribution for the parent blend. A significant reduction occurs on formation of the Illinois No. 6 fly ash because of the large pyritic mineral matter (Figure 38). The parent wheat straw particle sizes are shown as smaller than those of the coal, with little mineral matter larger than 22  $\mu\text{m}$ . However, this is probably due to underestimation of the flat, platelike silicate phytolith structures of the wheat straw by the CCSEM sizing procedure. A calculated size distribution of the blend fuel is shown, based on the blend ratio and the size distributions and mineral ash content of the parent fuels. An analogous calculated size distribution of the blend fly ash has been constructed from the ash content and parent fly ash particle-size distributions. The fly ash of the pure wheat straw is shifted to larger particle sizes than that of the parent fuel, indicating that agglomeration is occurring. However, the size distribution of the blend fly ash is shifted to smaller particle sizes than would be expected from the calculated fly ash size distribution. The blend fly ash contains even more fine particulate of less than 4.6 microns than the Illinois coal. The agglomeration that occurred for the pure wheat straw ash does not occur with the Illinois No. 6–wheat straw fly ash. This suggests that some interaction of the two ash components is hindering the agglomeration mechanism of the wheat straw ash.

A similar comparison of the Absaloka and wheat straw fuels and fly ashes (Figure 39) shows the Absaloka fly ash produces fly ash with much finer particle sizes than the minerals in the parent coal. Fragmentation of calcite and clays along with the organically bound alkalies and alkaline earths in the coal matrix are responsible. The Absaloka–wheat straw blend fly ash is shifted to larger particle sizes than the parent coal and is nearly the particle-size distribution for the blend fly ash predicted by the weighted average of the parent fly ashes. This suggests that either the presence of the Absaloka ash does not inhibit the wheat straw ash agglomeration or that interaction of the Absaloka and wheat straw fuel minerals is occurring.

Appendix G contains the cluster analysis results of the CCSEM unknowns for the blended ashes. Figures G13 through G16 show the clustering results of the 80% Illinois No. 6 coal–20% alfalfa stems ash. Figures G17 through G20 show the 80% Illinois No. 6 coal–20% hybrid poplar ash, and Figures G21 through G24 show the results of the 80% Illinois No. 6–20% wheat straw ash.

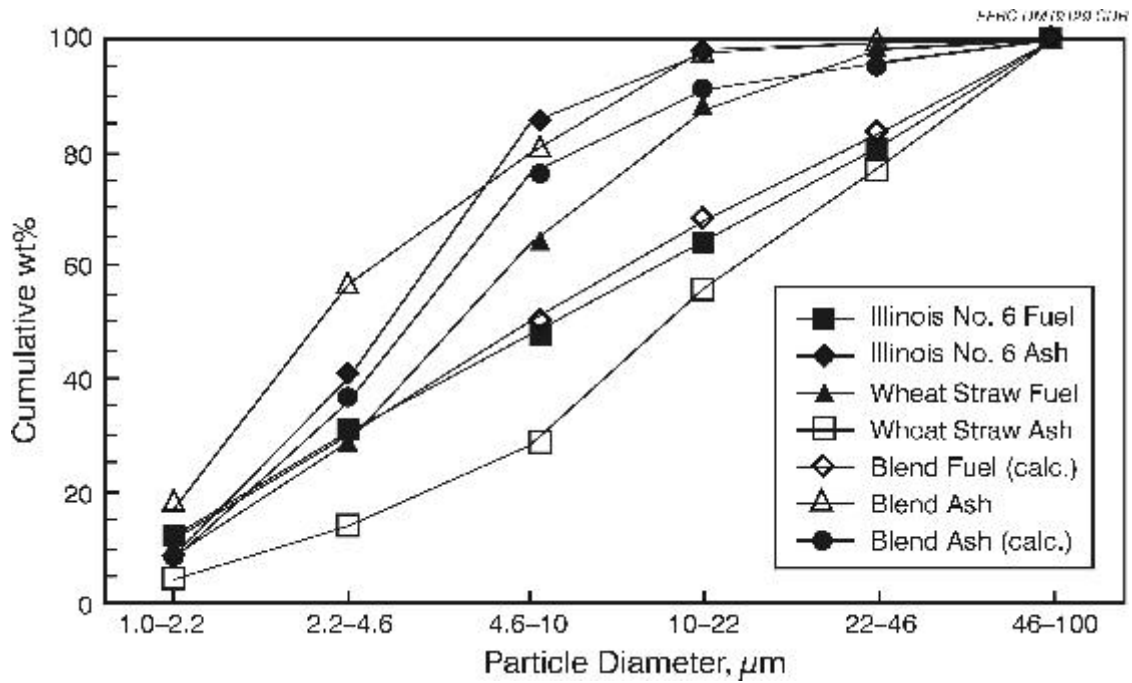


Figure 38. Illinois No. 6 and wheat straw fuel and fly ash mineral particle-size distribution.

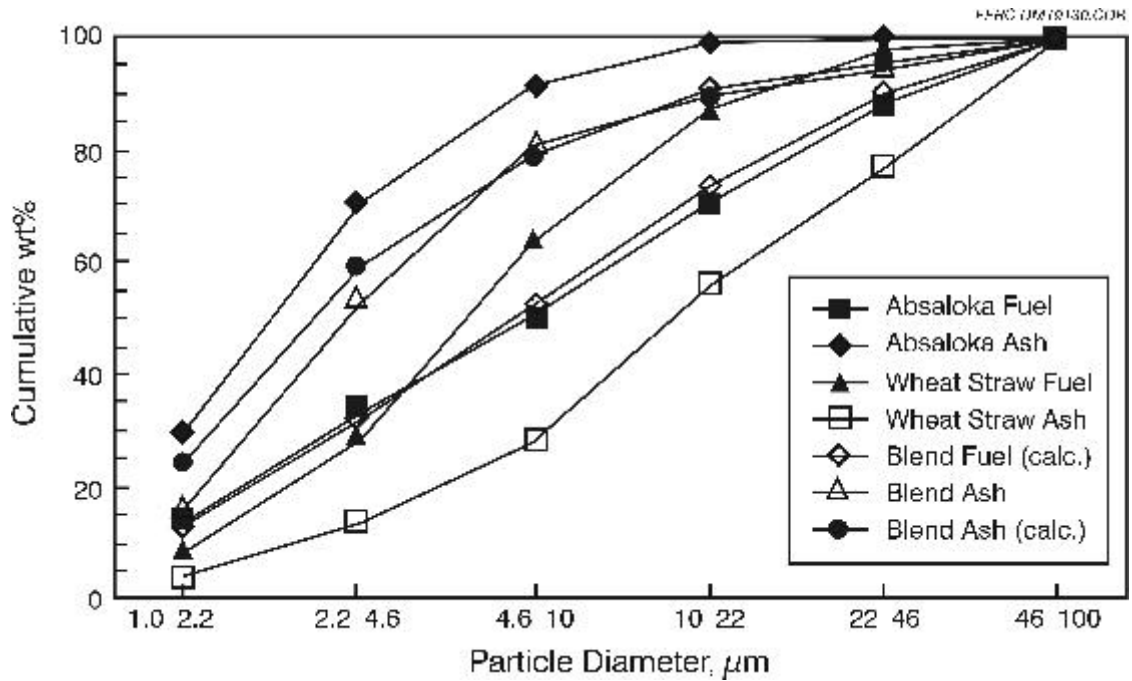


Figure 39. Absaloka and wheat straw fuel and fly ash mineral particle-size distribution.

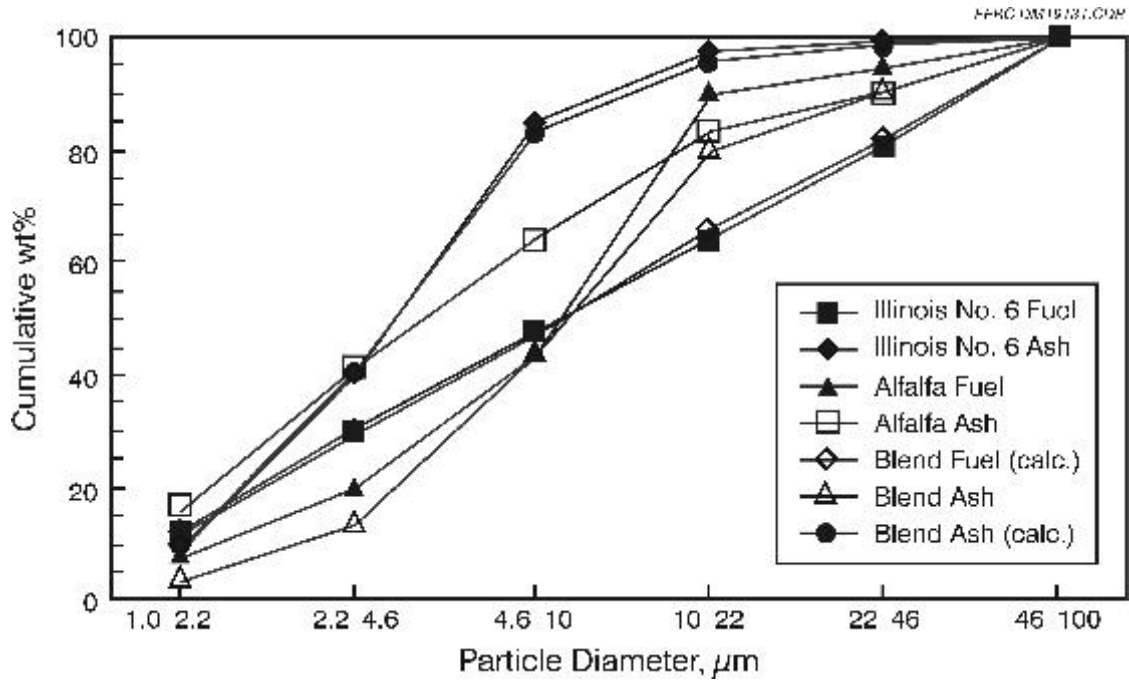


Figure 40. Illinois No. 6 and alfalfa stem fuel and fly ash mineral particle-size distribution.

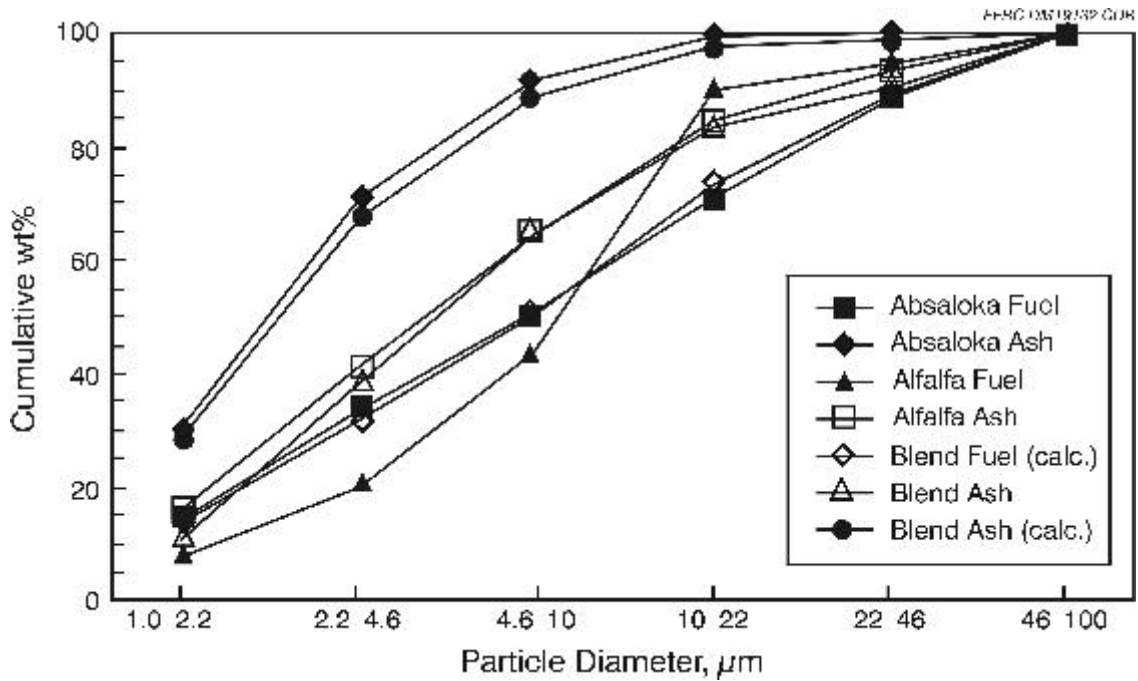


Figure 41. Absaloka and alfalfa stem fuel and fly ash mineral particle-size distribution.

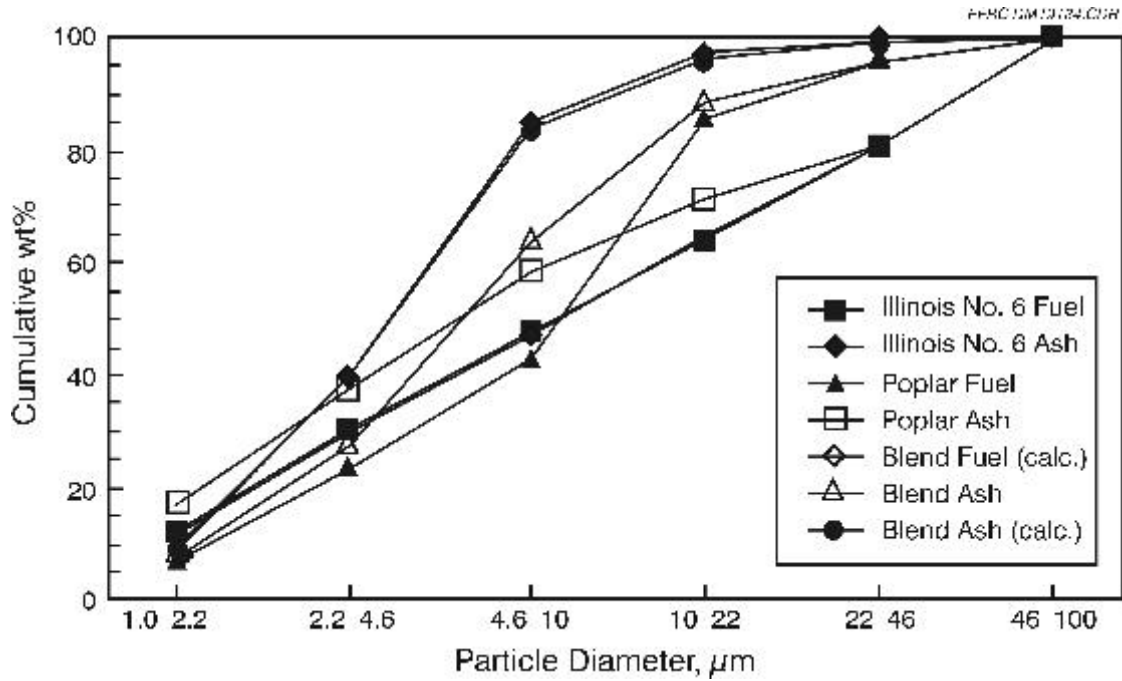


Figure 42. Illinois No. 6 and hybrid poplar fuel and fly ash mineral particle-size distribution.

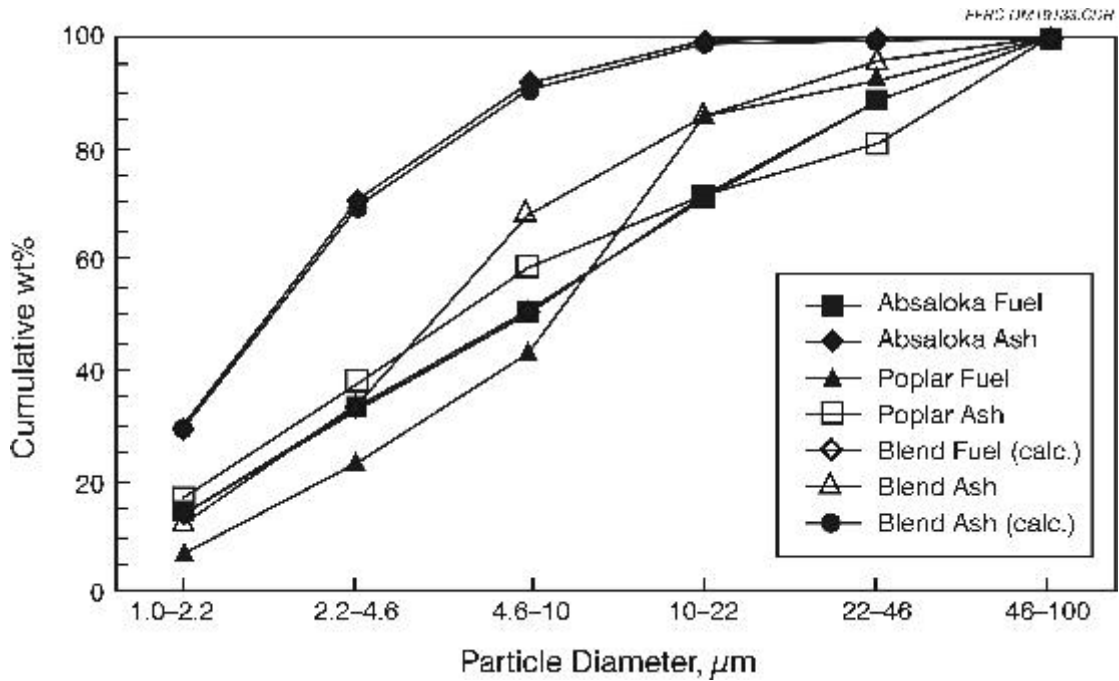


Figure 43. Absaloka and hybrid poplar fuel and fly ash mineral particle-size distribution.

Similar plots were made for the 80% Absaloka coal and the 20% biomass fuels. These are found in Figures G25 through G28 for the Absaloka–alfalfa stems blend, Figures G29 through G32 for the Absaloka–wheat straw blend, and Figures G33 through G36 for the Absaloka–hybrid poplar blend. For each of the blended fuels, there is a graph representing the bulk chemistry of the unknowns, the five most significant clusters, a frequency distribution of those clusters, and a particle-size-range distribution.

For the Illinois No. 6 and alfalfa stems (Figure 40), the alfalfa fly ash has a significantly smaller particle-size distribution than the minerals in the parent alfalfa fuel. This is the expected result of the high calcium and potassium content, which would result in the production of fine particulate as well as vapor-phase potassium species. The fly ash, as noted previously, showed enhancement of potassium and chlorine. The predicted blend fly ash distribution is nearly identical to that of the Illinois No. 6 fly ash as a result of the higher coal ash content. However, the experimental blend fly ash is much larger than predicted, similar to that of the mineral size distribution of the alfalfa fuel. This indicates interaction and agglomeration of the minerals from the parent coal and biomass, although no great enrichment of any elements was seen in the bulk fly ash chemistry. Behavior of the Absaloka and alfalfa stems (Figure 41) is similar, with the blend showing a much larger particle-size distribution than predicted from the parent fly ashes. Here, however, the blend particle-size distribution is nearly the same as that of the parent alfalfa fly ash, indicating that interaction and agglomeration may not be as extensive as with the Illinois No. 6 fly ash. In both cases, the presence of the alfalfa mineral matter has resulted in particle-size distributions larger than that seen for the parent coals and equal to or larger than those of the parent alfalfa. This suggests that biomass blending may have a beneficial effect in improving ash collectibility by increasing particle size.

The ashes for the Illinois No. 6 and hybrid poplar (Figure 42) also show a shift to larger particle sizes on blending over that of the predicted blend-size distribution. Here, the effect is not as pronounced, with the blend fly ash-size distribution being somewhat smaller than that of the parent hybrid poplar. However, the blend-size distribution is again larger than the parent Illinois No. 6 fly ash. Similar behavior (Figure 43) is seen for the Absaloka and hybrid poplar fly ash blend.

It is known that biomass combustion typically results in a large submicron particle fraction because of condensation of volatilized minerals, primarily potassium and sodium sulfates and chlorides. The amount of submicron particulate generated is an important issue. As part of the CEPS combustion testing with hybrid poplar, Absaloka coal, and an 80%–20% Absaloka–hybrid poplar blend, on-line measurements were made using an APS and a SMPS. These measurements indicated that there is a moderate shift in the submicron fraction to larger particle sizes (SMPS measurements) and, possibly, a small shift to larger particle sizes in the supermicron particle size range (APS measurements), as shown in Figure 44. Surprisingly, the coal appeared to have more fine submicron ash than either the hybrid poplar or the blend. A tentative hypothesis is that condensation of sticky potassium species from the biomass ash on fine coal ash particles is resulting in agglomeration of these particles. Further APS and SMPS measurements during pilot-scale combustion tests are planned to resolve this issue.

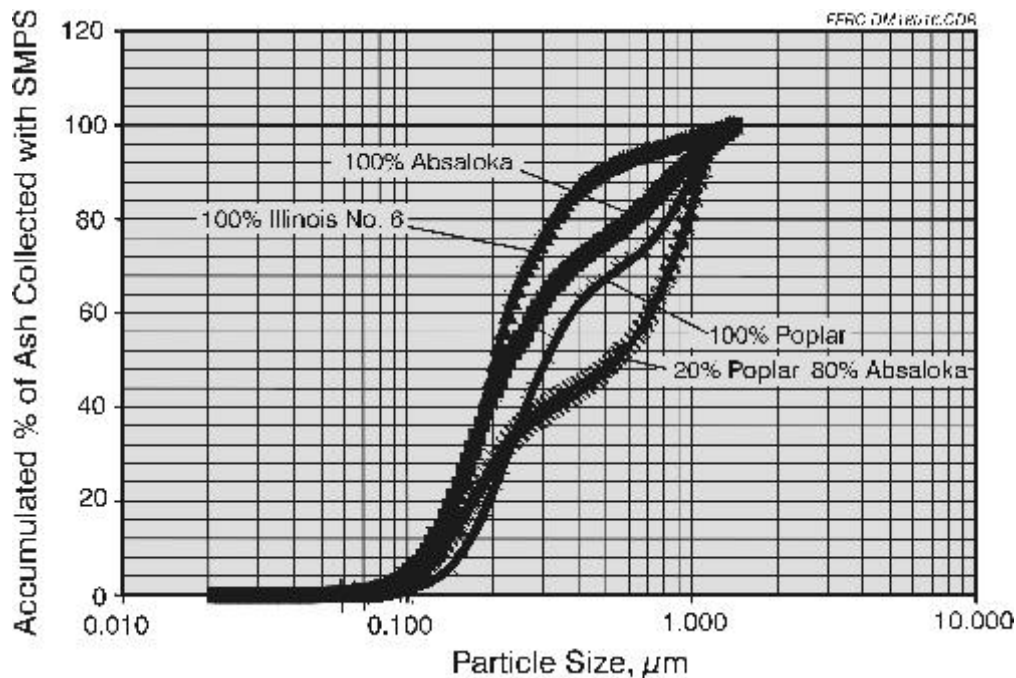


Figure 44. On-line APS-SMPS particle-size distributions.

Several mineral interactions and transformations are seen to occur during the production of the fly ash. The CCSEM analysis results for the major mineral phases have been given in Tables 8 and 19. The most striking is the behavior of iron between the parent Illinois No. 6 coal, the Illinois No. 6 fly ash, and the blend fly ash. The large particles of pyritic iron present in the coal decompose and fragment during the combustion process, leaving essentially no iron-rich material with a size greater than 22  $\mu\text{m}$ . Further, there is extensive interaction with minerals containing Al and Si show that most of the iron is found in the “unclassified” mineral category in combination with aluminum and silica. Smaller amounts of iron are also found in the mixed Al-Si category and the Si-rich category, while very little iron oxide and no pyritic minerals are present. The iron present in the blend fuel arises almost exclusively from pyritic minerals in the Illinois coal fraction. During combustion of the blend, the pyritic minerals fragment, again resulting in almost no particles greater than 22  $\mu\text{m}$ . Again, particle-by-particle examination of the analysis data shows a portion of the iron is found in the unclassified, silica-rich, and mixed Al-Si mineral categories, as occurred with the fly ash produced from the pure coal. However, a significant amount (18 wt%) of iron oxide is also identified. Cocombustion of the biomass with the Illinois No. 6 coal appears to have reduced the degree of assimilation of pyritic mineral matter into the Al- and Si-containing ash components. This may be because of dilution of the aluminosilicate coal minerals with nearly pure silica with high surface area from the wheat straw, an alteration in the aluminosilicate fly ash chemistry because of the increased Si and K derived from the wheat straw, or the presence of surface potassium compounds hindering the interaction of iron oxide with the aluminosilicate materials.

The second notable interaction during the production of fly ash is the behavior of potassium derived from the wheat straw fraction of the blend. Table 23 shows the average potassium

TABLE 23

Average Potassium Concentration of Illinois No. 6 and Blend Fly Ash		
	Illinois No. 6	Blend
	Fly Ash % K	Fly Ash % K
Quartz	5.6	4.0
Iron Oxide	0.4	0.6
Calcite	0.4	0.2
Kaolinite	3.7	0.0
K Al-Silicate	9.6	13.9
Mixed Al-Silicate	8.3	8.3
Pyrite	0.0	0.0
Pyrrhotite	0.0	0.0
Si-Rich	9.8	9.9
Unclassified	9.7	12.8

composition of the major mineral phases of the Illinois No. 6 and blend fly ash. Potassium is depleted in the quartz and kaolinite mineral phases, but shows strong increases in the potassium aluminosilicate and unclassified phases. This indicates that interaction of wheat straw-derived potassium with aluminosilicate minerals is occurring, particularly in the finer <math><22\text{-}\mu\text{m}</math> blend fly ash fractions. This may be a result of simple physical coating of aluminosilicate ash by condensation of potassium species on the ash or deposition of fine potassium aerosol particles. Examination of the morphology of the blend fly ash, as shown in Figure 45, indicates smoothly rounded particles, suggesting that coating with condensed potassium species is the likely mechanism. Although the blend fly ash contains appreciable submicron material, the composition is similar to that of the larger supermicron fraction, i.e., containing Si, Al, Fe, and K, with an increase in potassium content at smaller particle sizes. No pure potassium species such as chlorides or sulfides were identified. The lower percentage of potassium in the quartz mineral phase which is derived primarily from the wheat straw argues against a simple physical deposition mechanism only and suggests that a chemical interaction of potassium with the aluminosilicate material may also be occurring. The association of the potassium is significant because the presence of the coal ash components appears to be tying up some of the biomass-derived potassium, reducing the amount potentially released as a fine sulfate or chloride aerosol. In contrast, Figure 46 shows the morphology of the 100% wheat straw fly ash. This ash is characterized by very large, angular particles clearly related to the parent plant structures, along with rounded but imperfectly spherical ash particles. The chemistry of the larger particles is primarily silica, with lesser but still significant amounts of calcium, potassium, or both present. The other feature of the 100% wheat straw ash not seen in the blend ash is the presence of very fine (<math><2\text{-}\mu\text{m}</math>) particles consisting of potassium chloride, calcium sulfate, and, occasionally, calcium phosphate. These appear on the surface of the larger silicate particles, in the form of isolated discrete particles, and in apparent agglomerates of very fine particulate material.

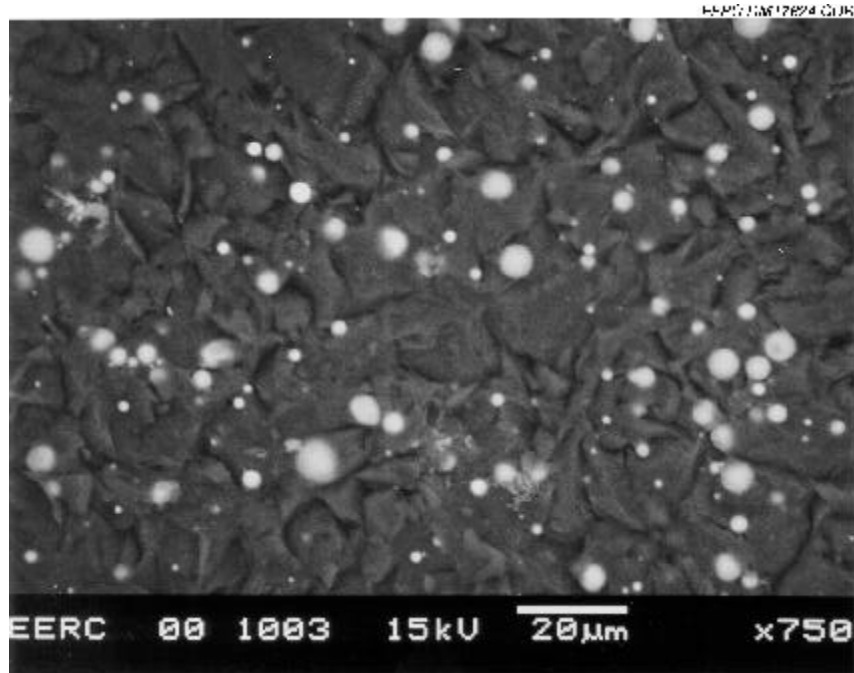


Figure 45. 80% Illinois No. 6–20% wheat straw fly ash.

### **MODELING OF FLY ASH AND AEROSOL FORMATION DURING COMBUSTION OF BIOMASS BY MODIFYING A CODE DEVELOPED FOR COAL COMBUSTION**

In Austria, the main focus on biomass combustion is in hot-water-producing combustion plants for district heating purposes. These units are mainly grate fired, and the dominant biomass fuel is bark. However, other biomass fuels such as waste wood and agricultural residues such as straw are used as well. Because of the small scale of these plants (typically 3–10 MW), flue gas particle control devices represent a major investment cost for these plants. However, because of increased awareness of the hazardous effects of particle emissions, the regulatory limits of particulate emissions are being steadily decreased for these plants, making installation of expensive particle control units a necessity.

The research group at the Technical University of Graz (TUG) is continuously collecting experimental data from Austrian biomass combustion plants, but by being able to model factors influencing the particle-size distribution during biomass combustion, new ideas and methods can be qualitatively tested prior to expensive full-scale test runs.

Dr. Jonas Dahl of TUG, Austria, worked in a postdoctoral position for 9 months at the EERC during the year 2000. Dr. Dahl investigated the feasibility of modifying and using a computer code developed for predicting ash transformation in coal combustion to model fly ash and aerosol formation in biomass combustion processes. Little is known on how cocombustion of coal with biomass will affect ash behavior in power plants. Such a model predicting the size distribution

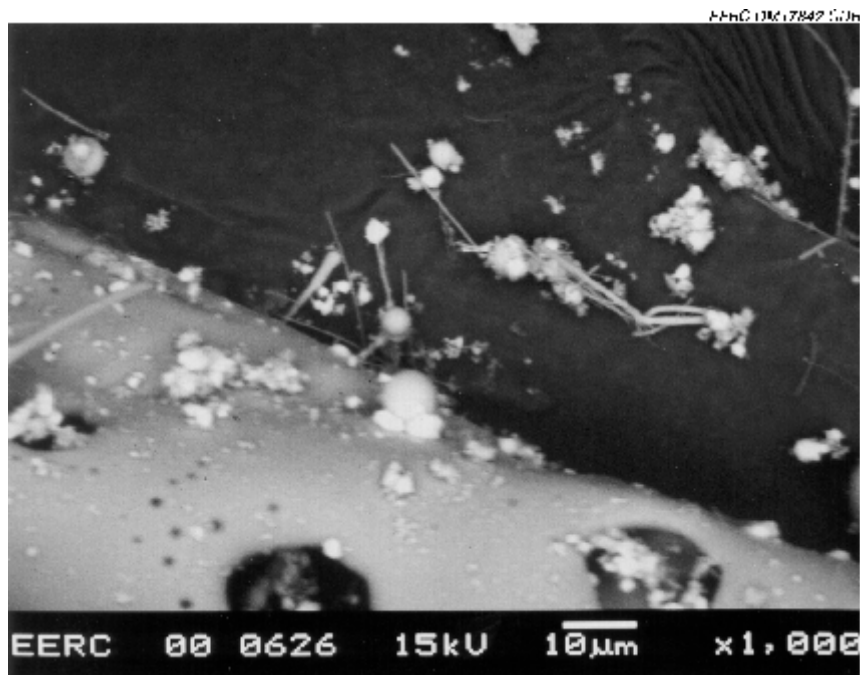
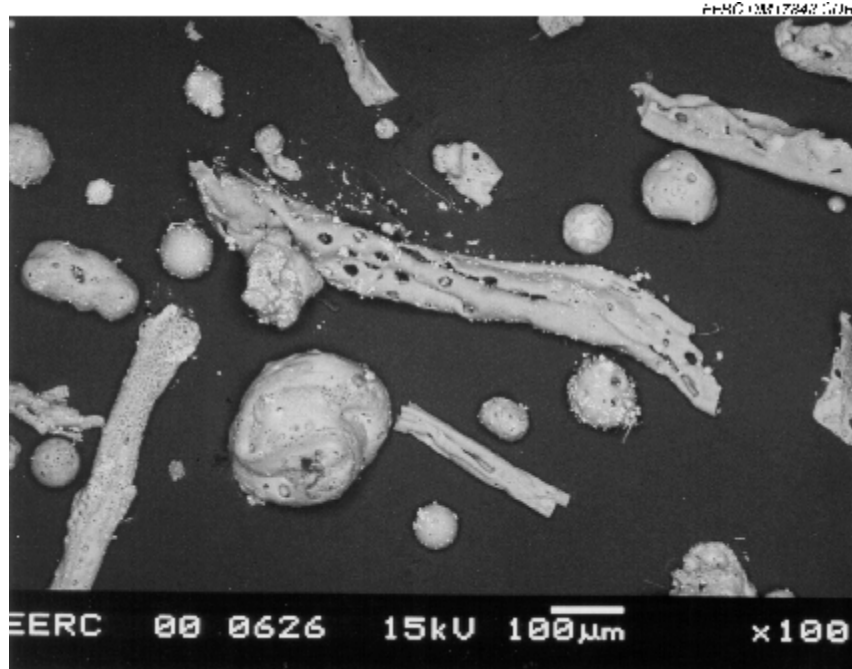


Figure 46. Wheat straw fly ash.

and chemical composition of fly ash would be an important tool to evaluate eventual deposition and slagging problems.

The original objective of the work was to adapt an ash transformation code developed for coal for predicting ash and aerosol formation in a biomass combustion system. However, because of poor existing documentation of the code, this objective had to be modified to concentrate on understanding and documenting the current algorithms of the code and, from this, suggest changes for application of the code to biomass fuels and aerosol formation predictions.

The starting point of the development of a biomass ash transformation model was the EERC TraceTran program. The core of the TraceTran code is the ATRAN code, which was developed to describes the transformation of the minerals during coal combustion. The work performed was mainly focused on understanding this part of the TraceTran code. The ATRAN code has been refined over the years and used for several types of thermal conversion processes of coal. Each of these processes has required their own special equations that have subsequently been added as options hardcoded into the source code.

### **The TraceTran (ATRAN) Program**

A general explanation of the functions of TraceTran is already given in the operation manual to the program (119). The manual also contains a detailed explanation of the required input to the program. This report does not, however, supply any information on the code itself or the algorithms used in the program. Thus, in order to be able to change the program for future projects and fuel types, the current work focused on obtaining a detailed insight of the algorithms used and the functioning of the code. However, because of the complexity of the code, the following description is preliminary and not yet a full documentation of the code.

The source code to TraceTran consist of 23 C++ files (.CPP) and 24 header files (.H) which, are listed in Table 24. The CPP files contain the algorithms and actual code, while the header files contain definitions of the format and content of functions, constants, and variables used in the respective CPP files.

The main section of the TraceTran program is the TRACTRAN.cpp. This part starts the program and calls upon the seven different ATRAN files that contain the main code for the ash transformation calculations. The basic function of these files are described Table 24 and are executed in the order of 1-5-2-3-6-4-7. These ATRAN files subsequently call the remaining subprograms listed in Table 25. The main function of each of these subprograms is also briefly described in Table 24.

It should be noted that COMATRAN and RANDOM appear to be old relics from previous versions of ATRAN or TraceTran and are not used in the present code. No function call to the COAMTRAN.CPP or its header file was found in the source code, and according to comments in the source code, the algorithm of the RANDOM.CPP has most likely been replaced by an internal C++ random number function.

TABLE 24

## Summary of the TraceTran Source Code Files

	CPP Files		Header Files
TRACTRAN.CPP	Windows interface to the program Input and start of the program	ATRAN.H	Defines maxparticles in system, organic-bound Si and % of vaporized elements in size bin <1.
ATRAN1.CPP	Data input, data formation, sulfur removal, and fragmentation	ATRAN1.H	Defines ATRAN1
ATRAN2.CPP	Coalescence of included particles	ATRAN2.H	Defines ATRAN2
ATRAN3.CPP	liberation	ATRAN3.H	Defines ATRAN3
ATRAN4.CPP	Data manipulation of ash, sorts minerals according to size and type of mineral	ATRAN4.H	Defines ATRAN4
ATRAN5.CPP	Mass balances (normalizes and compares data from CCSEM and XRF analyses)	ATRAN5.H	Defines ATRAN5
ATRAN6.CPP	Condensation reactions	ATRAN6.H	Defines ATRAN6
ATRAN7.CPP	Final output of data	ATRAN7.H FORMATS.H	Defines ATRAN7 Contains the format for the input and output files to ATRAN
STORAGE.CPP	Handles memory management	STORAGE.H	Defines STORAGE
SPHERES.CPP	V, A, and cross A of spheres	SPHERES.H	Defines SPHERES
GETTYPE.CPP	Returns fragmenting minerals to ATRAN 2	GETTYPE.H	Defines GETTYPE
GETSIZE.CPP	Sort particles into size bins	GETSIZE.H	Defines GETSIZE
GETPHASE.CPP	Writes mineral number for each particle	GETPHASE.H	Defines GETPHASE
FILEIO.CPP	Handles and stores input and output arrays for the seven ATRAN files	FILEIO.H	Defines FILEIO
CONVMAG.CPP	Converts three mag files into two	CONVMAG.HPP	Defines CONVMAG
COMPOUND.CPP	Mineral classification of CCSEM data from each particle	COMPOUND.H	Defines COMPOUND
COMMON.CPP	Common constants and error messages	COMMON.H	Defines COMMON
ELEMENTS.CPP	Normalizing routine for element input	ELEMENTS.H	Defines ELEMENTS
TRACE.CPP	Tracks the trace elements through the ash transformation, look-up tables for four coals, six conditions (C–O, steam), 27 temperatures (1500?–200?C), and six pressures (1–26)	TRACE.H	Defines TRACE
HOTGAS.CPP	Extra code for running the program in hot-gas mode	HOTGAS.HPP	Defines HOTGAS
HGELEM.CPP	Normalizing routine for elements in hot-gas mode	HGELEM.H	Defines HGELEM
COMATRAN.CPP	Mineral classification of CCSEM data from each particle	COMATRAN.H	Defines COMTRAN
RANDOM.CPP	Random number generator	RANDOM.H	Defines RANDOM

TABLE 25

Format of the CCSEM Analysis Files

#	T	Cts	Na	Mg	Al	Si	P	S	Cl	K	Ca	Fe	Ba	Ti	X	Y	Dia	Max	Min	Ar	Pe	Sh	F#	L-L
---	---	-----	----	----	----	----	---	---	----	---	----	----	----	----	---	---	-----	-----	-----	----	----	----	----	-----

Explanations:												Max	Max diameter											
#	Particle number											Min	Min diameter											
T	Type											Ar	Area											
Cts	X-ray counts											Pe	Perimeter											
X	x coordinate											Sh	Shape factor											
Y	y coordinate											F#	Frame number											
Dia	Average diameter											L-L	Locked or liberated particle											

### General Algorithms and Data Flow in TraceTran

Data from CCSEM analyses are input to the program as files made up of large arrays of data containing the chemistry, size (= cross section area which is recalculated as the diameter of a spherical particle), and mineral juxtaposition (locked or liberated) of each individual particle analyzed at three different magnifications (50 $\times$ , 250 $\times$ , and 800 $\times$ ). Each magnification contains data on particles in certain size ranges. The 800 $\times$  file contains particles between 1 and 4.6  $\mu\text{m}$ . The 250 $\times$  contains particles between 4.6 and 22  $\mu\text{m}$  and the 50 $\times$  between 22 and 100  $\mu\text{m}$ .

The standard CCSEM analysis method stops the automatic analyses either when 1200 particles have been analyzed (#) or when 100 frames (F#) have been analyzed (each area the SEM can scan without having to move the sample) at each magnification. This means that the maximum number of particle data entering the program would be 3600. However, at the lower-magnification analyses, the limit of 100 frames is typically reached before 1200 particles have been found in these size ranges.

The following numbered sections follow the flow sheet shown in Figure 47 describing the basic calculations of the TraceTran code. Both the flow sheet and the explanations in Sections 1 to 9 are a first basic version of a complete documentation of the algorithms in the code.

- 1) When the first version of ATRAN was programmed, only two magnifications were used for the CCSEM analyses, and thus, the three magnification files have to be converted into two before ATRAN can process them further. This is automatically done in the interface to TraceTran (see Figure 48 and Table 25) by dividing the data in the 250 $\times$  file into the other two files which then produces the two size ranges: low (1–10  $\mu\text{m}$ ) and high (10–100  $\mu\text{m}$ ).
- 2) The chemical compositions of the particles are compared with the composition of 35 minerals that have been identified in coal. The number of the identified mineral is then added after each particle in the input arrays. Some minerals behave in a similar way during combustion and, therefore, are identified with the same mineral number. The result is 32 different mineral numbers. If none of the compositions comply with the mineral identification, the particle is classified as unknown and is assigned the mineral number 33.

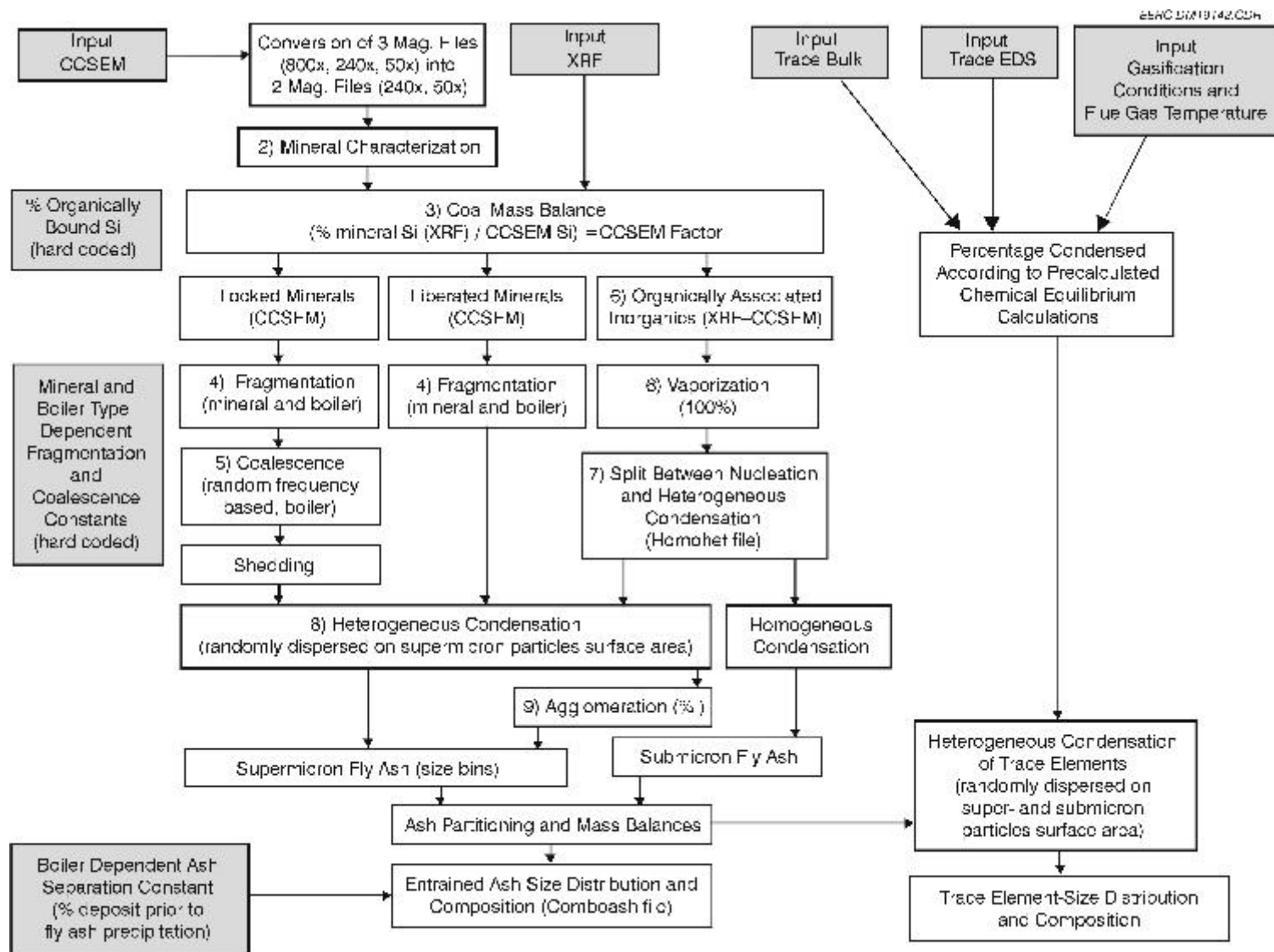


Figure 47. TraceTran program flow diagram.

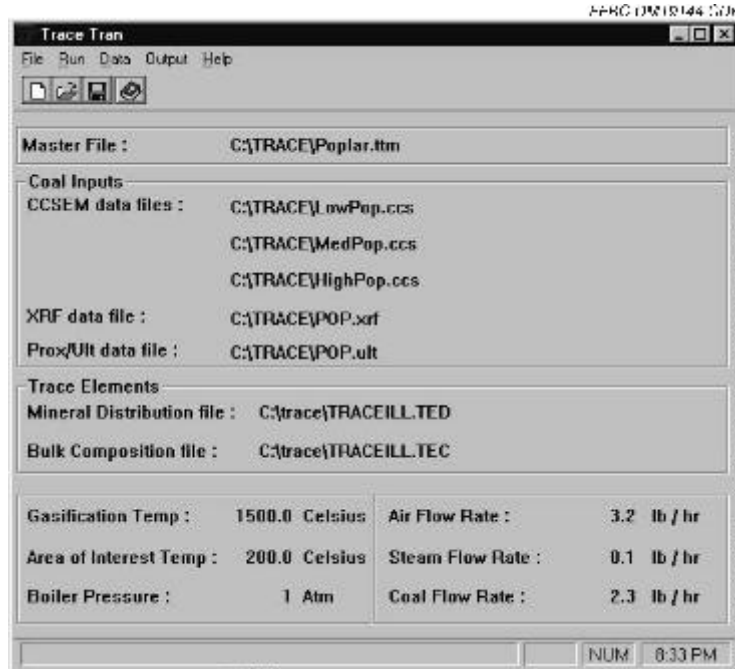


Figure 48. TraceTran program interface.

- 3) Concentrations of organically associated elements are identified by subtracting the CCSEM analysis from the XRF analysis. However, before this can be done, the two analysis methods have to be correlated with each other. This is done by converting all the major elements to oxides and then correcting the amount of SiO<sub>2</sub> found with XRF with the amount of SiO<sub>2</sub> found with CCSEM. In order to be able to do this correlation, it is assumed that 2% of the Si is organically bound in the coal or present as submicron particles in the fuel which are not analyzed by CCSEM. The ratio between 98% of the XRF Si and the CCSEM Si is then used as a factor for correlating the other elements analyzed by CCSEM. Finally, the amount of elements found by CCSEM is subtracted from the amount found by XRF. The difference is considered as organically associated elements. If the amount in the CCSEM is higher than the amount detected by XRF, the amount detected by XRF is used and the organically bound part set to 0.0001, as a value exactly equal to 0 will crash the program because of division by zero errors.
- 4) As the program progresses, several new arrays are created by extracting and sorting information from the input arrays, e.g., locked and liberated particles are divided into new arrays which are used for the fragmentation and coalescence calculations. Both locked and liberated mineral particles fragment during combustion. The extent of fragmentation depends on what type of mineral the particle contains. The minerals pyrite, oxidized pyrite, kaolinite, calcite, dolomite, and quartz fragment during combustion while the other minerals do not. Through experimental research and years of full-scale coal combustion experience, the EERC has developed different fragmentation factors which vary for the different mineral types and also with the combustion or gasification technology. The TraceTran code contains empirical measured factors for pressurized

bubbling fluidized-bed gasification (BFB), fluidized-bed combustion (FBC), low-NO<sub>x</sub> pulverized fuel (pc) combustion, and cyclone combustion (Table 26). No experimental measurements are available for stoker or grate combustion systems. All particles in all size ranges containing these fragmenting minerals fragment, but the fragmentation factors are randomly varied within a given size range. The new particles formed from the fragmentation maintain their identification number whether they were liberated or locked particles. Typically, fragmentation dramatically increases the number of particles. The program appears to allow for up to 10,000,000 particles after fragmentation, based on the defined size of the temporarily created memory array used for the fragmentation portion of the program.

During fragmentation, mineral particles containing sulfur are compensated for the loss of SO<sub>2</sub> and CO<sub>2</sub> during the combustion–gasification process by multiplying their individual area and diameter by appropriate factors. The result is that the sum of volume and mass of the fragmented particles is less than the volume and mass before removal. The factors vary with the mineral type, e.g., 0.7894 for iron carbonate (Fe<sub>2</sub>[CO<sub>3</sub>]<sub>3</sub>) and 0.7176 for gypsum (CaSO<sub>4</sub>).

- 5) Previous investigations have shown that liberated particles in coal do not interact significantly with any other particles once they enter the furnace. Thus only locked particles are allowed to grow because of coalescence. At the high temperatures prevailing during coal combustion, all minerals melt and can thus coalesce to form new particles. However,

TABLE 26

Fragmentation and Coalescence Constants in TraceTran

Mineral	Boiler Type					Gasification Hot Gas, TraceTran
	Fluidized	Pulverized	Low-NO <sub>x</sub>	Cyclone		
Pyrite	20	5	7	350	180	
Iron Carbonate	20	5	7	350	180	
Pyrrhotite and Ox. Pyrrhotite	20	5	7	390	180	
Gypsum	1	1	1	1	1	
Barite	1	1	1	1	1	
Ca–Al–P	1	1	1	1	5	
Kaolinite	30	70	20	100	5	
Calcite and Dolomite	9	1	1	1	5	
Quartz	15	150	25	1	55	
Coalescence	70	150	240	420	280	

the degree of coalescence is dependent on how the locked minerals are distributed in the coal particles. In the program, the coalescence is simulated by randomly combining locked particles based upon a frequency distribution until the total number of particles reaches a threshold value of 10,000 particles. The degree of coalescence is also based upon a coalescence value that varies with the combustion technology.

- 6) All organically bound elements are assumed to vaporize during coal combustion. The amount of organically bound elements is determined by subtracting the mineral bound elements determined by the CCSEM analyses from the total amount of major elements determined by the XRF bulk ash analysis, as described in Section 3.
- 7) The vaporized elements (i.e., organically bound elements) are then divided into nucleating and heterogeneously condensing groups. The split between these two is determined by empirical factors fitted to experimental data which differ for each element and boiler type. A certain amount of the submicron particles are allowed to agglomerate and form particles  $>1\mu\text{m}$ . These factors are contained in a file called homohet, which is different for each combustion–gasification technology.
- 8) The heterogeneously condensing elements are randomly distributed on the surface of the locked and liberated mineral particles.
- 9) The output from the calculations of the main elements are summarized in the comboash file.

### **Calculations with the TraceTran Code**

Initially, it was very difficult to get the TraceTran program to run using the new analysis data from biomass fuels. According to the description of the program, it should be able to accept the internal EERC standard format of CCSEM files. Apparently these standards had been changed since the program was first coded. The code expected as input three CCSEM files obtained from analyses performed at three magnifications: 800 $\times$ , 240 $\times$ , and 50 $\times$ . Because of the installation of new SEM instruments and concurrent changes in the automated SEM analysis routines, the new standard analyses at the EERC are now performed at magnifications of 800 $\times$ , 250 $\times$ , and 50 $\times$ . Furthermore, in these CCSEM files the chemical compositions are now reported in “floating point” numerical format. Examination of the TraceTran code appeared to indicate that it expect a floating point number format for the CCSEM input. However, the sample files containing data for Illinois No. 6 and Sufco coals that are installed along with the TraceTran program use an integer number format for these values. Initial tests with floating point numbers would cause the program to crash. By changing all input files to integer format for the CCSEM chemical compositions, calculations were finally carried out using the biomass data.

Calculations were performed for two coals (Illinois No. 6 bituminous coal and Absaloka subbituminous coal) and three biomass fuels (hybrid poplar, wheat straw, and Austrian bark). The results from the TraceTran calculations were then compared to the experimental particle-size distributions of baghouse ash determined by CCSEM analysis as shown in Figure 49.

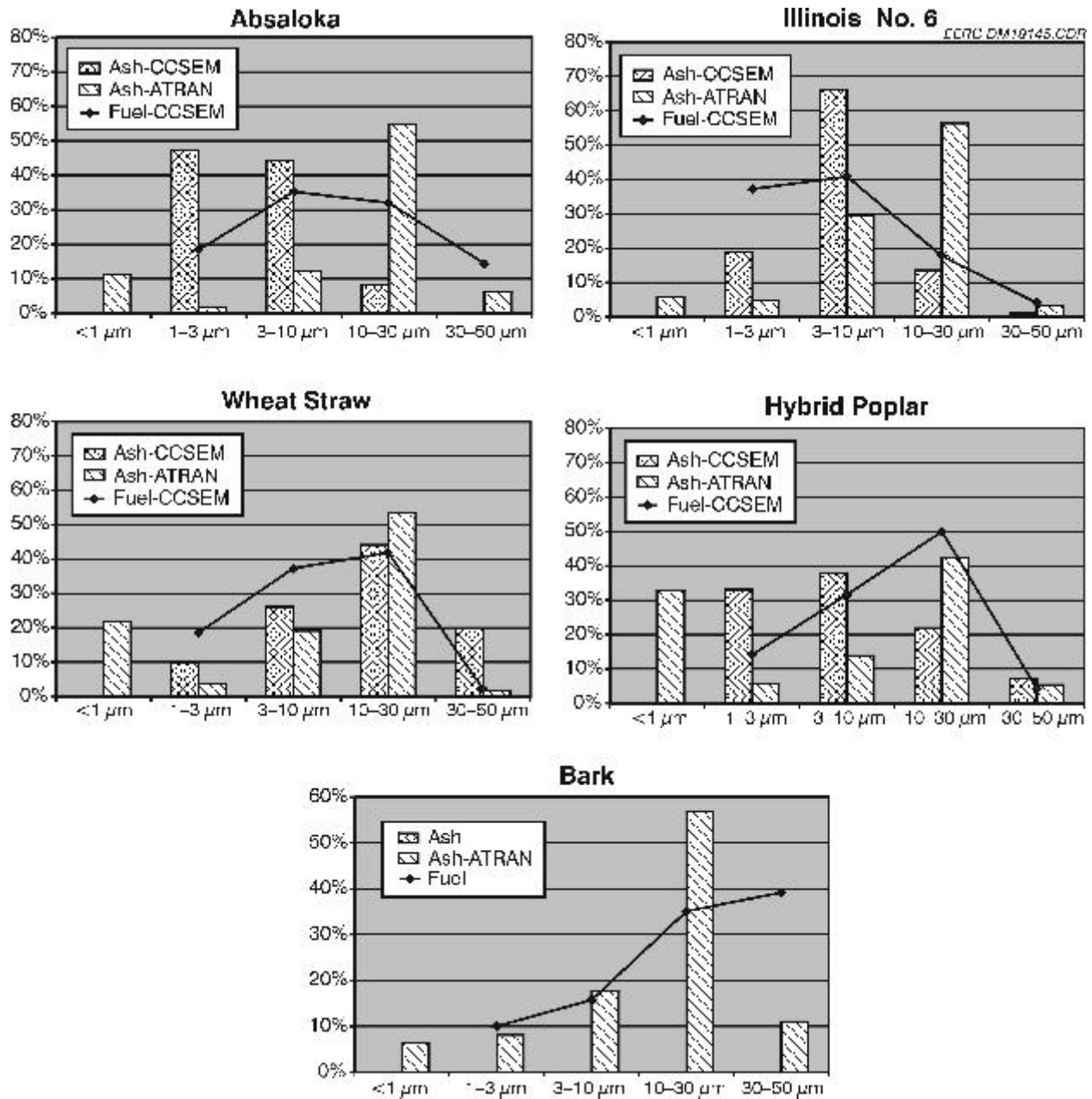


Figure 49. Results from the TraceTran model calculations compared to measured particle-size distribution of baghouse ash from CEPS combustion tests.

TraceTran requires input in the form of three CCSEM files (800×, 240×, and 50×), one XRD file (mineral bulk composition), one ULT file (ultimate analysis of fuel composition and ash content), and two files containing bulk content and mineral association of trace elements (see Figure 47). Details on the

content of these files are described in the TraceTran manual (119). Unfortunately, it turned out to be rather difficult to gather complete data sets (CCSEM analyses of fuel and ash and XRF analyses) from the same test runs for all fuels. Thus, for some of the fuels shown in Figure 49, the fuel analyses used in the model calculations are from a different test run than the ash analyses. The sample number or a note on the data source are also given in Table 27.

TABLE 27

EERC Identification Numbers for Data Used in the TraceTran Calculations				
	Fuel	Ash	XRF	Ult.
Illinois No. 6	Installed with TraceTran	000168	Installed with TraceTran	Installed with TraceTran
Absaloka	990047	990970	000283	000283
Straw	990415	000748	990415	990415
Hybrid Poplar	000683	000721	000683	000683
Austrian Bark	TUG	No analyses performed	TUG wet chemical analyses	Estimated from database values

As the trace elements were not investigated for the biomass materials and owing to the fact that these elements have a very small effect on the total particle-size distribution, the same dummy trace element files were used for all model calculations. The bulk trace element file does contain the bulk amount of Cl present. This was discovered after the calculations were performed and thus was not considered in the trace element calculations. This presumably could have affected the results for the submicron part of the TraceTran output.

The usual gasification conditions only affect the behavior of the trace elements in the TraceTran calculations and have no effect on the total particle-size distribution. Because of this, the same “dummy” gasification conditions were used for all calculations (see Figure 47).

### Discussion of Results

While comparing the results in Figure 49, it must be kept in mind that the CCSEM technique does not analyze particles smaller than 1  $\mu\text{m}$ . Thus the amount of submicron particles in the fly ashes are unknown, and a comparison with the TraceTran output is not possible for the submicron size bin. Comparison of TraceTran calculations with baghouse ash from bench-scale CEPS tests did not show a good correlation. Typically, ash particles in the size range 10–30  $\mu\text{m}$  are missing from the experimental data. These particles presumably are removed because of impaction, as the flue gas stream direction changes 90 degrees at the CEPS furnace exit. Comparison for these size ranges is thus not really relevant, although the wheat straw data fit rather well, with a significant peak in the 10–30- $\mu\text{m}$  range. It should be noted that

TraceTran predictions are based on aerodynamic diameter, while the CCSEM analysis measures physical particle diameter.

As seen in Figure 49, the calculated and the measured fly ash particle-size distributions do not fit very well. The TraceTran program was designed for coal so it was expected that biomass data probably would give a poor fit. However, the similar lack of fit for the coal data was unexpected. The most likely reason is that the coal fuel and ash data used were not from the same test runs. More calculations with other sets of data are, therefore, required to test the validity of the TraceTran predictions. Moreover, the default version of TraceTran was used in for the test calculations. Presumably, calculations in another mode such as “pulverized” or “low-NO<sub>x</sub>” (see Table 26) would give better results. Currently, the default mode is hardcoded into the program and can only be changed by modifying or recompiling the source code. No mode changes were attempted in these first test calculations. This will be done when the TraceTran code is reprogrammed and the modes are easier to change by the user.

### Results from Mineral Classification of Biomass Fuels

As previously explained, the calculation of fragmenting mineral particles in TraceTran is strongly dependent on the mineral composition identified in the CCSEM analyses. Therefore, it is crucial that the fragmenting minerals are correctly determined in the biomass fuels as well as in coal. Table 28 show the predominant minerals of the 32 minerals identified in the TraceTran code from CCSEM analyses of the fuels investigated. The fragmenting minerals are quartz, calcite, dolomite, kaolinite, pyrite, and pyrrhotite.

TABLE 28

Mineral	Predominant Minerals in the Fuels Investigated, wt%				
	Absaloka	Illinois No. 6	Poplar	Bark	Straw
Quartz*	18.4	15.3	1.9	26.1	26.1
Calcite*	8.9	3.5	68.6	8.3	4.5
Dolomite*	1.3	0	0.7	5.6	0.1
Kaolinite*	34.5	8.2	0.9	0	0
Pyrite*	0.1	2.6	0.1	0	0
Pyrrhotite*	9.1	46.3	0.7	0	0
Iron Oxide	4.4	1.1	9.1	1.9	1.5
K Al-Silicate	3.7	7.5	0.6	2.9	0
Ca Silicate	0	0	0	5.4	0.3
Si-Rich	1.6	2.4	0.4	2.3	11.4
Other	7.3	4.8	6.5	0.3	0.5
Unknown	10.3	8.2	9.3	39.6	55.3

\* Considered as fragmenting in the TraceTran code.

## Discussion

The modeling of fragmentation in TraceTran is heavily dependent on which fragmenting minerals are identified in the mineral classification part of the code. The identified fragmenting minerals in the biomass fuels were quartz, calcite, and dolomite. However, the analyses of bark and wheat straw also contained large numbers of mineral particles with compositions that did not match any of the 32 minerals which can be identified by the code. The reason for this is the different chemical structure of biomass fuels where a large part of the inherent minerals can consist of phytoliths. The composition of these phytoliths can vary greatly, depending on the species of the plant and on the soil it was grown in. In order to find trends in the composition of these new “minerals,” statistical cluster analyses of the chemical composition of mineral particles in biomass have been initiated by the EERC. The mineral particles in fuels and ashes are grouped by means of cluster analyses using the statistical software package Minitab version 13.1. Results from these statistical analyses have been reported in previous sections.

## Implementation of Aerosol Model Calculations

One of the major objectives of TUG is to gain information on possible influences controlling the formation of the submicron part of the fly ash during biomass combustion. Because the current version of TraceTran is not able to predict a submicron size distribution, a model for the formation and dynamics of submicron particles has to be developed for the TraceTran model.

## The General Dynamic Equation

To improve TraceTran and modify it to model biomass combustion and ash transformations, several important algorithms are suggested for expressing the combustion process and ash formation mechanisms.

The size and chemical composition change of fly ash particles in combustion processes are due to physical mechanisms such as chemical reactions, homogeneous nucleation, vapor condensation, coagulation, and deposition. The combination of these processes can be described by the General Dynamic Equation (GDE) (120), which is a population balance over a unit volume of the system. Consequently, by solving the GDE, the number concentration and size distribution of the fly ash can be calculated. However, the GDE is a nonlinear, partial integral-differential equation, and as such, its solution is complex and often

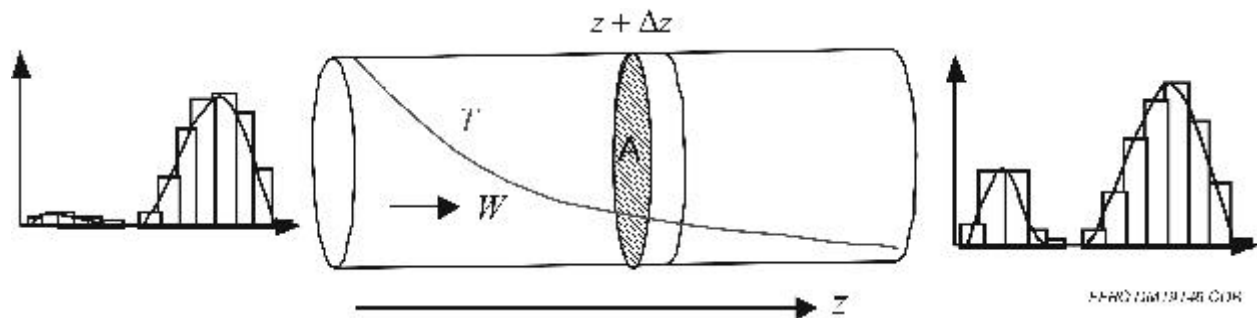


Figure 50. Illustration of the assumed plug flow and the discretized size distribution.

requires simplifying assumptions and numerical solution methods to obtain a solution. Several different schemes and approaches have previously been used to solve the GDE for aerosol dynamics (121).

The most common models used for combustion processes assume a flue gas which moves in plug flow and the temperature and composition of the gas uniform in any cross section of the flue gas duct (121, 122). The axial temperature profile and velocity of the gas are assumed to be known, and thus the time and temperature in every point on the z-axis are known as well. The numerical solution is then performed by stepwise calculation of the GDE for each  $z$  (Figure 50).

Furthermore, as a part of the numerical solution, the continuous size distribution is approximated by dividing it into discrete segments, or size bins. The finer this discrete size distribution is made, the better the resolution of the size distribution calculations, but at the cost of increased computational time.

Assuming the above-described approximations, the one-dimensional GDE for each size bin  $k$  can then be written as (122):

$$\frac{dn_k}{dz} = \frac{1}{u} J_n d(k - k^*) + \frac{c_{\text{coag}}}{\xi} \frac{dn_k}{dz} + \frac{c_{\text{grow}}}{\xi} \frac{dn_k}{dz} - \frac{v_d A_d}{uDV} n_k \quad [\text{Eq.1}]$$

where  $n_k$  is the particle number concentration for a size class  $k$  with particle diameter  $dp_k$ . The first term on the right corresponds to particle formation due to the homogeneous nucleation mechanism (formation of critical size embryo with the size  $dp^*$ ), the second term (coag) describes the coagulation mechanism, the third term (grow) describes the growth by condensation and chemical reactions, and the fourth term is the rate of particle deposition on boundary surfaces, where  $v_d$  is the particle deposition velocity,  $A_d$  is the deposition area, and  $V$  is the axial volume step.

In a previous EERC report, Dr. Flemming Frandsen reviewed and described in detail the equations for calculating the growth and nucleation term of the GDE in a hot flue gas (123). The explanations of these mechanisms will, therefore, not be repeated in this report, but the equations are described by Equations 1–3. Frandsen's report also contained a computer code HOMONUCL where the point of nucleation for a single condensing species in a cooling gas with a fixed chemical composition and a monodispersed source of primary particles could be calculated. Frandsen concluded that in order to be able to apply the code on a combustion system, the following additions to the code would be necessary:

- The gas-phase composition should be calculated using chemical equilibrium calculations, as the formation of condensing species is coupled to the global chemistry in the flue gas.
- A discrete particle-size distribution of the ash should be implemented instead of the monodispersed particles used in the code.
- Coagulation was not considered in the HOMONUCL code and should thus be considered in a new code.
- The effect of multicomponent nucleation should be considered.

- Data on surface tension for the nucleating species have to be collected. The calculation of nucleation is very sensitive to the surface tension, and thus good data are crucial.

Accordingly, the aim of this work has been to find possible solutions to the necessary additions to the HOMONUCL code and to identify necessary changes to the TraceTran code so that it can easily be connected to an improved HOMONUCL code. Thus a conceptual model was developed where the main calculations and order are described. This conceptual model is outlined in Figure 51.

The idea behind the conceptual model is that the TraceTran code will be used to create the input to the aerosol model by providing it with the amount of elements in the gas phase as well as a primary particle-size distribution. The TraceTran code identifies organic-bound elements. The major amount of these elements will vaporize during combustion; however, elements that form high- temperature stable oxides such as Mg, Al, Ca, and Si will form new particles in the boundary layer or on the surface of the burning char particles and, thus, form the submicron part of the primary mineral particle-size distribution. Other organically bound elements such as the alkali metals K and Na or volatile trace elements enter the main flue gas where they undergo gas-phase reactions mainly with Cl- and S-forming chloride or sulfates. If there is an excess of alkali to Cl and S, alkali hydroxides or carbonates are formed as well. These compounds either condense on the surface of the primary mineral particles or nucleate and form new submicron particles.

The condensation or nucleation of the alkali metals depends on the partial pressure of the species formed in the gas phase. The speciation and partial pressure ( $p_i$ ) of these species are determined by calculating the chemical equilibrium in the gas phase at temperature T. The temperature is, in turn, determined by the step taken on the z axis (see Figure 50). At the same temperature as the gas-phase equilibrium calculation, the saturation pressure of species i ( $p_{i,sat}$ ) is calculated over a particle containing the pure condensed species.

The mass transfer ratio I of the species i to the surface of the spherical primary mineral particles in size bin k with the average size of  $d_k$  can be determined by:

$$I_{i,k} = \frac{2 \cdot p_i \cdot d_k \cdot D_i}{R_g \cdot T} \cdot P_{load,k} \cdot (p_i - p_{i,sat}) \cdot C_{FS} \quad [\text{Eq. 2}]$$

where  $D_i$  is the diffusion coefficient for species i in the flue gas. The  $P_{load,k}$  is the number of particles in size bin k per volume unit, and  $C_{FS}$  is the Fuch-Sutugin correction factor which depends on the Knudsen number (123). If the temperature profile is steep enough and the concentration of species i is high in the gas phase, the gas-to-particle conversion by condensation may not be fast enough and  $p_i$  will reach the critical partial pressure  $p_{i,crit}$  for nucleation. The critical pressure is calculated by multiplying the saturation pressure  $p_{i,sat}$  by the critical saturation ratio  $S_{crit}$  which is a function of the temperature and of compound-specific properties of the condensed species such as its surface tension. Frandsen concluded in his investigations with the HOMONUCL code that the calculation of nucleation is very sensitive to the surface tension and that such data are typically difficult to obtain. New estimated data on the surface tension of KCl and  $K_2SO_4$  have been recently reported by Christensen and coworkers (121). Search for surface tension of other species such as ZnO and  $PbCl_2$  which can be important for certain waste wood fuels (124) needs to be done in future investigations.

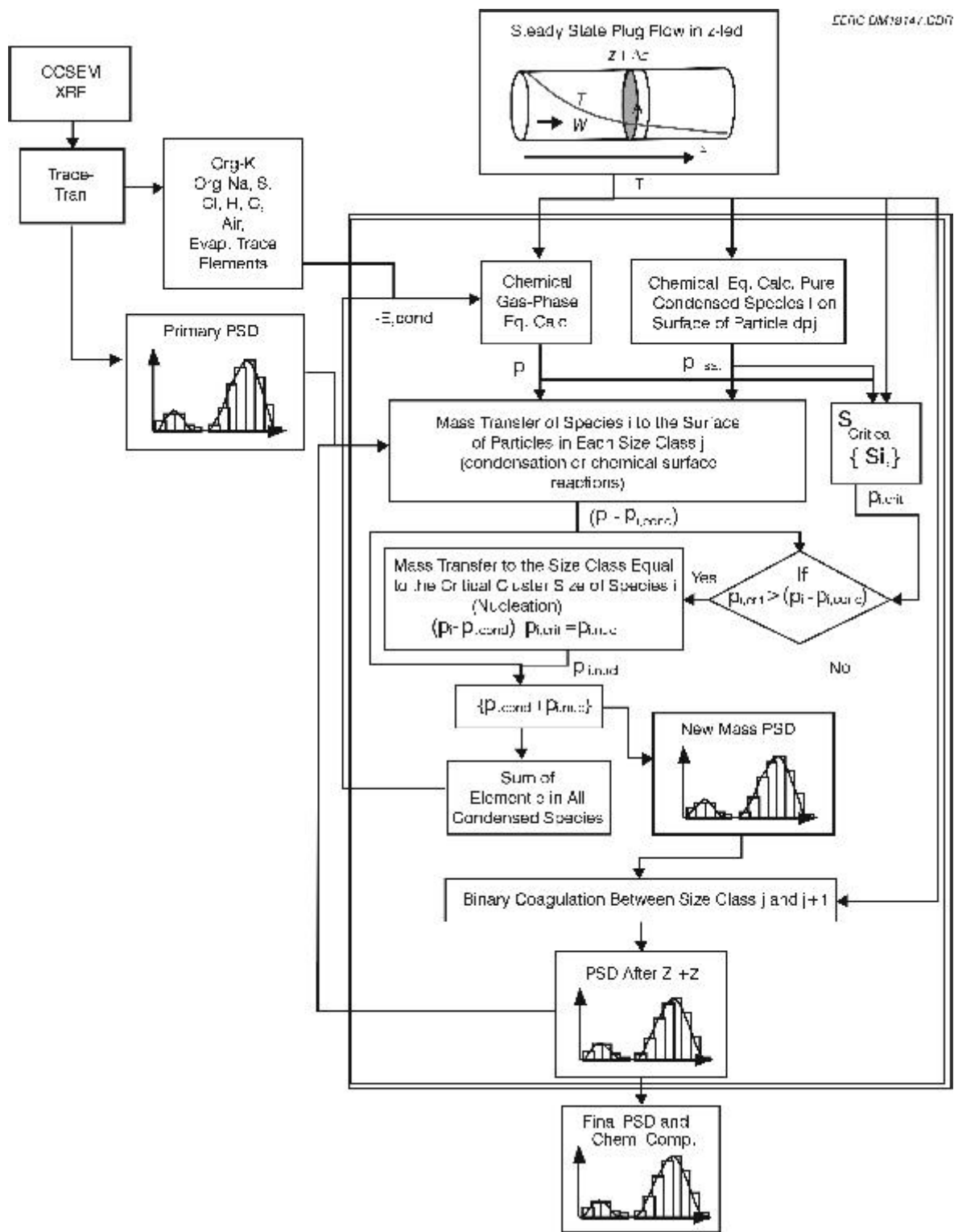


Figure 51. Conceptual flow diagram for an aerosol calculation model using TraceTran input data.

If nucleation occurs, it will add mass to the size bin with the same size as the critical cluster size for species *i*. The calculation of the critical cluster size was described in detail by Frandsen (123) and is thus not further discussed. The nucleated mass of species *i* is equal to the difference between the excess partial pressure and the critical partial pressure. Below the critical partial pressure, condensation on the newly formed particles will be the dominating gas-to-particle mechanism.

The masses added by condensation and nucleation by all condensing species are then summarized for respective size bins. Because of the fact that the number concentration of size bins larger than the nucleating particles is unchanged, the growth of these particles can then be calculated assuming spherical particles and a homogeneous chemical composition. This new size distribution is then subsequently used for the calculation of coagulation which will determine the final size distribution for each calculation step on the *z* axis.

The calculation of coagulation is typically the most complicated and calculation-intensive step in the solution of the GDE and often requires some type of matrix solution. In the discrete distribution calculations, the net rate of formation of particles of size *k* by collision of particles from size bin *i* and *j* and the loss of particles of size *k* by collision with other particles is given by Friedlander (120):

$$\frac{dn_k}{dt} = \frac{1}{2} \sum_{i+j=k} \beta_{i,j} n_i n_j - n_k \sum_{i=1}^{k-1} \beta_{i,k-i} n_i \quad [\text{Eq. 3}]$$

where  $\beta$  is the collision frequency function, which depends on the sizes of the colliding particles and on system properties such as temperature and pressure.

The calculation of  $\beta$  depends on which collision mechanism is considered. Typically Brownian coagulation is the most dominating mechanism for collision of submicron particles, while turbulent shear and gravitational settling are the governing mechanism for particles larger than a few microns (125). Thus a combination of all three mechanisms has to be considered to determine a  $\beta$  that will cover the whole investigated size spectra (<100  $\mu\text{m}$ ).

The use of a discrete size classification and coagulation calculation produces a huge amount of new size classes for each step in the axial direction *z*. Consequently, size classes must be merged in order to keep the number of equations and the computational time at a reasonable level. Examples of such merging are described by Jokiniemi and coworkers (122) and by Christensen and coworkers (121).

After each step (*z* +  $\Delta z$ ), a new size distribution is calculated that is subsequently used as the input size distribution for the condensation calculations at the next calculation step on the *z* axis. The total amount of element *e* in all condensed and nucleated species is summarized and subsequently withdrawn from the gas-phase equilibrium calculations for the next step on the *z* axis as well (e.g., the sum of *K* in condensed KCl and K<sub>2</sub>SO<sub>4</sub>).

The choice of step length of  $\Delta z$  and the number of size bins is typically a balance between accuracy and computational time and has to be tested and evaluated for each investigated system. According to a review of different mathematical models for aerosol dynamic calculations by Signeur and coworkers (126), typically 30–60 size bins evenly distributed on a logarithmic scale give acceptable results.

Moreover, it has to be noted that in the conceptual model in Figure 51, no calculations of particle losses to wall surfaces due to deposition are included. This effect will also have to be considered in the future as well.

Therefore, it is important that the output size distribution from the TraceTran code can be easily adjusted so that it will fit the size bins required by the aerosol model.

### **Improvements to the TraceTran Code**

Implementation of chemical equilibrium calculations will make the code flexible for use with both mass size distribution and trace element behavior predictions. This part could be programmed as well, but an easier solution would be to use readily available models that can be easily linked to any program code. GTT sells programs that can be implemented in C code (Chemapp) or in Excel (Chemsheet). However, in order to run these programs, databases for the calculations with Chemapp or Chemsheet have to be created from either Chemsage or FACT.

Both the TraceTran code and the conceptual model described in Figure 51 assume that all particles are spherical. This is true for most fly ash formed in pc combustion units but not for fly ash formed in grate-fired biomass combustion units. Because of the lower temperature in grate-fired biomass units and the low amount of large mineral particles in the fuel, coarse fly ash particles typically have the shape of agglomerates. This will significantly affect the particle surface area for a given particle size.

The TraceTran code was designed for coal and is heavily dependent on empirically fitted constants derived from experimental data from test runs with coal, but also on good CCSEM analyses. The main part of the transformations taking place are based on statistically randomized calculations around these empirical factors. The factors were gathered from thermal conversion techniques such as pulverized fuel combustion, PBF gasification, FBC, combustion, and cyclone combustion of coal. It is unlikely that these empirical factors will be correct for grate-fired biomass combustion.

Furthermore, the CCSEM analysis of biomass fuels will have to be checked for statistical repeatability. Elongated mineral particles in biomass could be an important factor in the reproducibility of the analyses.

The present TraceTran code models all particles as spherical and dense. This affects the surface area available for heterogeneous condensation, which is incorrect for agglomerated biomass ash particles, thus the particle size of the supermicron particles is incorrect as well. A possible change would be the addition of a fractal factor to the size calculation of the coarse fly ash particles, assuming that all (or a part) are agglomerates of smaller particles in a certain size range. Because the calculations are based on statistical

evaluations of the transformations, it needs a certain minimum number of particles in order to fulfill the statistical assumptions made.

### **Suggestions on Changes to the TraceTran (ATRAN) Code**

It is suggested that the EERC concentrate on reprogramming the ATRAN code so that it will be more flexible, allowing easy selection of input parameters in the calculations. The output from the ATRAN code should also be easily changeable in order to serve as input to future development of an aerosol module.

The following changes would be necessary:

- 1) The mode of plant that is calculated should be selectable as an input to the program.
- 2) The constants for fragmentation and coalescence should be removed from the source code and placed in an input file. This way, it will be much easier to include these factors for new fuels such as biomass.
- 3) The size bins in the output from TraceTran should be easily changeable. The reason for this is that the output would be linked to other aerosol modeling programs.
- 4) Zinc should be added to the trace element file or at least as an alternative, as for some fuels it can be a significant aerosol-forming element (e.g., waste wood [124]).
- 5) Chlorine should be included with the bulk XRF file or as a separate input file and not with the trace elements as in the current code.

## **CONCLUSIONS**

The work performed has involved an investigation of significant issues related to biomass cofiring with coal. Accomplishments of this work are summarized below.

### **Survey of Literature on Biomass Processing and Cofiring**

Biomass can be successfully cofired with coal in both wall- and tangentially fired pc boilers, cyclone boilers, fluidized-bed boilers, and spreader stokers. Woody biomass is the preferred cofire fuel because it contains less ash, silicates, potassium, and chlorine which could stimulate deposit formation. Herbaceous biomass (such as switchgrass and straw) contains more of the chlorine, silicates, and alkali metals that facilitate deposition, but they can be used if care is taken during selection and fuel preparation. Deposition rates have been found to depend strongly on interactions between the cofired fuels as well as on individual fuel properties. Biomass should not be stored outdoors for long periods of time, as the material tends to degrade during storage.

Proper fuel preparation is an important factor in successful cofiring. The biomass should be uniformly pulverized to at least  $\frac{1}{4}$  in. diameter (preferably  $\frac{1}{2}$  in.). Drum chippers work well for woody biomass comminution, while hammer mills are the most effective for pulverizing herbaceous biomass. Wet biomass should be pulverized to a smaller size to minimize residual carbon in the ash. The biomass should be fed to the boiler separately from the coal. Transport of the biomass can be made more consistent by adding vibration to the conveyors and bins.

$\text{NO}_x$  emissions are not adversely affected by the addition of biomass. In fact, when woody biomass is cofired with coal, the overall  $\text{NO}_x$  emissions are often reduced. Corrosion can be minimized by keeping the tube surface temperatures as low as possible and by firing higher-sulfur-content coal with higher-chlorine-containing biomass since less chlorine is present in deposits when sulfur is also present in the system.

With respect to ash deposition, woody biomass will decrease rates of ash deposition in hotter regions of a boiler where silicate-rich ash deposits can form and herbaceous biomass (e.g., straws and switchgrass) can cause increased fouling because of the presence of silicon, potassium, and chlorine in the biomass.

Many utilities are attempting to preserve lowest achievable levels of carbon in ash for ash resale, reuse, and disposal. With pressure on utilities to lower  $\text{NO}_x$ , more utilities are employing low- $\text{NO}_x$  burner technologies and staged combustion strategies, which generally increases carbon in fly ash. Burnout of biomass particles depends on moisture content and particle size. Processing will need to achieve small enough biomass sizes (i.e., top size of 3.2 mm, 0.125 in.) and low enough moisture to avoid adding additional poor burnout and increased residual carbon in the ash.

Barriers for biomass cofiring in large utility boilers are primarily related to economics. Currently, biomass is significantly more expensive than coal as a fuel feedstock, making utilities uninterested in this resource. Assuming that some sort of economic incentives are provided, such as by federal or state programs, then the barriers for biomass cofiring appear to focus primarily on consistent availability of biomass resources, efficient processing of biomass for incorporation into the boiler, and impacts on ash behavior.

### **The Effects of Plant Cell Chemistry on Cofiring Biomass with Coal**

Several mineral elements are essential for plant growth. A number of these elements which occur in higher concentrations can cause difficulties during firing of biomass or coal-biomass blends in utility boilers. Nitrogen in the biomass can increase  $\text{NO}_x$  levels, depending on the nitrogen content and the stoichiometry of the system. Silicon, potassium, chlorine, and alkali metals can all contribute to ash deposition, while chlorine and alkali metals can also corrode the boiler system.

A literature investigation into mineral uptake and storage by plants that are considered for biomass cofiring revealed the form and concentration of inorganic elements in plant matter. Sixteen essential elements, C, H, O, N, P, K, Ca, Mg, S, Zn, Cu, Fe, Mn, B, Mo, and Cl, are found throughout plants. Aside from H and O, the predominant inorganic elements are K and Ca, which are essential for the function

of all plant cells and will, therefore, be evenly distributed throughout the nonreproductive, aerial portions of herbaceous biomass. Some inorganic constituents, e.g., N, P, Ca, and Cl, are organically associated and incorporated into the structure of the plant. Cell vacuoles are the repository for excess ions in the plant. Minerals deposited in these ubiquitous organelles are expected to be most easily leached from dry material.

There are other elements obtained from soil interactions with roots, air interactions with aerial portions of the plants, and water interactions with both roots and aerial portions of plants. These elements may not have specific functions within the plant, but are nevertheless absorbed and fill a need. An example is Si, found in the form of monosilicic acid,  $\text{Si}(\text{OH})_4$ . In rice, it enhances resistance to fungus disease and increases the grain yield. The leaf blades of rice are more erect when silica slags are applied, and it has also been proven that rice plants showed retardation of their vegetative growth and a decreased degree of seed setting when the Si content was extremely low.

Another common nonessential element, Na is deposited throughout that plant despite its nonfunctional status. Its concentration will depend entirely on extrinsic factors regulating its availability in the soil solution, i.e., moisture and soil content. Similarly, Cl content is determined less by the needs of the plant than by availability in the soil solution; in addition to occurring naturally, Cl is present in excess as the anion complement in K fertilizer applications.

The overall plant development and maintenance depend on the chemical substances absorbed and transported by the roots. Nutrient supply to the roots is dependent on nutrient concentrations in the soil solution, the nature of nutrients, soil moisture status, and plant absorption capacity. The data suggest that although mineral content varies somewhat based on the needs of the plant, much is dependent on the availability of elements in the soil solution surrounding plant roots. This is most influenced by soil content, moisture availability, root uptake activity, and, in some cases, pH. Knowing the soil and moisture conditions, pH, and fertilizer history will provide insight into expected concentrations of elements in plants. Thus the geographic and climatic conditions have a strong effect on the variability in inorganic content of biomass material.

### **Geographic and Seasonal Differences in Switchgrass Elemental Composition**

An analysis was performed on data collected by the Chariton Valley RCD group, based in Centerville, Iowa, on switchgrass samples from ten different farms in the south-central portion of Iowa. The goal was to determine correlations between switchgrass elemental composition and geographical and seasonal changes so as to identify factors that influence the elemental composition of biomass. Switchgrass can be an acceptable energy fuel, showing low-moderate ash content, low sulfur, relatively low moisture, and acceptable heat contents. The most important factors in determining levels of various chemical compounds were found to be seasonal and geographical differences. From a standpoint of the amount of energy present in each sample, early spring was found to be the best harvest date in southern Iowa. The time with the lowest concentration of ash and various chemical compounds is April or May, although some oxides actually peak in the spring and are less abundant in the early fall. Overall, the best time to harvest a crop is late March or early April when the crops are coming out of dormancy. At this point, the viscosity of liquid phases formed during combustion would be higher because of lack of alkali and chlorine, and

boiler performance would be better. Moisture-free heat content is also high, and even the air-dried switchgrass readings (for which moisture is still present) show relatively high Btu/lb ratings. This is significant because of the energy requirements needed to dry the harvested switchgrass.

The switchgrass samples showed significant compositional variation due to local soil and moisture conditions. Geographically, the highest, driest areas generally produced samples with more Btu/lb and less  $K_2O$  than did low-lying wetlands. Growing at high elevations means less time air-drying and more heat content per pound, as well as lower  $K_2O$  concentrations, which will reduce the contribution of  $K_2O$  in forming fouling deposits in a boiler.

### **Characterization and Processing of Test Fuels**

Selection and analysis of fuels were based on biomass resources available in the upper midwestern United States: alfalfa stems from Minnesota, wheat straw from North Dakota, and hybrid poplar wood from a University of Minnesota–Crookston tree farm. Coals chosen for cocombustion with the biomass were an Illinois No. 6 bituminous coal and an Absaloka (Wyoming) Powder River Basin (PRB) subbituminous coal.

The basic chemistry and advanced analyses were completed on these biomass fuels, and small-scale tests demonstrated successful processing of alfalfa stems, wheat straw, and hybrid poplar to suitable size and moisture for cofiring.

### **Analytical Techniques Improvement**

The biomass chemical and mineralogical compositions derived for alfalfa stems and wheat straw were obtained along with observations of carbonate and phosphate minerals and amorphous silica phytolith structures.

Work in the area of understanding the mode of occurrence and chemical–physical properties of silica-rich phytoliths in herbaceous biomass such as wheat straw or alfalfa stems was undertaken. A leaching and separation technique was used to separate silica phytoliths from biomass, and these particles were analyzed using SEM. Some of the silica phytoliths contain minor amounts of potassium.

The chemical fractionation technique was modified and problems with determination of silica overcome by implementing acid digestion and wet-chemistry analysis of leachates instead of oven ashing and XRF analysis of the leached material.

Because the CCSEM classification scheme was designed for mineral phases in coal and the biomass material is phytolithic in origin, most of the chemical point analyses are unclassified by the standard CCSEM data reduction program. Statistical cluster analyses were performed on these unknowns. Clusters were defined by their average composition. Five abundant clusters for each of the biomass fuels were found. For the hybrid poplar, the Ca-rich cluster represents 68% of the particles analyzed. The alfalfa stems and wheat straw both showed a Si–K-rich cluster as the dominant chemical group.

Similarly, cluster analysis was performed on the CCSEM fly ash analysis results because of the high number of unclassified particles resulting from the presence of inorganic matter from the biomass. These analyses were performed in the same manner as the fuel cluster analyses. The wheat straw ash was found to show the greatest similarity from the fuel to the ash analyzed. A high percentage of analyses from both fuel and ash samples contained both Si and K. While Cl was a significant component in the fuel, very little was detected in the ash sample. In contrast, both the hybrid poplar and alfalfa stem fuels show little Cl, while the ash unknowns contain 10% and 28% Cl, respectively. These fuels exhibit a significant rearrangement of elements during combustion which can at least in part be attributed to the particle size being small (greater than 50% of the particles analyzed were below 10  $\mu\text{m}$  in diameter). Significant amounts of Ca and K tend to reduce the melting temperature of the Si-containing particles, allowing more components to be incorporated into the glassy matrix. Although SEM microprobe analysis cannot distinguish between any phases that may condense on the surface of the ash particle as it cools from that of the same element dispersed in the bulk of the particle, a significant amount of Cl was found with the alfalfa stem ash and a moderate amount of P was found with the hybrid poplar ash consistent with condensation of these elements on the ash particles.

### **Ash Formation and Deposition**

The biomass samples have a lower heating value and are characterized by much higher volatile matter and oxygen content and lower sulfur than the coals. The wheat straw ash level is similar to that of the Absaloka coal, with the alfalfa stems and hybrid poplar having a much lower ash content than the coals. Although the ash content is lower, each of the three biomass fuels has a distinctly different ash chemistry. The wheat straw ash contains primarily silica and significant potassium, while the alfalfa stems contain nearly equal amounts of silica, calcium, and potassium along with significant phosphorus. Both have very high chlorine content. In contrast, the hybrid poplar ash consists mostly of calcium and potassium, again with significant phosphorus present. The effect of the biomass ash composition on the blends is not as pronounced as would be expected, since the 80% coal–20% biomass are prepared by weight on an as-received basis. The higher moisture and ash content of the coals tend to dominate and mask the calcium, potassium, and phosphorus contribution of the biomass.

Entrained fly ash and fouling deposits were generated in the CEPS combustor for the parent coals, biomass materials, and blends of 80% coal with 20% biomass. Slagging and low-temperature fouling deposits were also produced for the blend of 80% Illinois No. 6 coal with 20% wheat straw. The slagging and fouling deposits were collected on a removable cooled probe for later analysis and determination of deposit strengths.

The slagging deposit for 20% wheat straw biomass cofired with 80% Illinois No. 6 coal was found to be generally hard and well sintered, with evidence of partial melting of the deposit material. Deposit morphologies showed distinct elongate silicate structures derived from the wheat straw material as well as distinct angular mineral matter derived from the coal, both being assimilated into the potassium–iron aluminosilicate melt phase. In contrast, a 100% Illinois No. 6 slagging deposit also shows some partial melting of ash, but the deposits are not as hard and resistant to removal.

In contrast, the Illinois No. 6–wheat straw fouling deposits, although growing rapidly, had very little strength or indication of sintering. All the coal–wheat straw blends, although growing more rapidly than the coal deposits, had effectively no strength. The rate of growth of the alfalfa and coal–alfalfa blends was similar, with the blend deposit strengths lower than that of the alfalfa and parent coals. Similar behavior is also seen for the hybrid poplar and coal–hybrid poplar blends. The blending of coal with biomass appears to dilute the coal minerals with the porous biomass ash, resulting in fouling deposits with lower strength and which are more easily removable. The weakness of the fouling deposits indicates that little interaction of the biomass potassium or calcium with the entrained ash occurs to produce low-viscosity melts in the temperature regime at which fouling deposits are produced.

CCSEM analysis was performed on the fly ash of the coals and blends. Although some quartz, clays, and aluminosilicates were identified, the great majority of the ash was classified as either unknown or silica-rich. The 80% Illinois No. 6–20% wheat straw blend ash also had a high level of iron oxide, similar to the fouling deposit. The standard mineral classifications provide little information about ash transformations and interactions, because of the large component of material classified as unknown. Using cluster analysis, the wheat straw ash was found to show the greatest similarity from the fuel to the ash analyzed. A high percentage of analyses from both fuel and ash samples contained both Si and K. While Cl was a significant component in the fuel, very little was detected in the ash sample. In contrast, cluster analysis of both the hybrid poplar and alfalfa stem fuels shows little Cl, while the ash unknowns contain 10% and 28% Cl, respectively. These fuels exhibit a significant rearrangement of elements during combustion which can at least in part be attributed to the particle size being small (greater than 50% of the particles analyzed were below 10  $\mu\text{m}$  in diameter).

The composition of the Illinois No. 6 ash is dominated by silica, alumina, and iron and the composition of the Absaloka ash by silica, alumina, and calcium. The wheat straw ash is predominantly silica, with 8% calcium and 9% potassium present. A small enrichment of iron occurs in the Illinois No. 6 deposit, while silica is enriched and calcium depleted in the Absaloka deposit relative to the chemistry of the parent coal inorganic material. There is also a slight depletion of calcium in the Absaloka fly ash. No enrichment or depletion of chlorine occurs for the deposits or fly ash for the coals. The wheat straw shows a depletion of potassium and an enrichment of silica in the deposit due to the impaction of large silica phytoliths along with the formation of vapor-phase or fine particulate potassium species which would not be expected to deposit. The blends of wheat straw with the coals has the major chemical constituents corresponding to the parent fuels. The 80% Absaloka–20% wheat straw blend composition also includes a significant amount of sulfur captured by the coal-derived calcium and the wheat straw-derived potassium. Although the wheat straw contains appreciable chlorine, there is little in either the wheat straw fly ash or the 80% Illinois No. 6–20% wheat straw blend fly ash. However, chlorine is a significant component of the 80% Absaloka–20% wheat straw blend fly ash. This suggests that the chlorine in the wheat straw and Illinois No. 6–wheat straw blend remains in the gas phase (possibly as HCl) or as a very fine submicron aerosol (possibly as KCl) which is too small to be analyzed by the CCSEM technique. The presence of chlorine in the Absaloka–wheat straw ash indicates either condensation or agglomeration of chlorine compounds such as KCl onto larger ash particles or competition of Absaloka-derived calcium with the wheat straw-derived potassium for chlorine capture. Some enrichment of silica and depletion of aluminum are seen in the Illinois No. 6–wheat straw and Absaloka–wheat straw deposits. The Absaloka–wheat straw

fly ash also contained much less silica than would be expected and significantly more chlorine as well as some enrichment of calcium. The lack of silica in the fly ash may be due to deposition in the CEPS ducting prior to the baghouse where the sample was collected.

The alfalfa deposit shows enrichment of phosphorus and potassium, along with depletion of silica, potassium, and chlorine. The alfalfa fly ash chemistry is comprised of silica, calcium, and potassium, with a significant amount of captured sulfur. A very high amount, 25% of the ash weight, is chlorine. There is a depletion of calcium, possibly due to the formation of fine calcium species. The 80% Illinois No. 6–20% alfalfa and 80% Absaloka–20% alfalfa blend fly ashes have silica and alumina content similar to the wheat straw blend fly ashes. The Absaloka–alfalfa blend fly ash does not exhibit the high sulfur capture shown by the Absaloka–wheat straw blend or the alfalfa fly ash. Although the Absaloka–alfalfa fly ash does contain more chlorine than the Illinois No. 6–alfalfa fly ash, it is approximately half that of the Absaloka–wheat straw blend, even though the chlorine content of the wheat straw and alfalfa are nearly the same. Indeed, there is only a small enrichment of chlorine (9%) in the Absaloka–alfalfa fly ash. As the coal–alfalfa blend deposits exhibited the highest strengths, this would suggest that interactions of the Absaloka and alfalfa minerals have occurred, with calcium now in a form less amiable to sulfur and chlorine capture.

The hybrid poplar deposit shows a depletion of potassium, with the fly ash showing a depletion of both calcium and potassium and some iron enrichment. Despite this, the hybrid poplar fly ash contains significant calcium, silica, and iron and 7% phosphorus and 7% potassium. There is also moderate capture of sulfur and chlorine, moderately higher than would be expected from the fuel chlorine content. Because of the low ash content of the hybrid poplar, the effect on the coal–poplar blends is not as pronounced, although the Absaloka–poplar blend fly ash does show a fair degree of chlorine capture and the deposit some enrichment of calcium.

The CCSEM mineral particle-size distributions of the coals and biomass fuels and fly ashes show that the Illinois No. 6 coal is dominated by large pyritic mineral particles. A significant reduction occurs on formation of the Illinois No. 6 fly ash because of the fragmentation of the large pyritic mineral matter. The parent wheat straw particle sizes are shown as smaller than those of the coal, with little mineral matter larger than 22  $\mu\text{m}$ . However, this is probably due to underestimation of the flat, platelike silicate phytolith structures of the wheat straw by the CCSEM sizing procedure. The fly ash of the pure wheat straw is shifted to larger particle sizes than that of the parent fuel, indicating that agglomeration is occurring. However, the size distribution of the blend fly ash is shifted to smaller particle sizes. The blend fly ash contains even more fine particulate less than 4.6 microns than the Illinois coal. The agglomeration which occurred for the pure wheat straw ash does not occur with the Illinois No. 6–wheat straw fly ash. This suggests that some interaction of the two ash components is hindering the agglomeration mechanism of the wheat straw ash.

A similar comparison of the Absaloka and wheat straw fuels and fly ash particle-size distributions shows that the Absaloka fly ash produces fly ash with much finer particle sizes than the minerals in the parent coal. The fragmentation of calcite and clays along with the organically bound alkalies and alkaline earths in the coal matrix are responsible. The Absaloka–wheat straw blend fly ash is shifted to larger particle sizes than the parent coal and is nearly the particle-size distribution for the blend fly ash predicted

by the weighted average of the parent fly ashes. This suggests that either the presence of the Absaloka ash does not inhibit the wheat straw ash agglomeration or that interaction of the Absaloka and wheat straw fuel minerals is occurring.

For the Illinois No. 6 and alfalfa stems, the alfalfa fly ash has a significantly smaller particle-size distribution than the minerals in the parent alfalfa fuel. This is the expected result of the high calcium and potassium content, which would result in the production of fine particulate and vapor-phase potassium species. The fly ash showed enhancement of potassium and chlorine. The predicted blend fly ash distribution is nearly identical to that of the Illinois No. 6 fly ash as a result of the higher coal ash content. However, the experimental blend fly ash is much larger than predicted, similar to that of the mineral-size distribution of the alfalfa fuel. This indicates interaction and agglomeration of the minerals from the parent coal and biomass, although no great enrichment of any elements was seen in the bulk fly ash chemistry. Behavior of the Absaloka and alfalfa stems was similar, with the blend showing a much larger particle-size distribution than predicted from the parent fly ashes. Here, however, the blend particle-size distribution is nearly the same as that of the parent alfalfa fly ash, indicating that interaction and agglomeration may not be as extensive as with the Illinois No. 6 fly ash. In both cases, the presence of the alfalfa mineral matter has resulted in particle-size distributions larger than that seen for the parent coals and equal to or larger than those of the parent alfalfa. This suggests that biomass blending may have a beneficial effect in improving ash collectibility by increasing particle size.

The ashes for the Illinois No. 6 and hybrid poplar show a shift to particle sizes larger than predicted on blending. Here, the effect is not as pronounced, with the blend fly ash-size distribution being somewhat smaller than that of the parent hybrid poplar. However, the blend-size distribution is again larger than the parent Illinois No. 6 fly ash. Similar behavior was seen for the Absaloka and hybrid poplar fly ash blend.

As part of the CEPS combustion testing with hybrid poplar, Absaloka coal, and an 80%–20% Absaloka–hybrid poplar blend, on-line measurements were made using an APS and a SMPS. These measurements indicated that there is a moderate shift in the submicron fraction to larger particle sizes (SMPS measurements) and, possibly, a small shift to larger particle sizes in the supermicron particle size range (APS measurements). The coal appeared to have more fine submicron ash than either the hybrid poplar or the blend. A tentative hypothesis is that condensation of sticky potassium species from the biomass ash on fine coal ash particles is resulting in agglomeration of these particles. Further APS and SMPS measurements during future pilot-scale combustion tests are planned to resolve this issue.

### **Modeling of Biomass Ash Transformations**

The TraceTran model shows promise for use as an ash transformation model for biomass combustion. Modifications that would be required include 1) implementation of chemical equilibrium calculations to estimate the critical biomass species present and their quantity; 2) modifying the code to represent the majority of biomass-derived ash particles as irregular agglomerates and not as spheres; 3) generating additional experimental and empirical data to better determine constants suitable for biomass for use in the program algorithms; and 4) making a series of code changes that will make the model more flexible, such as user-selectable power plant mode, placing empirical constants used in the algorithms in an

external input file rather than being embedded in the source code, allowing variable output size bins for fly ash distributions, and adding key biomass elemental constituents such as chlorine and zinc to the input files. These changes would be essential along with the changes in the fundamental algorithms to express ash formation using a general dynamic equation.

## FUTURE WORK

The direction for future work recommended here is based on the observation that U.S. utilities will become increasingly interested in cofiring biomass with coal as a practical low-cost option for reducing greenhouse gas emissions. In the Midwest, some interest in the use of switchgrass as a biomass fuel feedstock has already been expressed by Northern States Power Company, Otter Tail Power Company, and Great River Energy. At the present time, with the exception of wood waste used close to the source of supply, most sources of forest and agricultural biomass can be expected to cost \$2–\$3–MMBtu, which is significantly higher than the typical cost of PRB coal (typically \$0.75–MMBtu). If incentives are provided in the United States to make cofiring biomass profitable to utilities, then major issues of ash behavior will come to the forefront. Past work has demonstrated the importance of understanding why specific biomass types either enhance or diminish ash deposit formation in coal–biomass cofiring arrangements. However, a good theoretical model of inorganic transformations and interactions during biomass cofiring is still needed, especially for biomass types which may be the most likely candidates for U.S. utilities to exploit. It is recommended that additional research on the mechanisms of biomass ash formation and deposition be focused on hybrid poplar, switchgrass, and perhaps an additional readily available type of straw, such as rice straw. Excellent facilities for rigorous near-real-world cofiring combustion testing and product analysis at the EERC, plus ash deposition expertise, would be used to understand, and in some cases verify, other researchers' results in ash behavior during biomass combustion.

## REFERENCES

1. Mann, M.K.; Spath, P.L. The Net CO<sub>2</sub> Emissions and Energy Balances of Biomass and Coal-Fired Power Systems. In *Biomass: A Growth Opportunity in Green Energy and Value-Added Products, Proceedings of the 4th Biomass Conference of the Americas*; Overend, R.P.; Chornet, E., Eds.; 1999; Vol. 1, pp 379–385.
2. Bhattacharya, S.C. State of the Art of Biomass Combustion. *Energy Sources* **1998**, *20*, 113–135.
3. Easterly, J.L.; Burnham, M. Overview of Biomass and Waste Fuel Resources for Power Production. *Biomass Bioenergy* **1996**, *10* (2–3), 79–92.

4. Turnball, J.H. Strategies for Achieving a Sustainable, Clean and Cost-Effective Biomass Resource. *Biomass Bioenergy* **1996**, *10* (2–3), 93–100.
5. McGowin, C.R.; Wiltsee, G.A. Strategic Analysis of Biomass and Waste Fuels for Electric Power Generation. *Biomass Bioenergy* **1996**, *10* (2–3), 167–175.
6. Bauen, A.; Kaltschmitt, M. Contribution of Biomass Toward CO<sub>2</sub> Reduction in Europe. In *Biomass: A Growth Opportunity in Green Energy and Value-Added Products, Proceedings of the 4th Biomass Conference of the Americas*; Overend, R.P.; Chornet, E., Eds.; 1999; Vol. 1, pp 371–378.
7. Kwant, K.W.; van Leenders, C. Developments of Green Energy Market in the Netherlands and the Perspectives of Biomass. In *Biomass: A Growth Opportunity in Green Energy and Value-Added Products, Proceedings of the 4th Biomass Conference of the Americas*; Overend, R.P.; Chornet, E., Eds.; 1999; Vol. 1, p 1629.
8. Frandsen, F.J.; Nielsen, H.P.; Jensen, P.A.; Hansen, L.A.; Livbjerg, H.; Dam-Johansen, K.; Sorensen, H.S.; Larsen, O.H.; Sander, B.; Henriksen, N.; Simonsen, P. Deposition and Corrosion in Straw- and Coal-Straw Co-Fired Utility Boilers. In *Proceedings of the Engineering Foundation Conference on Impact of Mineral Impurities in Solid Fuel Combustion*; Kona, HI, Nov 2–7, 1997; Wall, T.F.; Baxter, L.L., Eds.; 14 p.
9. Frandsen, F.J.; Nielsen, H.P.; Hansen, L.A.; Hansen, P.F.B.; Andersen, K.H.; Sorensen, H.S. Ash Chemistry Aspects of Straw and Coal–Straw Cofiring in Utility Boilers. In *Proceedings of the 15th Annual International Pittsburgh Coal Conference*; Sept 14–18, 1998; 14 p.
10. Skrifvar, B.; Lauren, T.; Backman, R.; Hupa, M. The Role of Alkali Sulfates and Chlorides in Post Cyclone Deposits from Circulating Fluidized Bed Boilers Firing Biomass and Coal. In *Proceedings of the Engineering Foundation Conference on Impact of Mineral Impurities in Solid Fuel Combustion*; Kona, HI, Nov 2–7, 1997; Wall, T.F.; Baxter, L.L., Eds.; 10 p.
11. Jensen, P.A.; Stenholm, J.; Hald, P. Deposition Investigation in Straw-Fired Boilers. *Energy Fuels* **1997**, *11*, 1048–1055.
12. Olanders, B.; Steenari, B. Characterization of Ashes from Wood and Straw. *Biomass Bioenergy* **1995**, *8* (2), 105–115.
13. Nordin, A. Chemical Elemental Characteristics of Biomass Fuels. *Biomass Bioenergy* **1995**, *8* (2), 339–347.
14. Boylan, D.M. Southern Company Tests of Wood–Coal Cofiring in Pulverized Coal Units. *Biomass Bioenergy* **1996**, *10* (2–3), 139–147.

15. Brouwer, J.; Owens, W.D.; Harding, S.; Heap, J.P. Cofiring Waste Biofuels and Coal for Emission Reduction. In *Energy, Environment, Agriculture, and Industry, Proceedings of the 2nd Biomass Conference of the Americas*; Portland, OR, Aug 21–24, 1995; NREL/CP-200-8098, DE95009230; pp 390–399.
16. Rudinger, H.; Kicherer, A.; Greul, U.; Spliethoff, H.; Hein, K.R.G. Investigations in Combined Combustion of Biomass and Coal in Power Plant Technology. *Energy Fuels* **1996**, *10*, 789–796.
17. Hughes, E.; Tillman, D. Biomass Cofiring: Status and Prospects 1996. In *Biomass Usage for Utility and Industrial Power, Proceedings of the Engineering Foundation Conference*; Snowbird, UT, April 28 – May 3, 1996; 19 p.
18. Battista, J.; Tillman, D.; Hughes, E. Cofiring Wood Waste with Coal in a Wall-Fired Boiler: Initiating a 3-Year Demonstration Program. In *Expanding BioEnergy Partnerships, Proceedings of BioEnergy 98*; Madison, WI, Oct 4–8, 1998; pp 243–250.
19. Moore, T. Harvesting the Benefits of Biomass. *EPRI J.* **1996**, *May–June*, 16–25.
20. Prinzing, E.E.; Hunt, E.F. Impacts of Wood Cofiring on Coal Pulverization at the Shawville Generating Station. In *Biomass Usage for Utility and Industrial Power, Proceedings of the Engineering Foundation Conference*; Snowbird, UT, April 28 – May 3, 1996; 15 p.
21. Gold, B.A.; Tillman, D.A. Wood Cofiring Evaluation at TVA Power Plants. *Biomass Bioenergy* **1996**, *10* (2–3), 71–78.
22. Miles, T.R.; Miles, T.R., Jr.; Baxter, L.L.; Bryers, R.W.; Jenkins, B.M.; Oden, L.L. Boiler Deposits from Firing Biomass Fuels. *Biomass Bioenergy* **1996**, *10* (2–3), 125–138.
23. Moe, T.A. *Wastepaper Pellets as a Source of Fuel for Auxiliary Home Heating*; Final Report for Western Area Power Administration; Energy & Environmental Research Center: Grand Forks, ND, June 1995; 21 p.
24. Tillman, D.A.; Plasynski, S.; Hughes, E. Biomass Cofiring in Coal-Fired Boilers: Test Programs and Results. In *Biomass A Growth Opportunity in Green Energy and Value-Added Products, Proceedings of the 4th Biomass Conference of the America*; Overend, R.P.; Chornet, E., Eds.; Pergamon; Vol. 2, pp 1287–1291.
25. Aerts, D.J.; Ragland, K.W.; Cofiring Switchgrass in a 50 MW Pulverized Coal Utility: In *Expanding BioEnergy Partnerships, Proceedings of BioEnergy 98*; Madison, WI, Oct 4–8, 1998; pp 295–305.

26. Segrest, S.A.; Rockwood, D.L.; Stricker, J.A.; Green, A.E.S.; Smith, W.H.; Carter, D.R. Biomass Cofiring with Coal at Lakeland, FL, Utilities. In *Expanding BioEnergy Partnerships, Proceedings of BioEnergy 98*; Madison, WI, Oct 4–8, 1998; pp 315–325.
27. Kendall, A. Barriers to the Progress of BioEnergy. *Energy World* **1996**, May, 10–13.
28. Graham, R.L.; Lichtenberg, E.; Roningen, V.O.; Shapouri, H.; Walsh, M.E. The Economics of Biomass Production in the United States. In *Energy, Environment, Agriculture, and Industry, Proceedings of the 2nd Biomass Conference of the Americas*; Portland, OR, Aug 21–24, 1995; NREL/CP-200-8098, DE95009230; pp 1314–1323.
29. Piperno, D.R. *Phytolith Analysis*; Academic Press: New York, 1988.
30. Timpe, R.C.; Hauserman, W.B. The Catalytic Gasification of Hybrid Poplar and Common Cattail Plant Chars, In *Energy from Biomass Wastes XVI*; Klass, D.L., Ed.; Institute of Gas Technology, 1993; pp 903–920.
31. Galbreath, K.C.; Zygarlicke, C.J.; Olson, E.S.; Pavlish, J.H.; Toman, D.L. Evaluating Mercury Transformation Mechanisms in a Laboratory-Scale Combustion System. *The Science of the Total Environment* **2000**, in press.
32. Zygarlicke, C.J.; Eylands, K.E.; McCollor, D.P.; Musich, M.A.; Toman, D.L. Impacts of Cofiring Biomass with Fossil Fuels. In *Proceedings of the 25th International Technical Conference on Coal Utilization and Fuel Systems*; Clearwater, FL, March 6–9, 2000; pp 115–126.
33. Zygarlicke, C.J.; Galbreath, K.C.; McCollor D.P.; Toman, D.L. Development of Fireside Performance Indices for Coal-Fired Utility Boilers. In *Applications of Advanced Technology to Ash-Related Problems in Boilers*; Baxter, L.; DeSollar, R., Eds.; Plenum Press: New York, 1996; pp 617–636.
34. Zygarlicke, C.J. Predicting Ash Behavior in Conventional and Advanced Power Systems: Putting Models to Work. In *Impact of Mineral Impurities in Solid Fuel Combustion*; Gupta, R.; Wall, T.; Baxter, L., Eds.; Kluwer Academic–Plenum Publishers: New York, 1999; pp 709–722.
35. Benson, S.A.; Holm, P.L. Comparison of the Inorganic Constituents in Low-Rank Coals. *Ind. Eng. Chem. Prod. Res. Dev.* **1985**, *24*, 145.
36. Zygarlicke, C.J.; Steadman, E.N.; Advanced SEM Techniques to Characterize Coal Minerals. *Scan. Electr. Microsc.* **1990**, *4* (3), 579–590.
37. Galbreath, K.C.; Zygarlicke, C.J.; Casuccio, G.S.; Moore, T.A.; Gottlieb, P.J.; Agron-Olshina, N.; Huffman, G.P.; Shah, A.; Yang, N.Y.C.; Vleeskens, J.M.; Hamburg, G. Collaborative Study of

- Quantitative Coal Mineral Analysis Using Computer-Controlled Scanning Electron Microscopy. *Fuel* **1995**, 75 (4), 424–430.
38. Kalmanovitch, D.P.; Montgomery, G.G.; Steadman, E.N. ASME Paper No. 87-JPGC-FACT-4, 1987.
  39. University of Wisconsin–Madison College of Agricultural & Life Sciences Department of Soil Science. <http://www.soils.wisc.edu/~barak/soilscience326> (accessed June 2001).
  40. Robinson, A.; Baxter, L.; Junker, H.; Shaddix, C.; Freeman, M.; James, R.; Dayto, D. Fireside Issues Associated with Coal–Biomass Cofiring. In *Expanding BioEnergy Partnerships, Proceedings of BioEnergy '98*; Madison, WI, Oct 1998.
  41. Dayton, D.C.; Milne, T.A. Laboratory Measurement of Alkali Metal Containing Vapors Released During Biomass Combustion. In *Applications of Advanced Technology to Ash-Related Problems in Boilers*; Baxter, L.; DeSollar, R., Eds.; Plenum Press: New York, 1996; pp 161–186.
  42. Alberts, B.; Bray, D.; Lewis, J.; Raff, M.; Roberts, K.; Watson, J. *Molecular Biology of the Cell*, 2nd ed.; Garland Publishing, Inc.: New York, 1989; pp 48–51, 342–401, and 1137–1184.
  43. Fageria, N.K.; Baligar, V.C.; Jones, C.A. *Growth and Mineral Nutrition of Field Crops*; Marcel Dekker Inc.: New York, 1991.
  44. Taiz, L. The Plant Vacuole. *J. Experimental Biol.* **1992**, 172, 113–122.
  45. Carson, E.W. *The Plant Root and Its Environment: Proceedings of an Institute Sponsored by the Southern Regional Education Board*; Virginia Polytechnic Institute and State University, July 5–16, 1971; University Press of Virginia: Charlottesville, VA, 1974.
  46. Peel, A.J., *Transport of Nutrients in Plants*. Butterworth & Co. Ltd., John Wiley & Sons, 1974.
  47. Alloway, B.J. *Heavy Metals in Soils*; Blackie and Son Ltd.: Glasgow, 1990.
  48. Epstein, E. *Mineral Nutrition of Plants: Principles and Perspectives*; John Wiley and Sons: New York, 1972.
  49. Deckard, E. North Dakota State University, Fargo, ND, Personal communication, 2001.
  50. Energieonderzoek Centrum Nederland (ECN) Biomass Phyllis database for biomass and waste. <http://www.ecn.nl/phyllis/cgibin/DataTable.asp> (accessed June 2001).
  51. Russelle, M. University of Minnesota, Minneapolis, MN. Personal communication, 2001.

52. Calderini, D.F.; Torres-Leon, S.; Slafer, G.A. Consequences of Wheat Breeding on Nitrogen and Phosphorus Yield, Grain Nitrogen and Phosphorus and Associated Traits. *Ann. Botany* **1995**, *76*, 315–322.
53. Cramer, M.D.; Lewis, O.A.M. The Influence of Nitrate and Ammonia Nutrition on the Growth of Wheat (*Triticum aestivum*) and Maize (*Zea mays*) Plants. *Ann. Botany* **1993**, *72*, 359–365.
54. Cramer, M.D.; Lewis, O.A.M. The Influence of  $\text{NO}_3^-$  and  $\text{NH}_4^+$  Nutrition on the Gas Exchange Characteristics of the Roots of Wheat (*Triticum aestivum*) and Maize (*Zea mays*) Plants. *Ann. Botany* **1993**, *72*, 37–46.
55. Trolldenier, G. Techniques for Observing Phosphorus Mobilization in the Rhizosphere. *Biol. Fertil. Soils* **1992**, *14*, 121–125.
56. Romer, W.; Augustin, L.; Shilling, G. The Relationship Between Phosphate Absorption and Root Length in Nine Wheat Cultivars. In *Developments in Plant and Soil Sciences*; 1989; Vol. 36, pp 123–125.
57. Clarke, J.M.; Campbell, C.A.; Cutforth, H.W.; DePauw R.M.; Winkleman, G.E. Nitrogen and Phosphorus Uptake, Translocation, and Utilization Efficiency of Wheat in Relation to Environment and Cultivar Yield and Protein Levels. *Can. J. Botany* **1990**, *70*, 965–977.
58. Frank, A.B.; Bauer, A.; Black A.L. Carbohydrate, Nitrogen and Phosphorus Concentrations of Spring Wheat Leaves and Stems. *Agron. J.* **1989**, *81*, 524–528.
59. Elliot, D.E.; Reuter D.J.; Reddy G.D.; Abbott, R.J. Phosphorus Nutrition of Spring Wheat (*Triticum aestivum* L.) 4. Calibration of Plant Phosphorus Test Criteria from Rain-Fed Field Experiments. *Aust. J. Agri. Res.* **1997**, *48*, 883–897.
60. Goodroad, L.L.; Wilson, D.O. Influence of Sulfur on Growth and Nutrient Composition of Soft Red Winter Wheat. *J. Plant Nutri.* **1989**, *12* (8), 1029–1039.
61. Monaghan, J.M.; Scrimgeour, C.M.; Stein, W.M.; Zhao, F.J.; Evans, E.J. Sulphur Accumulation and Redistribution in Wheat (*Triticum aestivum*): A Study Using Stable Sulphur Isotope Ratios as a Tracer System. *Plant, Cell, Environ.* **1999**, *22*, 831–839.
62. Fitzgerald, M.A.; Ugalde, T.D.; Anderson, J.W. Sulphur Nutrition Changes the Source of S in Vegetative Tissues of Wheat During Generative Growth. *J. Experi. Botany* **1999**, *50* (333), 499–508.
63. Krol, E.; Trebacz, K. Way of Ion Channel Gating in Plant Cells. *Ann. Botany* **2000**, *86*, 449–469.
64. White, P.J. Calcium Channels in the Plasma Membrane of Root Cells. *Ann. Botany* *81*, 173–183.

65. Webb, M.J.; Loneragan, J.F. Effect of Zinc Deficiency on Growth, Phosphorus Concentration, and Phosphorus Toxicity of Wheat Plants. *Soil Sci. Soc. Am. J.* **1988**, *52*, 1676–1680.
66. Mugwira, L.M.; Patel, S.U.; Fleming, A.L. Aluminum Effects on Growth and Al, Ca, Mg, K and P Levels in Triticale, Wheat and Rye. *Plant Soil* **1980**, *57*, 467–470.
67. Johnson R.E.; Jackson, W.A. Calcium Uptake and Transport by Wheat Seedlings as Affected by Aluminum. In *Soil Science Society Proceedings*; 1964; pp 381–386.
68. Fleming, A. L. Ammonium Uptake by Wheat Varieties Differing in Al Tolerance. *Agron. J.* **1983**, *75*, 726–730.
69. Harvey, D.M.R.; Thorpe, J.R. Some Observations on the Effects of Salinity on Ion Distribution and Cell Ultrastructure in Wheat Leaf Mesophyll Cells. *J. Experi. Botany* **1986**, *37* (174), 1–7.
70. Beyrouthy, C.A.; Grigg, B.C.; Normann, R.J.; Wells, B.R. Nutrient Uptake by Rice in Response to Water Management. *J. Plant Nutri.* **1994**, *17* (1), 39–55.
71. Islam, M.M.; Ponnampereuma F.N. Soil and Plant Tests for Available Sulfur in Wetland Rice Soils. *Plant Soil* **1982**, *68*, 97–113.
72. Samosir, S.; Blair, G.J., Sulfur Nutrition of Rice. III. A Comparison of Fertilizer Sources for Flooded Rice. *Agron. J.* **1983**, *75* (2), 203–206.
73. Stout, W.L.; Jung G.A. Biomass and Nitrogen Accumulation in Switchgrass: Effects of Soil and Environment. *Agron. J.* **1995**, *87*, 663–669.
74. Reynolds, J.H.; Walker, C.L.; Kirchner, M.J., Nitrogen Removal in Switchgrass Biomass under Two Harvest Systems. *Biomass Bioenergy* **2000**, *19*, 281–286.
75. Boylan, D.; Bush, V.; Bransby, D.I. Switchgrass Cofiring: Pilot Scale and Field Evaluation. *Biomass Bioenergy* **2000**, *19*, 411–417.
76. Prychid, C.J.; Rudall, P.J. Calcium Oxalate Crystals in Monocotyledons: A Review of Their Structure and Systematics. *Ann. Botany* **1999**, *84*, 725–739.
77. Trockenbrodt, M. Calcium Oxalate Crystals in the Bark of *Quercus robur*, *Ulmus glabra*, *Populus tremula* and *Betula pendula*. *Ann. Botany* **1995**, *75*, 281–284.
78. Britannica.com, Inc. <http://www.britannica.com> (accessed June 2001).
79. Kidambi, S.P.; Matches, A.G.; Bolger, T.P. Mineral Concentrations in Alfalfa and Sainfoin as Influenced by Soil Moisture Level. *Agron. J.* **1990**, *82*, 229–236.

80. Smith, D.; Struckmeyer, B.E. Effects of High Levels of Chlorine in Alfalfa Shoots. *Can. J. Plant Sci.* **1977**, *57*, 293–296.
81. Wilson, S.A.; Severson, R.C.; Kennedy, K.R.; Shineman, A.R.; Kinney, S.A. Total and Water Extractable Selenium in Soils and Stream Sediments, and Total Selenium in Alfalfa from the Marty II Study Area, South Dakota. U.S. Department of the Interior U.S. Geological Survey Report in cooperation with the U.S. Bureau of Reclamation Great Plains Region and the U.S. Bureau of Reclamation, Denver Office; Open File Report 90-330; 1990.
82. Iler, R.K. *Colloid Chemistry of Silica and Silicates*; Cornell University: Ithaca, NY, 1955; pp 276–297.
83. Lanning, F.C.; Ponnaiya, B.W.X.; Crumpton, C.F. The Chemical Nature of Silica in Plants. In *Plant Physiology*; 1958; pp 339–343.
84. Ball, T.B. A Typologic and Morphometric Study of Variation in Phytoliths from Einkorn Wheat (*Triticum monococcum*). *Can. J. Botany* **1993**, *71*, 1182–1192.
85. Parry, D.W.; Smithson, F. Techniques for Studying Opaline Silica in Grass Leaves. *Ann. Botany* **1958**, *22*, 544–549.
86. Blackman, E.; Parry, D.W. Opaline Silica Deposition in Rye (*Secale cereale* L.). *Ann. Botany* **1968**, *32*, 199–206.
87. Blackman, E. Opaline Silica Bodies in the Range Grasses of Southern Alberta. *Can. J. Botany* **1970**, *49*, 769–781.
88. Ollendorf, A.L.; Mulholland, S.C.; Rapp, G. JR. Phytolith Analysis as a Means of Plant Identification: *Arundo donax* and *Phragmites communis*. *Ann. Botany* **1988**, *61*, 209–214.
89. Whang, S.S.; Kim, K.; Hess, W.M. Variation of Silica Bodies in Leaf Epidermal Long Cells Within and Among Seventeen Species of *Oryza* (Poaceae). *Am. J. Botany* **1998**, *85* (4), 461–466.
90. Blackman, E. The Pattern Sequence of Opaline Silica Deposition in Rye (*Secale cereale* L.). *Ann. Botany* **1968**, *32*, 206–218
91. Terrell, E.E.; Wergin, W.P.; Epidermal Features and Silica Deposition in Lemmas and Awns of *Zizania* (Gramineae). *Am. J. Botany* **1981**, *68* (5), 697–707.
92. Mitsui, S.; Takatoh, H. Nutritional Study of Silicon in Gramineous Crops. *Soil Sci. Plant Nutri.* **1963**, *9* (2), 12–16.
93. Yoshida, S. Sulfur Nutrition of Rice. *Soil Sci. Plant Nutri.* **1979**, *25* (4), 121–134.

94. Iowa Counties. <http://www.iowa-counties.com/indexmap.htm> (accessed 2001).
95. Weier, T. E.; Stocking, C.R.; Barbour, M.G. *Botany: An Introduction to Plant Biology*, 5th ed.; John Wiley & Sons, 1974.
96. Dayton, D.C.; Milne, T.A. Laboratory Measurement of Alkali Metal Containing Vapors Released During Biomass Combustion. In *Applications of Advanced Technology to Ash-Related Problems in Boilers*; Baxter, L.; DeSollar, R., Eds.; Plenum Press: New York, 1996; pp 161–186.
97. Davis, M.; Johnson, D.; Deutch, S.; Agblevor, F.; Fennell, J.; Ashley, P. Variability in the Composition of Short Rotation Woody Feedstocks. In *Proceedings of the 2nd Biomass Conference of the Americas*; Portland, OR, 1995; pp 216–225.
98. Johnson, D.; Ashley, P.; Deutch, S.; Davis, M.; Fennell, J. Compositional Variability in Herbaceous Energy Crops. In *Proceedings of the 2nd Biomass Conference of the Americas*; Portland, OR, 1995; pp 267–277.
99. McLaughlin, S.; Samson, R.; Bransby, D.; Wiselogel, A. Evaluating Physical, Chemical, and Energetic Properties of Perennial Grasses as Biofuels. In *Partnerships to Develop and Apply Biomass Technologies, Proceedings of BIOENERGY '96–The 7th National BioEnergy Conference*; Nashville, TN, Sept 1996.
100. Chum, H.; Milne, T.; Johnson, D.; Agblevor, F. Feedstock Characterization and Recommended Procedures. In *Proceedings of the 1st Biomass Conference of the Americas*; 1993; Vol. III, pp 1685–1703.
101. Wright, L.; Tuskan, G. Strategy, Results and Directions for Woody Crop Research Funded by the U.S. Department of Energy. In *Proceedings of the TAPPI Pulping Conference*; 1997.
102. Walsh, M. *Production Costs and Supply of Biomass by U.S. Region*; Report for U.S. Department of Energy Contract No. AC05–84OR21400; Oak Ridge National Laboratory: Oak Ridge, TN, 1995.
103. Graham, R.; Lichtenberg, E.; Roningen, V.; Shapouri, H.; Walsh, M. The Economics of Biomass Production in the United States. In *Proceedings of the 2nd Biomass Conference of the Americas*; Portland, OR, 1995.
104. Public Policy Associates. Urban Wood Waste in Michigan: Supply and Policy Issues, Final Report for U.S. Department of Energy Grant No. DE-FG05-830R21390; 1994.
105. Bransby, D.; Sladden, S.; Downing, M. Yield Effects on Bale Density and Time Required for Commercial Harvesting and Baling of Switchgrass. In *Partnerships to Develop and Apply Biomass*

- Technologies, Proceedings of BIOENERGY '96–The 7th National BioEnergy Conference*; Nashville, TN, Sept 1996.
106. Turhollow, A.; Downing, M.; Butler, J. The Cost of Silage Harvest and Transport Systems for Herbaceous Crops. In *Partnerships to Develop and Apply Biomass Technologies, Proceedings of BIOENERGY '96–The 7th National BioEnergy Conference*; Nashville, TN, Sept 1996.
  107. Weislogel, A.; Agblevor, F.; Johnson, D.; Deutch, S.; Fennell, J. Compositional Changes During Storage of Large Round Switchgrass Bales. *Bioresour. Technol.* **1996**, *56* (1), 103–109.
  108. Johnson, D.; Adam, P.; Ashley, P.; Chum, H.; Deutch, S.; Fennell, J.; Weislogel, A. Study of Compositional Changes in Biomass Feedstocks Upon Storage (Results). In *Proceedings of the International Energy Agency/BioEnergy Agreement Task IX Activity 5 Workshop*; New Brunswick, Canada, May 1993.
  109. Hartsough, B.; Yomogida, D.; Stokes, B. Harvesting Systems for Short Rotation Woody Crops. Presented at the 1st Conference of the Short Rotation Woody Crops Operations Working Group, Paducah, KY, Sept 1996.
  110. Brandon, D. The Ground Rules for Buying a Grinder. *Waste Age* **1999**, *Nov*, 80–85.
  111. Komar Industrial Auger Processors.<http://www2.thomasregister.com/ss/162436307/olc/komar/komaraug.htm> (accessed 2001).
  112. Center for Renewable Energy and Sustainable Technology. Bioenergy Mailing List, [www.crest.org/renewables/bioenergy-list-archive/9608](http://www.crest.org/renewables/bioenergy-list-archive/9608) (accessed 2001).
  113. Joppich, A.; Salman, H. Wood Powder Feeding, Difficulties and Solutions. *Biomass Bioenergy* **1999**, *16*, 191–198.
  114. Cobb, J.; Elder, W.; Freeman, M.; James, R.; McCreery, L.; Biedenbach, W.; Burnett, W. Demonstration Program for Wood/Coal Cofiring in Western Pennsylvania. In *Expanding BioEnergy Partnerships, Proceedings of BioEnergy '98*; Madison, WI, Oct 1998.
  115. Bundalli, N. Development of the “Moving Hole” Feeder for Biomass. In *Expanding BioEnergy Partnerships, Proceedings of BioEnergy '98*; Madison, WI, Oct 1998.
  116. Freeman, M.C.; Walbert, G.F.; Brown, D.K. Combustion of HiMicro-Processed Coal/Biomass Fuels: FETC CERF Preliminary Results. In *Expanding BioEnergy Partnerships, Proceedings of BioEnergy '98*; Madison, WI, Oct 1998.
  117. Baxter, L.; Miles, T.; Miles, T., Jr.; Jenkins, B.; Dayton, D.; Milne, T.; Bryers, R.; Oden, L. *Alkali Deposits Found in Biomass Boilers: The Behavior of Inorganic Material in Biomass-Fired*

- Power Boilers—Field and Laboratory Experiences*; Report for U.S. Department of Energy Contract No. AC36–83CH10093; 1996.
118. American Society for Testing and Materials. ASTM Procedure E 1755-95 Standard Test Method for Ash in Biomass, Annual Book of ASTM Standards, Vol. 11.05.
  119. Erickson, T.A.; Galbreath, K.C.; Zygarlicke, C.J.; Hetland, M.D.; Benson, S.A. *Trace Element Emissions Project*; Final Technical Report (Aug 5, 1992 – Dec 31, 1998) for U.S. Department of Energy Contract No. DE-AC21-92MC28016; EERC Publication 99-EERC-06-06; Energy & Environmental Research Center: Grand Forks, ND, 1999.
  120. Friedlander, S.K. *Smoke, Dust, and Haze: Fundamentals of Aerosol Dynamics*, 2nd ed.; John Wiley and Sons: New York, 1977.
  121. Christensen K.; Stenholm, M.; Livbjerg, H. The Formation of Submicron Aerosol Particles, HCl and SO<sub>2</sub> in Straw-Fired Boilers. *J. Aerosol Sci.* **1998**, 29 (4), 421–444.
  122. Jokiniemi, J.K.; Lazaridis, M.; Lehtinen, K.E.; Kauppinen, E.I. Numerical Simulation of Vapor-Aerosol Dynamics in Combustion Processes. *J. Aerosol Sci.* **1994**, 25, 429–446.
  123. Frandsen, F.K. (1994): The Stability of Aerosols – The Prediction of Homogeneous Nucleation, EERC report.
  124. Obernberger, I.; Brunner, T.; Dahl, J. Formation, Composition, and Particle Size Distribution of Fly Ashes from Biomass Combustion Plants. In *Proceedings of the 4th Biomass Conference of the Americas*; Pergamon: Oakland, CA, 1999.
  125. Christensen, K.A. The Formation of Submicron Particles from the Combustion of Straw. Ph.D. Thesis, Department of Chemical Engineering (ed), Technical University of Denmark, Lyngby, Denmark; ISBN 87-90142-04-7.
  126. Seigneur, C.; Hudischewsky, B.; Seinfeld, J.; Whitby, K.; Whitby, E.; Brock, J.; Barnes, H. *Aerosol Sci. Technol.* **1986**, 5, 205–222.

## **APPENDIX A**

# **BIOMASS LITERATURE SEARCH**

## BIOMASS LITERATURE SEARCH

### Plant Cell Chemistry

MindQuest.net. <http://mindquest.net/biology/cell-biology/outlines/ec7guide.html> (accessed 2001).

? Cell biology study guide outline

Schachtman, D.; Liu, W. Molecular Pieces to the Puzzle of the Interaction Between Potassium and Sodium Uptake in Plants. *Trends in Plant Science* **1999**, 4 (7), 281–287.

University of Edinburgh Institute of Ecology and Resource Management. <http://www.meranti.iern.ed.ac.uk/teaching/ecophys/stomata.html> (accessed 2001).

? Stomatal physiology and plant ecophysiology courses

University of Wisconsin–Madison College of Agricultural and Life Sciences Department of Soil Science. <http://www.soils.wisc.edu/~barak/soilscience326> (accessed 2001).

? Plant nutrient management course, Soil Science 326; Philip Barak, Instructor

### Biomass Characteristics

Chum, H. et al. Feedstock Characterization and Recommended Procedures. In *Proceedings of the 1st Biomass Conference of the Americas, Vol. III*; 1993; pp 1685–1703.

Davis, M. et al. Variability in the Composition of Short Rotation Woody Feedstocks. In *Proceedings of the 2nd Biomass Conference of the Americas*; Portland, OR, 1995; pp 216–225.

Dayton, D.; Milne, T. *Laboratory Measurements of Alkali Metal Containing Vapors Released During Biomass Combustion*; U.S. Department of Energy National Renewable Energy Laboratory, Industrial Technologies Division: Golden, CO.

Duke, J. *Medicago sativa L., Alfalfa, Handbook of Energy Crops*; [http://www.hort.purdue.edu/newcrop/duke\\_energy/Medicago\\_sativa.html](http://www.hort.purdue.edu/newcrop/duke_energy/Medicago_sativa.html).

? Unpublished 1983 report for Purdue University New Crop Resource On-Line Program

Johnson, D. et al. Compositional Variability in Herbaceous Energy Crops. In *Proceedings of the 2nd Biomass Conference of the Americas*; Portland, OR, 1995; pp 267–277.

McLaughlin, S. et al. Evaluating Physical, Chemical, and Energetic Properties of Perennial Grasses as Biofuels. In *Proceedings BIOENERGY '96–The 7th National BioEnergy Conference; Partnerships to Develop and Apply Biomass Technologies*; Nashville, TN, Sept 1996.

SRI International. *Data Summary of Municipal Solid Waste Management Alternatives; Volume I Report Text*; Report to the U.S. Department of Energy National Renewable Energy Laboratory; Document No. TP-431-4988A; Menlo Park, CA, 1992; Section 9.

### **Biomass Production, Harvesting, Transport, and Storage Issues**

Bransby, D. et al. Yield Effects on Bale Density and Time Required for Commercial Harvesting and Baling of Switchgrass. In *Proceedings of BIOENERGY '96–The 7th National BioEnergy Conference: Partnerships to Develop and Apply Biomass Technologies*; Nashville, TN, Sept 1996.

Graham R. et al. The Economics of Biomass Production in the United States. In *Proceedings of the 2nd Biomass Conference of the Americas*; Portland, OR, 1995.

Johnson, D. et al. Study of Compositional Changes in Biomass Feedstocks Upon Storage (Results). In *Proceedings of the International Energy Agency/BioEnergy Agreement Task IX Activity 5 Workshop*; New Brunswick, Canada, May 1993.

Public Policy Associates. *Urban Wood Waste in Michigan: Supply and Policy Issues*; Final Report for U.S. Department of Energy Grant No. DE-FG05-83OR21390; 1994.

Turhollow, A. et al. The Cost of Silage Harvest and Transport Systems for Herbaceous Crops. In *Proceedings of BIOENERGY '96–The 7th National BioEnergy Conference; Partnerships to Develop and Apply Biomass Technologies*; Nashville, TN, Sept 1996.

Walsh, M. *Production Costs and Supply of Biomass by U.S. Region*; Report for U.S. Department of Energy Contract No. AC05-84OR21400; Oak Ridge National Laboratory, TN, 1995.

Weislogel, A. et al. Compositional Changes During Storage of Large Round Switchgrass Bales.: *Bioresource Technol.* **1996**, 56 (1), 103–109.

Wright, L.; Tuskan, G. Strategy, Results and Directions for Woody Crop Research Funded by the U.S. Department of Energy. In *Proceedings of the TAPPI Pulping Conference*; 1997.

### **Biomass Grinding and Feeding Methods and Equipment**

Brandon, D. The Ground Rules for Buying a Grinder. *Waste Age* **1999**, Nov, 80–85.

Bundalli, N. Development of the “Moving Hole” Feeder for Biomass. In *Proceedings of BIOENERGY '98–Expanding BioEnergy Partnerships*; Madison, WI, Oct 1998.

Center for Renewable Energy and Sustainable Technology. <http://www.crest.org/renewables/bioenergy-list-archive/9608> (accessed 2001).

? Bioenergy Mailing List, Biomass Densification

Center for Renewable Energy and Sustainable Technology. <http://www.crest.org/renewables/bioenergy-list-archive/9903> (accessed 2001).

? Bioenergy Mailing List, Cofiring: Biomass Combustion Requirements for Fossil-Fired Utilities

Cobb, J. et al. Demonstration Program for Wood/Coal Cofiring in Western Pennsylvania. In *Proceedings of BIOENERGY '98-Expanding BioEnergy Partnerships*; Madison, WI, Oct 1998.

Freeman, M. et al. Combustion of HiMicro-Processed Coal/Biomass Fuels; FETC CERF Preliminary Results. In *Proceedings in BIOENERGY '98-Expanding BioEnergy Partnerships*; Madison, WI, Oct 1998.

Hartsough, B. et al. Harvesting Systems for Short Rotation Woody Crops. Presented at the 1st Conference of the Short Rotation Woody Crops Operations Working Group, Paducah, KY, Sept 1996.

Joppich, A.; Salman, H. Wood Powder Feeding, Difficulties and Solutions. *Biomass Bioenergy* **1999**, *16*, 191-198.

Komar Industrial Auger Processors. <http://www2.thomascregister.com/ss/162436307/olc/komar/komaraug.htm>.

### **Results of Biomass-Coal Cofiring Studies**

Aerts, D.; Ragland, K. Cofiring Switchgrass in a 50-MW Pulverized Coal Utility Boiler. In *Proceedings of BIOENERGY '98-Expanding BioEnergy Partnerships*; Madison, WI, Oct 1998.

Battista, J. et al. Cofiring Wood Waste With Coal in a Wall-Fired Boiler: Initiating a 3-Year Demonstration Program. In *Proceedings of BIOENERGY '98-Expanding BioEnergy Partnerships*; Madison, WI, Oct 1998.

Baxter, L. et al. *Alkali Deposits Found in Biomass Boilers; The Behavior of Inorganic Material in Biomass-Fired Power Boilers-Field and Laboratory Experiences*; Report for U.S. Department of Energy Contract No. AC36-83CH10093; 1996.

Robinson, A. et al. Fireside Issues Associated with Coal-Biomass Cofiring. In *Proceedings of BIOENERGY '98-Expanding BioEnergy Partnerships*; Madison, WI, Oct 1998.

Rollins, M. et al. Commercializing Cofiring at the Colbert Fossil Plant of TVA. In *Proceedings of BIOENERGY '98-Expanding BioEnergy Partnerships*; Madison, WI, Oct 1998.

U.S. Department of Energy Energy Efficiency and Renewable Energy Network. [http://www.eren.doe.gov/biopower/cofire\\_techdesc.htm](http://www.eren.doe.gov/biopower/cofire_techdesc.htm) (accessed 2001).

? BioPower Program cofiring technical description

**APPENDIX B**

**PLANT CELL CHEMISTRY LITERATURE  
SEARCH**

## PLANT CELL CHEMISTRY LITERATURE SEARCH

### Literature

Alberts, B.; Bray, D.; Lewis, J.; Raff, M.; Roberts, K.; Watson, J. *Molecular Biology of the Cell*, 2nd ed.; Garland Publishing: New York, 1989; pp 48–51, 342–401, and 1137–1184.

Alloway, B.J. *Heavy Metals in Soils*; Blackie and Son Ltd.: Glasgow, 1990.

Baligar, V.C.; Elgin, J.H. Jr.; Foy, C.D. Variability in Alfalfa for Growth and Mineral Uptake and Efficiency Ratios under Aluminum Stress. *Agron. J.* **1989**, *81*, 223–229.

Ball, T.B. A Typologic and Morphometric Study of Variation in Phytoliths from Einkorn Wheat (*Triticum monococcum*). *Can. J. Botany* **1993**, *71*, 1182–1192.

Barber, D.A.; Shone, M.G.T. The Absorption of Silica from Aqueous Solutions by Solutions by Plants. *J. Experi. Botany* **1966**, *17* (52), 569–578.

Batten, G.D. Concentrations of Elements in Wheat Grains Grown in Australia, North America, and the United Kingdom. *Aust. J. Experi. Agri.* **1994**, *34*, 51–56.

Beyrouthy, C.A.; Grigg, B.C.; Normann, R.J.; Wells, B.R. Nutrient Uptake by Rice in Response to Water Management. *J. Plant Nutri.* **1994**, *17* (1), 39–55.

Blackman, E. Observations on the Development of the Silica Cells of the Leaf Sheath of Wheat (*Triticum aestivum*). *Can. J. Botany* **1969**, *47*, 827–837.

Blackman, E. Opaline Silica Bodies in the Range Grasses of Southern Alberta. *Can. J. Botany* **1970**, *49*, 769–781.

Blackman, E. The Pattern Sequence of Opaline Silica Deposition in Rye (*Secale cereale* L.). *Ann. Botany* **1968**, *32*, 206–218.

Blackman, E.; Parry, D.W. Opaline Silica Deposition in Rye (*Secale cereale* L.). *Ann. Botany* **1968**, *32*, 199–206.

Boylan, D.; Bush, V.; Bransby, D.I. Switchgrass Cofiring: Pilot Scale and Field Evaluation. *Biomass Bioenergy* **2000**, *19*, 411–417.

Butler, D.L.; Wright, W.G.; Steward, K.C.; Osmundson, B.C.; Krueger, R.P.; Crabtree, D.W. *Detailed Study of Selenium and Other Constituents in Water, Bottom Sediment, Soil, Alfalfa, and Biota Uncompagne Project Area and in the Grand Valley, West-Central Colorado, 1991–93*; U.S. Geological Survey Water Resources Investigations Report 96-4138, Denver, CO, 1996.

- Calderini, D.F.; Torres-Leon, S.; Slafer, G.A. Consequences of Wheat Breeding on Nitrogen and Phosphorus Yield, Grain Nitrogen and Phosphorus and Associated Traits. *Ann. Botany* **1995**, *76*, 315–322.
- Carson, E.W. *The Plant Root and Its Environment: Proceedings of an Institute Sponsored by the Southern Regional Education Board*; Virginia Polytechnic Institute and State University, July 5–16, 1971; University Press of Virginia: Charlottesville, VA, 1974.
- Clark, D.H.; Cary, E.E.; Maryland, H.F. Analysis of Trace Elements in Forages by Near Infrared Reflectance Spectroscopy. *Agron. J.* **1989**, *81*, 91–95.
- Clarke, J.M.; Campbell, C.A.; Cutforth, H. W.; DePauw, R.M.; Winkleman, G.E. Nitrogen and Phosphorus Uptake, Translocation, and Utilization Efficiency of Wheat in Relation to Environment and Cultivar Yield and Protein Levels. *Can. J. Botany* **1990**, *70*, 965–977.
- Cramer, M.D.; Lewis, O.A.M. The Influence of  $\text{NO}_3^-$  and  $\text{NH}_4^+$  Nutrition on the Gas Exchange Characteristics of the Roots of Wheat (*Triticum aestivum*) and Maize (*Zea mays*) Plants. *Ann. Botany* **1993**, *72*, 37–46.
- Cramer, M.D.; Lewis, O.A.M. The Influence of Nitrate and Ammonia Nutrition on the Growth of Wheat (*Triticum aestivum*) and Maize (*Zea mays*) Plants. *Ann. Botany* **1993**, *72*, 359–365.
- Datta, K.S.; Kumar, A.; Varma, S.K.; Angrish, R. Differentiation of Chloride and Sulphate Salinity on the Basis of Ionic Distribution in Genetically Diverse Cultivars of Wheat. *J. Plant Nutri.* **1995**, *18* (10), 2199–2212.
- Elliot, D.E.; Reuter D.J.; Reddy G.D.; Abbott, R.J. Phosphorus Nutrition of Spring Wheat (*Triticum aestivum* L.) 4. Calibration of Plant Phosphorus Test Criteria from Rain-Fed Field Experiments. *Aust. J. Agri. Res.* **1997**, *48*, 883–897.
- Epstein, E. *Mineral Nutrition of Plants: Principles and Perspectives*; John Wiley and Sons: New York, 1972.
- Fageria, N.K.; Baligar, V.C.; Jones, C.A. *Growth and Mineral Nutrition of Field Crops*; Marcel Dekker Inc.: New York, 1991.
- Fisher, K.T.; Brummer, J.E.; Leininger, W.C.; Heil, D.M. Interactive Effects of Soil Amendments and Depth of Incorporation on Geyer Willow. *J. Environ. Qual* **2000**, *29*, 1786–1793.
- Fitzgerald, M.A.; Ugalde, T.D.; Anderson, J.W. Sulphur Nutrition Changes the Source of S in Vegetative Tissues of Wheat During Generative Growth. *J. Experi. Botany* **1999**, *50* (333), 499–508.

- Fleming, A.L. Ammonium Uptake by Wheat Varieties Differing in Al Tolerance. *Agron. J.* **1983**, 75, 726–730.
- Frank, A.B.; Bauer, A.; Black A.L. Carbohydrate, Nitrogen and Phosphorus Concentrations of Spring Wheat Leaves and Stems. *Agron. J.* **1989**, 81, 524–528.
- Gardiner, D.T.; Christensen, N.W. A Simple Model for Phosphorus Uptake Kinetics of Wheat Seedlings. *J. Plant Nutri.* **1997**, 20 (2 and 3), 271–277.
- Goodroad, L.L.; Wilson, D.O. Influence of Sulfur on Growth and Nutrient Composition of Soft Red Winter Wheat. *J. Plant Nutri.* **1989**, 12 (8), 1029–1039.
- Gol'yeva, A.A. Experience in Using Phytolith Analysis in Soil Science. *Eurasian Soil Sci.* **1996**, 28 (12), 248–256.
- Harvey, D.M.R.; Thorpe, J.R. Some Observations on the Effects of Salinity on Ion Distribution and Cell Ultrastructure in Wheat Leaf Mesophyll Cells. *J. Experi. Botany* **1986**, 37 (174), 1–7.
- Hewitt, E.J.; Smith, T.A. *Plant Mineral Nutrition*; The English Universities Press Ltd., 1974.
- Iler, R.K. *Colloid Chemistry of Silica and Silicates*; Cornell University: Ithaca, NY, 1955; pp 276–297.
- Iler, R.K. *The Chemistry of Silica: Solubility, Polymerization, Colloid and Surface Properties, and Biochemistry*; John Wiley & Sons: New York, 1979.
- Islam, M.M.; Ponnampereuma F.N. Soil and Plant Tests for Available Sulfur in Wetland Rice Soils. *Plant Soil* **1982**, 68, 97–113.
- Johnson R.E.; Jackson, W.A. Calcium Uptake and Transport by Wheat Seedlings as Affected by Aluminum. *Soil Science Society Proceedings*; 1964; pp 381–386.
- Jones, L.H.P.; Handreck, K.A. Studies of Silica in the Oat Plant III. Uptake of Silica from Soils by the Plant. *Plant Soil* **1965**, 23 (1), 79–96.
- Jones, L.H.P.; Milne, A.A.; Wadham, S.M. Studies of Silica in the Oat Plant II. Distribution of the Silica in the Plant. *Plant Soil* **1963**, 18 (3), 358–371.
- Judd, W.S.; Campbell, C.S.; Kellogg, E.A.; Stevens, P.F. *Plant Systematics: A Phylogenetic Approach*; Sinauer Associates Inc.: Sunderland, MA, 1999.
- Keltjens, W.G.; Tan, K. Interactions Between Aluminum, Magnesium and Calcium with Different Monocotyledonous and Dicotyledonous Plant Species. *Plant Soil* **1993**, 155–156, 485–488.

- Kidambi, S.P.; Matches, A.G.; Bolger, T.P. Mineral Concentrations in Alfalfa and Sainfoin as influenced by Soil Moisture Level. *Agron. J.* **1990**, *82*, 229–236.
- Krol, E.; Trebacz, K. Way of Ion Channel Gating in Plant Cells. *Ann. Botany* **2000**, *86*, 449–469.
- Lanning, F.C.; Ponnaiya, B.W.X.; Crumpton, C.F. The Chemical Nature of Silica in Plants. *Plant Physiol.* **1958**, 339–343.
- Lee, R.B. Control of Net Uptake of Nutrients by Regulation of Influx in Barley Plants Recovering from Nutrient Deficiency. *Ann. Botany* **1993**, *72*, 223–230.
- Lepp, N.W. *Effect of Heavy Metal Pollution on Plants, Volume 1*; Applied Science Publishers: London, 1981.
- Lindsay, W.L. *Chemical Equilibria in Soils*; John Wiley & Sons: New York, 1979.
- Ma, Z.; Wood, C.W.; Bransby, D.I. Impacts of Soil Management on Root Characteristics of Switchgrass. *Biomass Bioenergy* **2000**, *18*, 105–112.
- Metcalf, C.R. *Anatomy of the Monocotyledons*; Oxford University Press, 1960.
- Mitsui, S.; Takatoh, H. Nutritional Study of Silicon in Gramineous Crops. *Soil Sci. Plant Nutri.* **1963**, *9* (2), 12–16.
- Monaghan, J.M.; Scrimgeour, C.M.; Stein, W.M.; Zhao, F.J.; Evans, E.J. Sulphur Accumulation and Redistribution in Wheat (*Triticum aestivum*): A Study Using Stable Sulphur Isotope Ratios as a Tracer System. *Plant, Cell, Environ.* **1999**, *22*, 831–839.
- Mugwira, L.M.; Patel, S.U.; Fleming, A.L. Aluminum Effects on Growth and Al, Ca, Mg, K, and P Levels in Triticale, Wheat, and Rye. *Plant Soil* **1980**, *57*, 467–470.
- Ollendorf, A.L.; Mulholland, S.C.; Rapp, G. Jr. Phytolith Analysis as a Means of Plant Identification: *Arundo donax* and *Phragmites communis*. *Ann. Botany* **1988**, *61*, 209–214.
- Parry, D.W.; Smithson, F. Detection for Studying Opaline Silica in Grass Leaves. *Nature* **1957**, *179*, 975–976.
- Parry, D.W.; Smithson, F. Influence of Mechanical Damage on Opaline Silica Deposition in *Molinia caerulea* L. *Nature* **1963**, *199*, 925–926.
- Parry, D.W.; Smithson, F. Techniques for Studying Opaline Silica in Grass Leaves. *Ann. Botany* **1958**, *22*, 544–549.

- Peel, A.J. *Transport of Nutrients in Plants*; Butterworth & Co. Ltd., John Wiley & Sons, 1974.
- Piperno, D.R. *Phytolith Analysis: An Archeological and Geological Perspective*; Academic Press, Inc., 1988; pp 11–49.
- Pizer, N.H. *Trace Elements in Soils and Crops: Proceedings of a Conference organized by the Soil Scientists of the National Agricultural Advisory Service*; Feb 8–9, 1966; Her Majesty's Stationary Office: London, 1971.
- Prychid, C.J.; Rudall, P.J. Calcium Oxalate Crystals in Monocotyledons: A Review of their Structure and Systematics. *Ann. Botany* **1999**, *84*, 725–739.
- Reginato, J.C.; Palumbo, M.C.; Moreno, I.S.; Bernardo, I.Ch.; Tarzia, D.A. Modeling Nutrient Uptake Using a Moving Boundary Approach: Comparison with the Barber-Cushman Model. *Soil Sci. Soc. Am. J.* **2000**, *64*, 1363–1367.
- Rehmm G.W. Application of Phosphorus and Sulfur on Irrigated Alfalfa. *Agron. J.* **1987**, *79*, 973–979.
- Reich, P.B.; Lassoie, J.P.; Amundson, R.G. Reduction in Growth of Hybrid Poplar Following Field Exposure to Low Levels of O<sub>3</sub> and (or) SO<sub>2</sub>. *Can. J. Botany* **1984**, *62*, 2835–2841.
- Reynolds, J.H.; Walker, C.L.; Kirchner, M.J. Nitrogen Removal in Switchgrass Biomass under Two Harvest Systems. *Biomass Bioenergy* **2000**, *19*, 281–286.
- Romer, W.; Augustin, L.; Shilling, G. The Relationship Between Phosphate Absorption and Root Length in Nine Wheat Cultivars. *Develop. Plant Soil Sci.* **1989**, *36*, 123–125.
- Rorison, J.H. *Ecological Aspects of the Mineral Nutrition of Plants*; Blackwell Scientific Publications: Oxford, 1969.
- Samosir, S.; Blair, G.J. Sulfur Nutrition of Rice. III. A Comparison of Fertilizer Sources for Flooded Rice. *Agron. J.* **1983**, *75* (2), 203–206.
- Shone, M.G.T. Initial Uptake of Silica by Excised Barley Roots. *Nature* **1964**, *202*, 314–315.
- Smith, D.; Struckmeyer, B.E. Effects of High Levels of Chlorine in Alfalfa Shoots. *Can. J. Plant Sci.* **1977**, *57*, 293–296.
- Smithson, F. Plant Opal in Soil. *Nature* **1956**, *178*, 107.
- Stevens, B.J.; Sell, L.O.; Easty, D.B. Determination of Total Organic Chlorine in Pulp. *Tappi J.* **1989**, *72* (7), 181–182.

- Stiles, W. *Trace Elements in Plants*; Cambridge University Press, 1961.
- Stout, W.L.; Jung G.A. Biomass and Nitrogen Accumulation in Switchgrass: Effects of Soil and Environment. *Agron. J.* **1995**, *87*, 663–669.
- Taiz, L. The Plant Vacuole. *J. Experi. Biol.* **1992**, *172*, 113–122.
- Terrell, E.E.; Wergin, W.P. Epidermal Features and Silica Deposition in Lemmas and Awns of *Zizania* (Gramineae). *Am. J. Botany* **1981**, *68* (5), 697–707.
- Trockenbrodt, M. Calcium Oxalate Crystals in the Bark of *Quercus robur*, *Ulmus glabra*, *Populus tremula* and *Betula pendula*. *Ann. Botany* **1995**, *75*, 281–284.
- Trolldenier, G. Techniques for Observing Phosphorus Mobilization in the Rhizosphere. *Biol. Fertil. Soils* **1992**, *14*, 121–125.
- Viehoever, A.; Prusky, S.C. Biochemistry of Silica. *Am. J. Pharm.* **1938**, *10*, 99–120.
- Webb, M.J.; Loneragan, J.F. Effect of Zinc Deficiency on Growth, Phosphorus Concentration, and Phosphorus Toxicity of Wheat Plants. *Soil Sci. Soc. Am. J.* **1988**, *52*, 1676–1680.
- Wang, S.S.; Kim, K.; Hess, W.M. Variation of Silica Bodies in Leaf Epidermal Long Cells Within and Among Seventeen Species of *Oryza* (Poaceae). *Am. J. Botany* **1998**, *85* (4), 461–466.
- White, P.J. Calcium Channels in the Plasma Membrane of Root Cells. *Ann. Botany* **1998**, *81*, 173–183.
- Wilson, S.A.; Severson, R.C.; Kennedy, K.R.; Shineman, A.R.; Kinney, S.A. *Total and Water Extractable Selenium in Soils and Stream Sediments, and Total Selenium in Alfalfa from the Marty II Study Area, South Dakota*. Report in cooperation with the U.S. Bureau of Reclamation Great Plains Region and the U.S. Bureau of Reclamation, Denver Office; Open File Report 90-330; U.S. Department of the Interior, U.S. Geological Survey, 1990.

### **Electronic Sources**

BertelsmannSpringer. <http://link.springer-ny.com/search.htm> (accessed March 26, 2001).

Britannica.com Inc. [www.britannica.com](http://www.britannica.com) (accessed March 29, 2001).

Colorado State University College of Natural Resources. Nutrient Cycling: The Fundamental Concepts of Nitrogen and Phosphorus Dynamics in Ecosystems. <http://www.cnr.colostate.edu/~bobw/a/n/nitro1.htm> (accessed May 24, 2001).

? PowerPoint presentation by Dr. Bob Woodmansee

E-Journals.org. Electronic Sites of Leading Botany, Plant Biology, and Science Journals.  
<http://www.e-journals.org/botany/> (accessed March 26, 2001).

Farabee, M.J. Plant Hormones, Nutrition, and Transport.  
<http://gened.emc.maricopa.edu/bio/bio181/BIOBK/BioBookPLANTHORM.html#Plant%20Nutrition> (accessed Feb 22, 2001).

MoorMans, Inc. Variation in Trace Mineral Concentration of Native Grasses.  
<http://www.moormans.com/beef/BeefFF/9beefaug/mineral.htm> (accessed Feb 22, 2001).

University of Adelaide, Australia, Department of Plant Science. Plant Nutrition Group List of Recent Publications. <http://planta.waite.adelaide.edu.au/labs/rdg/recent.htm> (accessed Feb 22, 2001).

University of Minnesota–Minneapolis. Spring Wheat Research.  
<http://www.agro.agri.umn.edu/rp/projects/wheat.htm> (accessed Feb 22, 2001).

University of Missouri. Phytolith Database. <http://web.missouri.edu/~phyto/> (accessed Jan 17, 2001).

University of Wisconsin–Milwaukee Department of Geography. Phytolith Morphotype Catalog;  
<http://www.uwm.edu/People/fredlund/phytocat.htm> (accessed Jan 22, 2001).

U.S. Department of Agriculture Agricultural Research Service Federal Plant, Soil, and Nutrition Laboratory. <http://www.arserrc.gov/naa/home/fedpsnl.htm> (accessed Feb 23, 2001).

U.S. Department of Agriculture Agricultural Research Service Plant Science Research Unit, University of Minnesota, St. Paul. <http://link.springer-ny.com/search.htm> (accessed Feb 26, 2001).

## **APPENDIX C**

# **GLOSSARY OF BIOMASS TERMS**

## GLOSSARY OF BIOMASS TERMS

**Aerial:** Borne in the air rather than underground or underwater.

**Angiosperm:** A plant of the class Angiospermae, characterized by seeds enclosed in an ovary; a flowering plant.

**Anthesis:** The blooming or time of full bloom of a flower.

**Cambium:** A layer of cells in the stems and roots of vascular plants that gives rise to phloem and xylem.

**Chloroplast:** Specialized intracellular organelle that carry out photosynthesis during daylight hours.

**Cortex:** A layer of tissue in roots and stems lying between the epidermis and the vascular tissue.

**Culm:** The jointed stem of a grass or sedge.

**Cytosol:** The compartment of the cytoplasm that includes everything other than the membraned–bounded organelles. Site of protein synthesis and many of the reactions by which some small molecules are degraded and others are formed (intermediary metabolism of the cell).

**Druses:** Multiple crystals thought to have formed around a nucleation site to form a crystal conglomerate.

**Gramineae:** Family of grasses of which wheat, rice, and switchgrass are members.

**Idioblast:** A plant cell that differs noticeably in form from neighboring cells.

**Ligule:** A straplike structure, such as a ray flower of a daisy or a sheathlike organ at the base of a grass leaf.

***Medicago sativa:*** (alfalfa) Diploid.

**Meristems:** Special regions composed of self-renewing stem cells. Apical meristems at the tips of growing roots and shoots are involved in adding new cells that will elongate and differentiate into root tissues and stem tissues plus leaf primordia. Lateral meristems, circumferentially arranged inside the plant are involved in producing cells that increase the girth of the plant.

**Monosaccharide:** Aldehydes or ketones that also have two or more hydroxyl groups. General formula is  $(\text{CH}_2\text{O})_n$ , (where  $n = 3, 4, 5, 6, 7$ ). The aldehyde or ketone group provides the means for the molecule to exist either as a chain or a ring and for the linking of ringed monosaccharides to join, forming long chains of sugar molecules called polysaccharides.

**Opaline silica:** ( $\text{SiO}_2 \cdot n\text{H}_2\text{O}$ ) These deposits are known as silicophytoliths or opal phytoliths.

***Oryza sativa:*** (rice) Diploid.

***Panicum virgatum:*** (switch grass) Diploid.

**Petiole:** The stalk of a leaf; a leaf without a petiole is sessile.

**Phloem:** Complex set of living cells in the vascular tissue that is responsible for transporting sucrose from photosynthetic cells in the leaf to the rest of the plant.

**Phytolith:** (plant-rock) Deposit of silica as well as other types of plant mineral deposits.

**Poaceae:** Alternative name for family of grasses Gramineae.

**Polysaccharide:** A group of nine or more monosaccharides joined by glycosidic bonds, such as starch and cellulose.

***Populus tremuloides:*** (hybrid poplar) Diploid.

**Protoplasm:** A complex jellylike colloidal substance conceived of as constituting the living matter of plant and animal cells and performing the basic life functions.

**Stoma:** *pl. -mata* One of the minute pores in the epidermis of a leaf or stem through which gases and water vapor pass.

**Sucrose:** A crystalline disaccharide carbohydrate,  $\text{C}_{12}\text{H}_{22}\text{O}_{11}$ , found in many plants, mainly sugar cane and sugar beet, and used widely as a sweetener, preservative, and in the manufacture of plastics and cellulose. The major form in which sugar is transported between plant cells, sucrose is exported from the leaves via vascular bundles, providing the carbohydrate required for the rest of the plant.

**Taxon:** A group of organisms constituting one of the categories or formal units in taxonomic classification, such as phylum, order, family, genus, or species, and characterized by common characteristics in varying degrees of distinction.

**Tonoplast:** The single membrane that separates a vacuole from the cytoplasm in a plant cell.

***Triticum aestivum:*** (domestic wheat) Diploid.

***Triticum monococcum:*** (Einkorn wheat) Diploid wheat thought to have been domesticated from *Triticum boeoticum*. It has been cultivated since Neolithic times in Europe and the Ancient Near East and is currently grown in most countries of the European continent.

**Vacuole:** A small cavity in the protoplasm of a cell.

**Xylem:** Long tubes forming the strengthened wall of the vascular tissue that transport water and ion throughout the plant. The capillary movement within the xylem is related to water evaporation from the plant. In mature plants, they are dead cells with all the cytoplasm removed.

## **APPENDIX D**

# **SWITCHGRASS PROXIMATE, ULTIMATE, AND ASH CHEMISTRY ANALYSES**

Sample	Lodge Land #1	Lodge Land #2	G. Peterson #1	G. Peterson #2	Schultz #1	Schultz #3	Schultz #5	Schultz #7	Schultz #9	Schultz #11	Schultz #13	Schultz #15	Schultz #17	Van Patten #1	Van Patten #2	Krutsinger #1	Krutsinger #2
County	Appanoose	Appanoose	Lucas	Lucas	Lucas	Lucas	Lucas	Lucas	Lucas	Lucas	Lucas	Lucas	Lucas	Lucas	Lucas	Lucas	Lucas
Township	Chariton	Chariton	English	English	English	English	English	English	English	English	English	English	English	English	English	Liberty	Liberty
Farm	Lodge Land 1999	Lodge Land 1999	G. Peterson	G. Peterson	Schultz	Van Patten	Van Patten	Krutsinger	Krutsinger								
Date	1999	1999	2000	2000	1999	1999	1999	2000	2000	2000	2000	2000	2000	1999	1999	1999	1999
Status	Harvested	Harvested	Harvested	Harvested	Unharvested	Harvested	Harvested	Harvested	Harvested								
Proximate Analysis, wt% (as-received)																	
Moisture	23.05	13.66	12.09	17.61	11.77	12.77	11.37	12.40	11.14	14.00	10.28	17.33	14.29	14.20	16.36	12.87	12.79
Ash	4.01	3.98	3.18	3.46	4.90	4.74	5.00	4.18	3.97	4.46	3.49	2.55	2.98	4.12	4.10	3.93	4.70
Volatile	61.16	68.09	72.14	66.14	69.40	69.64	69.92	71.02	72.29	69.24	74.28	69.34	71.83	68.07	66.37	68.68	67.96
Fixed Carbon	11.78	14.27	12.59	12.79	13.93	12.85	13.71	12.40	12.60	12.30	11.95	10.78	10.90	13.61	13.17	14.52	14.55
Sulfur, wt% (fuel basis)	0.12	0.07	0.09	0.11	0.08	0.06	0.06	0.10	0.08	0.08	0.13	0.09	0.07	0.05	0.06	0.09	0.09
Btu-lb, HHV	6029	6837	7193	6742	7010	6884	7082	7057	7122	6754	7259	6733	6945	6868	6648	6997	6969
LHV, Btu-lb	5792	6696	7068	6561	7002	7401	7256	7486	7390	7440	7095	7543	6922	7175	7187	6479	6837
MMF, Btu-lb	6300	7144	7449	7002	7401	7256	7486	7390	7440	7095	7543	6922	7175	7187	6955	7306	7341
Air Dry Loss, wt% (fuel basis)	17.39	7.69	5.00	10.71	5.00	5.88	4.35	5.54	4.17	7.01	4.00	12.50	8.70	6.90	9.68	8.33	8.33
Ultimate Analysis, wt% (as-received)																	
Moisture	23.05	13.66	12.09	17.61	11.77	12.77	11.37	12.40	11.14	14.00	10.28	17.33	14.29	14.20	16.36	12.87	12.79
Carbon	36.41	41.34	42.45	39.73	41.75	41.69	42.04	41.79	42.61	40.96	43.34	40.28	41.66	41.04	39.76	41.88	41.48
Hydrogen	4.57	5.10	5.20	4.91	5.00	4.98	5.11	4.97	5.02	4.88	5.24	4.80	4.93	4.98	4.76	4.09	5.03
Nitrogen	0.61	0.57	0.57	0.79	0.42	0.37	0.33	0.31	0.37	0.33	0.33	0.31	0.33	0.27	0.29	0.34	0.29
Sulfur	0.12	0.07	0.09	0.11	0.08	0.06	0.06	0.10	0.08	0.08	0.13	0.09	0.07	0.05	0.06	0.09	0.09
Ash	4.01	3.98	3.18	3.46	4.90	4.74	5.00	4.18	3.97	4.46	3.49	2.55	2.98	4.12	4.10	3.93	4.70
Oxygen	31.23	35.28	36.42	33.39	36.08	35.39	36.09	36.25	36.81	35.29	37.19	34.64	35.74	35.34	34.67	36.80	35.62
Chlorine	0.25	0.20	0.03	0.04	0.05	0.06	0.07	0.01	0.03	0.02	0.01	0.01	0.01	0.06	0.05	0.08	0.11
Bulk Ash Chemistry, wt%																	
SiO <sub>2</sub>	58.43	57.37	72.76	72.15	67.93	69.83	69.82	74.76	75.90	79.64	71.35	68.10	73.21	70.87	63.87	67.92	62.77
Al <sub>2</sub> O <sub>3</sub>	0.87	0.30	0.59	0.76	0.43	0.35	0.81	0.37	0.08	0.07	0.01	0.41	1.25	0.59	0.29	0.01	0.07
TiO <sub>2</sub>	0.09	0.01	0.02	0.02	0.01	0.04	0.09	0.04	0.04	0.04	0.04	0.04	0.04	0.01	0.01	0.01	0.01
Fe <sub>2</sub> O <sub>3</sub>	0.36	0.33	0.42	0.53	0.39	0.27	0.31	0.35	0.30	0.22	0.46	0.57	0.78	0.35	0.45	0.36	0.30
CaO	7.70	7.28	8.86	10.50	6.96	7.51	9.44	10.30	10.20	9.46	12.50	14.50	13.80	7.88	7.48	6.72	6.67
MgO	6.08	4.38	3.77	4.59	3.02	3.75	3.55	3.21	3.26	2.75	3.19	3.69	2.93	3.50	2.99	3.03	2.27
Na <sub>2</sub> O	0.86	1.02	0.18	0.18	0.13	0.12	0.15	0.09	0.11	0.08	0.23	0.44	0.23	0.26	0.31	0.26	0.26
K <sub>2</sub> O	17.40	21.10	5.53	6.85	13.00	11.30	9.75	7.40	7.05	5.00	8.56	6.93	3.30	11.60	16.20	12.10	14.40
P <sub>2</sub> O <sub>5</sub>	4.81	3.91	2.43	3.17	9.13	8.52	7.32	4.69	4.46	4.08	4.49	4.83	3.34	7.57	7.69	8.37	8.69
SO <sub>3</sub>	2.19	2.90	1.74	2.44	1.12	0.96	1.27	1.15	1.05	0.97	1.01	1.39	1.05	1.05	1.79	1.26	0.95
Cl	3.10	1.47	0.15	0.31	0.37	0.41	0.45	0.11	0.18	0.10	0.28	0.41	0.11	0.21	0.20	0.38	0.54
Water-Soluble Alkalies, %																	
Na <sub>2</sub> O	0.012	0.018	0.004	0.004	0.001	0.001	0.001	0.002	0.002	0.004	0.002	0.001	0.001	0.001	0.001	0.001	0.001
	0.015	0.021	0.004	0.005	0.001	0.001	0.001	0.002	0.002	0.004	0.002	0.001	0.001	0.001	0.001	0.001	0.001
K <sub>2</sub> O	0.859	0.951	0.176	0.239	0.702	0.534	0.503	0.281	0.286	0.219	0.102	0.112	0.072	0.507	0.714	0.526	0.731
	0.116	1.101	0.200	0.290	0.796	0.612	0.568	0.321	0.321	0.254	0.113	0.135	0.084	0.591	0.854	0.604	0.838

Sample	Cross #1	Cross #2	Sellers #1	Sellers #2	Sellers #2	Sellers #4	Sellers #6	Sellers #8	Sellers #10	Sellers #12	Sellers #14	Sellers #16	Sellers #18	Sellers #21	Bills Brome #20	Cemensky #19	Peck Orchard #22
County	Wayne	Wayne	Wayne	Wayne	Wayne	Wayne	Wayne	Wayne	Wayne	Wayne	Wayne	Wayne	Wayne	Wayne	NA	NA	NA
Township	South Fork	South Fork	Union	Union	Union	Union	Union	Union	Union	Union	Union	Union	Union	Union	NA	NA	NA
Farm	Cross	Cross	Sellers	Sellers	Sellers	Sellers	Sellers	Sellers	Sellers	Sellers	Sellers	Sellers	Sellers	Sellers	Bills Brome	Cemensky	Peck Orchard
Date	1999	1999	1999	1999	1999	1999	1999	1999	2000	2000	2000	2000	2000	2000	2000	2000	2000
Status	Harvested	Harvested	Harvested	Harvested	Unharvested	NA	NA	NA									
Proximate Analysis, wt% (as-received)																	
Moisture	13.65	11.92	15.80	9.41	10.57	11.54	14.54	12.56	10.29	16.79	15.15	15.16	15.24	23.58	30.24	25.69	18.23
Ash	4.41	3.95	3.63	4.15	5.52	4.48	3.81	3.57	4.11	3.94	3.10	3.11	4.05	8.76	6.11	3.90	5.00
Volatile	69.04	71.68	66.97	72.07	68.10	69.03	67.88	70.76	72.11	67.24	69.87	70.44	69.53	57.28	54.02	60.69	64.35
Fixed Carbon	12.90	12.45	13.60	14.37	15.81	14.95	13.77	13.11	13.49	12.03	11.88	11.29	11.18	10.38	9.63	9.72	12.42
Sulfur, wt % (fuel basis)	0.07	0.07	0.20	0.23	0.21	0.12	0.13	0.09	0.11	0.12	0.12	0.11	0.11	0.14	0.11	0.13	0.12
Btu-lb, HHV	6929	7108	6731	7266	7114	6955	6823	6935	7220	6708	6881	6850	6817	5699	5295	5916	6378
LHV, Btu-lb	6788	6985	6568	7169													
MMF, Btu-lb	7275	7424	7004	7605	7563	7308	7114	7212	7555	7004	7118	7087	7128	6292	5667	6174	6740
Air Dry Loss, wt% (fuel basis)	5.56	4.35	10.71	4.35	5.56	6.25	8.33	7.14	4.35	11.11	9.09	9.09	9.09	17.65	25.00	20.00	12.50
Ultimate Analysis, wt% (as-received)																	
Moisture	13.65	11.92	15.80	9.41	10.57	11.54	14.54	12.56	10.29	16.79	15.15	15.16	15.24	23.58	30.24	25.69	18.23
Carbon	41.44	42.39	40.69	43.40	41.84	41.88	40.77	41.92	42.94	39.61	40.79	41.05	40.25	33.63	31.77	35.48	38.33
Hydrogen	4.87	5.11	4.86	5.53	5.36	5.28	5.06	5.22	5.37	4.95	5.14	5.06	4.99	4.32	4.08	4.44	4.63
Nitrogen	0.45	0.40	0.38	0.42	0.82	0.52	0.38	0.42	0.48	0.45	0.41	0.37	0.49	0.82	0.53	0.67	0.54
Sulfur	0.07	0.07	0.20	0.23	0.21	0.12	0.13	0.09	0.11	0.12	0.12	0.11	0.11	0.14	0.11	0.13	0.12
Ash	4.41	3.95	3.63	4.15	5.52	4.48	3.81	3.57	4.11	3.94	3.10	3.11	4.05	8.76	6.11	3.90	5.00
Oxygen	35.11	36.16	34.44	36.86	35.68	36.18	35.31	36.22	36.70	34.14	35.29	35.14	34.87	28.75	27.16	29.69	33.15
Chlorine	0.10	0.04	0.11	0.04	0.35	0.17	0.07	0.02	0.05	0.01	0.01	0.01	0.01	0.02	0.02	0.02	0.01
Bulk Ash Chemistry, wt%																	
SiO <sub>2</sub>	69.21	63.96	64.04	63.76	52.99	57.92	65.76	69.20	71.18	68.83	68.98	76.76	76.27	81.83	83.29	68.98	76.16
Al <sub>2</sub> O <sub>3</sub>	0.51	0.33	0.01	0.07	0.01	0.01	0.01	0.01	0.01	0.94	0.78	1.18	1.35	1.41	0.80	2.20	0.14
TiO <sub>2</sub>	0.01	0.01	0.09	0.04	0.17	0.22	0.04	0.04	0.04	0.04	0.04	0.04	0.04	0.04	0.13	0.14	0.07
Fe <sub>2</sub> O <sub>3</sub>	0.35	0.36	0.42	0.38	0.38	0.42	0.28	0.25	0.30	0.39	0.35	0.42	0.46	0.46	0.57	0.90	0.33
CaO	8.19	8.62	10.40	8.07	6.65	9.90	8.79	9.27	10.80	10.20	10.80	10.40	10.90	7.76	8.04	16.20	9.31
MgO	4.83	5.54	5.64	4.25	3.90	4.32	6.05	4.11	3.87	4.38	4.53	4.25	3.15	2.69	1.02	2.43	1.95
Na <sub>2</sub> O	0.50	0.38	0.28	0.10	0.13	0.18	0.13	0.12	0.15	0.15	0.10	0.09	0.08	0.08	0.19	0.20	0.22
K <sub>2</sub> O	10.40	12.30	13.50	12.40	21.50	15.50	10.80	6.87	6.45	6.37	3.87	3.45	2.16	3.80	3.20	4.46	5.70
P <sub>2</sub> O <sub>5</sub>	5.82	5.18	5.17	5.03	9.10	8.09	4.99	3.38	3.81	2.50	2.52	2.01	2.26	2.75	2.28	3.17	3.92
SO <sub>3</sub>	2.02	2.14	1.90	2.33	1.06	1.68	2.10	1.42	1.49	1.46	1.48	2.45	1.49	1.74	0.97	1.81	1.14
Cl	0.47	0.24	0.71	0.60	5.10	2.50	0.82	0.23	0.36	0.18	0.15	0.06	0.05	0.06	0.05	0.10	0.13
Water-Soluble Alkalies, %																	
Na <sub>2</sub> O	0.001	0.001	0.002	0.002	0.002	0.001	0.001	0.001	0.001	0.003	0.001	0.001	0.001	0.001	0.001	0.001	0.002
K <sub>2</sub> O	0.543	0.533	0.514	0.496	1.256	0.696	0.386	0.226	0.239	0.201	0.121	0.103	0.075	0.158	0.184	0.169	0.239
	0.629	0.605	0.611	0.548	1.404	0.786	0.452	0.258	0.267	0.241	0.143	0.121	0.089	0.207	0.263	0.227	0.292

## **APPENDIX E**

# **ANALYTICAL CHARACTERIZATIONS FOR VARIOUS TYPES OF BIOMASS**

TABLE E-1

## Analytical Characterizations for Various Types of Biomass

	Planer Shavings	Eucalyptus	Poplar	Switchgrass	Rice Straw	Wheat Straw
Proximate Analysis (as-received)						
Ash, wt%	NA <sup>1</sup>	0.48	1.16	4.22	17.79	7.48
Volatile Matter, wt%	NA	78.52	80.99	72.73	57.92	68.60
Fixed Carbon, wt%	NA	11.66	13.05	14.89	12.56	14.73
Moisture, wt%	NA	9.34	4.80	8.16	11.73	9.19
Heating Value, Btu-lb	8760	8262	8382	8012	6339	7599
Ultimate Analysis (as-received)						
C	34.50	44.89	47.05	43.04	34.64	40.88
H	3.76	5.21	5.71	5.37	4.39	5.14
O (by difference)	26.65	39.92	41.01	38.58	29.70	36.06
N	0.16	0.13	0.22	0.53	1.12	0.83
S	0.01	0.03	0.05	0.10	0.09	0.17
Cl <sup>2</sup>	0.02	0.05	<0.01	0.46	0.55	0.24
Ash Composition (as-received)						
Si	0.024	0.04	0.05	0.94	6.71	2.29
Fe	0.014	— <sup>3</sup>	—	—	0.11	0.054
Al	0.021	0.02	0.02	0.03	0.14	0.077
Na	0.005	0.02	0.001	0.007	0.11	0.116
K	0.057	0.038	0.311	0.989	0.12	0.938
Ca	0.116	0.091	0.392	0.223	0.25	0.149
Mg	0.013	0.021	0.081	0.117	0.22	0.118
P	—	0.061	0.075	0.284	0.13	0.044

<sup>1</sup> Analytical results not available.<sup>2</sup> Not usually reported as part of an ultimate analysis.<sup>3</sup> None detected.

Continued . . .

TABLE E-1 (continued)

	Corn Stover	Wood Waste No. 1	Wood Waste No. 2	Wheat Straw No. 1	Wheat Straw No. 2	Wheat Stems
Proximate Analysis (as-received)						
Ash, wt%	4.75	6.21	6.58	5.25	3.21	4.96
Volatile Matter, wt%	75.96	67.31	67.61	71.05	67.09	66.44
Fixed Carbon, wt%	13.23	16.26	16.53	13.96	12.29	12.78
Moisture, wt%	6.06	10.22	9.28	9.74	17.41	15.82
Heating Value, Btu-lb	7782	8164	7868	7988	7905	7847
Ultimate Analysis (as-received)						
S	0.10	0.07	0.03	0.10	0.08	0.08
Cl <sup>2</sup>	0.25	0.11	0.03	0.23	0.14	0.37
Ash Composition (as-received)						
Si	1.20	1.67	1.71	1.55	0.82	1.34
Fe	— <sup>3</sup>	0.22	0.22	0.05	0.02	0.02
Al	0.05	0.34	0.37	0.06	0.01	0.01
Na	0.006	0.12	0.11	0.04	0.04	0.03
K	1.08	0.25	0.24	0.46	0.34	0.64
Ca	0.294	0.46	0.66	0.35	0.28	0.27
Mg	0.175	0.11	0.12	0.05	0.05	0.05
P	0.180	0.004	0.04	0.08	0.06	0.06

<sup>1</sup> Analytical results not available.<sup>2</sup> Not usually reported as part of an ultimate analysis.<sup>3</sup> None detected.

Continued . . .

TABLE E-1 (continued)

	Alfalfa Stems No. 1	Alfalfa Stems No. 2	Summer Switchgrass	Dakota Switchgrass	Willow	Willow Tops
Proximate Analysis (as-received)						
Ash, wt%	4.78	4.83	2.33	3.15	0.85	2.17
Volatile Matter, wt%	71.59	73.77	71.93	71.07	76.52	73.92
Fixed Carbon, wt%	14.34	13.80	12.47	13.14	12.40	16.70
Moisture, wt%	9.29	7.60	13.27	12.64	10.23	7.21
Heating Value, Btu-lb	8025	8014	7979	8014	8330	8424
Ultimate Analysis (as-received)						
C	42.79	43.23	41.21	41.45	44.07	45.86
H	5.44	5.5	5.03	5.02	5.29	5.47
O (by difference)	35.09	36.00	37.81	37.02	39.21	38.28
N	2.43	2.66	0.31	0.65	0.32	0.89
S	0.18	0.18	0.04	0.07	0.03	0.12
Cl <sup>2</sup>	0.45	0.46	<0.01	0.03	<0.01	<0.01
Ash Composition (as-received)						
Si	0.13	0.07	0.67	0.90	0.03	0.02
Fe	0.01	0.01	0.02	0.02	0.004	0.01
Al	0.001	0.001	0.02	0.01	0.01	0.02
Na	0.04	0.05	0.01	0.01	0.02	0.04
K	1.11	1.14	0.16	0.20	0.09	0.33
Ca	0.63	0.67	0.18	0.27	0.28	0.53
Mg	0.30	0.27	0.07	0.10	0.01	0.04

<sup>1</sup> Analytical results not available.<sup>2</sup> Not usually reported as part of an ultimate analysis.<sup>3</sup> None detected.

Continued . . .

TABLE E-1 (continued)

	Sandia Switchgrass	Pistachio Shells	Almond Shells	Almond Hulls	Wastepaper
Proximate Analysis (as-received)					
Ash, wt%	5.64	1.30	2.80	5.67	7.51
Volatile Matter, wt%	66.49	75.49	70.13	67.22	78.61
Fixed Carbon, wt%	13.68	15.67	19.22	18.93	8.71
Moisture, wt%	13.68	7.53	7.85	8.18	5.17
Heating Value, Btu-lb	8126	8469	8189	8069	9126
Ultimate Analysis (as-received)					
C	40.90	46.41	46.20	42.70	46.76
H	4.90	5.83	5.48	5.48	6.7
O (by difference)	33.78	38.05	36.94	36.83	33.01
N	0.48	0.63	0.68	1.06	0.66
S	0.05	0.20	0.03	0.04	0.14
Cl <sup>2</sup>	0.08	0.04	0.01	0.05	— <sup>3</sup>
Ash Composition (as-received)					
Si	1.72	0.05	0.16	0.19	0.88
Fe	0.14	0.32	0.07	0.04	0.03
Al	0.21	0.01	0.04	0.04	3.11
Na	0.04	0.04	0.05	0.04	0.07
K	0.33	0.20	0.72	2.29	0.02
Ca	0.29	0.09	0.34	0.34	0.54
Mg	0.11	0.03	0.11	0.11	0.10
P	0.07	0.07	0.12	0.12	0.01

<sup>1</sup> Analytical results not available.<sup>2</sup> Not usually reported as part of an ultimate analysis.<sup>3</sup> None detected.

## **APPENDIX F**

# **FUEL CCSEM ANALYSIS RESULTS**

TABLE F-1

## CCSEM Analysis of Illinois No. 6 Coal

Mineral Fraction:	19.442						Total	% Excluded
Size Bins:	1.0-2.2	2.2-4.6	4.6-10	10-22	22-46	46-100		
Quartz	3.7	5.3	4.3	1.6	0.3	0.1	15.3	26.2
Iron Oxide	0.0	0.0	0.1	0.0	0.2	0.9	1.1	98.5
Periclase	0.0	0.0	0.0	0.0	0.0	0.0	0.0	0.0
Rutile	0.0	0.0	0.0	0.0	0.0	0.0	0.0	49.0
Alumina	0.0	0.0	0.0	0.0	0.0	0.0	0.0	0.0
Calcite	0.1	0.4	0.4	0.5	0.9	1.3	3.5	88.0
Dolomite	0.0	0.0	0.0	0.0	0.0	0.0	0.0	0.0
Ankerite	0.1	0.0	0.0	0.0	0.0	0.0	0.1	56.0
Kaolinite	1.2	2.5	1.7	1.7	0.4	0.8	8.2	35.6
Montmorillonite	0.2	0.6	0.2	0.2	0.1	0.0	1.4	33.0
K Al-Silicate	1.6	3.0	1.9	0.9	0.1	0.1	7.5	21.0
Fe Al-Silicate	0.0	0.4	0.2	0.1	0.0	0.0	0.7	26.1
Ca Al-Silicate	0.0	0.0	0.0	0.0	0.0	0.0	0.0	0.0
Na Al-Silicate	0.0	0.0	0.1	0.0	0.0	0.0	0.1	12.3
Aluminosilicate	0.1	0.1	0.1	0.1	0.0	0.0	0.3	41.1
Mixed Al-Silica	0.1	0.6	0.2	0.1	0.1	0.0	1.2	26.9
Fe Silicate	0.0	0.0	0.0	0.0	0.0	0.0	0.0	0.0
Ca Silicate	0.0	0.0	0.0	0.0	0.0	0.0	0.0	0.0
Ca Aluminate	0.0	0.0	0.0	0.0	0.0	0.0	0.0	0.0
Pyrite	0.0	0.0	0.3	0.3	0.6	1.4	2.6	89.6
Pyrrhotite	1.3	2.5	5.7	9.6	13.0	14.2	46.3	80.1
Oxidized Pyrrhotite	0.1	0.0	0.0	0.0	0.1	0.0	0.1	24.7
Gypsum	0.1	0.1	0.1	0.1	0.1	0.1	0.6	69.7
Barite	0.0	0.0	0.0	0.0	0.0	0.0	0.0	0.0
Apatite	0.0	0.0	0.0	0.0	0.0	0.0	0.0	0.0
Ca Al-Phosphate	0.0	0.0	0.0	0.0	0.0	0.0	0.0	0.0
KCl	0.1	0.0	0.1	0.0	0.0	0.0	0.2	14.2
Gypsum-Barite	0.0	0.0	0.0	0.0	0.0	0.0	0.0	0.0
Gypsum-Al-Silicate	0.0	0.0	0.0	0.0	0.0	0.0	0.1	16.8
Si-Rich	0.9	0.6	0.5	0.2	0.1	0.0	2.4	18.0
Ca-Rich	0.0	0.0	0.0	0.1	0.0	0.0	0.1	78.0
Ca-Si-Rich	0.0	0.0	0.0	0.0	0.0	0.0	0.0	0.0
Unknown	2.3	2.5	1.5	1.0	0.6	0.3	8.2	28.2
Totals	11.9	18.4	17.2	16.6	16.7	19.2	100.0	

TABLE F-2

## CCSEM Analysis of Absaloka Coal

Mineral Fraction:	8.449						Total	% Excluded
Size Bins:	1.0-2.2	2.2-4.6	4.6-10	10-22	22-46	46-100		
Quartz	1.2	1.9	3.0	5.0	4.9	1.7	17.7	63.9
Iron Oxide	0.2	0.5	0.4	0.6	1.0	1.5	4.2	90.3
Periclase	0.0	0.0	0.0	0.0	0.0	0.0	0.0	0.0
Rutile	0.1	0.0	0.0	0.2	0.2	0.0	0.6	81.7
Alumina	0.0	0.1	0.0	0.0	0.0	0.0	0.1	89.0
Calcite	0.3	1.0	0.8	1.4	2.7	5.3	11.5	87.5
Dolomite	0.0	0.0	0.1	0.0	0.2	0.0	0.3	91.1
Ankerite	0.0	0.2	0.0	0.0	0.0	0.0	0.2	81.2
Kaolinite	3.6	8.3	9.1	6.1	3.1	0.7	30.9	37.3
Montmorillonite	0.2	0.0	0.1	0.3	0.0	0.2	0.9	43.8
K Al-Silicate	0.3	0.7	0.5	1.0	0.5	0.3	3.3	61.7
Fe Al-Silicate	0.1	0.2	0.0	0.0	0.0	0.2	0.5	77.9
Ca Al-Silicate	1.6	1.1	0.3	0.3	0.1	0.0	3.5	12.5
Na Al-Silicate	0.0	0.0	0.0	0.0	0.0	0.0	0.1	70.7
Aluminosilicate	0.0	0.2	0.1	0.0	0.0	0.0	0.3	0.0
Mixed Al-Silica	0.1	0.1	0.0	0.2	0.1	0.0	0.5	36.3
Fe Silicate	0.0	0.0	0.0	0.0	0.0	0.0	0.0	0.0
Ca Silicate	0.1	0.0	0.0	0.0	0.0	0.0	0.1	12.8
Ca Aluminate	0.0	0.0	0.0	0.0	0.0	0.0	0.0	0.0
Pyrite	0.0	0.0	0.0	0.1	0.1	0.0	0.2	100.0
Pyrrhotite	0.2	0.4	0.9	3.0	3.1	1.1	8.6	92.1
Oxidized Pyrrhotite	0.2	0.0	0.3	0.0	0.7	0.2	1.4	82.7
Gypsum	0.1	0.3	0.4	0.4	0.1	0.0	1.3	80.5
Barite	0.1	0.0	0.0	0.0	0.0	0.0	0.2	29.7
Apatite	0.1	0.1	0.1	0.4	0.0	0.0	0.7	62.8
Ca Al-Phosphate	0.3	0.6	0.2	0.2	0.0	0.0	1.3	11.0
KCl	0.0	0.0	0.0	0.0	0.0	0.0	0.0	0.0
Gypsum-Barite	0.0	0.0	0.0	0.0	0.0	0.0	0.0	0.0
Gypsum-Al-Silicate	1.0	0.2	0.0	0.1	0.1	0.0	1.5	6.3
Si-Rich	0.5	0.1	0.1	0.2	0.1	0.1	1.1	19.2
Ca-Rich	0.1	0.1	0.1	0.0	0.0	0.0	0.3	15.4
Ca-Si-Rich	0.0	0.0	0.0	0.0	0.0	0.0	0.0	0.0
Unknown	3.5	2.9	0.7	1.0	0.6	0.0	8.7	23.3
Totals	14.0	19.3	17.3	20.4	17.7	11.3	100.0	

TABLE F-3

## CCSEM Analysis of Wheat Straw

Mineral Fraction:	0.855						Total	% Excluded
Size Bins:	1.0-2.2	2.2-4.6	4.6-10	10-22	22-46	46-100		
Quartz	1.0	3.9	8.6	9.6	2.5	0.5	26.1	20.4
Iron Oxide	0.1	0.6	0.7	0.0	0.1	0.0	1.5	22.3
Periclase	0.0	0.0	0.0	0.0	0.0	0.0	0.0	0.0
Rutile	0.0	0.0	0.0	0.0	0.0	0.0	0.0	0.0
Alumina	0.0	0.0	0.0	0.0	0.0	0.0	0.0	0.0
Calcite	1.6	2.7	0.2	0.0	0.0	0.0	4.5	25.1
Dolomite	0.0	0.0	0.0	0.0	0.1	0.0	0.1	39.7
Ankerite	0.0	0.0	0.0	0.0	0.0	0.0	0.0	0.0
Kaolinite	0.0	0.0	0.0	0.0	0.0	0.0	0.0	0.0
Montmorillonite	0.0	0.0	0.0	0.0	0.0	0.0	0.0	0.0
K Al-Silicate	0.0	0.0	0.0	0.0	0.0	0.0	0.0	0.0
Fe Al-Silicate	0.0	0.0	0.0	0.0	0.0	0.0	0.0	0.0
Ca Al-Silicate	0.0	0.0	0.0	0.0	0.0	0.0	0.0	0.0
Na Al-Silicate	0.0	0.0	0.0	0.0	0.0	0.0	0.0	0.0
Aluminosilicate	0.0	0.0	0.0	0.0	0.0	0.0	0.0	0.0
Mixed Al-Silica	0.0	0.0	0.0	0.0	0.0	0.0	0.0	0.0
Fe Silicate	0.0	0.0	0.0	0.0	0.1	0.0	0.1	0.0
Ca Silicate	0.0	0.0	0.3	0.0	0.0	0.0	0.3	26.2
Ca Aluminate	0.0	0.0	0.0	0.0	0.0	0.0	0.0	0.0
Pyrite	0.0	0.0	0.0	0.0	0.0	0.0	0.0	0.0
Pyrrhotite	0.0	0.0	0.0	0.0	0.0	0.0	0.0	0.0
Oxidized Pyrrhotite	0.0	0.0	0.0	0.0	0.1	0.0	0.1	100.0
Gypsum	0.0	0.0	0.0	0.0	0.0	0.0	0.0	0.0
Barite	0.0	0.0	0.0	0.0	0.0	0.0	0.0	0.0
Apatite	0.0	0.0	0.0	0.0	0.0	0.0	0.0	0.0
Ca Al-Phosphate	0.0	0.0	0.0	0.0	0.0	0.0	0.0	0.0
KCl	0.0	0.0	0.0	0.0	0.0	0.0	0.0	0.0
Gypsum-Barite	0.0	0.0	0.0	0.0	0.0	0.0	0.0	0.0
Gypsum-Al-Silicate	0.0	0.0	0.0	0.0	0.0	0.0	0.0	0.0
Si-Rich	0.6	2.5	3.3	3.1	1.9	0.0	11.4	17.2
Ca-Rich	0.0	0.0	0.1	0.0	0.1	0.0	0.2	67.4
Ca-Si-Rich	0.1	0.1	0.2	0.0	0.0	0.0	0.3	0.0
Unknown	5.4	9.9	21.7	11.5	5.7	1.1	55.3	21.0
Totals	8.8	19.8	35.0	24.1	10.6	1.7	100.0	0.0

TABLE F-4

## CCSEM Analysis of Alfalfa Stems

Mineral Fraction:	2.412						Total	% Excluded
Size Bins:	1.0-2.2	2.2-4.6	4.6-10	10-22	22-46	46-100		
Quartz	2.5	3.0	6.4	16.1	2.0	4.3	34.3	79.4
Iron Oxide	0.0	0.1	0.2	0.0	0.0	0.0	0.3	35.1
Periclase	0.0	0.0	0.0	0.0	0.0	0.0	0.0	0.0
Rutile	0.0	0.0	0.0	0.0	0.0	0.0	0.0	0.0
Alumina	0.0	0.0	0.0	0.0	0.0	0.0	0.0	0.0
Calcite	0.4	2.7	10.1	23.9	0.6	0.0	37.7	4.3
Dolomite	0.0	0.0	0.0	0.2	0.1	0.0	0.3	0.0
Ankerite	0.0	0.0	0.0	0.0	0.0	0.0	0.0	0.0
Kaolinite	0.0	0.0	0.0	0.0	0.0	0.0	0.0	0.0
Montmorillonite	0.0	0.0	0.0	0.0	0.0	0.0	0.0	0.0
K Al-Silicate	0.0	0.1	0.2	0.2	0.0	0.0	0.5	14.0
Fe Al-Silicate	0.0	0.0	0.0	0.0	0.0	0.0	0.0	0.0
Ca Al-Silicate	0.0	0.0	0.0	0.0	0.0	0.0	0.0	0.0
Na Al-Silicate	0.0	0.0	0.0	0.1	0.0	0.0	0.1	0.0
Aluminosilicate	0.0	0.0	0.0	0.0	0.0	0.0	0.0	0.0
Mixed Al-Silica	0.0	0.0	0.0	0.0	0.0	0.0	0.0	0.0
Fe Silicate	0.0	0.0	0.0	0.0	0.0	0.0	0.0	0.0
Ca Silicate	0.0	0.1	0.0	0.0	0.0	0.0	0.1	26.6
Ca Aluminate	0.0	0.0	0.0	0.0	0.0	0.0	0.0	0.0
Pyrite	0.0	0.0	0.0	0.0	0.0	0.0	0.0	0.0
Pyrrhotite	0.0	0.0	0.0	0.0	0.0	0.0	0.0	0.0
Oxidized Pyrrhotite	0.0	0.0	0.0	0.0	0.0	0.0	0.0	0.0
Gypsum	0.0	0.0	0.0	0.0	0.0	0.0	0.0	0.0
Barite	0.0	0.0	0.0	0.0	0.0	0.0	0.0	0.0
Apatite	0.0	0.0	0.1	0.1	0.0	0.0	0.2	0.0
Ca Al-Phosphate	0.0	0.0	0.0	0.0	0.0	0.0	0.0	0.0
KCl	0.0	0.0	0.0	0.0	0.0	0.0	0.0	0.0
Gypsum-Barite	0.0	0.0	0.0	0.0	0.0	0.0	0.0	0.0
Gypsum-Al-Silicate	0.0	0.0	0.0	0.0	0.0	0.0	0.0	0.0
Si-Rich	0.6	0.9	1.6	1.2	0.6	0.3	5.1	70.5
Ca-Rich	0.6	1.0	0.8	0.1	0.0	0.0	2.5	2.7
Ca-Si-Rich	0.0	0.0	0.0	0.1	0.0	0.0	0.1	19.7
Unknown	3.4	4.2	4.6	4.3	1.3	0.8	18.6	18.6
Totals	7.6	12.1	23.9	46.2	4.8	5.5	100.0	

TABLE F-5

## CCSEM Analysis of Hybrid Poplar

Mineral Fraction:	2.299						Total	% Excluded
Size Bins:	1.0-2.2	2.2-4.6	4.6-10	10-22	22-46	46-100		
Quartz	0.1	0.2	0.4	0.4	0.2	0.6	1.9	13.9
Iron Oxide	0.9	3.9	2.8	1.4	0.1	0.0	9.1	11.5
Periclase	0.0	0.0	0.0	0.0	0.0	0.0	0.0	0.0
Rutile	0.0	0.0	0.0	0.1	0.0	0.0	0.1	0.0
Alumina	0.0	0.0	0.1	0.0	0.0	0.0	0.1	0.0
Calcite	2.7	6.6	10.7	38.0	8.7	2.0	68.6	9.4
Dolomite	0.2	0.1	0.2	0.0	0.2	0.0	0.7	0.0
Ankerite	0.0	0.0	0.0	0.0	0.0	0.0	0.0	0.0
Kaolinite	0.0	0.0	0.0	0.3	0.0	0.5	0.9	2.9
Montmorillonite	0.0	0.0	0.0	0.2	0.0	0.0	0.2	0.0
K Al-Silicate	0.0	0.1	0.2	0.2	0.0	0.0	0.6	3.4
Fe Al-Silicate	0.0	0.0	0.2	0.2	0.0	0.0	0.4	15.6
Ca Al-Silicate	0.0	0.1	0.1	0.1	0.0	0.0	0.3	4.2
Na Al-Silicate	0.0	0.0	0.0	0.0	0.0	0.0	0.1	0.0
Aluminosilicate	0.0	0.0	0.0	0.0	0.0	0.0	0.0	0.0
Mixed Al-Silica	0.0	0.0	0.0	0.2	0.0	0.0	0.2	0.0
Fe Silicate	0.1	0.8	0.7	0.1	0.0	0.0	1.6	5.8
Ca Silicate	0.0	0.0	0.0	0.0	0.0	0.0	0.0	33.5
Ca Aluminate	0.0	0.0	0.0	0.0	0.0	0.0	0.0	0.0
Pyrite	0.0	0.0	0.1	0.0	0.0	0.0	0.1	0.0
Pyrrhotite	0.0	0.3	0.4	0.0	0.0	0.0	0.7	25.5
Oxidized Pyrrhotite	0.2	0.5	1.0	0.3	0.0	0.0	2.0	0.0
Gypsum	0.0	0.1	0.2	0.1	0.0	0.0	0.3	0.0
Barite	0.0	0.0	0.0	0.0	0.0	0.0	0.0	0.0
Apatite	0.3	0.4	0.2	0.1	0.0	0.2	1.1	8.7
Ca Al-Phosphate	0.0	0.0	0.0	0.0	0.0	0.0	0.0	0.0
KCl	0.0	0.0	0.0	0.0	0.0	0.0	0.0	0.0
Gypsum-Barite	0.0	0.0	0.0	0.0	0.0	0.0	0.0	0.0
Gypsum-Al-Silicate	0.0	0.1	0.0	0.0	0.0	0.0	0.1	0.0
Si-Rich	0.0	0.0	0.3	0.0	0.1	0.0	0.4	14.3
Ca-Rich	0.3	0.3	0.1	0.2	0.1	0.1	1.2	3.7
Ca-Si-Rich	0.0	0.0	0.0	0.0	0.0	0.0	0.0	0.0
Unknown	2.0	2.8	1.8	1.3	0.8	0.5	9.3	11.1
Totals	6.9	16.3	19.5	43.0	10.4	3.9	100.0	

## **APPENDIX G**

# **CLUSTER ANALYSIS OF BIOMASS FUEL CCSEM DATA**

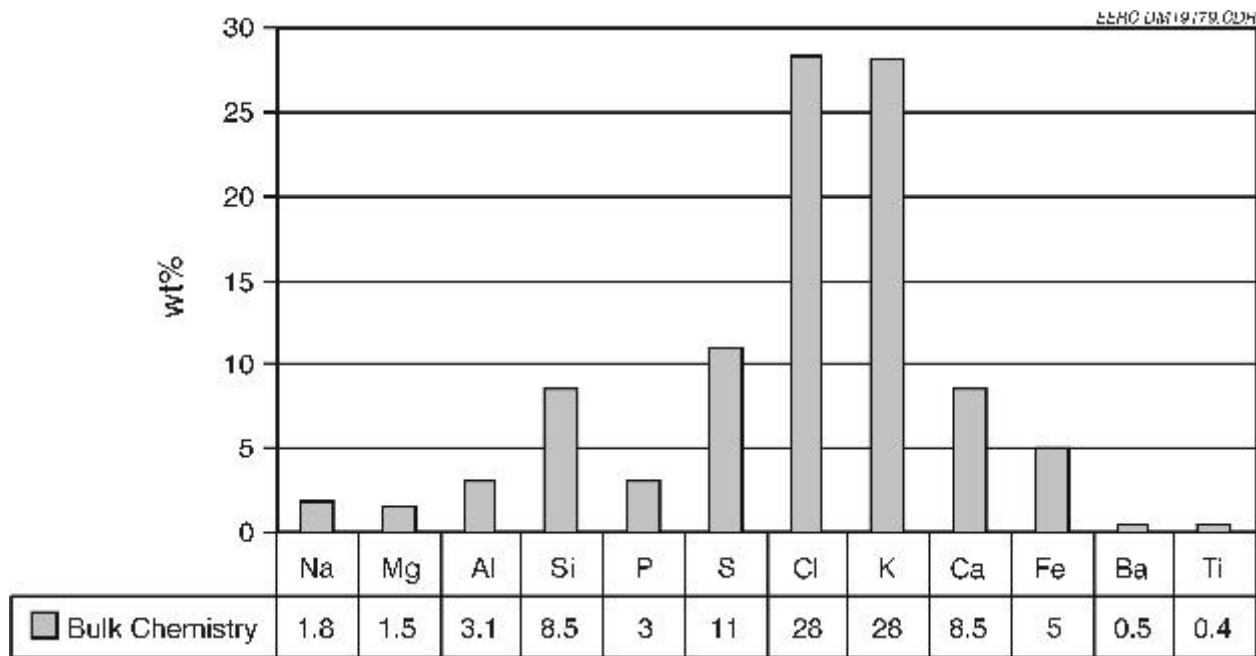


Figure G-1. Bulk chemistry of alfalfa stem baghouse ash.

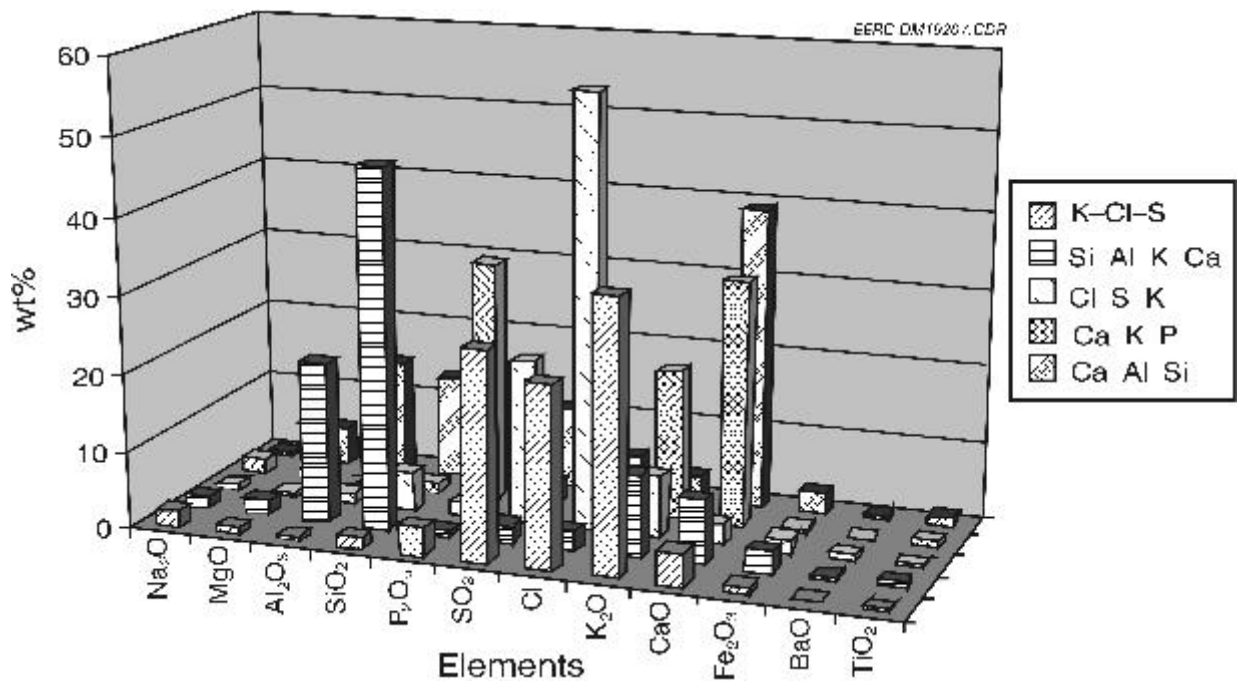


Figure G-2. The five most significant clusters from alfalfa stem baghouse ash.

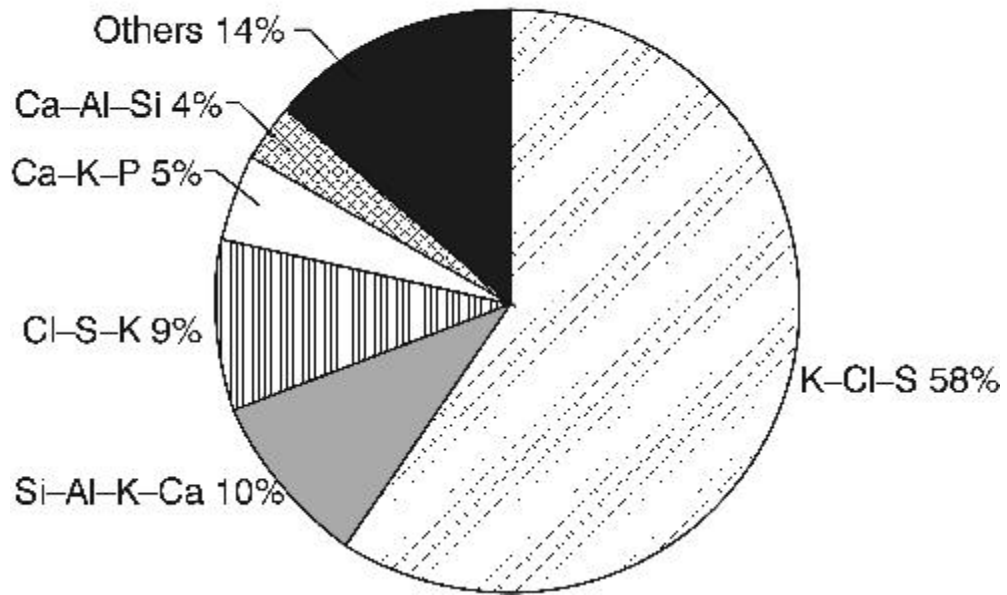


Figure G-3. Frequency distribution for alfalfa stem baghouse ash.

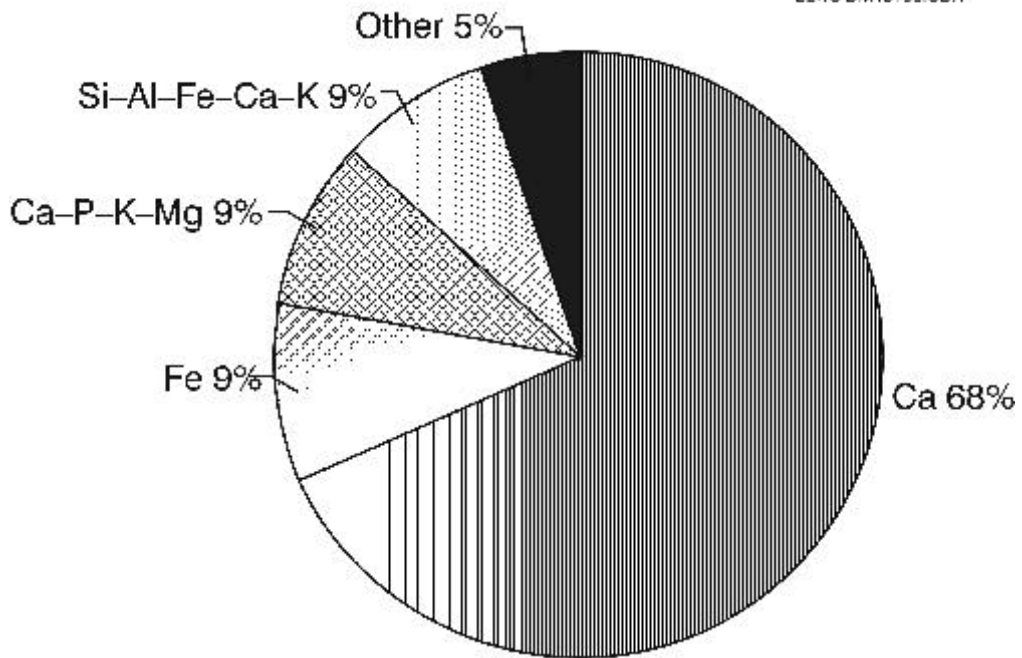


Figure G-4. Particle-size distribution for alfalfa stem baghouse ash.

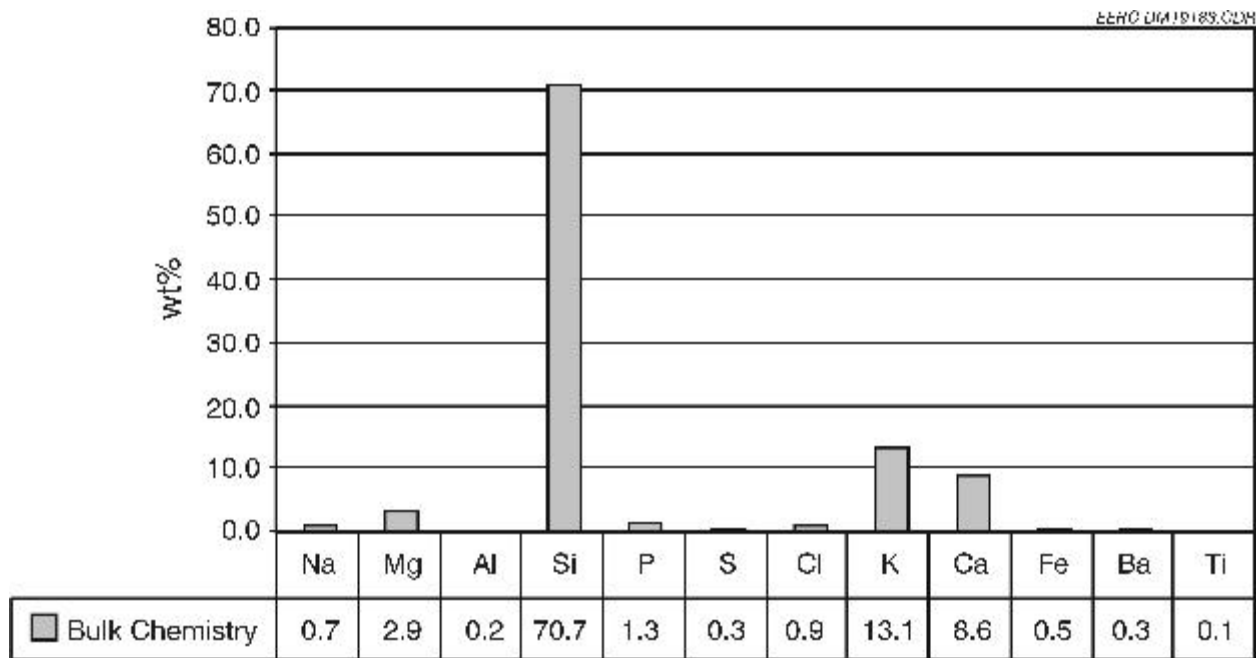


Figure G-5. Bulk chemistry of wheat straw filter ash.

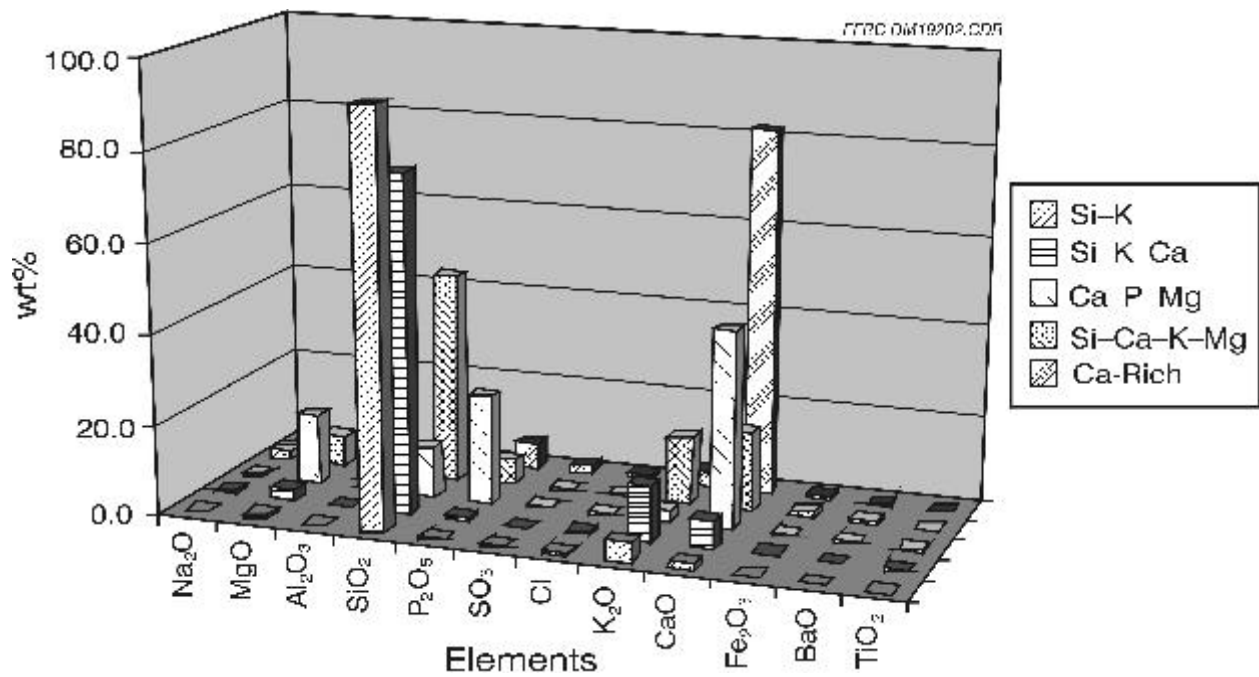


Figure G-6. The five most significant clusters from wheat straw filter ash.

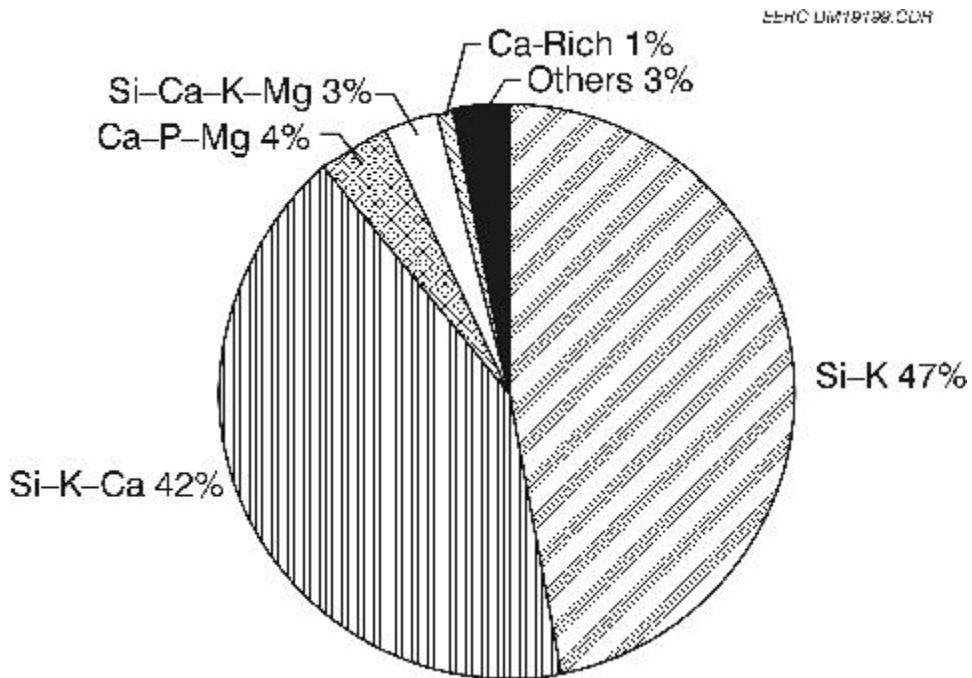


Figure G-7. Frequency distribution of chemical groups, based on cluster analysis.

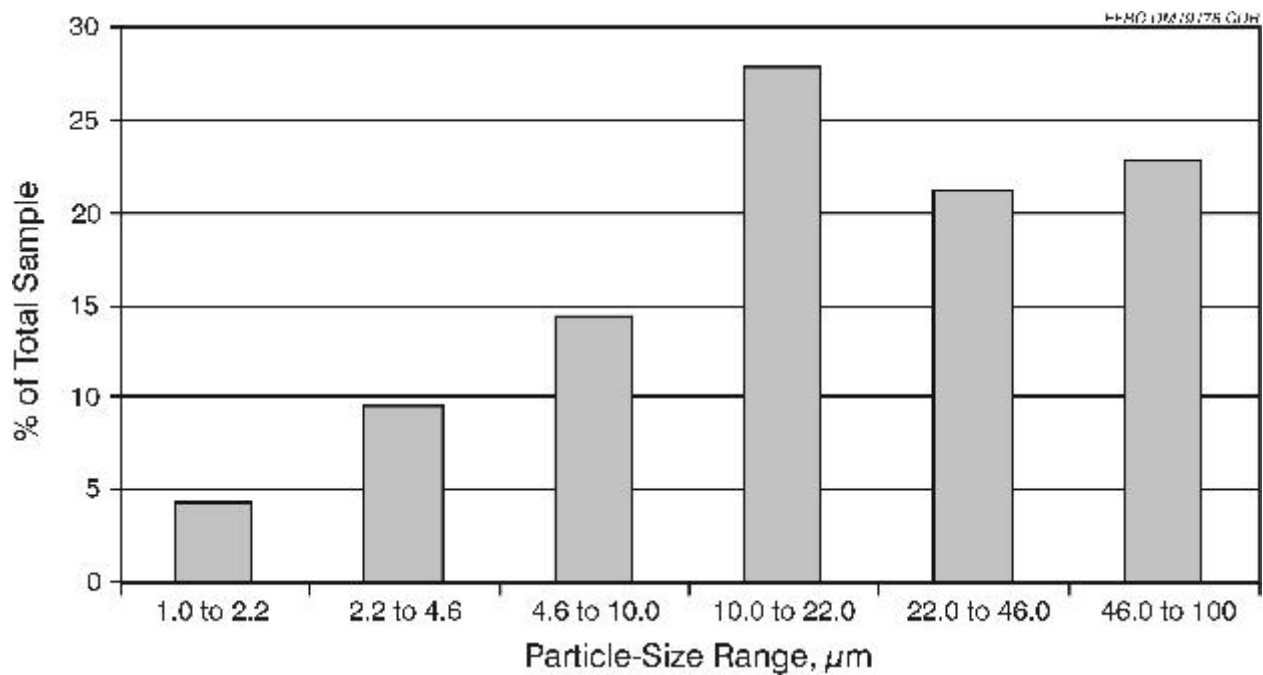


Figure G-8. Particle-size distribution for wheat straw filter ash.

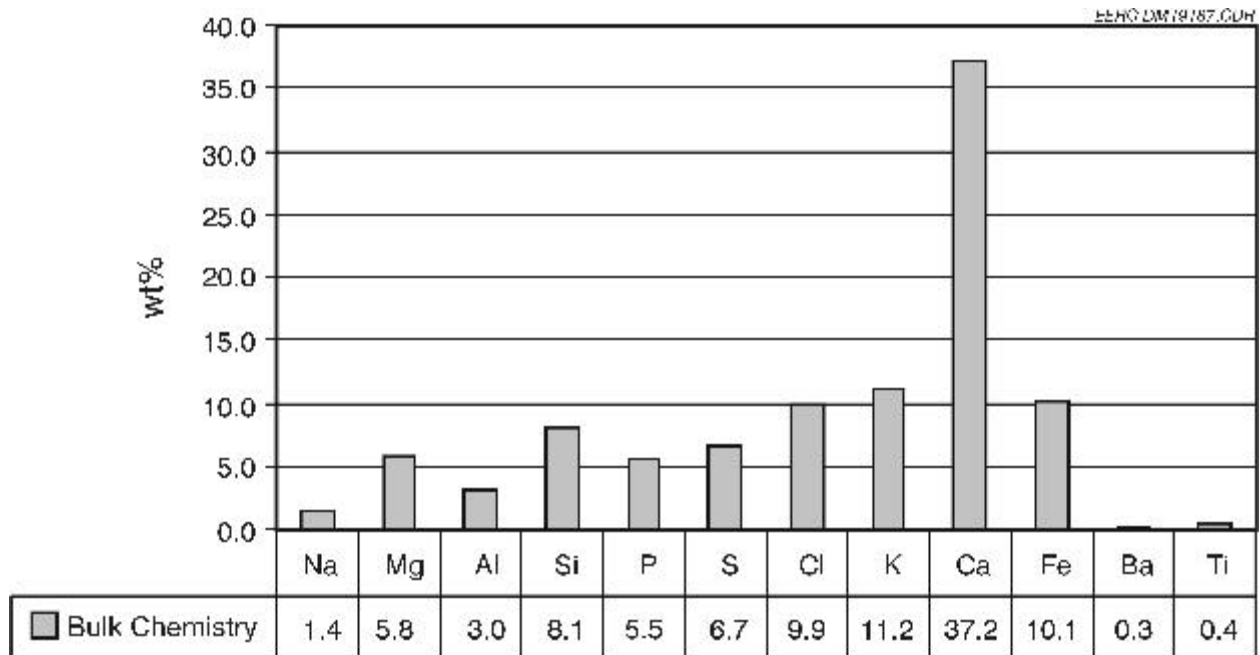


Figure G-9. Bulk chemistry of hybrid poplar ash.

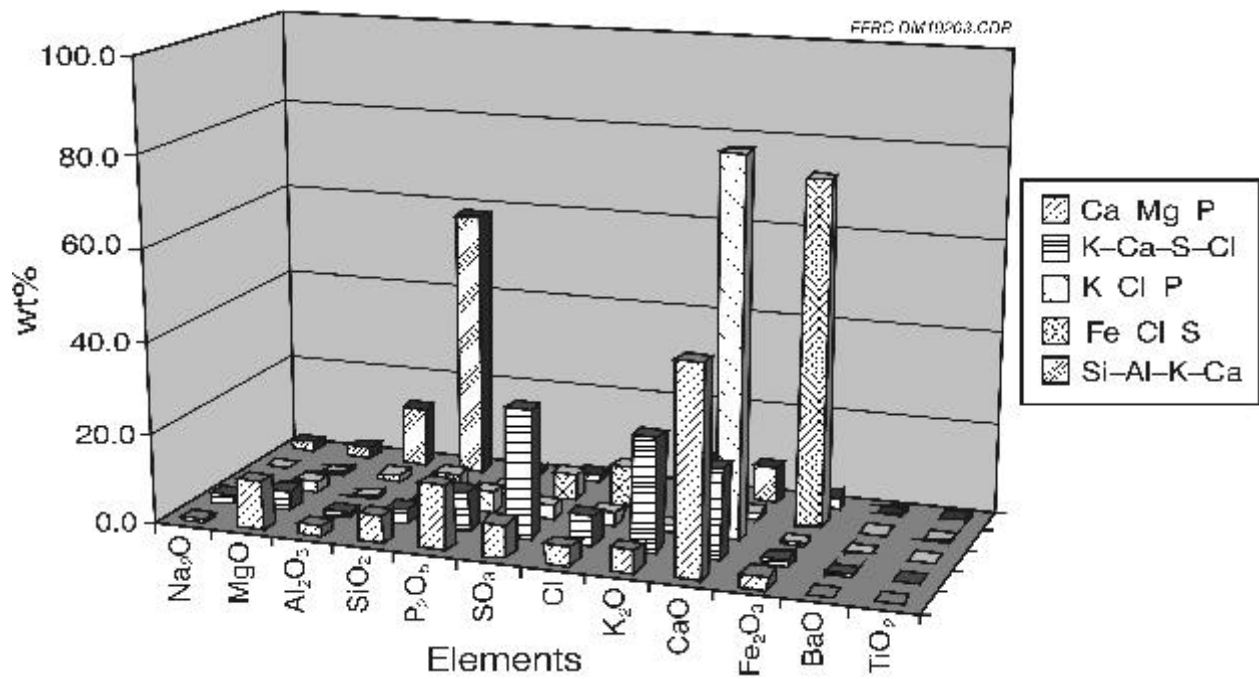


Figure G-10. The five most significant clusters from hybrid poplar ash.

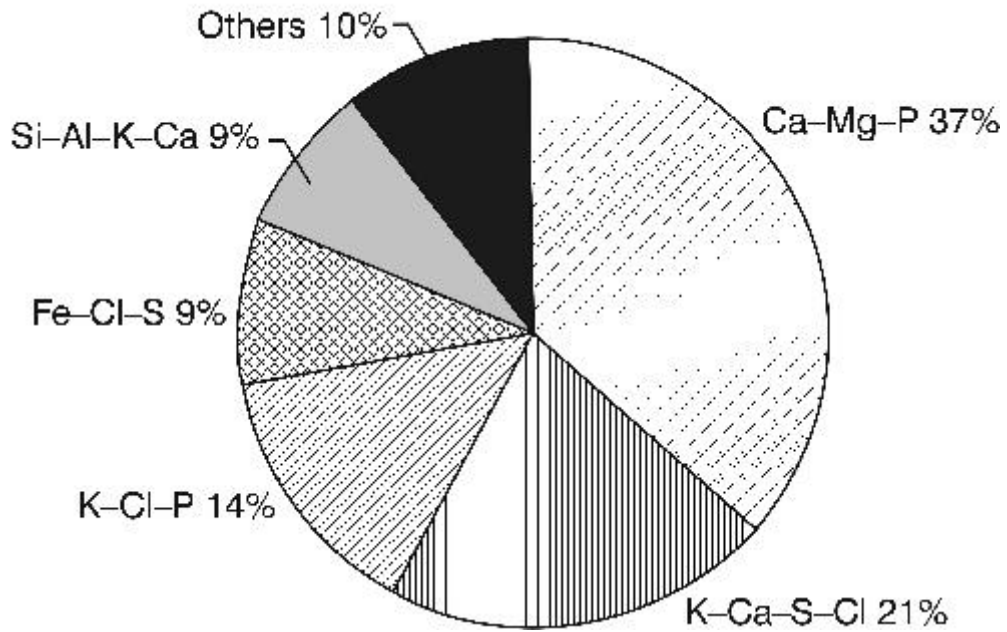


Figure G-11. Frequency distribution of chemical groups, based on cluster analysis.

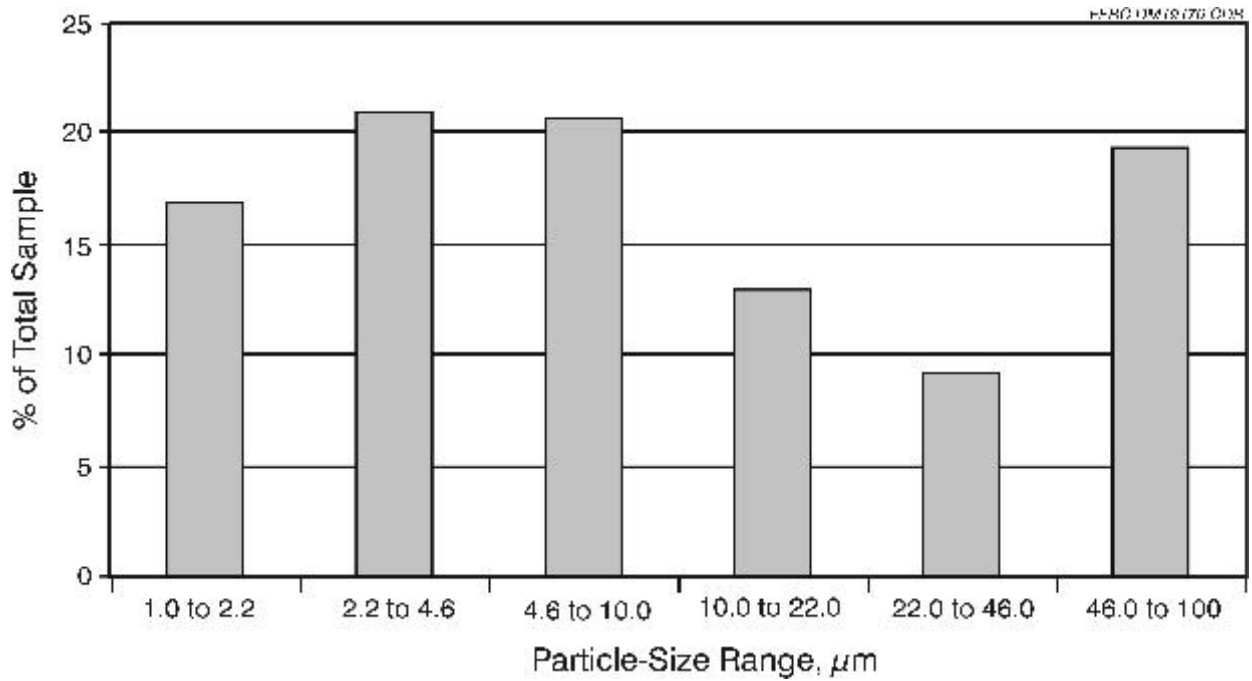


Figure G-12. Particle-size distribution for hybrid poplar ash.

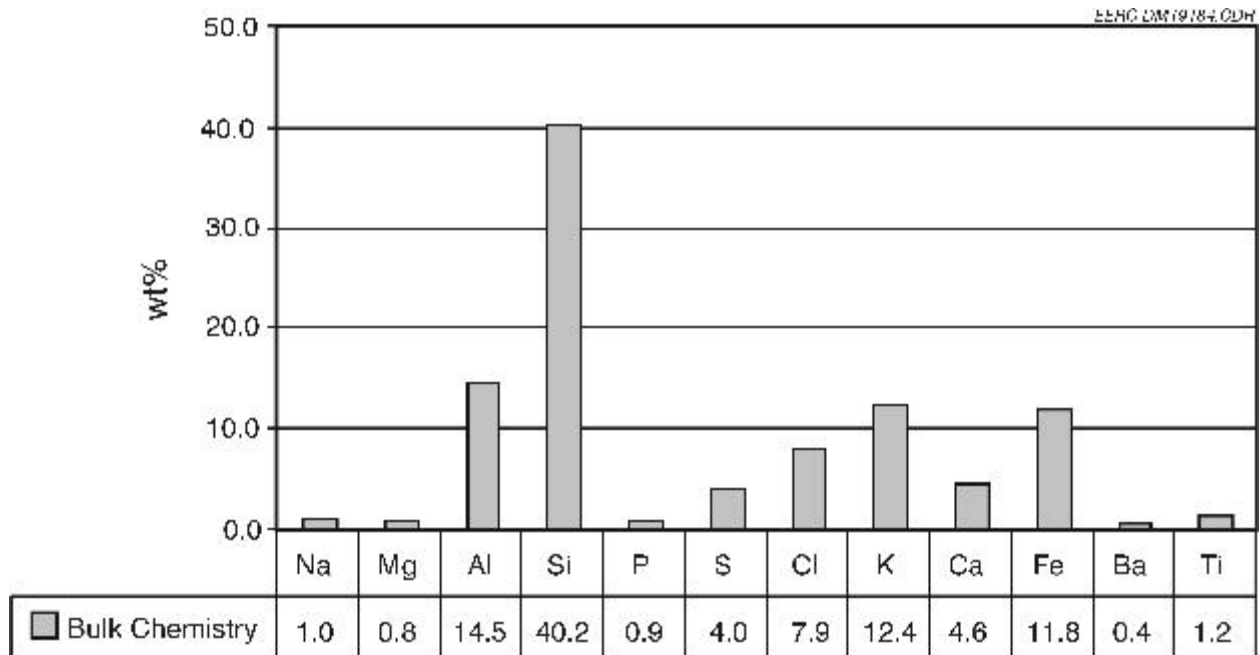


Figure G-13. Bulk chemistry of Illinois No. 6 and alfalfa stem blend ash.

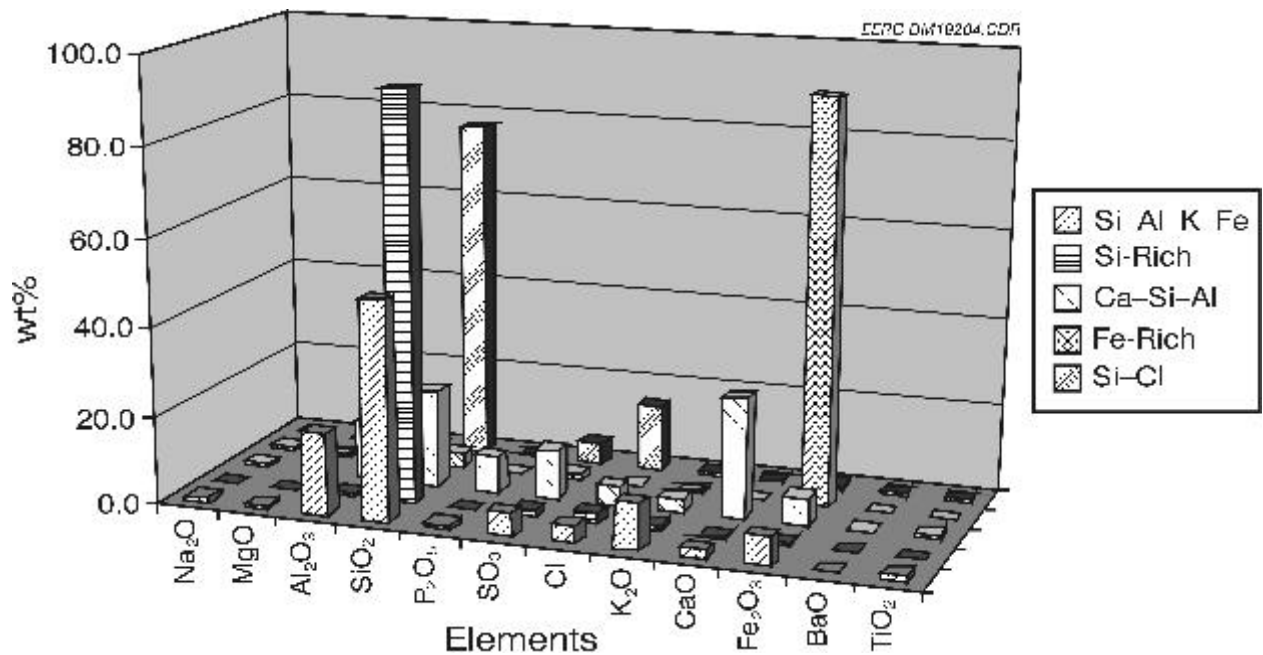


Figure G-14. The five most significant clusters from Illinois No. 6 and alfalfa stem blend ash.

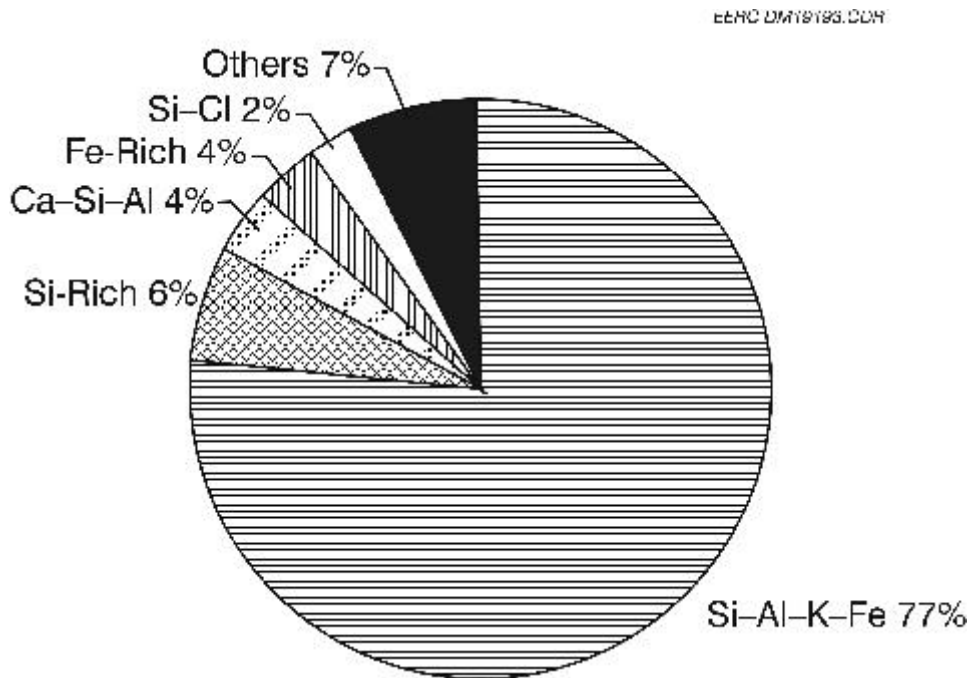


Figure G-15. Frequency distribution of chemical groups, based on cluster analysis.

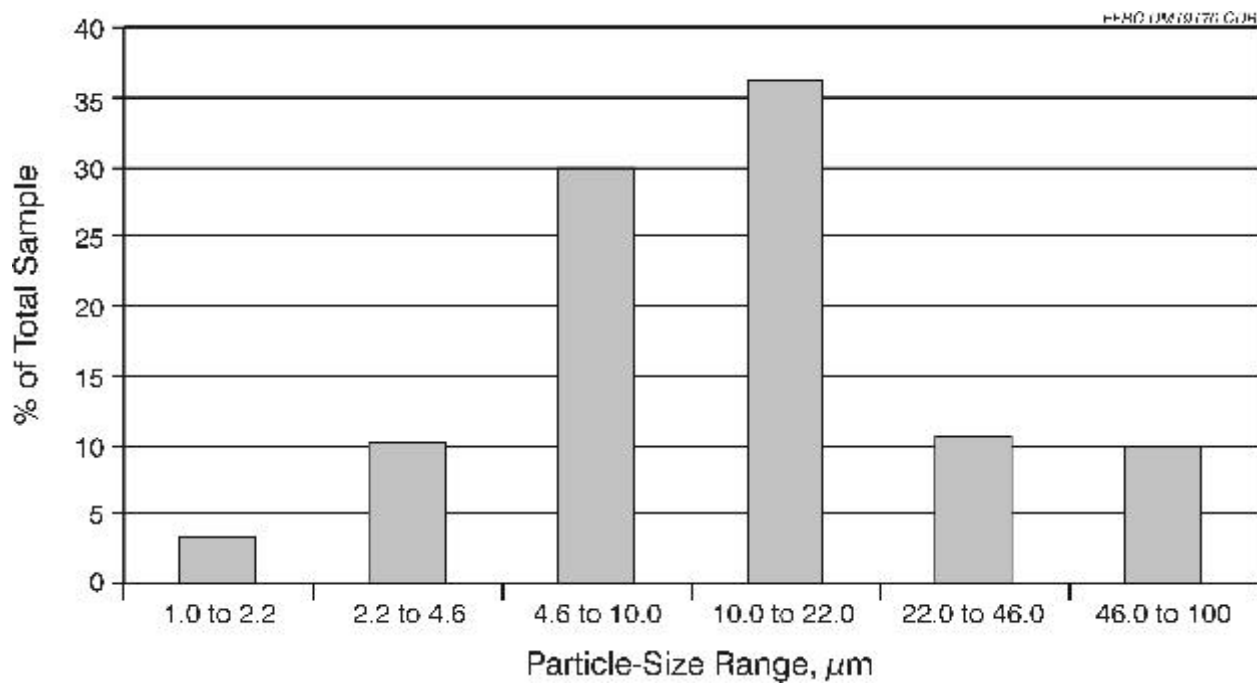


Figure G-16. Particle-size distribution for Illinois No. 6 and alfalfa stem blend ash.

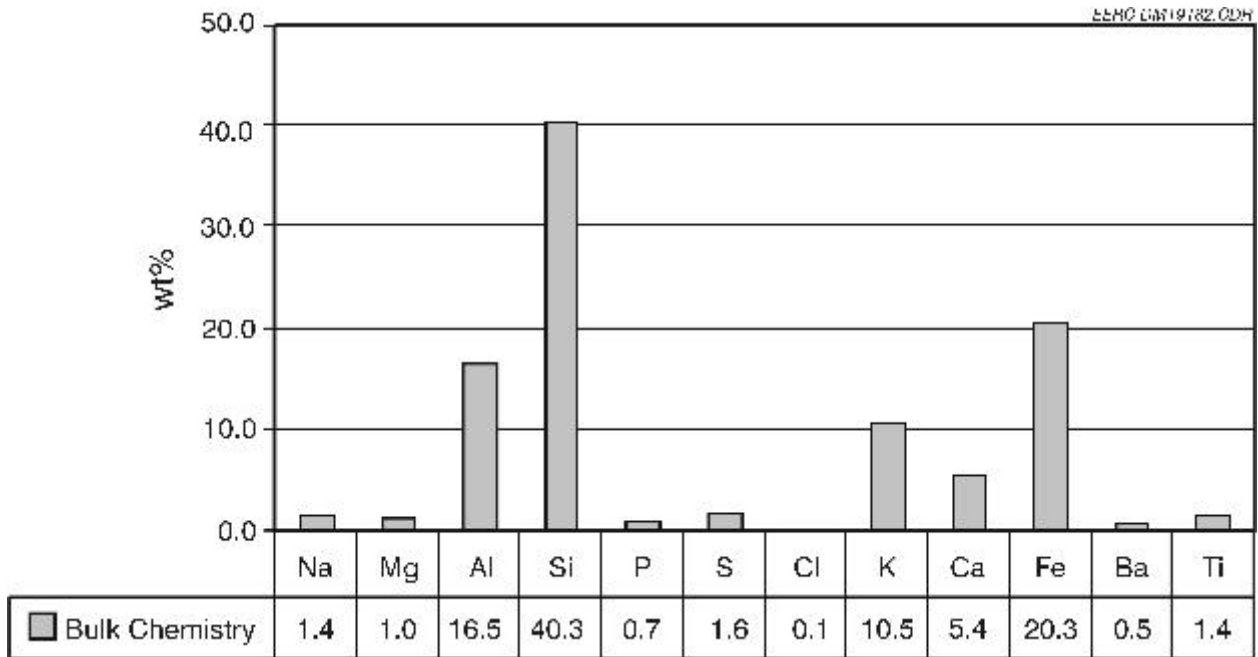


Figure G-17. Bulk chemistry of Illinois No. 6 and wheat straw blend ash.

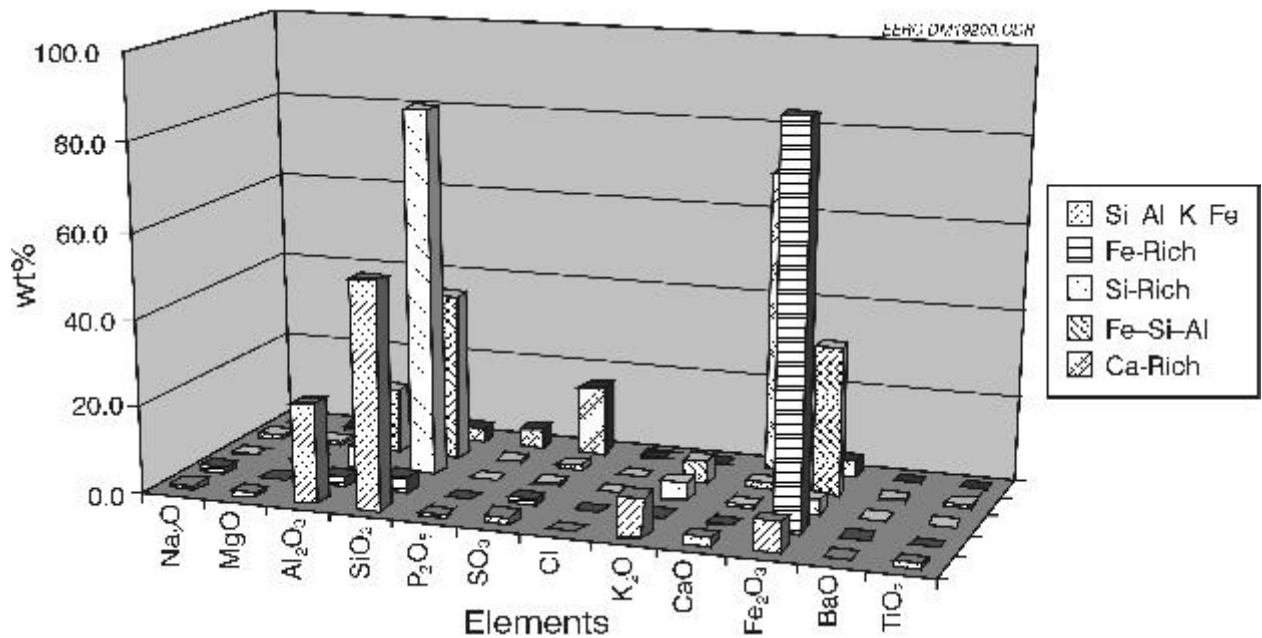


Figure G-18. The five most significant clusters from Illinois No. 6 and wheat straw blend ash.

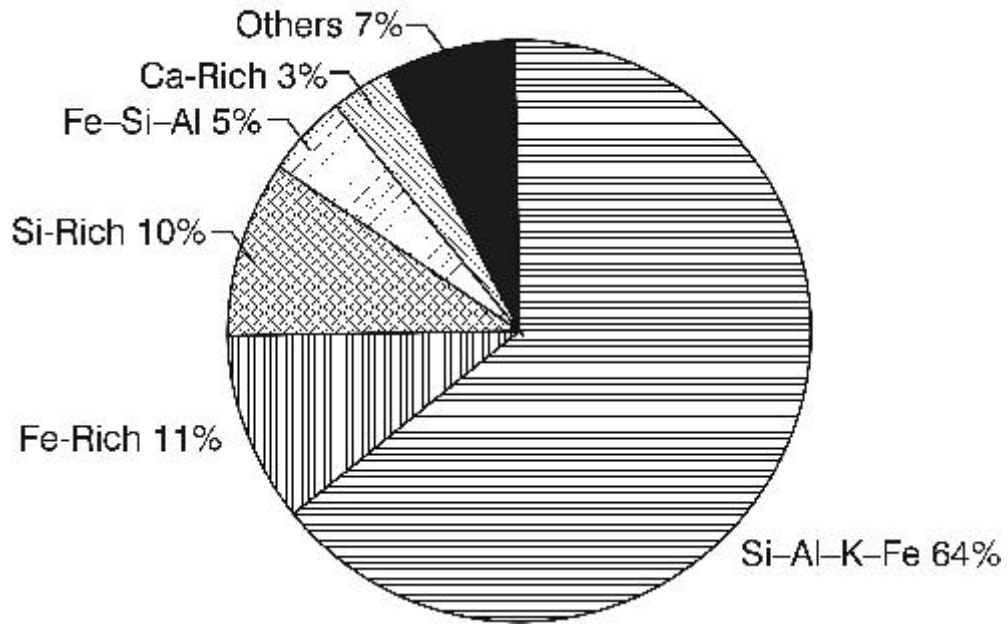


Figure G-19. Frequency distribution of chemical groups, based on cluster analysis.

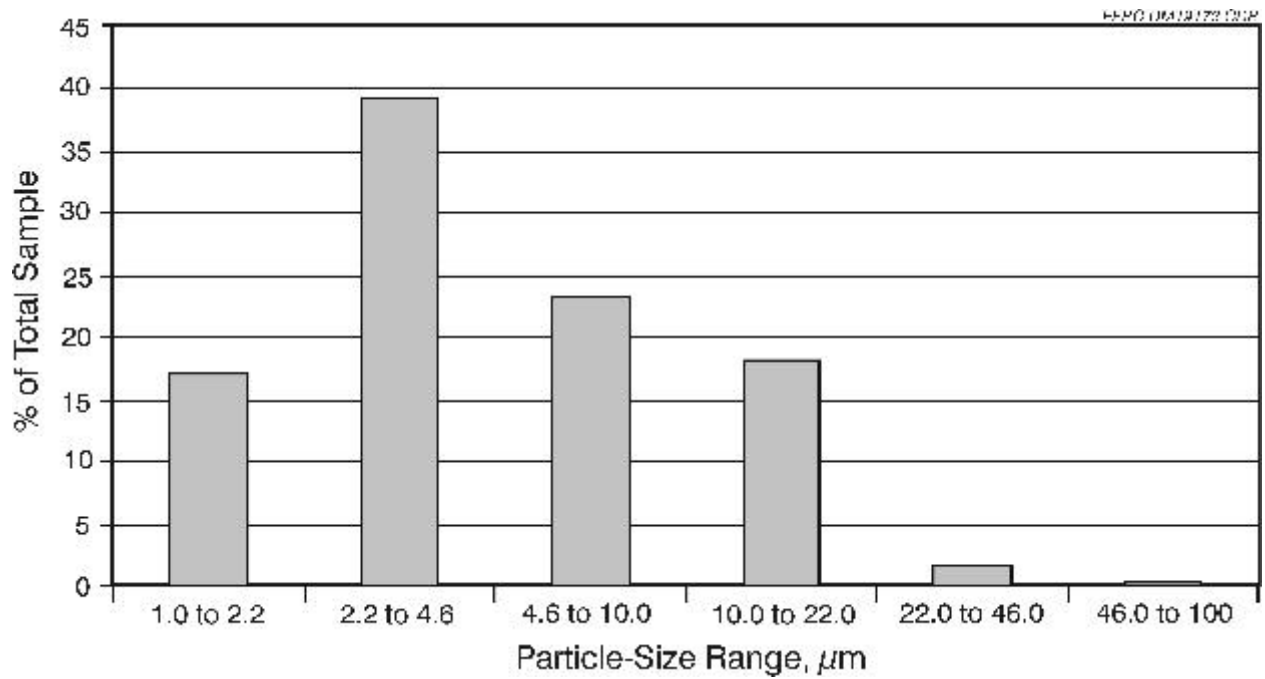


Figure G-20. Particle-size distribution for Illinois No. 6 and wheat straw blend ash.

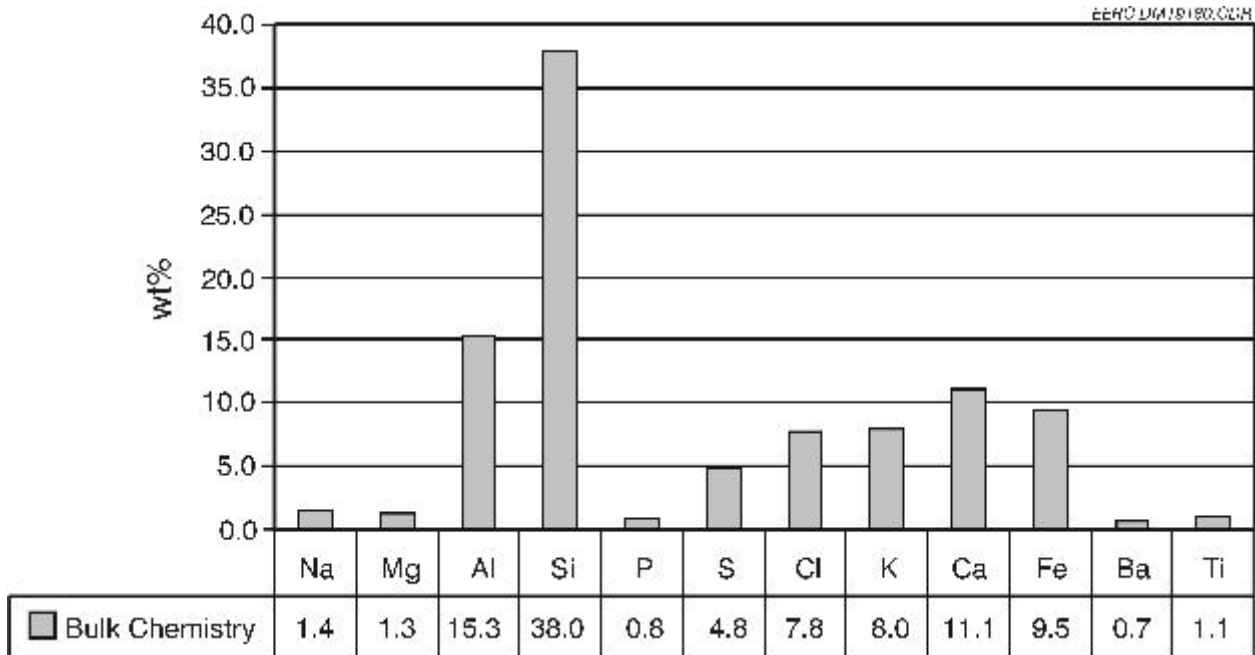


Figure G-21. Bulk chemistry of Illinois No. 6 and hybrid poplar blend ash.

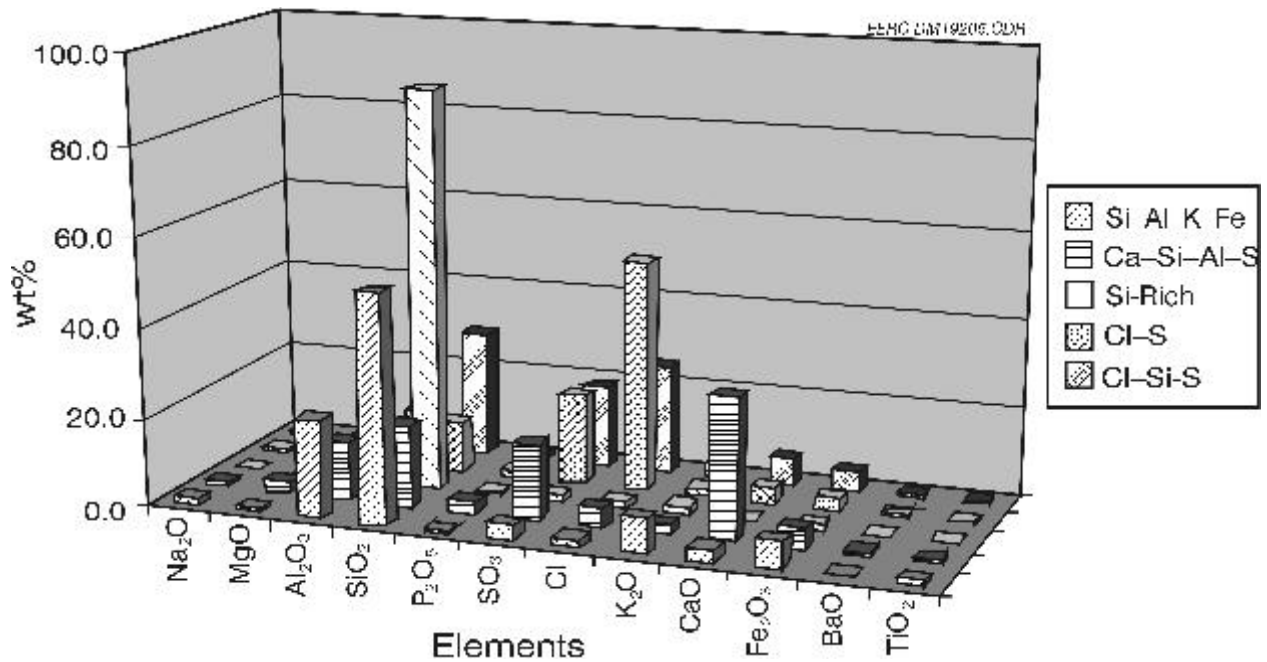


Figure G-22. The five most significant clusters from Illinois No. 6 and hybrid poplar blend ash.

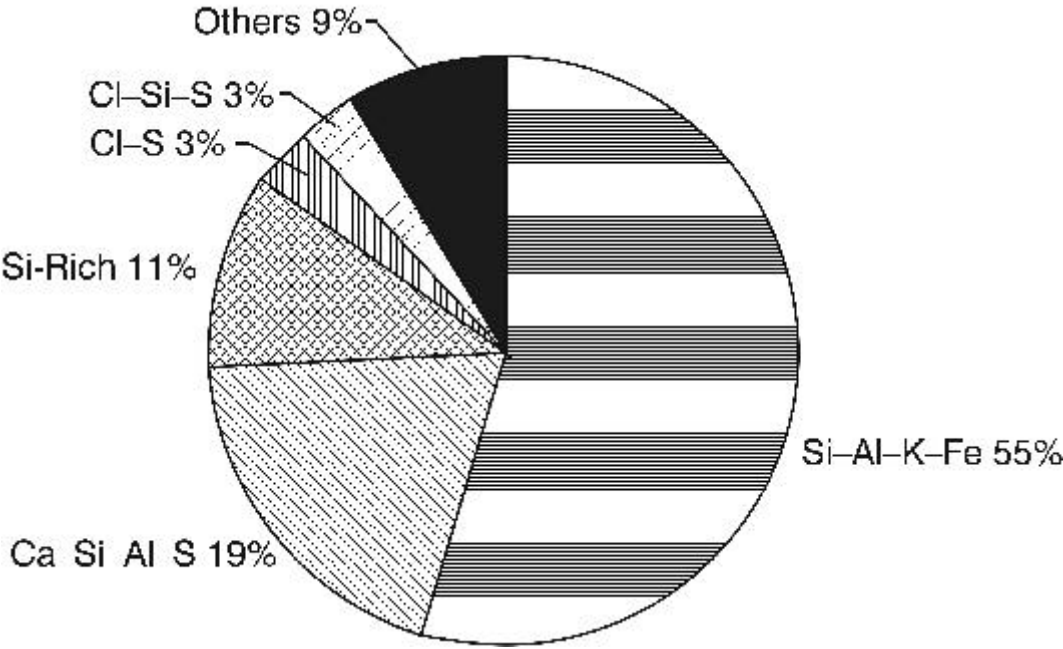


Figure G-23. Frequency distribution of chemical groups, based on cluster analysis.

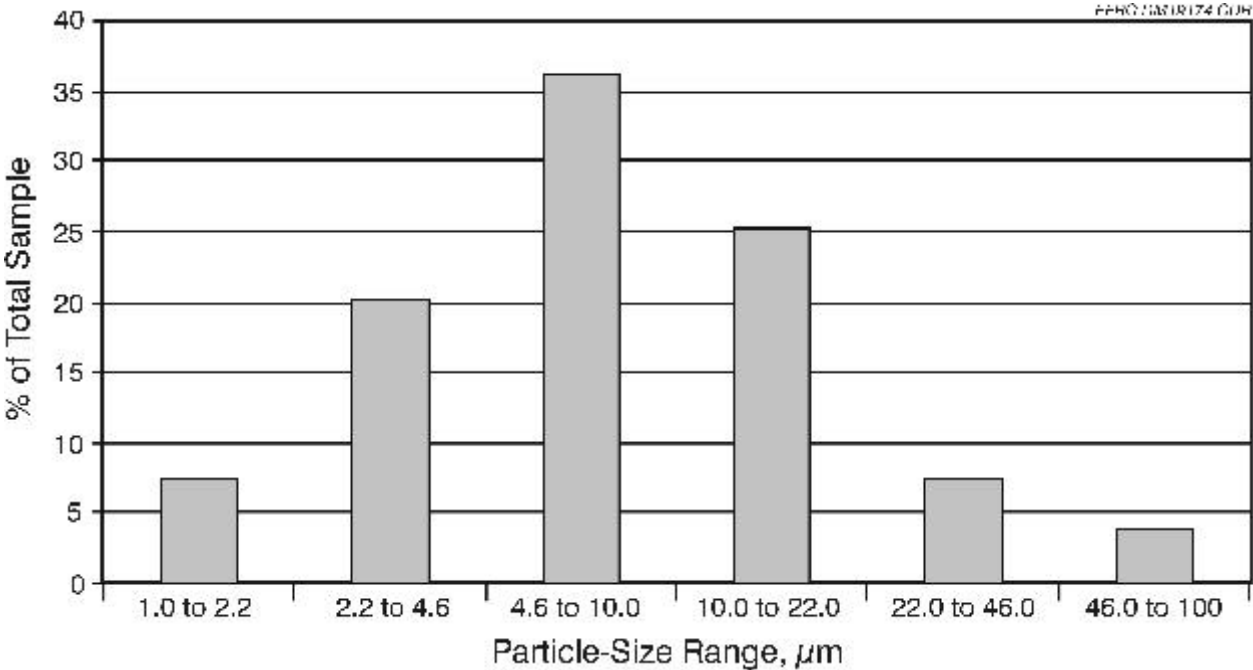


Figure G-24. Particle-size distribution for Illinois No. 6 and hybrid poplar blend ash.

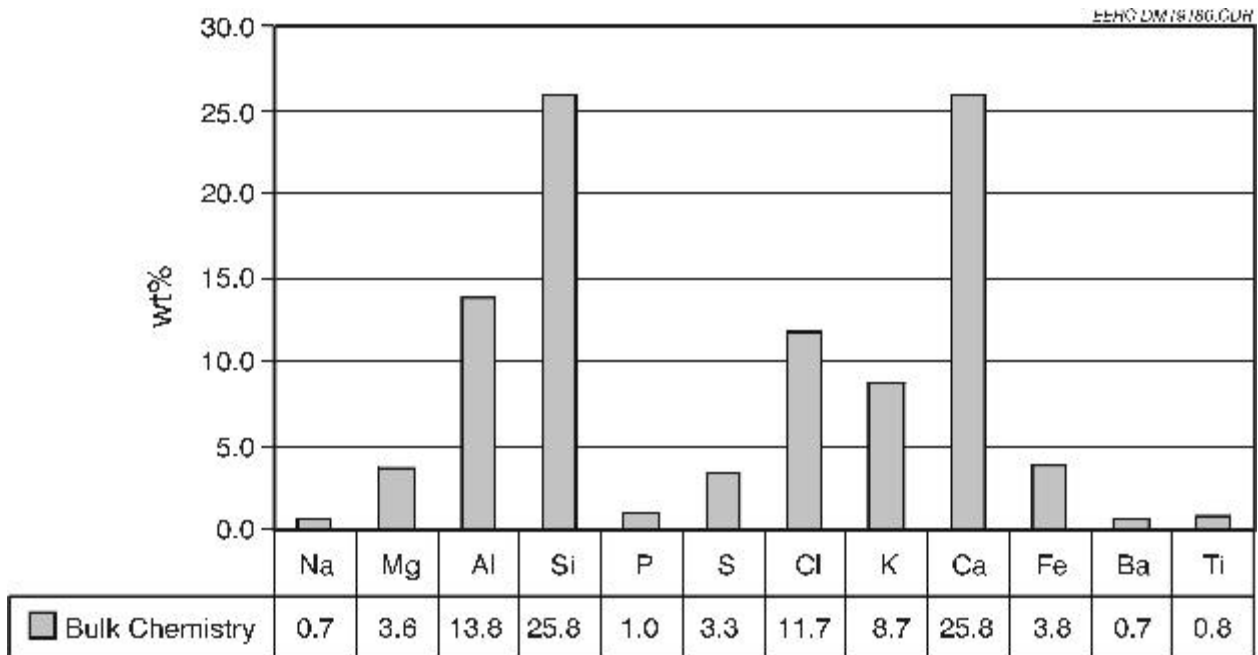


Figure G-25. Bulk chemistry of Absaloka and alfalfa stem blend ash.

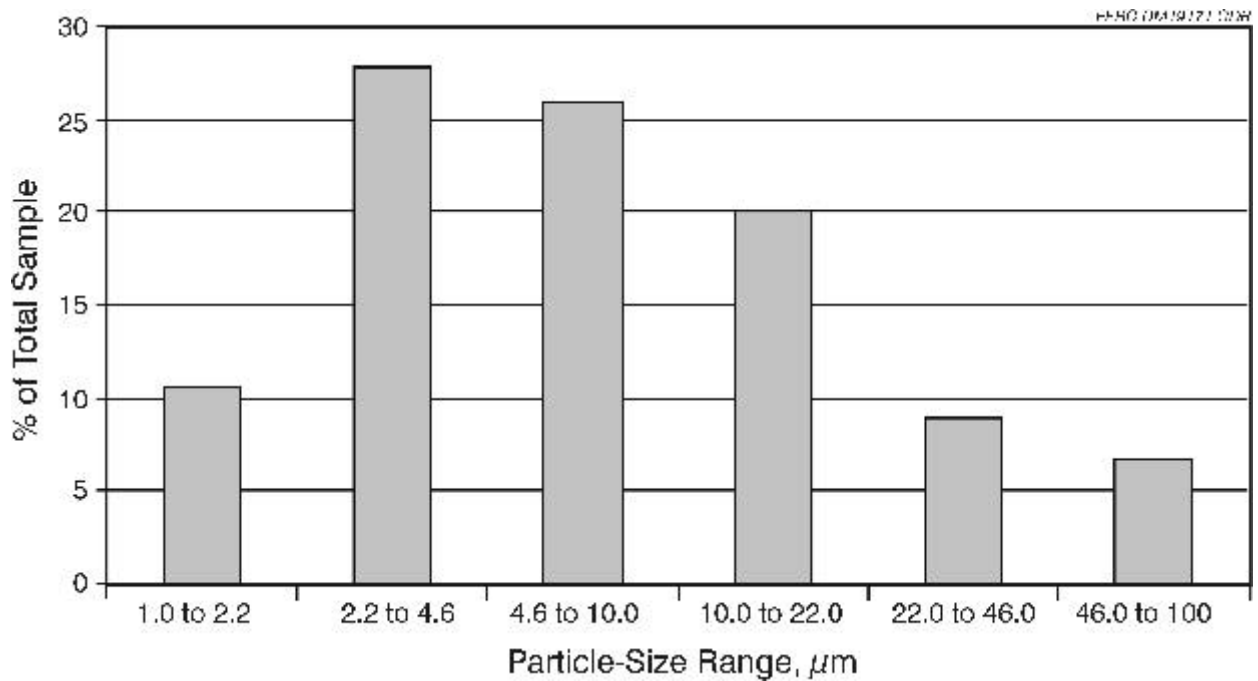


Figure G-26. The five most significant clusters from Absaloka and alfalfa stem blend ash.

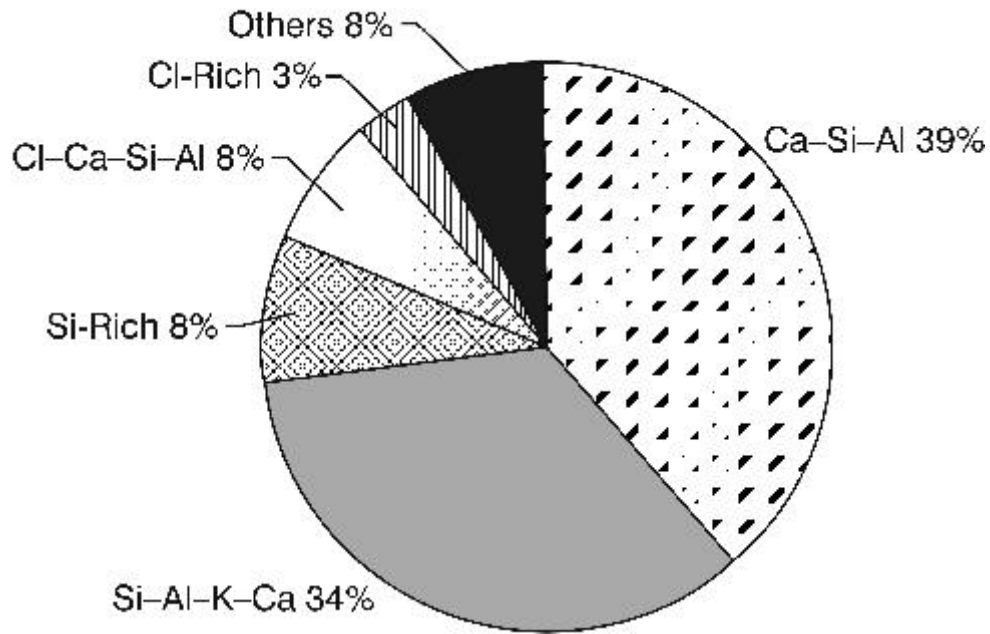


Figure G-27. Frequency distribution of chemical groups, based on cluster analysis.

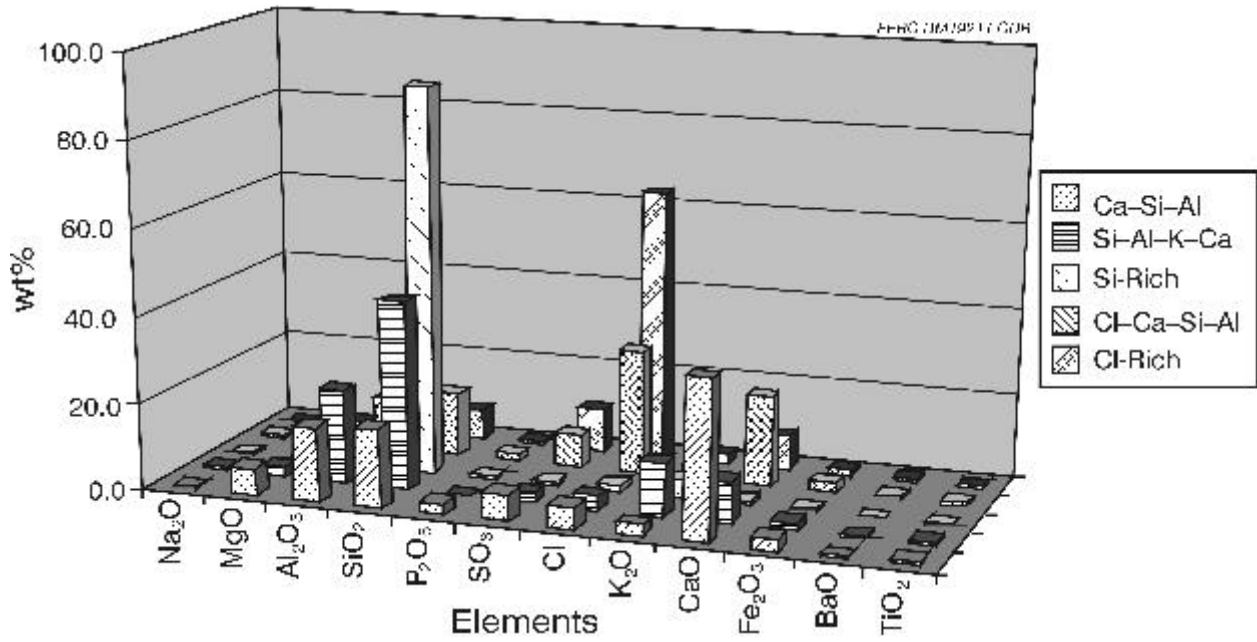


Figure G-28. Particle-size distribution for Absaloka and alfalfa stem blend ash.

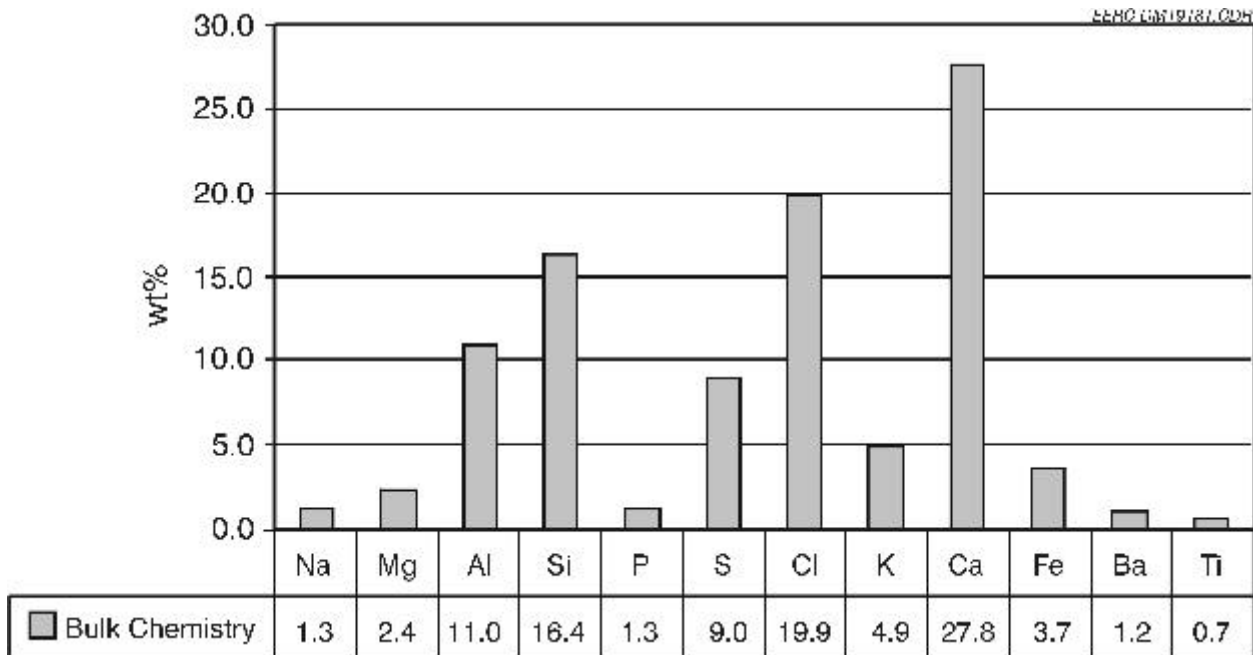


Figure G-29. Bulk chemistry of Absaloka and wheat straw blend ash.

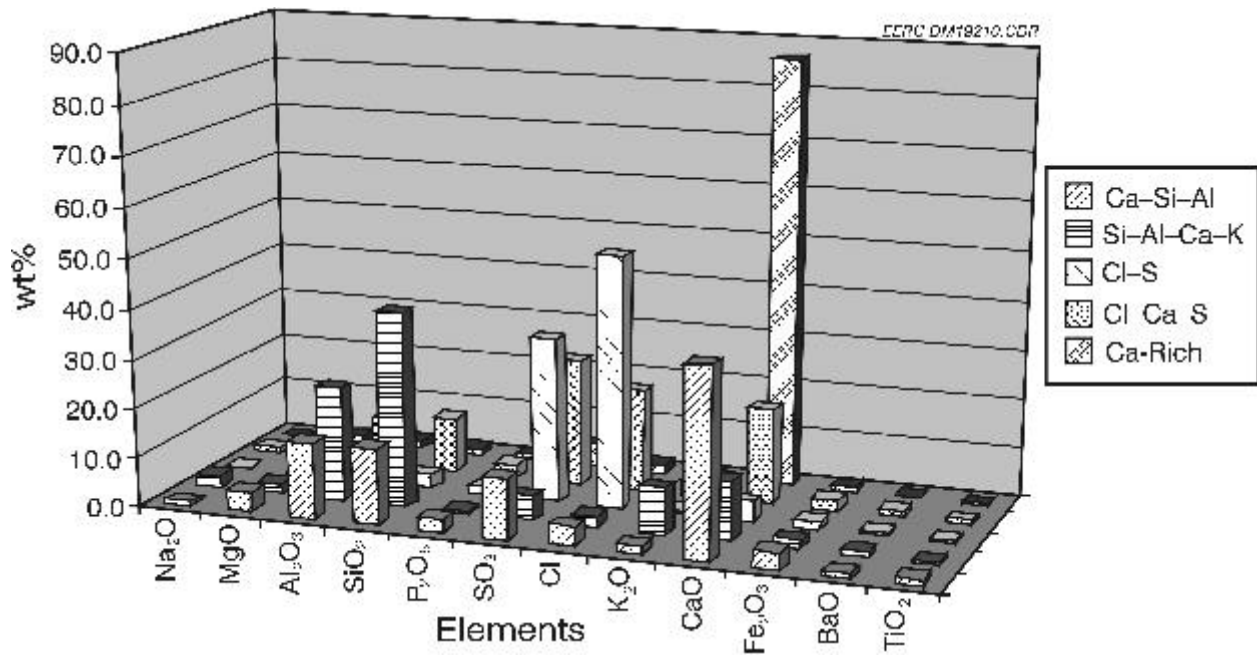


Figure G-30. The five most significant clusters from Absaloka and wheat straw blend ash.

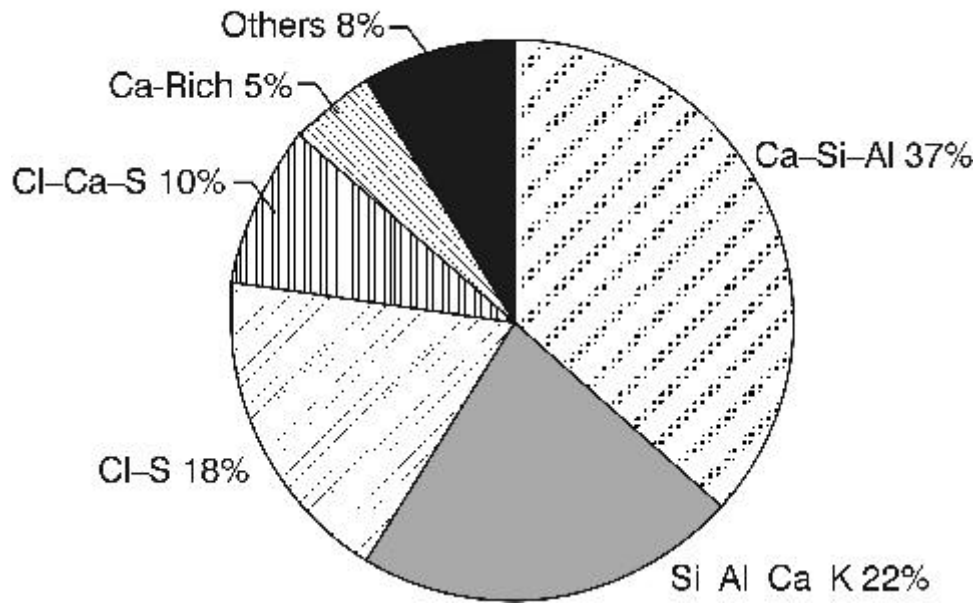


Figure G-31. Frequency distribution for chemical groups, based on cluster analysis.

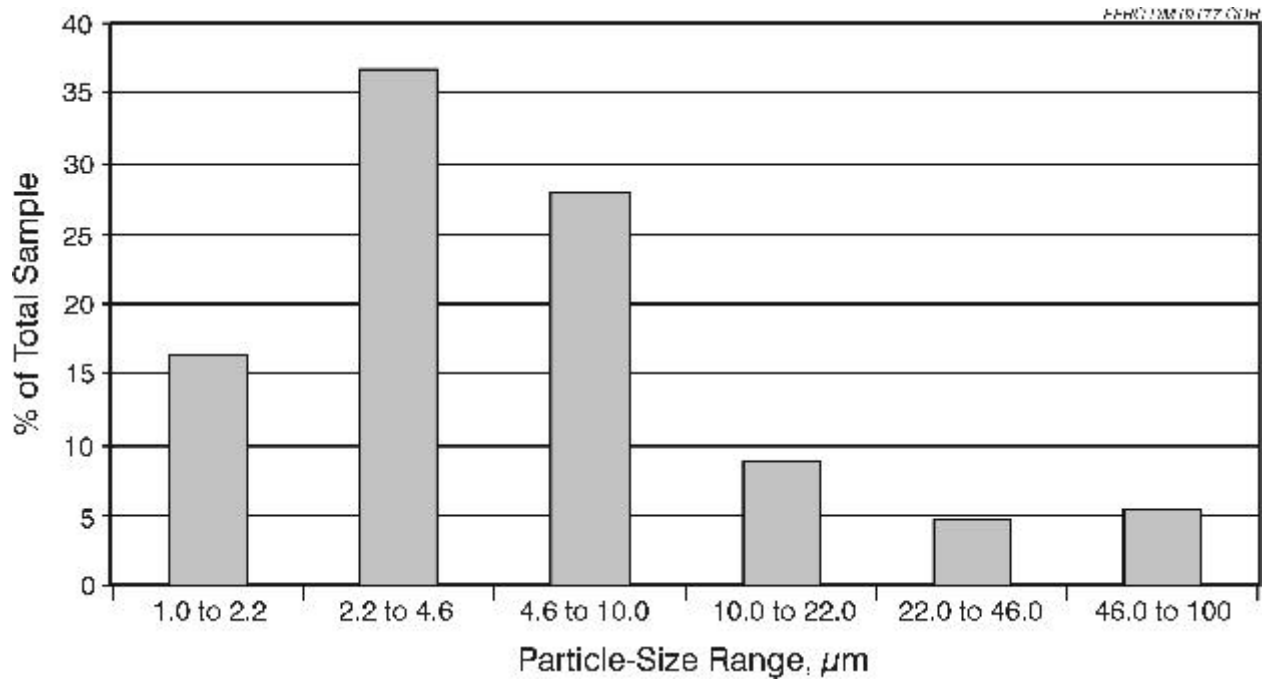


Figure G-32. Particle-size distribution for Absaloka and wheat straw blend ash.

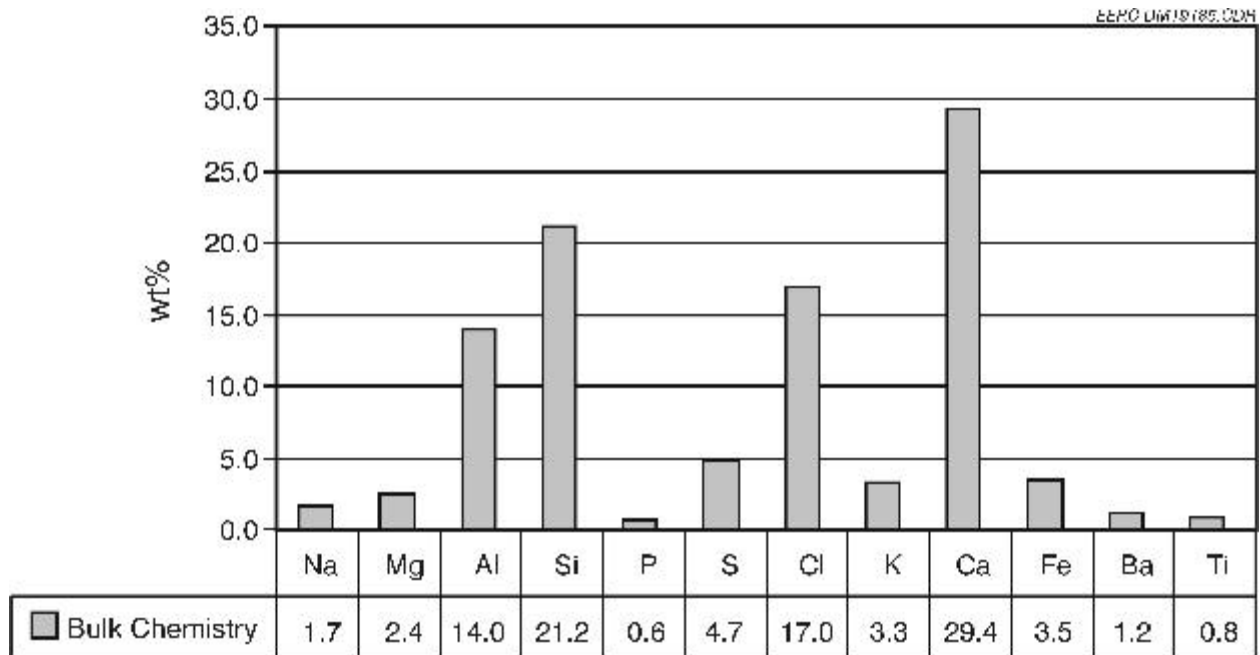


Figure G-33. Bulk chemistry of Absaloka and hybrid poplar blend ash.

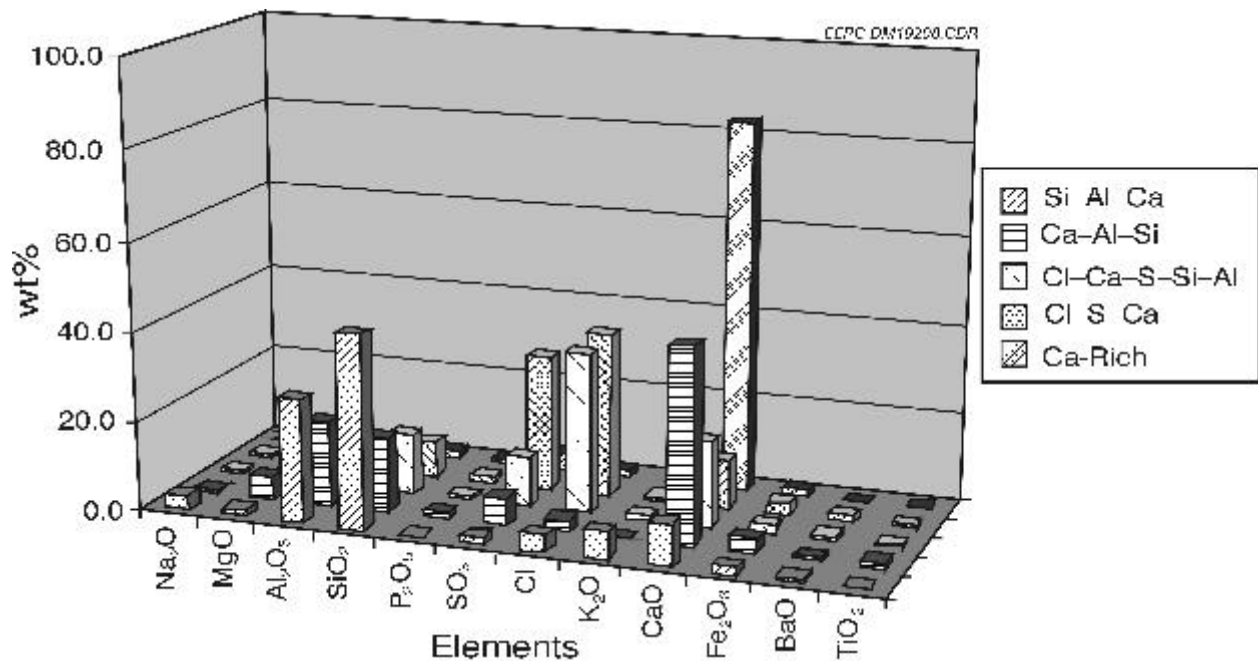


Figure G-34. The five most significant clusters from Absaloka and hybrid poplar blend ash.

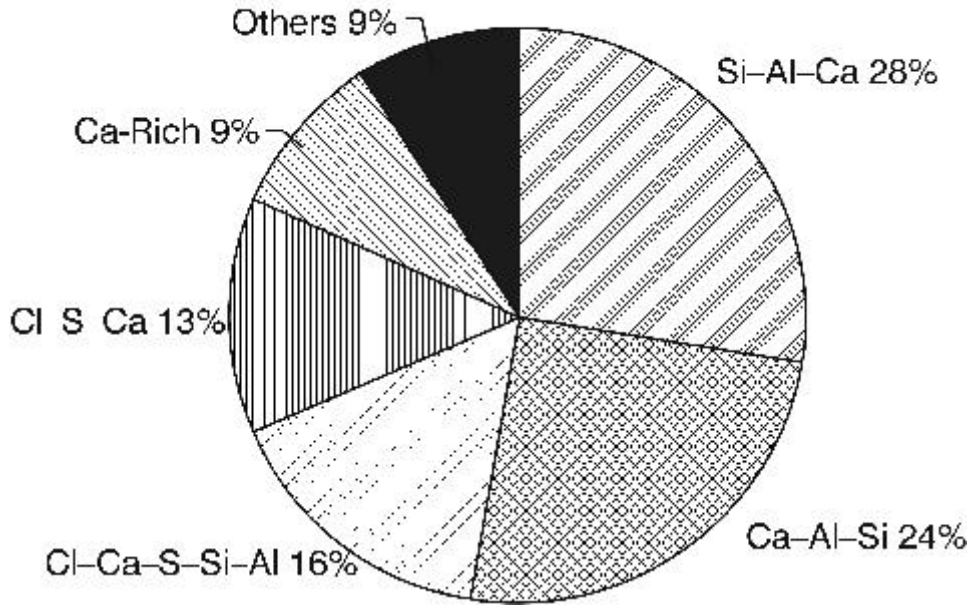


Figure G-35. Frequency distribution of chemical groups, based on cluster analysis.

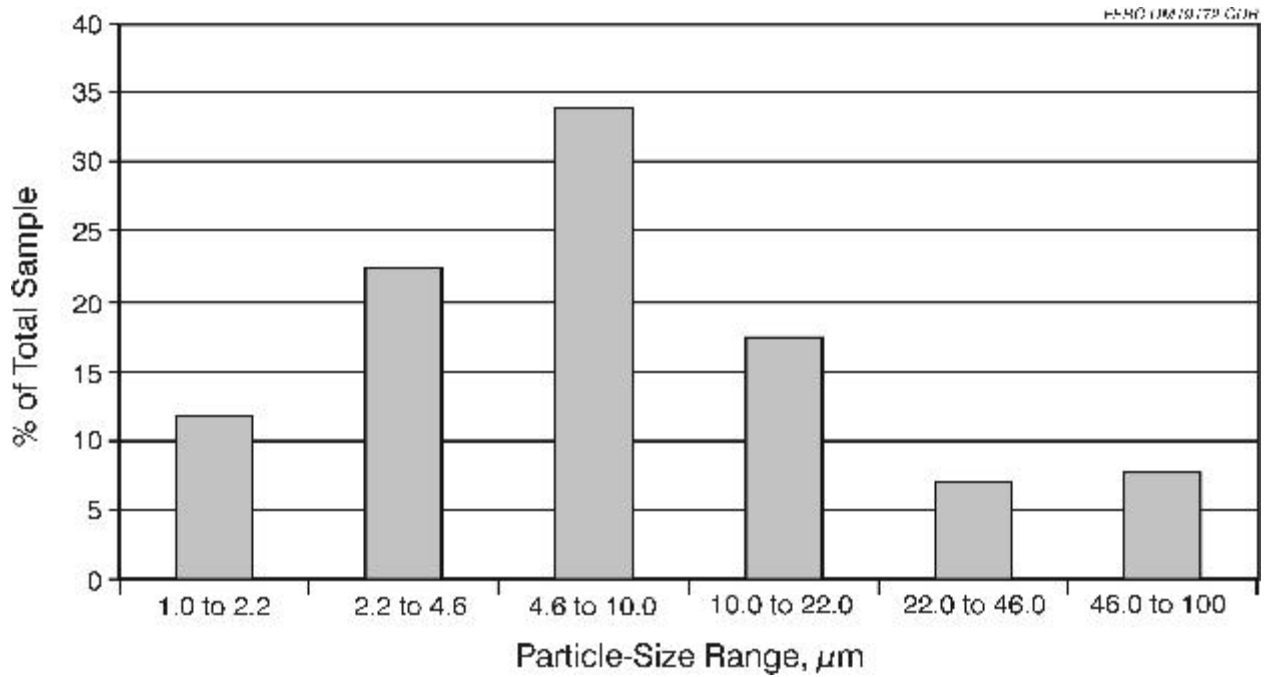


Figure G-36. Particle-size distribution for Absaloka and hybrid poplar blend ash.

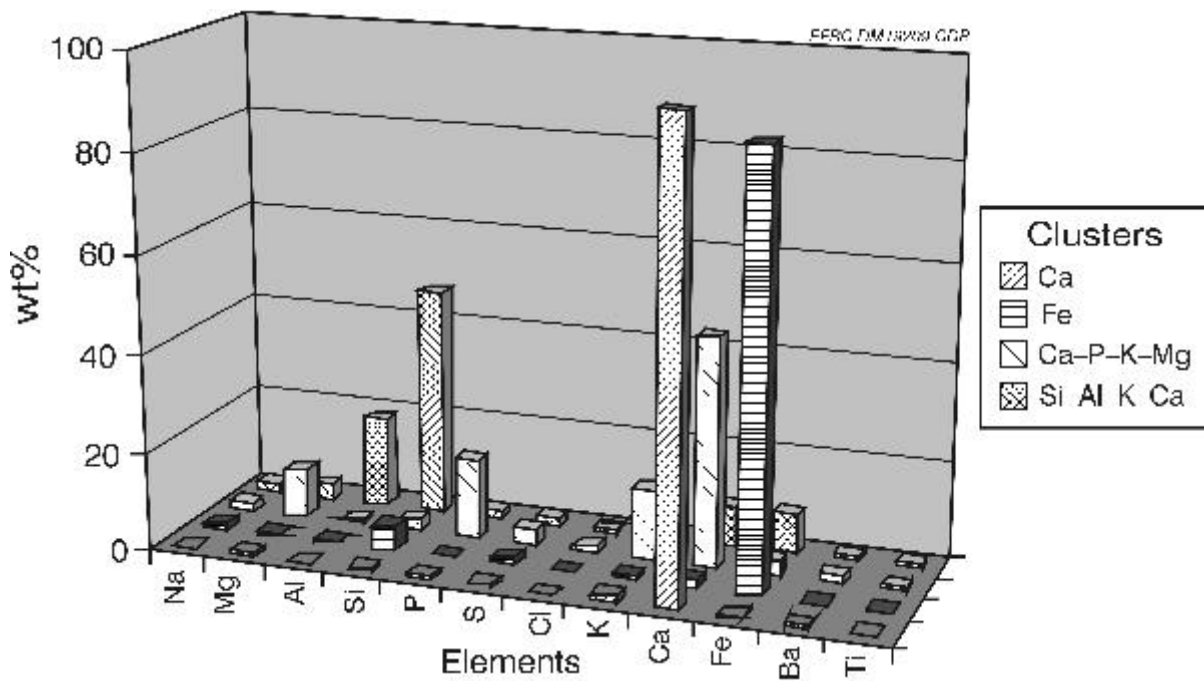


Figure G-37. Significant clusters from hybrid poplar fuel.

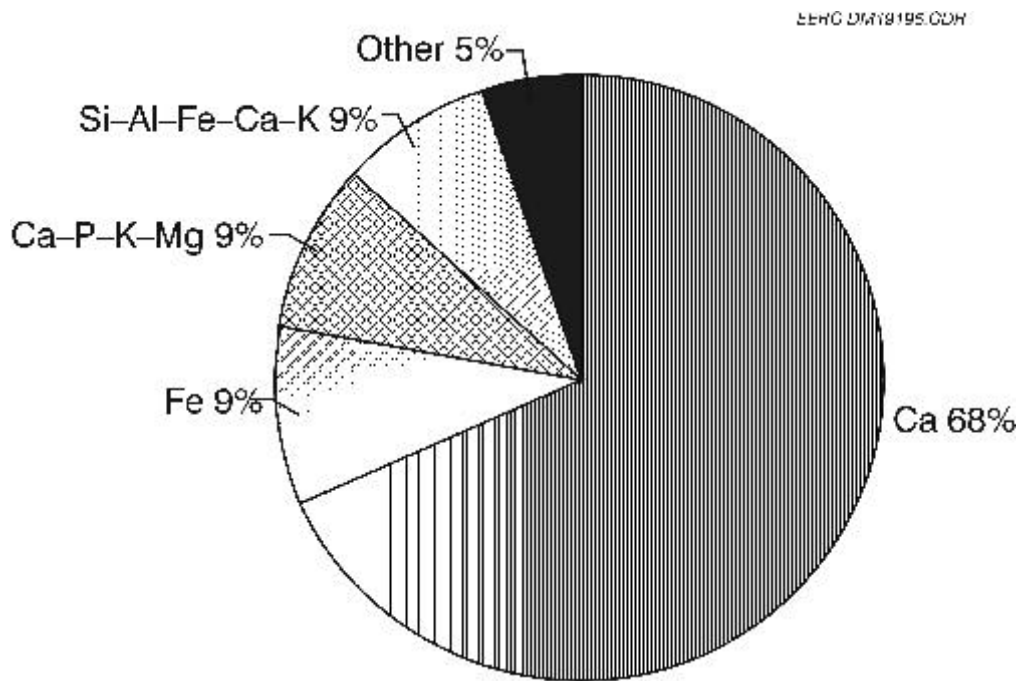


Figure G-38. Frequency distribution of chemical groups, based on cluster analysis.

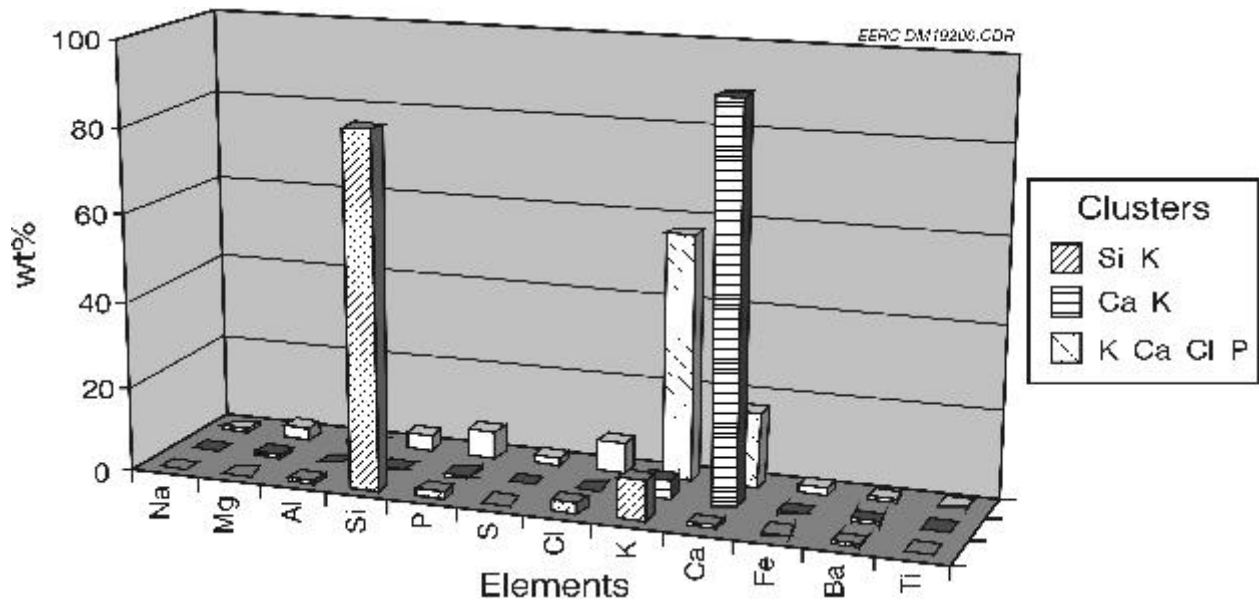


Figure G-39. Significant clusters from alfalfa stems fuel.

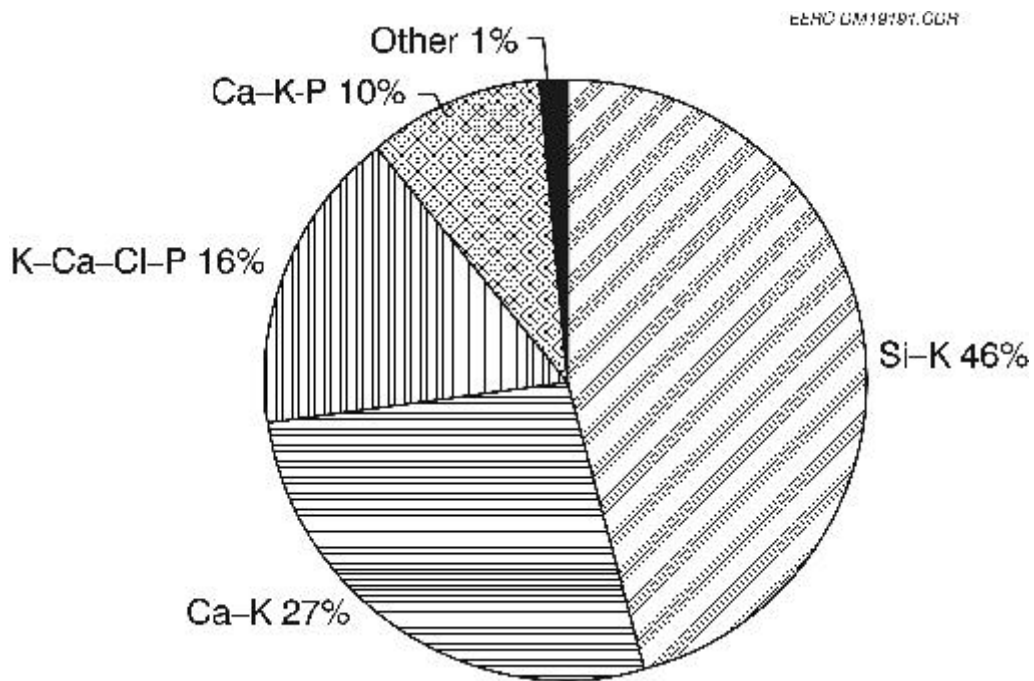


Figure G-40. Frequency distribution of chemical groups, based on cluster analysis.

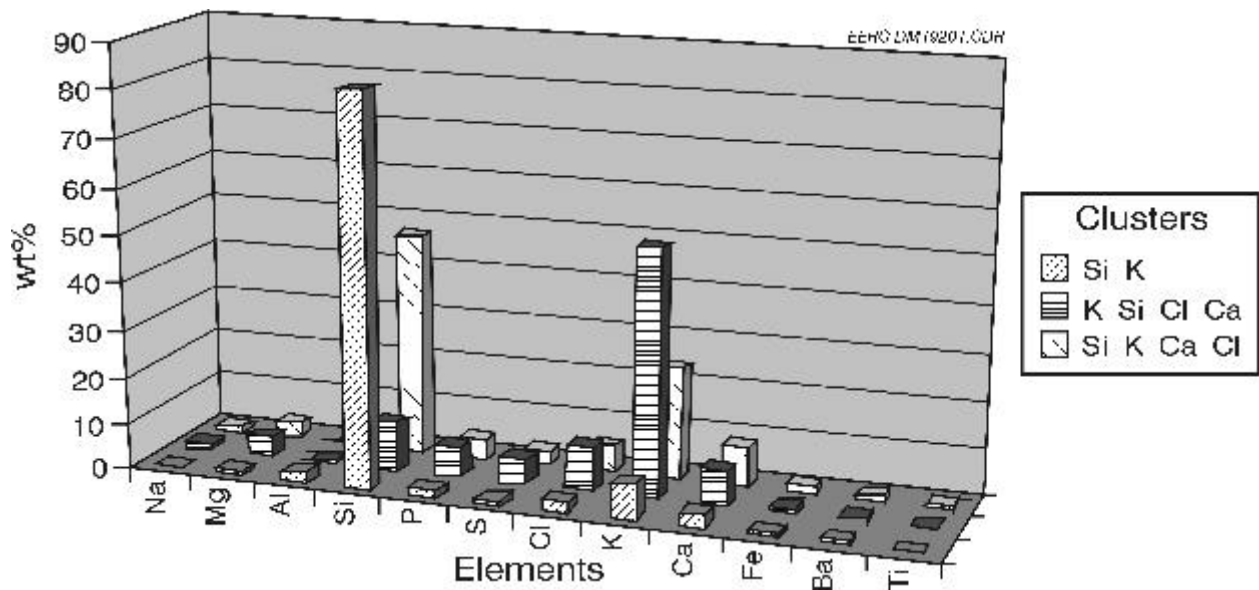


Figure G-41. Significant clusters from wheat straw fuel.

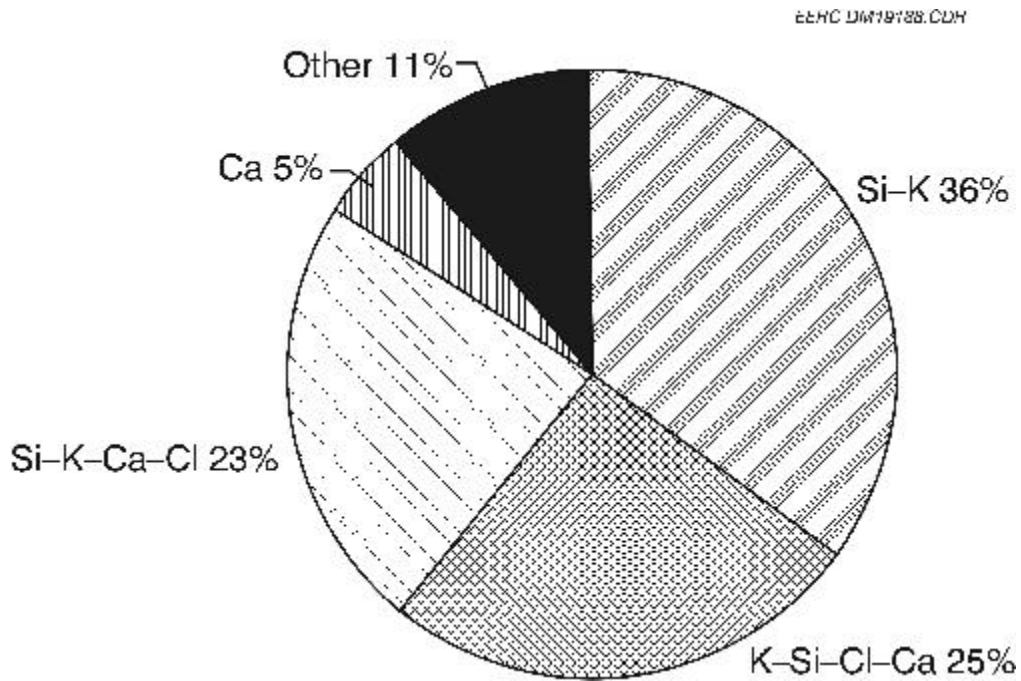


Figure G-42. Frequency distribution of chemical groups, based on cluster analysis.

## **APPENDIX H**

### **FLY ASH CCSEM ANALYSIS RESULTS**

TABLE H-1

## CCSEM Analysis of Illinois No. 6 Fly Ash

Size Bins, $\mu\text{m}$	1.0–2.2	2.2–4.6	4.6–10	10–22	22–46	46–100	Total
Quartz	0.0	0.0	0.1	0.0	0.0	0.0	0.1
Iron Oxide	0.2	0.6	0.8	0.0	0.0	0.0	1.7
Periclase	0.0	0.0	0.0	0.0	0.0	0.0	0.0
Rutile	0.0	0.1	0.0	0.0	0.0	0.0	0.1
Alumina	0.0	0.0	0.0	0.0	0.0	0.0	0.0
Calcite	0.0	0.0	0.2	0.0	0.0	0.0	0.2
Dolomite	0.0	0.0	0.0	0.0	0.0	0.0	0.0
Ankerite	0.0	0.0	0.0	0.0	0.0	0.0	0.0
Kaolinite	0.0	0.0	0.0	0.0	0.1	0.0	0.1
Montmorillonite	0.0	0.0	0.0	0.2	0.0	0.0	0.2
K Al-Silicate	0.0	0.2	1.5	1.7	0.7	0.0	4.2
Fe Al-Silicate	0.2	0.3	0.6	0.3	0.1	0.1	1.6
Ca Al-Silicate	0.0	0.0	0.1	0.0	0.0	0.0	0.1
Na Al-Silicate	0.0	0.0	0.0	0.0	0.0	0.0	0.0
Aluminosilicate	0.0	0.0	0.0	0.0	0.0	0.0	0.0
Mixed Al-Silicate	0.1	2.3	7.7	2.5	0.4	0.1	13.2
Fe Silicate	0.0	0.1	0.0	0.0	0.0	0.0	0.1
Ca Silicate	0.0	0.0	0.0	0.0	0.0	0.0	0.0
Ca Aluminate	0.0	0.0	0.0	0.0	0.0	0.0	0.0
Pyrite	0.0	0.0	0.0	0.0	0.0	0.0	0.0
Pyrrhotite	0.0	0.0	0.0	0.0	0.0	0.0	0.0
Oxidized Pyrrhotite	0.0	0.0	0.0	0.0	0.0	0.0	0.0
Gypsum	0.0	0.0	0.0	0.0	0.0	0.0	0.0
Barite	0.0	0.0	0.0	0.0	0.0	0.0	0.0
Apatite	0.0	0.1	0.0	0.0	0.0	0.0	0.2
Ca Al-Phosphate	0.0	0.0	0.0	0.0	0.0	0.0	0.0
KCl	0.0	0.0	0.0	0.0	0.0	0.0	0.0
Gypsum–Barite	0.0	0.0	0.0	0.0	0.0	0.0	0.0
Gypsum–Al-Silicate	0.0	0.0	0.3	0.2	0.0	0.0	0.4
Si-Rich	0.1	0.4	1.0	0.7	0.1	0.0	2.3
Ca-Rich	0.0	0.4	0.9	0.2	0.0	0.0	1.5
Ca–Si-Rich	0.0	0.0	0.0	0.0	0.0	0.0	0.0
Unknown	8.1	26.9	31.6	6.5	0.8	0.1	74.1
Totals	8.8	31.4	44.7	12.4	2.3	0.4	100.0

TABLE H-2

## CCSEM Analysis of Absaloka Fly Ash

Size Bins, $\mu\text{m}$	1.0–2.2	2.2–4.6	4.6–10	10–22	22–46	46–100	Total
Quartz	0.0	0.0	0.0	0.0	0.0	0.0	0.0
Iron Oxide	0.2	0.6	0.3	0.0	0.0	0.0	1.2
Periclase	0.0	0.0	0.0	0.0	0.0	0.0	0.0
Rutile	0.0	0.0	0.1	0.0	0.0	0.0	0.1
Alumina	0.0	0.0	0.0	0.0	0.0	0.0	0.0
Calcite	0.1	1.5	1.2	0.5	0.1	0.0	3.2
Dolomite	0.1	0.3	0.2	0.0	0.0	0.0	0.6
Ankerite	0.0	0.0	0.1	0.0	0.0	0.0	0.1
Kaolinite	0.1	0.7	3.2	2.5	0.1	0.0	6.6
Montmorillonite	0.0	0.0	0.1	0.0	0.0	0.0	0.1
K Al-Silicate	0.1	1.3	2.1	0.6	0.0	0.0	4.1
Fe Al-Silicate	0.1	1.1	1.6	0.2	0.0	0.0	3.0
Ca Al-Silicate	2.9	6.6	4.2	1.4	0.1	0.0	15.2
Na Al-Silicate	0.0	0.0	0.1	0.0	0.0	0.0	0.1
Aluminosilicate	0.0	0.0	0.0	0.0	0.0	0.0	0.0
Mixed Al-Silicate	1.1	3.7	1.2	0.2	0.0	0.0	6.2
Fe Silicate	0.0	0.0	0.0	0.0	0.0	0.0	0.0
Ca Silicate	0.0	0.6	0.2	0.2	0.0	0.0	1.0
Ca Aluminate	0.2	1.2	0.4	0.0	0.0	0.0	1.9
Pyrite	0.0	0.0	0.0	0.0	0.0	0.0	0.0
Pyrrhotite	0.0	0.0	0.0	0.0	0.0	0.0	0.0
Oxidized Pyrrhotite	0.0	0.0	0.0	0.0	0.0	0.0	0.0
Gypsum	0.0	0.0	0.1	0.1	0.0	0.0	0.2
Barite	0.0	0.0	0.0	0.0	0.0	0.0	0.0
Apatite	0.0	0.0	0.0	0.0	0.0	0.0	0.0
Ca Al-Phosphate	0.0	0.0	0.0	0.0	0.0	0.0	0.0
KCl	0.0	0.0	0.0	0.0	0.0	0.0	0.0
Gypsum–Barite	0.0	0.0	0.0	0.0	0.0	0.0	0.0
Gypsum–Al-Silicate	1.0	1.4	0.3	0.2	0.0	0.0	2.9
Si-Rich	0.1	0.0	0.1	0.1	0.0	0.0	0.3
Ca-Rich	0.3	0.7	0.4	0.1	0.0	0.0	1.4
Ca–Si-Rich	0.0	0.0	0.2	0.1	0.0	0.0	0.3
Unknown	23.3	21.4	4.5	2.0	0.1	0.0	51.4
Totals	29.7	41.1	20.6	8.2	0.4	0.0	100.0

TABLE H-3

## CCSEM Analysis of Wheat Straw Fly Ash

Size Bins, $\mu\text{m}$	1.0–2.2	2.2–4.6	4.6–10	10–22	22–46	46–100	Total
Quartz	3.0	5.7	4.3	6.5	7.2	5.3	31.9
Iron Oxide	0.0	0.0	0.0	0.0	0.0	0.0	0.0
Periclase	0.0	0.0	0.0	0.0	0.0	0.0	0.0
Rutile	0.0	0.0	0.0	0.0	0.0	0.0	0.0
Alumina	0.0	0.0	0.0	0.0	0.0	0.0	0.0
Calcite	0.0	0.0	0.1	0.2	0.0	0.9	1.2
Dolomite	0.0	0.1	0.0	0.1	0.3	0.1	0.7
Ankerite	0.0	0.0	0.0	0.0	0.0	0.0	0.0
Kaolinite	0.0	0.0	0.0	0.0	0.0	0.0	0.0
Montmorillonite	0.0	0.0	0.0	0.0	0.0	0.0	0.0
K Al-Silicate	0.0	0.0	0.0	0.1	0.0	0.0	0.1
Fe Al-Silicate	0.0	0.0	0.0	0.0	0.0	0.0	0.0
Ca Al-Silicate	0.0	0.0	0.0	0.0	0.0	0.0	0.0
Na Al-Silicate	0.0	0.0	0.0	0.0	0.0	0.0	0.0
Aluminosilicate	0.0	0.0	0.0	0.0	0.0	0.0	0.0
Mixed Al-Silicate	0.0	0.0	0.0	0.0	0.0	0.0	0.0
Fe Silicate	0.0	0.0	0.0	0.0	0.0	0.0	0.0
Ca Silicate	0.0	0.0	0.0	0.1	0.1	0.2	0.3
Ca Aluminate	0.0	0.0	0.0	0.0	0.0	0.0	0.0
Pyrite	0.0	0.0	0.0	0.0	0.0	0.0	0.0
Pyrrhotite	0.0	0.0	0.0	0.0	0.0	0.0	0.0
Oxidized Pyrrhotite	0.0	0.0	0.0	0.0	0.0	0.0	0.0
Gypsum	0.0	0.0	0.0	0.0	0.0	0.0	0.0
Barite	0.0	0.0	0.0	0.0	0.0	0.0	0.0
Apatite	0.0	0.1	0.0	0.1	0.3	0.1	0.6
Ca Al-Phosphate	0.0	0.0	0.0	0.0	0.0	0.0	0.0
KCl	0.0	0.1	0.0	0.1	0.0	0.0	0.2
Gypsum–Barite	0.0	0.0	0.0	0.0	0.0	0.0	0.0
Gypsum–Al-Silicate	0.0	0.0	0.0	0.0	0.0	0.0	0.0
Si-Rich	0.8	2.3	4.7	10.3	8.0	10.0	36.1
Ca-Rich	0.0	0.0	0.1	0.2	0.1	0.1	0.5
Ca–Si-Rich	0.0	0.1	0.1	0.3	0.2	0.3	1.0
Unknown	0.4	1.1	5.0	9.8	5.1	6.0	27.4
Totals	4.3	9.6	14.3	27.8	21.2	22.8	100.0

TABLE H-4

CCSEM Analysis of Alfalfa Fly Ash							
Size Bins, $\mu\text{m}$	1.0–2.2	2.2–4.6	4.6–10	10–22	22–46	46–100	Total
Quartz	0.0	0.1	0.4	0.7	0.2	0.2	1.5
Iron Oxide	0.0	0.2	0.3	1.0	0.3	0.0	1.8
Periclase	0.0	0.0	0.0	0.0	0.0	0.0	0.0
Rutile	0.0	0.0	0.0	0.0	0.0	0.0	0.0
Alumina	0.0	0.0	0.0	0.0	0.0	0.0	0.0
Calcite	0.0	0.0	0.2	0.1	0.0	0.0	0.3
Dolomite	0.0	0.0	0.0	0.2	0.0	0.0	0.2
Ankerite	0.0	0.0	0.0	0.0	0.0	0.0	0.0
Kaolinite	0.0	0.0	0.0	0.0	0.0	0.2	0.2
Montmorillonite	0.0	0.0	0.0	0.0	0.0	0.0	0.0
K Al-Silicate	0.0	0.0	0.6	0.6	0.2	0.0	1.4
Fe Al-Silicate	0.0	0.0	0.0	0.0	0.0	0.0	0.0
Ca Al-Silicate	0.0	0.1	0.3	0.1	0.1	0.0	0.5
Na Al-Silicate	0.0	0.0	0.0	0.0	0.0	0.0	0.0
Aluminosilicate	0.0	0.0	0.0	0.0	0.0	0.0	0.0
Mixed Al-Silicate	0.0	0.0	0.1	0.1	0.0	0.0	0.2
Fe Silicate	0.0	0.0	0.0	0.0	0.0	0.0	0.0
Ca Silicate	0.0	0.0	0.0	0.0	0.0	0.0	0.0
Ca Aluminate	0.0	0.0	0.0	0.0	0.0	0.0	0.0
Pyrite	0.0	0.0	0.0	0.0	0.0	0.0	0.0
Pyrrhotite	0.0	0.0	0.0	0.0	0.0	0.0	0.0
Oxidized Pyrrhotite	0.0	0.0	0.0	0.0	0.1	0.0	0.1
Gypsum	0.0	0.0	0.1	0.0	0.1	0.2	0.3
Barite	0.0	0.0	0.0	0.0	0.0	0.0	0.0
Apatite	0.0	0.0	0.1	0.2	0.1	0.1	0.5
Ca Al-Phosphate	0.0	0.0	0.0	0.0	0.0	0.0	0.0
KCl	3.2	4.9	0.8	0.5	0.2	0.1	9.6
Gypsum–Barite	0.0	0.0	0.0	0.0	0.0	0.0	0.0
Gypsum–Al-Silicate	0.0	0.0	0.0	0.0	0.0	0.0	0.1
Si-Rich	0.0	0.0	0.4	0.5	0.1	0.0	1.0
Ca-Rich	0.0	0.0	0.1	0.1	0.0	0.0	0.2
Ca–Si-Rich	0.0	0.0	0.0	0.1	0.0	0.0	0.1
Unknown	12.4	20.3	19.9	15.0	5.8	8.7	82.2
Totals	15.7	25.6	23.2	18.8	7.2	9.5	100.0

TABLE H-5

## CCSEM Analysis of Hybrid Poplar Fly Ash

Size Bins, $\mu\text{m}$	1.0–2.2	2.2–4.6	4.6–10	10–22	22–46	46–100	Total
Quartz	0.1	0.1	0.2	0.5	0.2	0.3	1.4
Iron Oxide	0.0	0.0	0.6	1.9	1.5	4.9	9.0
Periclase	0.0	0.0	0.0	0.0	0.0	0.0	0.0
Rutile	0.0	0.0	0.0	0.0	0.0	0.0	0.0
Alumina	0.1	0.1	0.1	0.1	0.2	0.0	0.6
Calcite	0.7	1.8	3.4	1.5	0.4	0.0	7.9
Dolomite	0.1	1.3	3.0	1.5	0.5	0.0	6.3
Ankerite	0.0	0.1	0.0	0.0	0.0	0.0	0.2
Kaolinite	0.0	0.0	0.0	0.0	0.1	0.0	0.1
Montmorillonite	0.0	0.0	0.0	0.0	0.0	0.0	0.0
K Al-Silicate	0.0	0.0	0.2	0.0	0.4	0.1	0.6
Fe Al-Silicate	0.0	0.2	0.0	0.0	0.0	0.0	0.3
Ca Al-Silicate	0.0	0.0	0.0	0.0	0.0	0.0	0.0
Na Al-Silicate	0.0	0.0	0.0	0.0	0.0	0.0	0.0
Aluminosilicate	0.0	0.0	0.0	0.1	0.1	1.4	1.6
Mixed Al-Silicate	0.0	0.1	0.1	0.2	0.0	0.3	0.7
Fe Silicate	0.0	0.0	0.0	0.0	0.0	0.0	0.0
Ca Silicate	0.0	0.0	0.0	0.0	0.0	0.0	0.0
Ca Aluminate	0.0	0.1	0.0	0.0	0.0	0.0	0.1
Pyrite	0.0	0.0	0.0	0.0	0.0	0.0	0.0
Pyrrhotite	0.0	0.0	0.0	0.0	0.0	0.0	0.0
Oxidized Pyrrhotite	0.0	0.0	0.1	0.2	0.1	4.0	4.3
Gypsum	0.0	0.0	0.2	0.3	0.0	0.0	0.5
Barite	0.0	0.0	0.0	0.0	0.0	0.0	0.0
Apatite	0.0	0.4	0.9	0.5	0.1	0.0	1.9
Ca Al-Phosphate	0.0	0.0	0.0	0.0	0.0	0.0	0.0
KCl	0.0	0.0	0.1	0.1	0.0	0.0	0.2
Gypsum–Barite	0.0	0.0	0.0	0.0	0.0	0.0	0.0
Gypsum–Al-Silicate	0.0	0.1	0.1	0.1	0.0	0.0	0.3
Si-Rich	0.0	0.1	0.3	0.1	0.0	0.1	0.6
Ca-Rich	0.5	2.3	2.2	0.9	0.3	0.0	6.1
Ca–Si-Rich	0.0	0.0	0.1	0.0	0.0	0.0	0.1
Unknown	15.4	14.1	9.0	5.1	5.4	8.2	57.2
Totals	16.9	20.9	20.7	13.0	9.2	19.3	100.0

TABLE H-6

## CCSEM Analysis of 80% Illinois No. 6-20% Wheat Straw Blend Fly Ash

Size Bins, $\mu\text{m}$	1.0-2.2	2.2-4.6	4.6-10	10-22	22-46	46-100	Total
Quartz	1.0	2.6	0.5	0.7	0.0	0.0	4.8
Iron Oxide	0.7	4.0	6.2	6.9	0.7	0.0	18.4
Periclase	0.0	0.0	0.0	0.0	0.0	0.0	0.0
Rutile	0.0	0.0	0.0	0.0	0.0	0.0	0.0
Alumina	0.0	0.0	0.0	0.0	0.0	0.0	0.0
Calcite	0.0	0.0	0.1	0.1	0.1	0.0	0.3
Dolomite	0.0	0.0	0.0	0.0	0.0	0.0	0.0
Ankerite	0.0	0.0	0.0	0.0	0.0	0.0	0.0
Kaolinite	0.0	0.0	0.0	0.0	0.0	0.0	0.0
Montmorillonite	0.0	0.0	0.0	0.0	0.0	0.0	0.0
K Al-Silicate	0.1	0.7	1.8	1.6	0.0	0.0	4.2
Fe Al-Silicate	0.0	0.1	0.0	0.2	0.0	0.0	0.3
Ca Al-Silicate	0.0	0.0	0.0	0.0	0.0	0.0	0.0
Na Al-Silicate	0.0	0.0	0.0	0.0	0.0	0.0	0.0
Aluminosilicate	0.0	0.0	0.0	0.0	0.0	0.0	0.0
Mixed Al-Silicate	0.1	0.3	0.4	1.2	0.1	0.0	2.1
Fe Silicate	0.0	0.0	0.1	0.0	0.0	0.0	0.1
Ca Silicate	0.0	0.0	0.0	0.0	0.0	0.0	0.0
Ca Aluminate	0.0	0.0	0.0	0.0	0.0	0.0	0.0
Pyrite	0.0	0.0	0.0	0.0	0.0	0.0	0.0
Pyrrhotite	0.0	0.0	0.0	0.0	0.0	0.0	0.0
Oxidized Pyrrhotite	0.0	0.0	0.1	0.0	0.0	0.0	0.1
Gypsum	0.0	0.0	0.0	0.0	0.0	0.0	0.0
Barite	0.0	0.0	0.0	0.0	0.0	0.0	0.0
Apatite	0.0	0.1	0.0	0.0	0.0	0.0	0.2
Ca Al-Phosphate	0.0	0.0	0.0	0.0	0.0	0.0	0.0
KCl	0.0	0.0	0.0	0.0	0.0	0.0	0.0
Gypsum-Barite	0.0	0.0	0.0	0.0	0.0	0.0	0.0
Gypsum-Al-Silicate	0.1	0.4	0.0	0.0	0.0	0.0	0.4
Si-Rich	1.0	1.9	0.8	0.5	0.1	0.0	4.3
Ca-Rich	0.0	0.6	0.7	0.4	0.0	0.0	1.7
Ca-Si-Rich	0.0	0.0	0.0	0.0	0.0	0.0	0.0
Unknown	14.1	28.8	12.4	6.5	0.7	0.3	62.8
Totals	17.1	39.4	23.3	18.1	1.7	0.3	100.0

TABLE H-7

## CCSEM Analysis of 80% Illinois No. 6–20% Alfalfa Stem Blend Fly Ash

Size Bins, $\mu\text{m}$	1.0–2.2	2.2–4.6	4.6–10	10–22	22–46	46–100	Total
Quartz	0.2	0.8	2.3	2.8	0.2	0.4	6.7
Iron Oxide	0.0	0.1	2.3	3.4	1.0	0.3	7.1
Periclase	0.0	0.0	0.0	0.0	0.0	0.0	0.0
Rutile	0.0	0.0	0.0	0.0	0.0	0.0	0.0
Alumina	0.0	0.0	0.0	0.0	0.1	0.0	0.1
Calcite	0.0	0.0	0.0	0.0	0.1	0.0	0.1
Dolomite	0.0	0.0	0.0	0.0	0.0	0.0	0.0
Ankerite	0.0	0.0	0.0	0.0	0.0	0.0	0.0
Kaolinite	0.0	0.0	0.0	0.3	0.2	0.1	0.6
Montmorillonite	0.0	0.0	0.0	0.0	0.0	0.0	0.0
K Al-Silicate	0.0	0.1	2.7	9.2	2.2	0.9	15.1
Fe Al-Silicate	0.0	0.0	0.1	0.0	0.0	0.0	0.1
Ca Al-Silicate	0.0	0.1	0.0	0.1	0.0	0.0	0.2
Na Al-Silicate	0.0	0.0	0.0	0.0	0.0	0.0	0.0
Aluminosilicate	0.0	0.0	0.0	0.0	0.0	0.0	0.0
Mixed Al-Silicate	0.0	0.2	0.1	0.5	0.1	0.0	0.9
Fe Silicate	0.0	0.0	0.1	0.0	0.0	0.0	0.1
Ca Silicate	0.0	0.0	0.1	0.0	0.0	0.0	0.1
Ca Aluminate	0.0	0.0	0.0	0.0	0.0	0.0	0.0
Pyrite	0.0	0.0	0.0	0.0	0.0	0.0	0.0
Pyrrhotite	0.0	0.0	0.0	0.0	0.0	0.0	0.0
Oxidized Pyrrhotite	0.0	0.0	0.3	0.2	0.1	0.0	0.6
Gypsum	0.0	0.0	0.0	0.2	0.1	0.0	0.3
Barite	0.0	0.0	0.0	0.0	0.0	0.0	0.0
Apatite	0.0	0.0	0.0	0.0	0.0	0.0	0.0
Ca Al-Phosphate	0.0	0.0	0.0	0.0	0.0	0.0	0.0
KCl	0.0	0.0	0.0	0.0	0.0	0.0	0.0
Gypsum–Barite	0.0	0.0	0.0	0.0	0.0	0.0	0.0
Gypsum–Al-Silicate	0.0	0.0	0.0	0.2	0.0	0.0	0.2
Si-Rich	0.4	0.6	1.5	2.1	0.4	0.2	5.3
Ca-Rich	0.0	0.0	0.2	0.1	0.0	0.0	0.3
Ca–Si-Rich	0.0	0.0	0.0	0.0	0.0	0.0	0.0
Unknown	2.7	8.2	20.0	17.0	6.0	7.9	62.0
Totals	3.3	10.2	29.9	36.1	10.7	9.8	100.0

TABLE H-8

## CCSEM Analysis of 80% Illinois No. 6–20% Hybrid Poplar Blend Fly Ash

Size Bins, $\mu\text{m}$	1.0–2.2	2.2–4.6	4.6–10	10–22	22–46	46–100	Total
Quartz	0.7	1.6	3.5	2.4	0.2	0.4	8.7
Iron Oxide	0.0	1.6	1.7	0.9	0.3	0.1	4.5
Periclase	0.0	0.0	0.0	0.0	0.0	0.0	0.0
Rutile	0.0	0.0	0.0	0.0	0.0	0.0	0.0
Alumina	0.0	0.0	0.0	0.0	0.0	0.0	0.0
Calcite	0.0	0.0	0.1	0.1	0.1	0.0	0.3
Dolomite	0.0	0.0	0.1	0.0	0.0	0.0	0.1
Ankerite	0.0	0.1	0.0	0.0	0.0	0.0	0.1
Kaolinite	0.0	0.0	0.0	0.1	0.0	0.0	0.2
Montmorillonite	0.0	0.0	0.0	0.0	0.0	0.0	0.0
K Al-Silicate	0.0	0.5	3.6	7.1	0.9	0.0	12.2
Fe Al-Silicate	0.0	0.1	0.2	0.0	0.0	0.1	0.4
Ca Al-Silicate	0.0	0.2	0.3	0.0	0.0	0.0	0.5
Na Al-Silicate	0.0	0.0	0.0	0.0	0.0	0.0	0.0
Aluminosilicate	0.0	0.0	0.0	0.0	0.0	0.0	0.0
Mixed Al-Silicate	0.1	0.9	2.5	1.2	0.3	0.0	5.0
Fe Silicate	0.0	0.0	0.1	0.0	0.0	0.0	0.1
Ca Silicate	0.0	0.0	0.0	0.0	0.0	0.0	0.0
Ca Aluminate	0.0	0.0	0.1	0.0	0.0	0.0	0.1
Pyrite	0.0	0.0	0.0	0.0	0.0	0.0	0.0
Pyrrhotite	0.0	0.0	0.0	0.0	0.0	0.0	0.0
Oxidized Pyrrhotite	0.0	0.0	0.0	0.0	0.0	0.0	0.0
Gypsum	0.0	0.0	0.2	0.7	0.1	0.0	1.1
Barite	0.0	0.0	0.0	0.0	0.0	0.0	0.0
Apatite	0.0	0.0	0.0	0.0	0.0	0.0	0.0
Ca Al-Phosphate	0.0	0.0	0.0	0.0	0.0	0.0	0.0
KCl	0.0	0.0	0.0	0.0	0.0	0.0	0.1
Gypsum–Barite	0.0	0.0	0.0	0.0	0.0	0.0	0.0
Gypsum–Al-Silicate	0.1	0.2	0.4	0.2	0.3	0.1	1.3
Si-Rich	0.3	0.8	1.7	0.7	0.2	0.2	3.9
Ca-Rich	0.0	0.3	0.3	0.4	0.1	0.0	1.1
Ca–Si-Rich	0.0	0.0	0.1	0.0	0.0	0.0	0.1
Unknown	6.1	13.8	21.4	11.3	4.7	2.9	60.2
Totals	7.5	20.1	36.1	25.1	7.3	3.8	100.0

TABLE H-9

## CCSEM Analysis of 80% Absaloka–20% Wheat Straw Blend Fly Ash

Size Bins, $\mu\text{m}$	1.0–2.2	2.2–4.6	4.6–10	10–22	22–46	46–100	Total
Quartz	0.0	0.8	0.4	0.2	0.1	0.0	1.6
Iron Oxide	0.0	0.2	0.7	0.2	0.0	0.1	1.2
Periclase	0.0	0.0	0.0	0.0	0.0	0.0	0.0
Rutile	0.0	0.0	0.0	0.0	0.0	0.0	0.0
Alumina	0.0	0.0	0.0	0.0	0.0	0.0	0.0
Calcite	0.0	0.8	0.9	1.1	0.4	0.0	3.2
Dolomite	0.0	0.2	0.2	0.1	0.0	0.0	0.5
Ankerite	0.0	0.0	0.1	0.0	0.0	0.0	0.2
Kaolinite	0.0	0.0	0.0	0.0	0.0	0.0	0.0
Montmorillonite	0.0	0.0	0.0	0.0	0.0	0.0	0.0
K Al-Silicate	0.0	0.0	1.2	0.9	0.2	0.1	2.3
Fe Al-Silicate	0.0	0.1	0.0	0.0	0.0	0.0	0.1
Ca Al-Silicate	0.0	0.5	1.1	0.4	0.0	0.1	2.1
Na Al-Silicate	0.0	0.0	0.0	0.0	0.0	0.0	0.0
Aluminosilicate	0.0	0.0	0.0	0.0	0.0	0.0	0.0
Mixed Al-Silicate	0.0	0.0	0.0	0.0	0.0	0.0	0.0
Fe Silicate	0.0	0.0	0.0	0.0	0.0	0.0	0.0
Ca Silicate	0.0	0.0	0.0	0.0	0.0	0.0	0.0
Ca Aluminate	0.0	0.1	0.5	0.2	0.0	0.0	0.8
Pyrite	0.0	0.0	0.0	0.0	0.0	0.0	0.0
Pyrrhotite	0.0	0.0	0.0	0.0	0.0	0.0	0.0
Oxidized Pyrrhotite	0.0	0.0	0.0	0.0	0.0	0.0	0.0
Gypsum	0.0	0.0	0.0	0.0	0.0	0.0	0.0
Barite	0.0	0.0	0.0	0.0	0.0	0.0	0.0
Apatite	0.0	0.0	0.0	0.0	0.0	0.0	0.0
Ca Al-Phosphate	0.0	0.1	0.0	0.0	0.0	0.0	0.2
KCl	0.0	0.0	0.0	0.0	0.0	0.0	0.0
Gypsum–Barite	0.0	0.0	0.0	0.0	0.0	0.0	0.0
Gypsum–Al-Silicate	0.0	1.7	1.2	0.5	0.4	0.4	4.2
Si-Rich	0.1	0.1	0.8	0.7	0.1	0.0	1.8
Ca-Rich	0.0	0.5	0.7	0.1	0.1	0.2	1.7
Ca–Si-Rich	0.0	0.0	0.1	0.0	0.0	0.0	0.1
Unknown	16.2	31.6	19.8	4.4	3.3	4.7	80.0
Totals	16.3	36.7	27.9	8.8	4.8	5.5	100.0

TABLE H-10

## CCSEM Analysis of 80% Absaloka–20% Alfalfa Stem Blend Fly Ash

Size Bins, $\mu\text{m}$	1.0–2.2	2.2–4.6	4.6–10	10–22	22–46	46–100	Total
Quartz	0.1	0.4	1.3	3.2	0.8	0.1	5.8
Iron Oxide	0.0	0.0	0.9	1.8	0.2	0.0	2.9
Periclase	0.0	0.0	0.0	0.0	0.0	0.0	0.0
Rutile	0.0	0.0	0.0	0.0	0.0	0.0	0.0
Alumina	0.0	0.0	0.0	0.0	0.0	0.0	0.0
Calcite	0.0	0.0	0.3	0.1	0.3	0.0	0.7
Dolomite	0.0	0.0	0.0	0.2	0.0	0.0	0.3
Ankerite	0.0	0.0	0.1	0.0	0.0	0.0	0.2
Kaolinite	0.0	0.0	0.0	0.0	0.0	0.0	0.1
Montmorillonite	0.0	0.0	0.0	0.0	0.0	0.0	0.0
K Al-Silicate	0.0	1.0	2.3	3.8	0.9	0.1	8.2
Fe Al-Silicate	0.0	0.0	0.0	0.0	0.0	0.0	0.0
Ca Al-Silicate	0.0	1.0	1.5	0.2	0.2	0.0	2.9
Na Al-Silicate	0.0	0.0	0.0	0.0	0.0	0.0	0.0
Aluminosilicate	0.0	0.0	0.0	0.0	0.0	0.0	0.0
Mixed Al-Silicate	0.0	0.0	0.1	0.0	0.0	0.0	0.1
Fe Silicate	0.0	0.0	0.0	0.1	0.0	0.0	0.1
Ca Silicate	0.0	0.0	0.0	0.0	0.0	0.0	0.0
Ca Aluminate	0.0	0.2	0.5	0.4	0.0	0.0	1.1
Pyrite	0.0	0.0	0.0	0.0	0.0	0.0	0.0
Pyrrhotite	0.0	0.0	0.0	0.0	0.0	0.0	0.0
Oxidized Pyrrhotite	0.0	0.0	0.0	0.0	0.0	0.0	0.0
Gypsum	0.0	0.2	0.0	0.2	0.2	0.0	0.6
Barite	0.0	0.0	0.0	0.0	0.0	0.0	0.0
Apatite	0.0	0.3	0.0	0.0	0.0	0.0	0.3
Ca Al-Phosphate	0.0	0.0	0.0	0.0	0.0	0.0	0.0
KCl	0.0	0.0	0.0	0.0	0.0	0.0	0.0
Gypsum–Barite	0.0	0.0	0.0	0.0	0.0	0.0	0.0
Gypsum–Al-Silicate	0.0	0.0	0.2	0.2	0.2	0.4	1.0
Si-Rich	0.2	0.3	0.9	0.3	0.2	0.0	1.9
Ca-Rich	0.0	0.2	0.3	0.1	0.1	0.2	1.0
Ca–Si-Rich	0.0	0.0	0.1	0.2	0.0	0.1	0.4
Unknown	10.2	24.2	17.4	9.4	5.5	5.7	72.4
Totals	10.6	27.8	26.0	20.0	8.9	6.7	100.0

TABLE H-11

## CCSEM Analysis of 80% Absaloka–20% Hybrid Poplar Blend Fly Ash

Size Bins, $\mu\text{m}$	1.0–2.2	2.2–4.6	4.6–10	10–22	22–46	46–100	Total
Quartz	0.1	0.3	1.4	2.2	0.3	0.1	4.5
Iron Oxide	0.0	0.2	0.9	0.2	0.1	0.0	1.5
Periclase	0.0	0.0	0.0	0.0	0.0	0.0	0.0
Rutile	0.0	0.0	0.0	0.0	0.0	0.0	0.0
Alumina	0.0	0.0	0.0	0.0	0.0	0.0	0.0
Calcite	0.0	0.8	2.2	2.9	0.8	0.2	7.0
Dolomite	0.0	0.1	0.3	0.1	0.0	0.0	0.5
Ankerite	0.0	0.2	0.1	0.0	0.0	0.0	0.3
Kaolinite	0.0	0.0	0.0	0.0	0.0	0.0	0.0
Montmorillonite	0.0	0.0	0.0	0.0	0.0	0.0	0.0
K Al-Silicate	0.0	0.1	0.1	0.9	0.6	0.0	1.7
Fe Al-Silicate	0.0	0.0	0.0	0.0	0.0	0.0	0.0
Ca Al-Silicate	0.1	1.5	3.2	1.6	0.3	0.0	6.6
Na Al-Silicate	0.0	0.0	0.0	0.0	0.0	0.0	0.0
Aluminosilicate	0.0	0.0	0.0	0.0	0.0	0.0	0.0
Mixed Al-Silicate	0.1	0.5	1.5	1.4	0.6	0.1	4.1
Fe Silicate	0.0	0.0	0.0	0.0	0.0	0.0	0.0
Ca Silicate	0.0	0.1	0.1	0.0	0.0	0.1	0.3
Ca Aluminate	0.0	0.5	0.9	0.3	0.0	0.0	1.7
Pyrite	0.0	0.0	0.0	0.0	0.0	0.0	0.0
Pyrrhotite	0.0	0.0	0.0	0.0	0.0	0.0	0.0
Oxidized Pyrrhotite	0.0	0.0	0.0	0.0	0.0	0.0	0.0
Gypsum	0.0	0.0	0.0	0.1	0.0	0.0	0.1
Barite	0.0	0.0	0.0	0.0	0.0	0.0	0.0
Apatite	0.0	0.0	0.1	0.0	0.0	0.0	0.1
Ca Al-Phosphate	0.0	0.0	0.0	0.0	0.0	0.0	0.0
KCl	0.0	0.0	0.0	0.0	0.0	0.0	0.0
Gypsum–Barite	0.0	0.0	0.0	0.0	0.0	0.0	0.0
Gypsum–Al-Silicate	0.2	0.9	0.7	0.1	0.5	0.8	3.3
Si-Rich	0.2	0.4	0.6	0.0	0.1	0.0	1.3
Ca-Rich	0.1	0.8	1.2	0.5	0.1	0.1	2.8
Ca–Si-Rich	0.0	0.0	0.1	0.3	0.0	0.0	0.4
Unknown	11.0	15.8	20.4	6.8	3.3	6.2	63.6
Totals	11.8	22.4	33.9	17.5	6.9	7.6	100.0